Aus dem Max von Pettenkofer-Institut für Hygiene und Medizinische Mikrobiologie
der Ludwig-Maximilians-Universität München
Lehrstuhl: Bakteriologie
Kommissarischer Vorstand: Prof. Dr. Rainer Haas

Metabolism of Glycerol and Inositol by *Legionella pneumophila*

Dissertation
zum Erwerb des Doktorgrades der Naturwissenschaften
an der medizinischen Fakultät der
Ludwig-Maximilians-Universität München

vorgelegt von

Christian Gerhard Manske

aus Tirschenreuth

2015

Gedruckt mit Genehmigung der Medizinischen Fakultät

der Ludwig-Maximilians-Universität München

Betreuer:

Prof. Dr. Hubert Hilbi

Zweitgutachter:

Prof. Dr. Heinrich Jung

Dekan der medizinischen Fakultät:

Prof. Dr. med. dent. Reinhard Hickel

Tag der mündlichen Prüfung: 23.06.2016

Eidesstattliche Versicherung

Ich, Christian Gerhard Manske, erkläre hiermit an Eides statt, dass ich die vorliegende Dissertation mit dem Thema

"Metabolism of Glycerol and Inositol by *Legionella pneumophila*"

selbständig verfasst, mich außer der angegebenen keiner weiteren Hilfsmittel bedient und alle Erkenntnisse, die aus dem Schrifttum ganz oder annähernd übernommen sind, als solche kenntlich gemacht und nach ihrer Herkunft unter Bezeichnung der Fundstelle einzeln nachgewiesen habe. Ich erkläre des Weiteren, dass die hier vorgelegte Dissertation nicht in gleicher oder in ähnlicher Form bei einer anderen Stelle zur Erlangung eines akademischen Grades eingereicht wurde.

_____ _____

Ort, Datum Unterschrift

Table of Contents

List of Abbreviations

°C	degrees Celsius
%	percent
µF	microfarad
µL	microliter
µm	micrometer
2-NBDG	2-(N-(7-nitrobenz-2-oxa-1,3-diazol-4-yl)amino)-2-deoxyglucose
3-HBA	3-hydroxybutyrate
6-PG	6-phosphoglycerate
AA	amino acid
ACES	N-(2-acetamido)-2-aminoethanesulfonic acid
ADP	adenosine diphosphate
Ala	alanine
Amp	ampicillin
Arg	arginine
Asn	asparagine
Asp	aspartate
ATP	adenosine triphosphate
BCYE	buffered charcoal yeast extract
CA	cellulose acetate
CDM	chemically defined medium
CE MDM	carbon-enriched minimal defined medium
cfu	colony forming unit
Cho	chorismate
Cm / Cm^R	chloramphenicol / resistance to chloramphenicol
cm^2	square centimeter
cpm	counts per minute
CYE	charcoal yeast extract
Cys	cysteine
DAP	diaminopimelic acid

DAPI	4′,6-diamidine-2-phenylindol
DM	defined medium
DMSO	dimethylsulfoxide
DNA	deoxyribonucleic acid
dNTP	deoxynucleotide triphosphate
ED	Entner-Doudoroff
EDTA	ethylenediaminetetraacetate
eEF1A	eukaryotic elongation factor 1A
EGTA	ethylene glycol tetraacetic acid
EPF	exponential phase form
ER	endoplasmic reticulum
Ess	essential amino acid medium
eV	electron Volt
FA	fatty acid
FAD	flavin adenine dinucleotide
FCS	fetal calf serum
FF	filamentous form
g	gram
GC/MS	gas chromatography/mass spectrometery
GDP	guanosine diphosphate
GFP	green fluorescent protein
GFP (ASV)	unstable green fluorescent protein
Gk	glycerol kinase
Gln	glutamine
Glu	glutamate
Gly	glycine
GTP	guanosine triphosphate
h	hour
HEPES	2-(4-(2-hydroxyethyl)piperazine-1-yl)ethanesulfonic acid
HGA	homogentisic acid
His	histidine
icm/dot	intracellular multiplication/defective organelle trafficking

IHF	integration host factor
Ile	isoleucine
IPTG	isopropyl-β-D-thiogalactopyranoside
kB	kilobase
KDPG	2-keto-3-deoxy-6-phosphogluconate
Km / Km^R	kanamycin / resistance to kanamycin
kPa	kilo Pascal
kV	kilovolt
l	litre
LAI-1	*Legionella* autoinducer 1
LB	Lysogeny Broth
LBs	lipid bodies
LCV	*Legionella*-containing vacuole
Leu	leucine
Lpn	*Legionella pneumophila*
Lys	lysine
M	molar
MDM	minimal defined medium
Met	methionine
mg	milligram
MI	*myo*-inositol
MIF	mature infectious form
min	minutes
mL	milliliter
mm	millimeter
mM	millimolar
MOI	multiplicity of infection
MOMP	major outer membrane protein
MP	macropinosome
NAD(P)H	nicotinamide adenine dinucleotide (phosphate)
ng	nanogram
NMR	nuclear magnetic resonance

OD_{600}	optical density at 600 nanometer
PBS	phosphate-buffered saline
PCR	polymerase chain reaction
PFA	paraformaldehyde
pH	negative common logarithm of the concentration of hydrogen ions
PHB	polyhydroxybutyrate
Phe	phenylalanine
PI	phosphatidylinositol
PI4KIIIβ	phosphatidylinositol-4-kinase-IIIβ
ppGpp	guanosine-3',5'-bispyrophosphate
PPP	pentose phosphate pathway
Pro	proline
PtdIns*P*	phosphatidylinositol phosphate
PYG	peptone yeast extract glucose broth
RFU	relative fluorescence unit
RNA	ribonucleic acid
RPF	replicative phase form
rpm	rounds per minute
RT	retention time
s	seconds
SD	standard deviation
Ser	serine
Shi	shikimate
SNARE	soluble N-ethylmaleimide sensitive factor attachment protein receptor
SorC	Sörensen phosphate buffer
SPF	stationary phase form
Suc	sucrose
T1SS	type I secretion system
T2SS	type II secretion system
T4SS	type IV secretion system
TBDMS	tert-butyl-dimethylsilyl
TCA	tricarbolic acid

TFB1/2	transformation buffer 1/2
Thr	threonine
TMS	trimethylsilyl
tRNA	transfer RNA
Trp	tryptophane
Tyr	tyrosine
UV	ultra violet
Val	valine
VBNCC	viable but not culturable cell
WT	wild-type
α-KGA	α-ketoglutarate
Ω	ohm

List of Publications

Manske C., Schell U., Hilbi H. (**2016**). Metabolism of *myo*-inositol by *Legionella pneumophila* promotes infection of amoeba and macrophages. Applied and Environmental Microbiology, 2016 Jun 10. pii: AEM.01018-16.

Häuslein I.[#], **Manske C.**[#], Goebel W., Eisenreich W., Hilbi H. (**2015**). Pathway analysis using ^{13}C-glycerol and other carbon tracers reveals a bipartite metabolism of *Legionella pneumophila*. Molecular Microbiology, 2016 Apr;100(2):229-46. doi: 10.1111/mmi.13313.

Manske C., Finsel I., Hoffmann C., Hilbi H. (**2015**). Analysis of *Legionella* metabolism by pathogen vacuole proteomics. Methods in Molecular Biology, submitted.

Harrison CF., Chiriano G., Finsel I., **Manske C.**, Hoffmann C., Steiner B., Kranjc A., Patthey-Vuadens O., Kickal S., Trofimov V., Ouertatani-Sakouhi H., Soldati T., Scapozza L., Hilbi H. (**2015**). Amoebae-based screening reveals a novel family of compounds restricting intracellular *Legionella pneumophila*. ACS Infectious. Diseases, 1 (7), pp 327–338.

Manske C., Hilbi H. (**2014**). Metabolism of the vacuolar pathogen *Legionella* and implications for virulence. Frontiers in Cellular and Infection Microbiology, Sep 9; 4:125.

# Authors contributed equally to this work

Summary

Legionella pneumophila is a gram-negative, opportunistic pathogen that naturally parasitizes environmental amoeba, but can also infect human alveolar macrophages, thus causing a severe and potentially lethal pneumonia called "Legionnaires' disease". *L. pneumophila* is an obligate aerobe organism that prefers amino acids as main source of carbon and energy. Nevertheless, the genome of *Legionella* encodes complete pathways that are needed for carbohydrate catabolism, making it possible that more substrates besides amino acids are used for nutrition by the bacteria. In this study a novel growth medium was designed and used to investigate the metabolism of glycerol and inositol by *L. pneumophila*. Previous studies of the transcriptome of *L. pneumophila* growing inside macrophages revealed that the expression of glycerol kinase (*lpg1414*) and glycerol-3-phosphate dehydrogenase (*glpD*) was highly upregulated compared to extracellular growing bacteria (Faucher *et al.*, 2011). In line with this study, we found that glycerol did not enhance extracellular growth of *L. pneumophila*. However, glycerol did promote intracellular growth in *Acanthamoeba castellanii* and macrophages in a *glpD*-dependent manner, and a *glpD* deletion mutant had a severe growth disadvantage compared to wild-type bacteria. Isotopologue profiling experiments with [U-$^{13}C_3$]glycerol, [U-$^{13}C_6$]glucose or [U-$^{13}C_3$]serine as precursors revealed that all three carbon sources were metabolized by *L. pneumophila*. Glycerol and glucose were mainly used to synthesize mannose and histidine, which proved that gluconeogenesis and the PPP are active in *L. pneumophila*, while serine was mainly used in the glycolytic pathway and the TCA cycle for energy generation. This work revealed that *L. pneumophila* employs a bipartite metabolism, where serine is used for energy generation, while glucose and glycerol are exclusively used for anabolic purposes. This metabolic concept seems also to apply for intracellularly growing *L. pneumophila* and other intracellular pathogens.

Furthermore, the genome of *L. pneumophila* harbors a cluster of genes with homologies to genes implicated in inositol metabolism in other prokaryotes. These genes were also shown to be upregulated upon infection of macrophages (Faucher *et al.*, 2011). In this work, the first protein of this cluster, Lpg1653, was identified as inositol transporter, as it enabled *L. pneumophila* to transport ^{14}C-inositol. The transporter was termed IolT, according to inositol transporters in other bacteria. Similar to glycerol, inositol did not enhance extracellular growth in different media, but promoted intracellular growth of *L. pneumophila* in *A. castellanii* and murine macrophages, and therefore might also be used as an intracellular carbon source. Interestingly, the expression of

iolT was regulated by RpoS, a central regulator of differentiation and virulence genes of *L. pneumophila*.

Taken together, the work outlined in this thesis expanded the understanding of *L. pneumophila* metabolism and proved that the bacteria can metabolize glycerol and inositol. The concept of a bipartite metabolism that was shown here might be important to understand the intimate relations and interactions between intracellular pathogens and their host cells. These insights might in consequence help to find new therapies for *L. pneumophila* and other intracellular pathogens.

Zusammenfassung

Legionella pneumophila ist ein Gram-negatives, opportunistisches Pathogen, welches natürlicherweise Amöben in der freien Natur parasitiert, aber auch in der Lage ist, Alveolarmakrophagen zu infizieren und dadurch eine schwere und potentiell tödliche Pneumonie, die sogenannte Legionärskrankheit, auslösen kann. *L. pneumophila* ist ein obligat aerobes Bakterium, das Aminosäuren als bevorzugte Kohlenstoff- und Energiequelle nutzt. Es ist allerdings möglich, dass weitere Substrate neben Aminosäuren den Bakterien als Nahrungsgrundlage dienen, da im Genom der Legionellen offenbar komplette Stoffwechselwege für den Kohlenhydratmetabolismus kodiert sind.

In dieser Arbeit wurde ein neuartiges Wachstumsmedium für Legionellen entwickelt und dazu benutzt, den Glyzerin- und Inositolstoffwechsel von *L. pneumophila* zu untersuchen. Vorgängige Transkriptomstudien von Legionellen, die intrazellulär in Makrophagen wuchsen, zeigten, dass verglichen mit extrazellulär wachsenden Bakterien, die Expression der Glyzerinkinase (*lpg1414*) und der Glyzerin-3-Phosphat Dehydrogenase (*glpD*), stark hochreguliert war (Faucher *et al.*, 2011). Damit übereinstimmend zeigten wir in der vorliegenden Studie, dass Glyzerin keinen Einfluss auf das extrazelluläre Wachstum von *L. pneumophila* hat, jedoch das intrazelluläre Wachstum in *Acanthamoeba castellanii* und Makrophagen fördert. Dies war abhängig von GlpD, und eine *glpD* Deletionsmutante hatte einen schweren Wachstumsnachteil im direkten Vergleich mit Wildtypbakterien. Isotopologisches Profiling mit [U-$^{13}C_3$]Glyzerin, [U-$^{13}C_6$]Glukose oder [U-$^{13}C_3$]Serin als Ausgangssubstanzen zeigte, dass *L. pneumophila* alle drei Substrate verstoffwechseln kann. Glyzerin und Glukose wurden dazu benutzt, Mannose und Histidin zu synthetisieren, wodurch bewiesen wurde, dass die Glukoneogenese und der Pentosephosphatweg in *L. pneumophila* ablaufen. Serin anderseits wurde in der Glykolyse und im TCA-Zyklus verwendet, um Energie zu gewinnen. Es konnte dadurch gezeigt werden, dass Legionellen einen zweigeteilten Stoffwechsel betreiben, in dem Serin zur Energiegewinnung und Glukose sowie Glyzerin ausschließlich zu anabolen Zwecken verwendet werden. Dieses Stoffwechselkonzept scheint auch auf intrazellulär wachsende Legionellen und andere intrazelluläre Pathogene anwendbar zu sein.

Das Genom von Legionellen enthält eine Gruppe an Genen, die große Homologien zu Genen zeigen, welche in anderen Prokaryoten mit dem Stoffwechsel von Inositol assoziiert sind. Transkriptomstudien zeigten, dass die Expression dieses Clusters in Makrophagen hochreguliert war (Faucher *et al.*, 2011). In der vorliegenden Arbeit wurde das erste Protein dieses Clusters,

Lpg1653, als Inositoltransporter identifiziert, da es *L. pneumophila* erlaubte ^{14}C-Inositol zu transportieren. In Anlehnung an die Namensgebung in anderen Bakterien wurde das Protein IolT genannt. Ähnlich wie Glyzerin, hatte Inositol keinen Einfluss auf das extrazelluläre Wachstum von *L. pneumophila*, verbesserte aber wiederum das intrazelluläre Wachstum in *A. castellanii* und Makrophagen. Inositol könnte deshalb als intrazelluläre Kohlenstoff- und Energiequelle verwendet werden. Interessanterweise wurde die Expression von *iolT* durch RpoS gesteuert, einem der zentralen Regulatoren der Genexpression in *L. pneumophila*.

Zusammenfassend lässt sich sagen, dass die vorliegende Arbeit das Verständnis des Stoffwechsels von *L. pneumophila* erweitert und nachweist, dass die Bakterien Glyzerin und Inositol verstoffwechseln können. Das Konzept eines zweigeteilten Metabolismus trägt zu einem verbesserten Verständnis der Beziehungen zwischen intrazellulären Pathogenen und ihren Wirtszellen bei. Diese Einsichten könnten nützlich sein, um neue Therapien gegen *L. pneumophila* und andere intrazelluläre Pathogene zu finden.

„Je mehr man kennt, desto mehr man weiß,

erkennt man: alles dreht im Kreis."

Johann Wolfgang von Goethe

1. Introduction

1.1 *Legionella pneumophila*

1.1.1 Discovery, Epidemiology and Ecology

Legionella pneumophila is a flagellated, rod-shaped obligate aerobe bacterium belonging to the family of *Legionellaceae* within the γ-proteobacteria (Brenner *et al.*, 1979). *L. pneumophila* is furthermore the causative agent of Legionnaires' disease, a severe and atypical pneumonia with a relatively high mortality rate of 15%. *L. pneumophila* was first isolated in 1943 from guinea pigs and described as "Rickettsia-like" (Tatlock, 1944). Another strain was isolated in 1953 from soil samples, showing the ability to infect free-living amoeba (Drozanski, 1956). These strains were subsequently classified as members of the genus *Legionella* in 1996 (Hookey *et al.*, 1996). The bacterium gained first attention as a human pathogen at a convention of the American Legion in 1976, where over 180 people were infected and developed symptoms of pneumonia. 29 people died in consequence of the infection. The disease was termed Legionnaires' disease in accordance to this outbreak, and the soon identified bacterium causing the outbreak was named *Legionella pneumophila* (Fraser *et al.*, 1977; McDade *et al.*, 1977). Following the identification of the bacterium, also other unsolved outbreaks of respiratory illness could be traced back to *L. pneumophila* showing the epidemiological relevance of this bacterium (Thacker *et al.*, 1978). Patients infected with *L. pneumophila* do not necessarily develop pneumonia but might only suffer from the milder flu-like form of Legionnaires' disease termed Pontiac fever (Glick *et al.*, 1978) or might not show any symptoms at all (Boshuizen *et al.*, 2001). There are more than 50 *Legionella* species described today. *L. pneumophila* and *L. longbeachae* are responsible for most of the clinical cases, although more than half of all described species can be associated with human disease (Newton *et al.*, 2010; Hilbi *et al.*, 2011a). Several genome sequences are available including the sequences of *L. pneumophila* and *L. longbeachae* (Chien *et al.*, 2004; Cazalet *et al.*, 2010).

Infection with *Legionella* spp. normally occurs via the inhalation of contaminated aerosols. Man-made artificial water sources like household water systems, water towers, air conditioners and also whirlpools are common reservoirs for the bacteria (Fields, 1996; Nguyen *et al.*, 2006). Of special interest in the epidemiology of *L. pneumophila* are nosocomial infections. The main problem here is that the bacteria impact high risk groups – elderly, ill or immunocompromised

persons – and are frequently underdiagnosed, as manifestations are often non-specific and require specialized testing (Sabria and Yu, 2002). With further urbanization, demographic changes and the rising number of people suffering from autoimmune disorders or immune deficiencies, the impact of Legionellosis on the population will further rise.

The bacteria are naturally found as parasites in free-living protozoa (Rowbotham, 1980) and associated with complex aquatic biofilms formed by species such as *Pseudomonas aeruginosa* or *Klebsiella pneumoniae* (Murga *et al.*, 2001; Mampel *et al.*, 2006; Abdel-Nour *et al.*, 2013). Protozoan predators like amoeba are also part of these communities and feed on bacteria residing within these biofilms (Abdel-Nour *et al.*, 2013) (Figure 1.1 A). *L. pneumophila* is able to infect and replicate within a broad range of natural occurring hosts including *Acanthamoeba castellanii* (Holden *et al.*, 1984), *Hartmannella vermiformis* (Fields *et al.*, 1993) or *Dictyostelium discoideum* (Hägele *et al.*, 2000; Solomon and Isberg, 2000). Furthermore, *L. pneumophila* can infect and replicate in human epithelial cells and alveolar macrophages, which were identified as the bacterial targets in human disease (Nash *et al.*, 1984). Notably, there is no indication that *L. pneumophila* can be transmitted from person to person, showing that humans are an evolutionary dead end for the pathogen (Ensminger *et al.*, 2012).

The processes involved in bacterial survival within naturally occurring protozoa or macrophages are very similar and seem to be evolutionarily conserved as a result of the selection for virulence factors that support growth within a wide range of host cells (Brüggemann *et al.*, 2006; Hoffmann *et al.*, 2014b). Although it is believed that *L. pneumophila* is not able to replicate independently of a host cell in natural water sources (Declerck, 2010), the bacteria can persist in many extracellular niches. The optimal conditions for *L. pneumophila* are at 35°C with neutral or slightly acidic pH (Fields *et al.*, 2002). Nevertheless, *Legionellaceae* have been isolated from physically challenging habitats such as extremely acidic environments (Sheehan *et al.*, 2005; Hao *et al.*, 2010), Antarctic freshwater lakes (Carvalho *et al.*, 2008) and from water sources with temperatures over 60°C. Although, under such high temperatures the bacteria are only able to survive in association with thermotolerant amoeba (Taylor *et al.*, 2009).

1.1.2 Life Cycle and Developmental Forms of *Legionella pneumophila*

As described earlier, *L. pneumophila* can exist in extracellular niches as part of biofilm communities but can also replicate intracellularly within a great number of eukaryotic hosts. Early studies showed that *L. pneumophila* bacteria do alternate between at least two

morphologically distinct forms, differing in motility, shape and energy-rich polymers (Rowbotham, 1986). Based on these observations a model for the *L. pneumophila* life cycle was proposed that consists of two phases: replication and transmission. The bacteria do alternate between a transmissive and a replicative form in response to environmental and metabolic stimuli (Molofsky and Swanson, 2004). While the transmissive form is motile, resistant to environmental stresses like UV light, heat, osmotic pressure, nutrient limitation and is also infectious, the replicative form lacks all these traits, but is able to replicate intracellularly (Rowbotham, 1986; Molofsky and Swanson, 2004; Brüggemann *et al.*, 2006). In its simplest form the life cycle is therefore biphasic (Figure 1.1 A): transmissive bacteria are taken up by a host cell and establish an intracellular niche that provides protection from lysosomal degradation (see section 1.1.3 for details). Availability of nutrients and other favourable factors then lead to the repression of transmissive traits and activate replicative traits that allow the bacteria to multiply intracellularly. When nutrients become limiting, a regulatory cascade leads to the downregulation of replicative traits and the bacteria switch back to the transmissive form (Molofsky and Swanson, 2004). At this point the bacteria also exhibit pore-forming activity that allows lysis and escape from the spent host cell (Alli *et al.*, 2000). As the developmental state of *L. pneumophila* determines successful intracellular replication, the switch between transmission and replication has to be strictly regulated. Key players to facilitate this switch are, among others, the global regulator CsrA (Molofsky and Swanson, 2003), the second messenger guanosine 3´,5´-bispyrophosphate (ppGpp) (Dalebroux *et al.*, 2010), the stringent response enzymes RelA and SpoT (Dalebroux *et al.*, 2009), the alternative sigma factor RpoS (Hales and Shuman, 1999b) and several two component systems, all of which will be described in detail in section 1.2.4.

Favourable for *in vitro* studies is the fact that the biphasic life cycle of *L. pneumophila* can be modelled in broth cultures, where the bacteria switch between an exponential phase form (EPF), resembling the replicative form *in vivo*, and a stationary phase form (SPF), resembling the transmissive form *in vivo*, which is motile and virulent (Molofsky and Swanson, 2004; Robertson *et al.*, 2014). Indeed, many features of *L. pneumophila*, like regulation through nutrients, virulence and motility, are mimicked in the broth model (Molofsky and Swanson, 2004) (Figure 1.1 B), while others, like the requirement of an acidic pH for successful intracellular replication in macrophages (Sturgill-Koszycki and Swanson, 2000), are not. This cycle presumably not only happens in artificial culture media, but allegedly resembles growth in biofilm communities, where *L. pneumophila* could feed on dead microorganisms (Temmerman *et al.*, 2006) or

metabolise nutrients released by other bacteria (Wadowsky and Yee, 1985; Tison, 1987) (Figure 1.1 A).

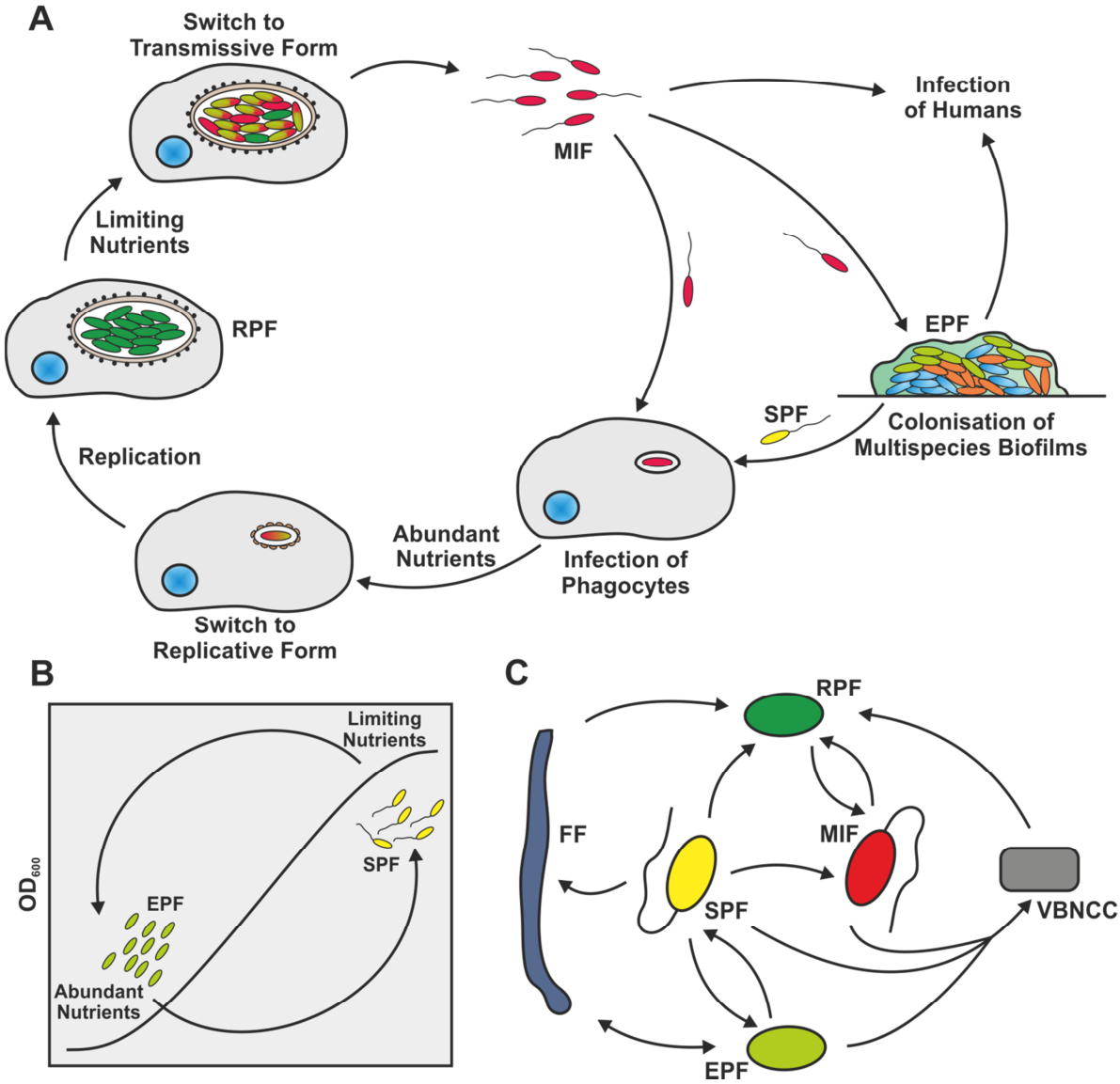

Figure 1.1: The life cycle and developmental forms of *L. pneumophila*. Infectious *L. pneumphila* (**MIF**) are taken up by amoeba or other phagocytes and establish a replication-permissive compartment. Availability of nutrients triggers the switch to the replicative phase form (**RPF**) and bacteria divide intracellularly. When nutrients become limiting, the bacteria switch back to the transmissive form, and virulent and motile bacteria leave the spent host cell. *L. pneumophila* also colonizes multispecies biofilms, where the bacteria alter between an exponential phase form (**EPF**) and a stationary phase form (**SPF**) that is infective. When contaminated aerosols are inhaled by humans, the bacteria can infect human alveolar macrophages, causing a severe pneumonia (**A**) (adapted from (Molofsky and Swanson, 2004)). The switch between replicative and transmissive form in response to nutrients can be modelled in broth, which is believed to resemble growth in biofilms in nature (**B**). The developmental forms of *L. pneumophila* are interconnected by a complex network. In addition to forms that resemble *in vivo* phenomena (**RPF**, **MIF**) and forms that resemble *in vitro* phenomena (**EPF**, **SPF**), bacteria can develop into a filamentous form (**FF**), especially in response to stress and into a spore like form (**VBNCC**) that can persist in water environments, both of which are virulent against eukaryotic cells (**C**) (adapted from (Robertson *et al.*, 2014)).

Besides the two previously described EPFs and SPFs, more developmental forms of *L. pneumophila* have been found to date, all of which might be interconnected by a complex network (Al-Bana *et al.*, 2014; Robertson *et al.*, 2014). These other forms include mature infectious forms (MIFs), replicative phase forms (RPFs), filamentous forms (FFs), viable but not culturable cells (VBNCCs) and many intermediate forms (Figure 1.1 C). MIFs and RPFs are the *in vivo* counterparts of exponential phase (EPFs) and stationary phase (SPFs) bacteria, respectively, in broth. While EPFs and RPFs are at least morphologically indifferent from one another (Faulkner and Garduno, 2002), MIFs differ from SPFs in the regard that MIFs are metabolically inert and loaded with inclusions of poly-3-hydroxybutyrate, more resistant to antibiotics and in general more infectious than SPFs (Garduno *et al.*, 2002). MIFs represent the transmissive form of *L. pneumophila* that exits a spent host cell after intracellular growth, while SPFs are most likely produced within biofilms in nature (Robertson *et al.*, 2014) (Figure 1.1 A). The filamentous form of *L. pneumophila* is believed to develop in response to stress, like nutrient limitation (Warren and Miller, 1979), high temperature (Piao *et al.*, 2006) or UV light (Charpentier *et al.*, 2011). FFs are found in broth, in water environments and infected lung tissue (Prashar *et al.*, 2012) and are known to be infectious to macrophages (Prashar *et al.*, 2013). Interestingly, as a consequence of FF uptake by macrophages, the filamentous cells undergo fragmentation and differentiate into RPFs (Prashar *et al.*, 2013), a process also occurring *in vitro* in broth cultures where they differentiate into EPFs (Piao *et al.*, 2006). At last, *L. pneumophila* exhibits a VBNCC state that is developed extracellularly in response to stress (Al-Bana *et al.*, 2014) and can be produced from EPFs, SPFs and MIFs (Ohno *et al.*, 2003; Al-Bana *et al.*, 2014). VBNCCs can persist in water environments for extended periods of time, until they receive a signal to wake up (Robertson *et al.*, 2014). That signal can be the uptake of VBNCCs by amoeba, upon which the bacteria differentiate into replicating cells and grow inside the host cell (Al-Bana *et al.*, 2014). The fact that these different forms of *L. pneumophila* can develop from each other and also the observation that *L. pneumophila* reaches different developmental endpoints in different host cells (Garduno *et al.*, 2002; Abdelhady and Garduno, 2013), shows that the *Legionella* life cycle could indeed be more complex than the biphasic model would suggest (Figure 1.1 C).

1.1.3 Virulence and Intracellular Replication

The key component for *L. pneumophila* virulence and successful intracellular replication is the Icm/Dot (intracellular multiplication/defective organelle trafficking) type IV secretion system (T4SS) consisting of 27 proteins forming two subcomplexes that span the inner and outer bacterial membrane (Burns, 2003; Segal *et al.*, 2005; Vincent *et al.*, 2006). The main function of the Icm/Dot T4SS is the delivery of a vast number of effector proteins into the host cell, of which currently over 300 have been identified. The high number of these effectors often results in functional redundancy and is considered to be due to host diversity (O'Connor *et al.*, 2011). Many of these effectors target central cell processes, which ultimately leads to the formation of an ER-derived compartment called the *Legionella*-containing vacuole (LCV) that enables *L. pneumophila* to replicate intracellularly (Shin and Roy, 2008). Eukaryotic pathways targeted by these effectors include endocytic, secretory or retrograde trafficking, and the bacteria exploit small GTPases, phosphoinositide lipids as well as ubiquitinylation and apoptosis factors to form the LCV (Hubber and Roy, 2010; Rolando and Buchrieser, 2012; Haneburger and Hilbi, 2013; Hoffmann *et al.*, 2014a; Horenkamp *et al.*, 2014; Finsel and Hilbi, 2015). The importance of the Icm/Dot secretion system is reflected by the fact that mutants lacking the T4SS are not able to replicate intracellularly, but are rapidly degraded in the lysosomal pathway upon uptake by the host cell (Roy and Isberg, 1997; Zink *et al.*, 2002).

In addition to the Icm/Dot T4SS *L. pneumophila* also possesses the Lvh T4SS, a type V secretion system, an Lss type I secretion system and an Lsp type II secretion system (T2SS). The T2SS was shown to be essential for intracellular growth of *L. pneumophila* in amoeba and macrophages (Hales and Shuman, 1999a; Liles *et al.*, 1999). Interestingly, the possibility that the Lvh T4SS protein VirD4 is able to complement the virulence defect of a *dotA* mutant was reported (Bandyopadhyay *et al.*, 2007; Bandyopadhyay *et al.*, 2013), indicating a role of this additional T4SS for the virulence of *L. pneumophila*. Functionality of the Lss type I secretion system was also recently shown, since an *lssBD* mutant, lacking the inner membrane transporter LssB and the periplasmic membrane fusion protein LssD, showed strongly attenuated virulence (Fuche *et al.*, 2015).

The intracellular replication cycle of *L. pneumophila* basically consists of four phases: adhesion and uptake, formation of the LCV, replication and finally exit from the spent host cell (Figure 1.2). The Icm/Dot T4SS is important for bacterial uptake as *L. pneumophila* can actively stimulate macropinocytotic internalisation, and Icm/Dot mutants are less efficiently taken up by

amoeba and HL-60 cells (Hilbi *et al.*, 2001; Watarai *et al.*, 2001; Lu and Clarke, 2005). *L. pneumophila* RtxA is a homologue of LapA of *Pseudomonas putita*, which was shown to act as adhesin involved in cell-cell interactions (Cirillo *et al.*, 2001). RtxA is also a substrate of the *L. pneumophila* Lss T1SS, and mutants lacking RtxA or the T1SS were defective for entry into host cells (Cirillo *et al.*, 2001; Fuche *et al.*, 2015).

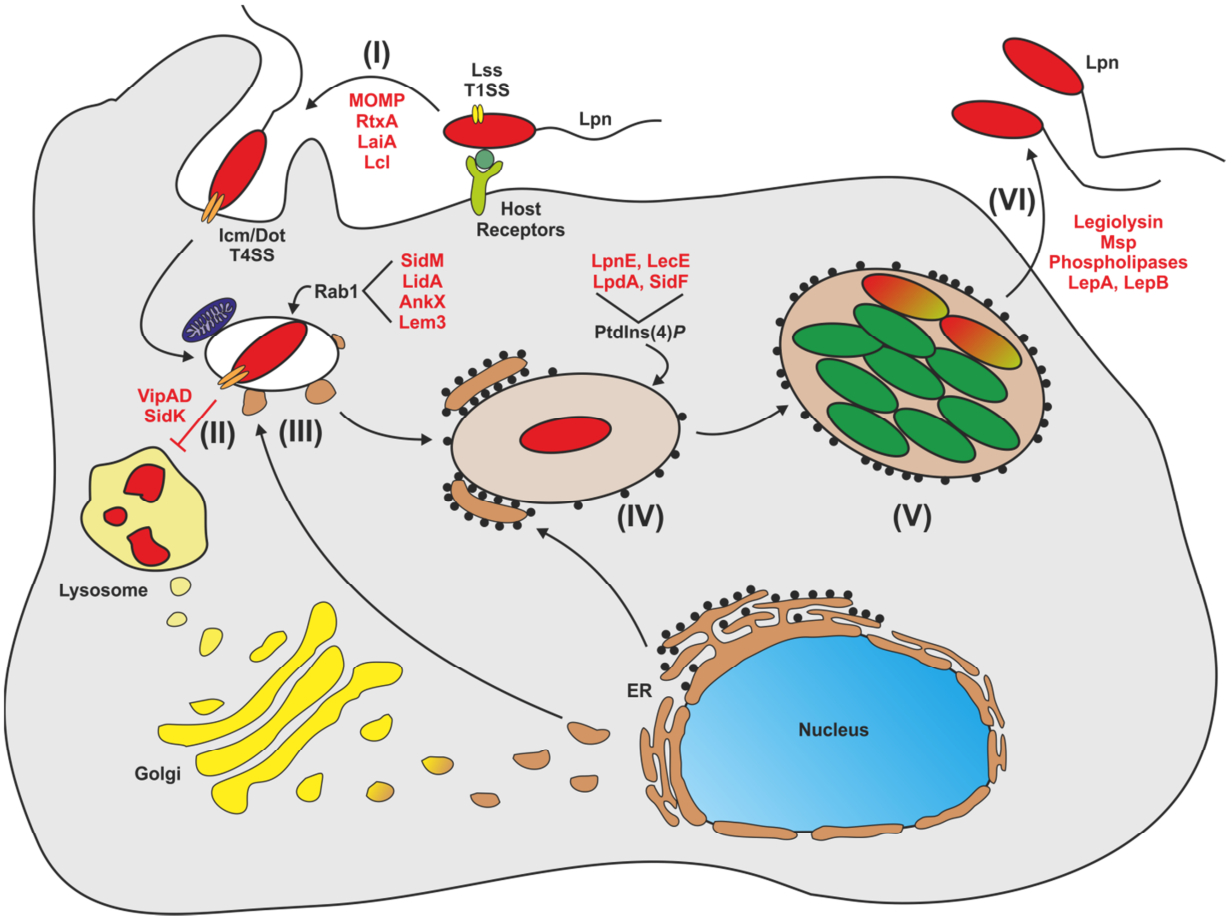

Figure 1.2: Intracellular infection and replication cycle of *L. pneumophila*. The bacteria bind to host cell receptors and promote their uptake by type-I and type-IV secreted effectors (**I**). After uptake, fusion with lysosomes is blocked (**II**), the LCV merges with ER exit site vesicles, and mitochondria associate with the LCV (**III**). Ribosomes and membranes derived from the rough ER fuse with the LCV and PtdIns(4)*P* specifically accumulates in the LCV membrane (**IV**). The bacteria switch to their replicative form (**green**) and replicate in a compartment resembling the ER (**V**). At the end of their replication cycle the bacteria switch back to the transmissive form (**red**) and escape from their spent host cell (**VI**). *L. pneumophila* virulence factors and effector proteins are shown in red, see text for details.

Other factors relevant for effective adhesion of *L. pneumophila* to host cells include the integrin analogue LaiA (Chang *et al.*, 2005), the collagen-like protein Lcl binding to the extracellular matrix of host cells and supporting infection in *A. castellanii* (Duncan *et al.*, 2011; Abdel-Nour *et*

al., 2014) and the major outer membrane proteins (MOMPs) that are targets of the complement system of the innate immune system, facilitating binding to macrophage complement receptors (Bellinger-Kawahara and Horwitz, 1990).

Host cell factors and effector proteins involved in formation of the LCV are numerous and will not all be discussed in detail here (for a review refer to Finsel and Hilbi, 2015). Interference with the endocytic pathway and therefore evasion of phagolysosome fusion is the essential first step after uptake. The effector protein VipA was found to directly bind actin and polymerize microfilaments, thus altering organelle trafficking in the host cell (Franco *et al.*, 2012). VipD is a phospholipase that binds the activated GTPase Rab5 on endosomes eventually blocking their fusion with the LCV (Gaspar and Machner, 2014). Also, acidification of the phagosome is inhibited by *L. pneumophila*. The Icm/Dot substrate SidK prevents acidification of the LCV by targeting the host cell V-ATPase subunit VatA and therefore inhibiting ATP hydrolysis, proton translocation and ultimately vacuole acidification (Xu *et al.*, 2010). Communication with the endocytic pathway is not completely inhibited as marker of late endosomes/lysosomes were found to be present on the LCV (Urwyler *et al.*, 2009).

Simultaneously with the avoidance of lysosomal degradation, *L. pneumophila* modifies the LCV to a compartment that resembles the endoplasmic reticulum (ER) and allows replication of the bacteria (Tilney *et al.*, 2001). As an initial step, mitochondria and smooth ER exit site vesicles associate with the LCV shortly after uptake into the host cell (Horwitz, 1983; Kagan and Roy, 2002). However, the frequency of mitochondria and smooth vesicles decreases again after a few hours and ribosomes associate with the LCV (Horwitz, 1983; Swanson and Isberg, 1995). Also, ER-specific enzymes, like glucose-6-phosphatase, or the chaperone calnexin (Kagan and Roy, 2002; Robinson and Roy, 2006) localize with the LCV, suggesting that the ribosomes do not originate from the cytoplasm but rather from the fusion of rough ER membranes with the LCV (Robinson and Roy, 2006).

An important factor for LCV formation is the exploitation of the host cell phosphoinositide (PI) metabolism. PI lipids control the identity of organelles and vesicle trafficking pathways by providing binding sites for host regulatory proteins (Di Paolo and De Camilli, 2006). *L. pneumophila* perturbs and exploits the PI pattern of the LCV to anchor Icm/Dot substrates to the vacuole (Hilbi *et al.*, 2011b). Several Icm/Dot effectors might actively enrich the levels of PtdIns(4)*P* in the LCV membrane, including LpnE, which is associated with the PtdIns(4,5)P_2-5-phosphatase OCRL and the PtdIns-4-kinase-IIIβ (PI4KIIIβ) of the host cell (Weber *et al.*, 2009).

The effectors LecE and LpdA recruit protein kinases to the LCV, which subsequently might bind PI4KIIIβ (Viner *et al.*, 2012). Finally, the effector SidF, a phosphatidylinositol polyphosphate-3-phosphatase might directly enrich PtdIns(4*)P* in the LCV membrane (Hsu *et al.*, 2012). Another effector, LppA, was shown to hydrolyse phosphorylated PIs *in vitro*, although it did not affect the PI pattern of LCVs *in vivo*. LppA acts as a hexakisphosphate inositol (phytate) phosphatase and might promote intracellular replication by removing the iron chelator phytate from the intracellular milieu (Weber *et al.*, 2014a). Overall, PtdIns(4)*P* represents an LCV lipid marker that steadily accumulates on the membrane of the pathogen compartment in the course of 2 h post infection (Weber *et al.*, 2014b), acts as binding target for several Icm/Dot effectors and may also contribute to the acquisition of ER vesicles (Weber *et al.*, 2006).

GTPases are key regulators of vesicle transport that interact with downstream proteins and can switch between an inactive, GDP-bound, and an active, GTP-bound, conformation (Stenmark, 2009). *L. pneumophila* also exploits small GTPases; an especially well-studied example is Rab1. Rab1 is localized to the LCV by several Icm/Dot substrates (Kagan *et al.*, 2004). The effector protein SidM, also known as DrrA, binds to PtdIns(4)*P* and acts as a guanine nucleotide exchange factor that activates Rab1 (Brombacher *et al.*, 2009; Schoebel *et al.*, 2009). LidA interacts with activated Rab1, keeping the GTPase in its active state (Neunuebel *et al.*, 2012). Another Icm/Dot substrate, AnkX, was also shown to interact with Rab1. The effector can modify inactive Rab1 by phosphocholination, which leads to the incorporation of Rab1 into the LCV membrane, where it is dephosphocholinated by Lem3 (Mukherjee *et al.*, 2011; Goody *et al.*, 2012). Activated Rab1 ultimately leads to the recruitment of ER exit site vesicles (Kagan *et al.*, 2004; Arasaki *et al.*, 2012). Besides Rab1 also other small GTPases of the Rab family have been found in the proteome of purified LCVs from macrophages and also seem to be involved in formation of the replication-permissive compartment (Hoffmann *et al.*, 2014a). Interaction with ER exit site vesicles is believed to prepare the LCV for interaction with rough ER vesicles, converting the LCV from a plasma membrane-derived vacuole to a compartment resembling the host ER, where the bacteria will replicate with a doubling time of about 2 h (Tilney *et al.*, 2001). Other studies report that ER recruitment is not essential to trigger replication of *L. pneumophila*, as mutants defective for the acquisition of ER membranes were not impaired in initial replication (Weber *et al.*, 2014b).

For replication, the bacteria undergo a major transcriptional switch that alters the expression of almost half the genome, representing the replicative phase (Brüggemann *et al.*, 2006; Faucher *et*

al., 2011). Nutrients are the key factor for this switch. Especially, genes involved in amino acid synthesis as well as uptake (Wieland *et al.*, 2005; Faucher *et al.*, 2011) and iron uptake systems (Cianciotto, 2007) are upregulated and important to initiate replication. Also, the availability and uptake of nucleosides was shown to be important for intracellular replication (Fonseca *et al.*, 2014).

The limitation of nutrients is also a key factor for switching back to the transmissive phase at the end of the intracellular replication cycle of *L. pneumophila*, where virulence traits such as the flagellar machinery and Icm/Dot substrates are upregulated (Brüggemann *et al.*, 2006). The intracellular replication cycle is closed by lysis of the host and the release of flagellated, virulent *L. pneumophila* cells to the environment. Several processes have been described that might facilitate host cell lysis. Haemolytic proteins such as legiolysin (Rdest *et al.*, 1991) and Msp (Szeto and Shuman, 1990; Poras *et al.*, 2012) as well as several phospholipases (Bender *et al.*, 2009; Lang *et al.*, 2012; Aurass *et al.*, 2013) might actively lyse the host cell. The effector proteins LepA and LepB have been shown to promote the nonlytic egress from protozoa (Chen *et al.*, 2004), and also induction of apoptosis in macrophages (Müller *et al.*, 1996) has been discussed as possible exit strategy of *L. pneumophila*.

1.2 Metabolism of *Legionella pneumophila*

1.2.1 Amino Acid Metabolism

L. pneumphila is an obligate aerobe organism (Warren and Miller, 1979). Early studies of the metabolism of *L. pneumophila* showed the preference for amino acids as main source of carbon and energy (Pine *et al.*, 1979; George *et al.*, 1980; Ristroph *et al.*, 1981; Tesh and Miller, 1981; Tesh *et al.*, 1983). Cell growth in chemically defined media revealed auxotrophies for the amino acids arginine, cysteine, isoleucine, leucine, methionine, threonine and valine (George *et al.*, 1980; Tesh and Miller, 1981). Serine as well as threonine were discussed as major carbon sources for *L. pneumophila* (George *et al.*, 1980). This need for amino acids is reflected in the genome of *L. pneumophila,* where around 12 classes of ATP binding cassette transporters, amino acid permeases and proteases are found, which are likely implicated in amino acid uptake (Cazalet *et al.*, 2004; Chien *et al.*, 2004). The absence of biosynthetic pathways for certain amino acids in the genomes of several *L. pneumophila* strains (Cazalet *et al.*, 2004; Chien *et al.*, 2004; Steinert *et al.*, 2007; D'Auria *et al.*, 2010; Schroeder *et al.*, 2010) and *L. longbeachae* (Cazalet *et al.*, 2010; Kozak *et al.*, 2010) corresponds to amino acid auxotrophies that were investigated and confirmed in defined media. *L. pneumophila* employs several well-studied systems to cope with these auxotrophies, some of which will be described below.

L. pneumphila lacks enzymes that allow the synthesis of arginine from glutamate, as the conversion of glutamate to N-acetylglutamate did not occur in chemically defined medium and activity of the N-acetylglutamate synthetase was not measurable in bacterial cell extracts (Tesh and Miller, 1983). Supplementation of the medium with arginine or ornithine and citrulline, which are precursors of arginine emerging in later steps of the synthesis from glutamate, restored growth (Tesh and Miller, 1983). Availability of arginine might also function as a regulatory switch during intracellular growth, as mutants lacking the arginine repressor ArgR were unable to replicate inside host cells (Hovel-Miner *et al.*, 2010). Several genes, including parts of the Icm/Dot T4SS and translocated effector proteins, were differentially expressed in *argR* deletion mutants compared to wild-type bacteria (Hovel-Miner *et al.*, 2010). In addition, the eukaryotic arginine transporter SLC7A2 was upregulated in infected macrophages (Portier *et al.*, 2015) and is supposedly incorporated in the membrane of LCVs (Hoffmann *et al.*, 2014a), which might facilitate the uptake of arginine into the LCV.

The common solid growth medium for *L. pneumophila* is buffered charcoal yeast extract (BCYE) agar, supplemented with L-cysteine and ferric pyrophosphate (Feeley *et al.*, 1979).

L. pneumophila lacks the key cysteine biosynthetic enzymes serine acetyltransferase and cysteine synthase, and no activity of these enzymes was detected in cell extracts (Chien *et al.*, 2004; Ewann and Hoffman, 2006). *L. pneumophila* is therefore auxotroph for cysteine and employs at least two energy-dependent cysteine transporters. Interestingly, the amount of cysteine in BCYE agar is much higher than what is required for bacterial growth, as the main part of cysteine is rapidly oxidized to cystine within the medium, which *L. pneumophila* cannot utilize (Ewann and Hoffman, 2006).

The phagosomal transporter A (PhtA) was identified as an important factor for replication and differentiation in macrophages (Sauer *et al.*, 2005) (Figure 1.3). PhtA is a threonine transporter, and mutants lacking *phtA* did not grow in chemically defined medium, but were rescued by excess tryptone or dipeptides containing threonine, indicating that PhtA is not the only threonine uptake system in *L. pneumophila* (Sauer *et al.*, 2005). Like ArgR mutants (Hovel-Miner *et al.*, 2010), bacteria lacking the PhtA transporter were not able to replicate inside macrophages, due to their inability to differentiate from the transmissive to the replicative state. Also PhtJ, a valine transporter, was needed for successful differentiation and replication within macrophages (Sauer *et al.*, 2005; Chen *et al.*, 2008), proving the importance of these transporters and the availability of certain amino acids as key regulators for *L. pneumphila* differentiation. The Pht-family also includes the *phtC-phtD* locus (Chen *et al.*, 2008). Expression of *phtC* in *E. coli* strains, lacking all known nucleoside transporters, allowed these strains to transport pyrimidines. PhtC and PhtD function as thymidine transporters required for replication in macrophages and survival of thymidine deprivation (Fonseca *et al.*, 2014). A recent study also demonstrated the importance of the shikimate pathway for intracellular replication in macrophages. The aromatic amino acids phenylalanine, tryptophan and tyrosine are synthesized by this pathway, and mutants lacking key enzymes were not able to replicate within macrophages, which are auxotrophic for tryptophan and phenylalanine. The mutant bacteria were still able to replicate normally in *Acanthamoeba* spp., which synthesize aromatic amino acids, indicating that aromatic amino acids can also be taken up from the host cell (Jones *et al.*, 2015).

Already in early studies, serine was discussed as a major carbon source for *L. pneumophila* (George *et al.*, 1980). Using the method of isotopologue profiling, which is based on the incorporation of precursors labelled with stable isotopes into key metabolites such as protein-derived amino acids or storage compounds (Zamboni *et al.*, 2009), it was shown that serine is indeed taken up in large amounts by *L. pneumophila* growing in broth (Eylert *et al.*, 2010). Serine

was incorporated directly into proteins, but also used to synthesize other amino acids and poly-3-hydroxybutyrate (Eylert *et al.*, 2010), proving its role as an effective and important carbon and energy source for *L. pneumophila.*

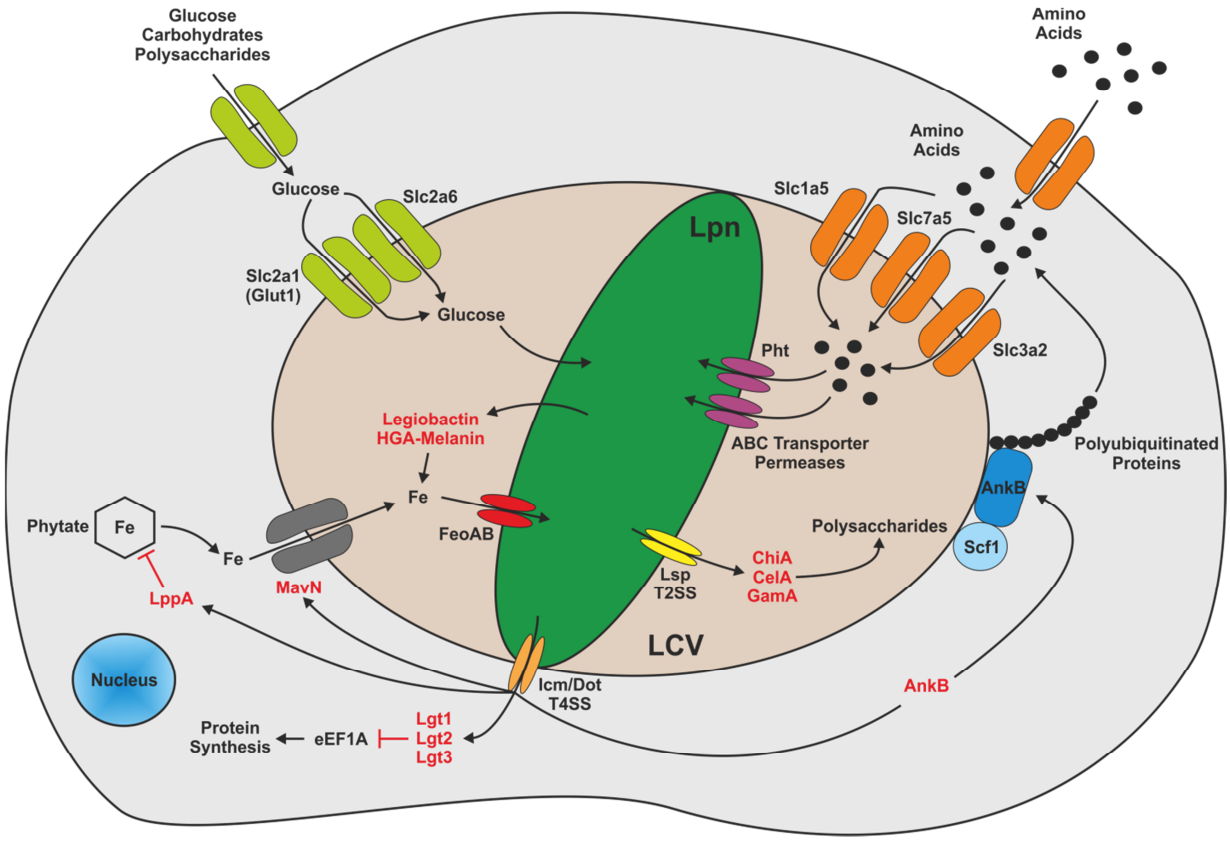

Figure 1.3: Intracellular metabolism of *L. pneumophila*. Several host cell glucose transporters (**green**) and amino acid transporters (**orange**) are presumably located in the LCV membrane and facilitate nutrient uptake. The genome of *L. pneumophila* encodes several ABC transporters, permeases and transporters belonging to the phagosomal transporter (**Pht**) family (**violet**), which are used to take up amino acids. Iron reducing factors (**HGA-melanin**) and the siderophore **legiobactin**, together with iron transporters like **FeoAB**, are used to take up iron. Several type-II secreted effector proteins, like the chitinase **ChiA**, the endoglucanase **CelA** or the glycoamylase **GamA**, degrade polysaccharides. Finally, Icm/Dot effector proteins are used to interfere with host protein synthesis (**Lgt1**, **Lgt2**, **Lgt3**), build up a pool of free amino acids by employing the host proteasome (**AnkB**), act as a phytase (**LppA**) or function as an iron transporter in the LCV membrane (**MavN**). *L. pneumophila* effector proteins are shown in red.
Abbreviations: **Lpn**, *Legionella pneumophila*; **LCV**, *Legionella*-containing vacuole; **eEF1A**, eukaryotic elongation factor 1A; **SCF1**, ubiquitin ligase complex.

To take up and utilize amino acids, *L. pneumophila* also relies on and exploits host metabolic functions. The eukaryotic neutral amino acid transporter SLC1A5 is upregulated in macrophages infected with *L. pneumophila*, and depletion of this transporter by RNA interference or competitive pharmacological inhibition abolishes intracellular growth of the bacteria (Wieland *et al.*, 2005). Proteomic analysis of LCVs isolated from infected macrophages suggested that

SLC1A5, together with other amino acid transporters (SLC7A5, SLC3A2) and glucose transporters (SLC2A1, SLC2A6), is located in the LCV membrane and might facilitate uptake of nutrients into the LCV lumen (Hoffmann *et al.*, 2014a) (Figure 1.3).

Also, Icm/Dot-translocated effector proteins are used to modulate host cell metabolic functions (Figure 1.3). Several effectors were identified that directly block host protein translation. Among them are the glycosyltransferases Lgt1, Lgt2 and Lgt3, that modify eukaryotic elongation factor eEF1A, which leads to the inhibition of protein synthesis and ultimately to the death of the host cell (Belyi *et al.*, 2011). Another effector, AnkB, leads to increased levels of free amino acids in the host cell by utilizing the host cell proteasome (Price *et al.*, 2011). AnkB can interact with the host SCF1 ubiquitin ligase complex via an F-box domain, harbours two ANK domains, which mediate protein-protein interactions in eukaryotes, and a CaaX motive that is modified by farnesylation (Price *et al.*, 2009; Ensminger and Isberg, 2010; Lomma *et al.*, 2010; Price *et al.*, 2010; Price and Kwaik, 2010). AnkB is farnesylated inside the host cell and thus anchored to the LCV membrane. Polyubiquitinated proteins generated by AnkB are then degraded by the host proteasome generating a pool of free amino acids (Price *et al.*, 2011).

1.2.2 Carbohydrate Metabolism

The genomes of *L. pneumophila* (Cazalet *et al.*, 2004; Chien *et al.*, 2004; Steinert *et al.*, 2007; D'Auria *et al.*, 2010; Schroeder *et al.*, 2010) and *L. longbeachae* (Cazalet *et al.*, 2010; Kozak *et al.*, 2010) encode a complete glycolytic pathway, the Entner-Doudoroff (ED) pathway, as well as an incomplete pentose phosphate pathway (PPP), suggesting the capacity of carbohydrate catabolism. Indeed, studies with ^{14}C-radio-labelled substrates indicated that glucose, pyruvate, glycerol and acetate are metabolized by *L. pneumophila* (Pine *et al.*, 1979; Weiss *et al.*, 1980; Tesh *et al.*, 1983). Glucose was not rapidly metabolized upon growth in a chemically defined medium, and the catabolic route of glucose metabolism remained unclear, although it was suggested that glucose metabolism occurs via the pentose phosphate pathway and the ED pathway, rather than by the glycolytic pathway (Weiss *et al.*, 1980; Tesh *et al.*, 1983). Consistent with the notion that glycerol might be metabolized by *L. pneumophila*, it was observed that genes required for glycerol catabolism were highly upregulated during infection of macrophages, compared to growth in broth (Faucher *et al.*, 2011). Also, genes associated with the ED pathway, as well as a glucokinase and a glucoamylase were upregulated upon growth in *A. castellanii* (Brüggemann *et al.*, 2006). The ED pathway was meanwhile identified as the route of glucose

catabolism *in L. pneumophila*. Isotopologue profiling revealed the uptake of ^{13}C-labelled glucose by *L. pneumophila* growing in broth, and carbon flow from glucose into downstream metabolites was dependent on the *zwf* gene encoding the glucose-6-phosphate dehydrogenase (Eylert *et al.*, 2010). Mutants lacking other genes of the ED pathway were also not able to metabolize glucose anymore and were defective for intracellular growth in *Acanthamoeba culbertsoni* and mammalian cells (Harada *et al.*, 2010). Besides the simple sugar glucose, also polysaccharides are metabolized by *L. pneumophila*, and several T2SS substrates involved in the degradation of complex carbohydrates have been described. The bacteria secrete a chitinase (ChiA), an endoglucanase (CelA) that was indeed found to degrade cellulose, as well as a glucoamylase (GamA) that degraded carboxymethyl cellulose, glycogen and starch (DebRoy *et al.*, 2006; Pearce and Cianciotto, 2009; Herrmann *et al.*, 2011) (Figure 1.3). The T2SS is essential for intracellular growth of *L. pneumophila* in amoebae and macrophages (Hales and Shuman, 1999a; Liles *et al.*, 1999) and although neither ChiA, CelA nor GamA were required for successful intracellular growth, complex carbohydrates might well be used as a source of carbon and energy inside a host. At last, the polyamine spermidine moderately favoured intracellular replication of *L. pneumophila* (Nasrallah *et al.*, 2011) and mutants lacking PotD, a spermidine-binding protein, were not able to initiate intracellular replication (Nasrallah *et al.*, 2014), suggesting the possibility of polyamines as carbon source or regulatory components.

1.2.3 Micronutrient Requirements

Microorganisms require metals as cofactors for many enzymes. *L. pneumophila* is no exception, especially as it is an intracellular pathogen and limitation of certain metal ions is a key component of host immunity against pathogens. Iron, calcium, magnesium and zinc were shown to stimulate extracellular growth of *L. pneumophila* in chemically defined medium (Reeves *et al.*, 1981), and accordingly, iron is an essential component of *L. pneumophila* standard growth media (Feeley *et al.*, 1979) and chemically defined media (Reeves *et al.*, 1981; Ristroph *et al.*, 1981). Calcium and magnesium might also be important for biofilm formation, as they were shown to enhance the adherence of *L. pneumophila* to surfaces (Koubar *et al.*, 2013).

Iron is essential for most, if not all bacteria, as it is cofactor for many enzymes within prosthetic groups like heme or iron-sulfur clusters (Ratledge and Dover, 2000; Andreini *et al.*, 2008). Iron exists in two forms, ferrous (Fe^{2+}) and ferric (Fe^{3+}) iron, the latter of which is insoluble. The form predominantly present is mostly dependent on the pH and availability of oxygen (Williams, 2012;

Becker and Skaar, 2014). Iron limitation is also an important factor of immunity against pathogens, and reduction of available ferric iron is important to restrict bacterial growth. In eukaryotic cells, iron is either bound in prosthetic groups or complexed in the storage protein ferritin to make it unavailable for intracellular pathogens and to prevent iron toxicity (Recalcati *et al.*, 2008).

L. pneumophila grown under iron-limiting conditions showed reduced virulence and was unable to survive within host cells (James *et al.*, 1995). Also, host cells treated with iron chelators did not support growth of *L. pneumophila* anymore (Gebran *et al.*, 1994; Byrd and Horwitz, 2000), highlighting the importance of iron availability for *L. pneumophila in vivo*. Not surprisingly, the bacteria therefore employ many systems for iron reduction, complexation and transport. *L. pneumophila* has at least two ferric reductases devoted to the assimilation of iron within the bacterial cell (Johnson *et al.*, 1991; Poch and Johnson, 1993) and at least one secreted factor necessary for iron reduction, called homogentisic acid (HGA) (Chatfield and Cianciotto, 2007). HGA is produced in the course of phenylalanine and tyrosine metabolism of *L. pneumophila* and can be polymerized to HGA-melanin (Flydal *et al.*, 2012). HGA and HGA-melanin can restore bacterial growth under iron-limiting conditions, enhance the uptake of iron and release ferrous iron from transferrin and ferritin, two major iron chelators of mammalian cells (Zheng *et al.*, 2013). Also Icm/Dot substrates might facilitate the acquisition of iron (Figure 1.3). LppA is a type IV-secreted phytase of *L. pneumophila* that might help to counteract iron-limiting conditions within natural hosts of *L. pneumophila*, such as *D. discoideum* and *A. castellanii*. Phytate is not only an abundant phosphor storage compound ,but also a strong iron chelator that could be used to limit intracellular iron for pathogens (Weber *et al.*, 2014a). Another type IV-secreted effector protein, called MavN, was identified as a mediator of iron acquisition in *L. pneumophila*. MavN is inserted into the LCV membrane, binds iron and presumably is an iron transporter, facilitating the uptake of iron into the LCV (Isaac *et al.*, 2015). MavN, also known as IroT, was found to be highly induced under iron-limiting conditions and mutants lacking the transporter were highly impaired for growth in *A. castellanii* and human macrophages (Portier *et al.*, 2015). (Figure 1.3).

L. pneumophila produces the high-affinity iron siderophore legiobactin, used to chelate and transport iron (Liles *et al.*, 2000; Starkenburg *et al.*, 2004). Important for synthesis and function of legiobactin are at least four proteins: The cytoplasmic LbtA, which is a siderophore synthetase, LbtB the inner-membrane efflux transporter of legiobactin, LbtU located in the outer-membrane and acting as receptor of ferrilegiobactin and finally LbtC which is predicted to be the transporter

of ferrilegiobactin located in the inner membrane (Allard *et al.*, 2006; Chatfield *et al.*, 2011; Chatfield *et al.*, 2012). The structure of legiobactin was recently elucidated and constitutes a polycarboxylate identical in structure to rhizoferrin, a siderophore made by funghi (Burnside *et al.*, 2015). Legiobactin is also very important *in vivo*, as *lbtA* mutant strains of *L. pneumophila* showed reduced ability to infect lungs of A/J mice (Allard *et al.*, 2009). Other iron transporters have also been identified in *L. pneumophila*, including the FeoAB system, a homologue of the well-characterized *E. coli* system, which is also important for *in vivo* growth (Robey and Cianciotto, 2002) (Figure 1.3).

1.2.4 Regulation of Differentiation and Virulence by Metabolism

The availability of certain nutrients is essential for the switch between transmission and replication, as seen for example for *L. pneumophila* mutants lacking the arginine transcriptional regulator ArgR or the threonine transporter PhtA, which are no longer able to switch from the transmissive to the replicative form inside host cells (see section 1.2.1). As amino acids represent the main carbon and energy source for *L. pneumophila*, it is not surprising that they are also main regulatory factors for the phenotypic switch (Byrne and Swanson, 1998; Sauer *et al.*, 2005). The network of factors that mediate this switch is complex and will be dissected in the following paragraphs (Figure 1.4).

The second messenger guanosine-3`,5`-bispyrophosphate (ppGpp) is central for the switch between the replicative/non-motile to the virulent/motile form of *L. pneumophila* in response to amino acid or nutrient limitation (Hammer and Swanson, 1999; Dalebroux *et al.*, 2010). ppGpp is the trigger of the so-called stringent response and alters the preference of RNA polymerase for certain sigma factors, thus facilitating changes in gene expression profiles (Dalebroux *et al.*, 2010). The alarmone ppGpp is synthesized by two enzymes in *L. pneumophila*, RelA and SpoT. RelA is a ribosome-associated enzyme that is activated when uncharged tRNAs accumulate at the ribosome as a consequence of low amino acid levels in the cell (Dalebroux *et al.*, 2009). SpoT interacts with the acyl-carrier protein ACP and is activated by the reduction in the rate of fatty acid biosynthesis or increased levels of short chain fatty acids (Edwards *et al.*, 2009). The enzyme therefore synthesizes ppGpp, not in response to low amino acid levels but by monitoring fatty acid biosynthesis. Furthermore, during exponential growth SpoT acts as a ppGpp-hydrolase, which keeps the concentration of the alarmone within the cell low to assure that transmissive traits are not expressed during replication (Dalebroux *et al.*, 2009).

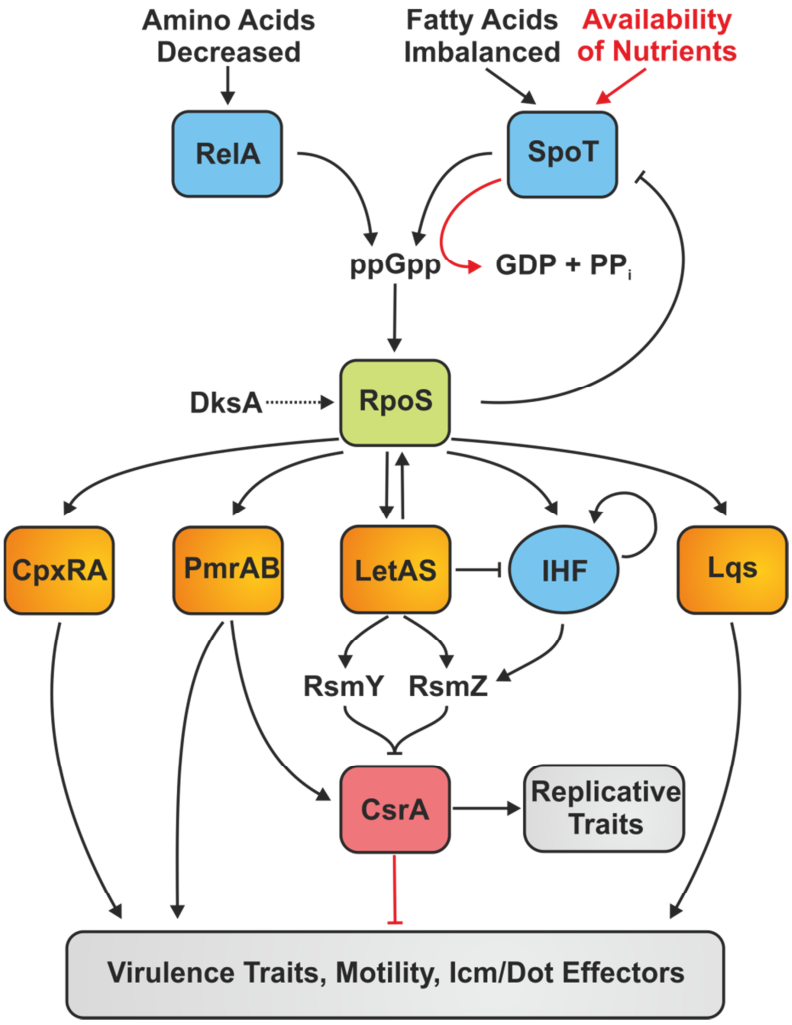

Figure 1.4: Regulation of replicative and transmissive traits by *L. pneumophila*. As long as nutrients are available, the global regulator CsrA prevents the expression of virulence traits and promotes expression of replicative traits. Also, SpoT hydrolases ppGpp, blocking the downstream regulatory cascade. When nutrients become limiting, ppGpp is synthesized by RelA and SpoT, leading to production of the alternative sigma factor RpoS, which in turn regulates the two component systems CpxRA, PmrAB, LetAS, the integration host factor IHF and the *Legionella* quorum sensing system Lqs. CsrA is silenced by the two regulatory RNAs RsmY and RsmZ, which leads to the swtich from replicative to transmissive phase and to the expression of virulence traits, motility and Icm/Dot effector proteins (model adapted from (Manske and Hilbi, 2014)).

High levels of ppGpp lead to an increase in stability and activity of RpoS, the alternative sigma factor σ^{38}/σ^{S} that acts as the central regulator of differentiation in the *L. pneumophila* life-cycle (Bachman and Swanson, 2001; Zusman *et al.*, 2002). RpoS regulates 208 genes in exponential and 571 genes in stationary growth phase including genes required for central metabolism (Hovel-Miner *et al.*, 2009), small regulatory RNAs, two component systems, ArgR and the quorum sensing regulator LqsR (see below). An *rpoS* mutant of *L. pneumophila* does grow normally in broth, but is not able to replicate intracellularly in amoeba (Hales and Shuman,

1999b), highlighting its role as a central regulator of the *L. pneumophila* life-cycle. Another factor that might be important for activation of RpoS is the ribosome-binding protein DksA. Deletion mutants lacking *dksA* still produce ppGpp but are defective for flagellar gene expression and macrophage cytotoxicity, and DksA is believed to cooperate with ppGpp (Dalebroux *et al.*, 2010). However, it is not known whether DksA also influences the expression of RpoS as shown for *E. coli*, where deletion of *dksA* results in significantly lower levels of RpoS, even when ppGpp is produced (Brown *et al.*, 2002). Furthermore, there also exists a regulatory feedback loop between RpoS and SpoT that negatively regulates expression of *spoT* to prevent hydrolytic degradation of ppGpp. Mutants of *rpoS* showed decreased levels of ppGpp and failed to induce the stringent response upon growth in water (Trigui *et al.*, 2015).

Downstream of RpoS are at least three two component systems and one quorum sensing system influencing the virulence of *L. pneumophila*. The CpxRA system, consisting of the response regulator CpxR and the cognate sensor kinase CpxA, was the first two component system in *L. pneumophila* that was shown to regulate an *icm/dot* virulence gene (Gal-Mor and Segal, 2003a). Until now several other *icm/dot* genes and several Icm/Dot-translocated substrates have been found to be regulated by CpxR, establishing CpxRA as an important regulator of the Icm/Dot T4SS (Altman and Segal, 2008). Also, the PmrAB two component system is known to be regulated by RpoS (Hovel-Miner *et al.*, 2009) and acts itself as a regulator of several Icm/Dot substrates (Zusman *et al.*, 2007). Mutants lacking *pmrAB* are severely attenuated for intracellular growth and differentially express a large number of genes, including metabolic genes and the flagellar machine (Al-Khodor *et al.*, 2009). Furthermore, *pmrAB* mutants exhibit significantly lower levels of another important regulatory protein, the “carbon storage regulator” CsrA (Al-Khodor *et al.*, 2009), and the two component system is therefore integral part of the link between metabolism and virulence (see below). The third two component system is the LetAS system that acts as an inducer of transmissive traits (Hammer *et al.*, 2002). In mutants lacking the response regulator LetA several *icm/dot* genes were differentially expressed (Gal-Mor and Segal, 2003b), and also expression of *rpoS* was reduced, demonstrating that RpoS is also influenced by downstream two component systems (Lynch *et al.*, 2003). The induction of transmissive traits is facilitated in an indirect fashion, as LetAS acts as a repressor of CsrA (Sahr *et al.*, 2009) by inducing the expression of two small RNAs, *rsmY* and *rsmZ* (Rasis and Segal, 2009). CsrA is a RNA-binding protein that blocks translation of transcripts encoding stationary phase and transmissive trait proteins in exponentially growing cells, and therefore, acts as an antagonist for

the stringent response. When *rsmY* and *rsmZ* are expressed, they bind to CsrA, allowing translation of previously blocked transmissive traits, promoting the switch from replicative to transmissive phase (Rasis and Segal, 2009). At last, the *Legionella* quorum sensing (*lqs*) cluster is also involved in this regulatory cascade. The Lqs system consists of the autoinducer synthase LqsA producing the α-hydroxyketone signaling molecule LAI-1 (Spirig *et al.*, 2008), the sensor kinases LqsS (Tiaden *et al.*, 2010) and LqsT (Kessler *et al.*, 2013) and the response regulator LqsR (Tiaden *et al.*, 2007). Expression of *lqsR* is growth-phase dependent and regulated by RpoS and to a lesser extent by LetA (Tiaden *et al.*, 2007). In a mutant lacking the whole *lqs* cluster, genes involved in protein production, amino acid and carbohydrate metabolism and other replicative traits were upregulated, whereas genes associated with transmissive traits were downregulated, suggesting that also Lqs acts as a regulator of the life-style switch (Tiaden *et al.*, 2008). Finally, the integration host factor (IHF) is a DNA-binding protein that is important for the differentiation of replicative *L. pneumophila* to transmissive bacteria (Morash *et al.*, 2009). Expression of IHF is positively regulated by RpoS, and IHF itself also auto-regulates its own expression (Zhao *et al.*, 2007). Regulation through IHF and the LetAS two component system is intertwined, as LetA negatively regulates IHF expression but IHF also cooperates with LetA to induce transcription of *rsmY* and *rsmZ* (Zhao *et al.*, 2007).

1.3 Central Carbon Metabolism, Amino Acid Biosynthesis and Inositol Metabolism

1.3.1 Central Carbon Metabolism and Amino Acid Biosynthesis

Central carbon metabolism describes the enzymatic reactions that degrade different nutrients to produce precursor molecules for biosynthesis pathways as well as for energy storage (Csete and Doyle, 2004). Central metabolism includes several metabolic pathways like the glycolytic pathway, the PPP and the tricarbolic acid (TCA) cycle (Donachie and Begg, 1970; Konopka, 1984). The glycolytic pathway converts glucose to two molecules pyruvate and delivers two molecules ATP; pyruvate then being fed into the TCA cycle, which again delivers ATP as well as NAD(P)H/H^+ and precursors for several biosynthesis pathways, including fatty acid biosynthesis. The PPP is central for the interconversion of glucose or fructose into C_4-, C_5- and C_7-sugars, which are important for many biosynthesis pathways like cell wall synthesis or purine metabolism. The pathway consists of an oxidative part that delivers NADPH/H^+ and a non-oxidative part that catalyzes the interconversion of carbohydrates, resulting in fructose-6-phosphate and glyceraldehyde-3-phosphate as intermediates of the glycolytic pathway. Some bacteria have an additional pathway, the ED pathway that can be used to metabolize glucose. Here, glucose is catabolized to the specific intermediate of the ED pathway, 2-keto-3-deoxy-6-phosphogluconate (KDPG) that is then cleaved to form glyceraldehyde-3-phosphate and pyruvate (Entner and Doudoroff, 1952). In absence of usable sugars, intermediates of the glycolytic pathway as well as glucose can be made in the gluconeogenic pathway that is closely related to the glycolytic pathway, but not its exact reversion (Anderson and Cooper, 1969). Another reason why these pathways are so central for metabolism is the fact that many nutrients besides glucose, enter these central pathways at some point of their catabolism, as for example seen for inositol (Kröger and Fuchs, 2009) or glycerol (Joseph *et al.*, 2008). *L. pneumophila* also possesses these central metabolic pathways, including the ED pathway, the glycolytic pathway, the TCA cycle and a PPP which, however, lacks the transaldolase as well as the 6-phosphogluconate dehydrogenase (Chien *et al.*, 2004).

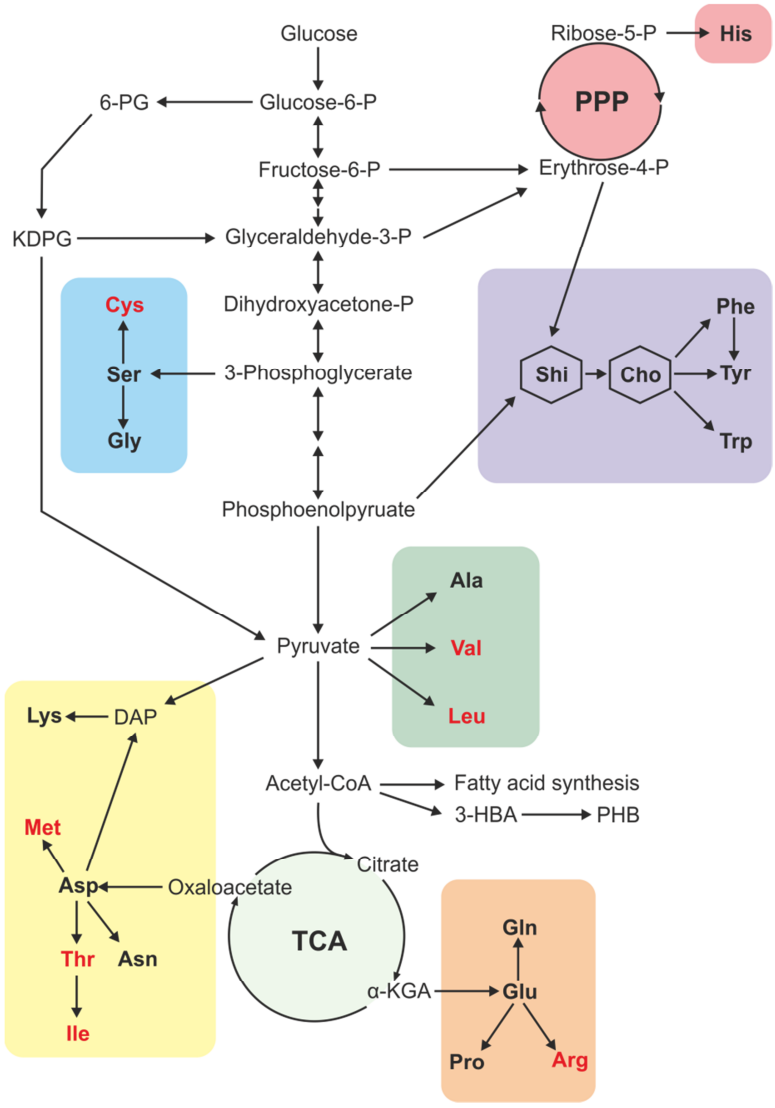

Figure 1.5: Central carbon metabolism and amino acid synthesis by *L. pneumophila*. The central carbon metabolism of *L. pneumophila* consists of the Entner-Doudoroff (**ED**) pathway, the glycolytic pathway, the citric acid cycle (**TCA**) and the pentose phosphate pathway (**PPP**) that delivers intermediates and precursors for biosynthesis of e.g. fatty acids or storage compounds (**3-HBA**, **PHB**). Amino acids are also synthesized from intermediates of this central metabolism and are grouped into five biosynthesis families: 3-phosphoglycerate group (**blue**), pyruvate group (**green**), α-ketoglutarate group (**orange**), oxaloacetate group (**yellow**) and aromatic group (**purple**). Histidin is derived from intermediates of the PPP (**red**). Amino acids are shown in 3-letter code and essential amino acids for *L. pneumophila* are shown in red.
Abbreviations: **6-PG**, 6-phosphogluconate; **KDPG**, 2-keto-3-desoxy-phosphogluconate; **Shi**, shikimate; **Cho**, chorismate; **DAP**, diaminopimelic acid; **α-KGA**, α-Ketoglutarate; **3-HBA**, 3-hydroxybutyrate; **PHB**, polyhydroxybutyrate.

Amino acids are the building blocks of proteins and can be synthesized in several fundamentally different biosynthesis pathways, which will not be described in detail here. Nevertheless, all amino acids share one common feature. The backbone of amino acids is derived from different

intermediates of central carbon metabolism, and amino acids can be, depending on their initial precursor, grouped into five biosynthetic families: the 3-phsophoglycerate group comprising Ser, Cys and Gly; the pyruvate group containing Ala, Val and Leu; the α-ketoglutarate group with Glu, Gln, Pro and Ala; the oxaloacetate group comprising Asp, Asn, Thr, Ile, Met and Lys (as intermediate between pyruvate and oxaloacetate group) and finally the group of aromatic amino acids with Phe, Tyr and Trp that are derived from the shikimate pathway. Histidine is a special case, as it is standing aside of the other amino acids and is being derived from the PPP with ribose-5-phosphate as precursor (Figure 1.5). Not all organisms can synthesize all amino acids themselves, which defines the term essential amino acid. This means that these amino acids have to be taken up from the environment, making the organism auxotrophic for a given amino acid. *L. pneumophila* is auxotrophic for several amino acids, including Cys, Val, Leu, Met, Thr, Ile and Arg (see section 1.2.1) (Figure 1.5).

1.3.2 Inositol Metabolism

Inositol is a polyol, a sugar alcohol, which exists in nine stereoisomeric forms, with *myo*-inositol (MI) being the most abundant stereoisomer (Turner *et al.*, 2002). MI is abundant in soil and aquatic environments and normally exists in various states of phosphorylation with between one and six phosphate groups (Turner *et al.*, 2002; Mao *et al.*, 2009). The most common form of inositol in soil is the six-fold phosphorylated inositol hexakisphosphate, also known as phytic acid or phytate, which serves as a major phosphorus storage compound in plants and seeds (Sakai *et al.*, 2015) and makes up for more than 80% of organic phosphate in soil (Turner *et al.*, 2002). Phytate is highly negatively charged and can complex a variety of ions, including iron, and is also highly resistant to enzymatic hydrolysis, which might account for its accumulation in the ground (Turner *et al.*, 2002). A special group of enzymes, so-called phytases, are used to catalyze the stepwise removal of phosphate from phytate (Lei *et al.*, 2013), a crucial step for recycling organic phosphate. MI is furthermore the key component of phosphoinositide lipids that are important for the definition of subcellular compartments and membrane dynamics in eukaryotic cells (Haneburger and Hilbi, 2013). The biosynthesis of inositol proceeds through a conserved metabolic pathway in eukaryotes and archaea that consists of two steps, the isomerization of glucose-6-phosphate to inositol-3-phosphate by inositol synthase enzymes, followed by the dephosphorylation to inositol by inositol monophosphatases (Fischbach *et al.*, 2006). Moreover, environmental inositol or inositol-3-phosphate can be used directly for the synthesis of phytate or

its differentially phosphorylated intermediates, e.g. by *D. discoideum* (Stephens and Irvine, 1990).

As MI is naturally occurring in many ecosystems, it is not surprising that also a large number of microorganisms can grow on MI as sole source of carbon and energy, including *Bacillus subtilis* (Yoshida *et al.*, 2008), *Lactobacillus casei (Yebra et al., 2007)* or *Salmonella enterica* (Kröger and Fuchs, 2009). The molecular genetics of bacterial MI catabolism have been best described in *B. subtilis*, where two operons, *iolABCDEFGHIJ* and *iolRS* as well as the gene *iolT*, are responsible for MI degradation (Yoshida *et al.*, 2008). IolT and IolF have been identified as inositol transporters belonging to the major facilitator superfamily, but only IolT is essential, as mutants lacking *iolT* did show major growth defects (Yoshida *et al.*, 2002). Another central component of inositol catabolism is the regulator protein IolR that, in the absence of inositol, binds to the operator sites within the *iol* operon (Yoshida *et al.*, 1999). In the presence of MI, 2-deoxy-5-keto-D-gluconic-acid-6-phosphate, a central intermediate of MI catabolism, antagonizes the repressor IolR and allows expression of the *iol* operon (Yoshida *et al.*, 1997). The degradation of MI then finally results in dihydroxyacetone phosphate, acetyl-CoA and CO_2 as end products (Kröger and Fuchs, 2009) (Figure 1.6). Although the genetic organization of *iol* genes can differ from organism to organism and must not necessarily consist of all genes found in the genome of *B. subtilis*, the principal reactions seem to be conserved and consist of seven stepwise reactions (Yoshida *et al.*, 2008; Kröger and Fuchs, 2009).

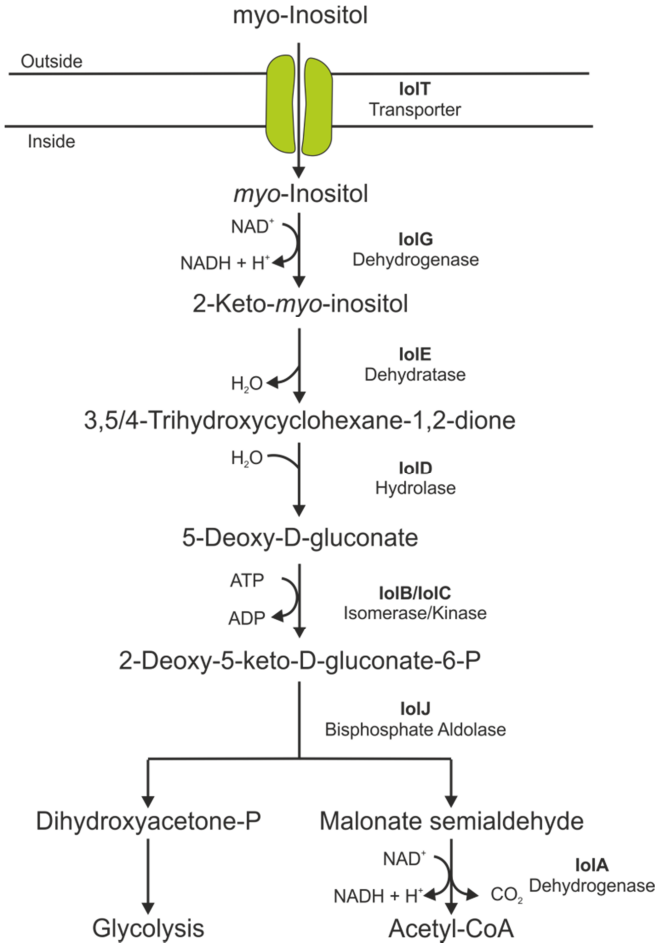

Figure 1.6: Schematic pathway of *myo*-inositol catabolism. *Myo*-inositol is transported across the cell membrane by IolT and then degraded in several enzymatic steps to dihydroxyacetone phosphate and acetyl-CoA which then enter the central carbon metabolism (model adapted from (Yoshida *et al.*, 2008; Kröger and Fuchs, 2009)).

After import of MI by IolT, the first reaction is the dehydrogenation of MI to 2-keto-*myo*-inositol catalyzed by IolG, followed by dehydration to 3,5/4-trihydroxycyclohexane, catalyzed by IolE. The next reaction, catalyzed by the hydrolase IolD, breaks the hexane ring, yielding 5-deoxy-glucuronic acid, which is then isomerized by IolB to 2-deoxy-5-keto-D-gluconic acid. The next step is the ATP-dependent phosphorylation of the compound, catalyzed by IolC, which yields the central intermediate 2-deoxy-5-keto-D-gluconic-acid-6-phosphate, subsequently cleaved by the bisphosphate aldolase IolJ into dihydroxyacetone phosphate and malonate semialdehyde. The latter is then finally converted into acetyl-CoA in a dehydrogenase reaction catalyzed by IolA, which releases CO_2. The endproducts dihydroxyacetone phosphate and acetyl-CoA can then be channeled into the central metabolism (Figure 1.6).

1.4 Aims of the Thesis

L. pneumophila colonizes a variety of extra- and intracellular niches and is therefore exposed to a plethora of different possible carbon and energy sources. Nevertheless, not much is known about the nutrition of *L. pneumophila*. The bacteria are auxotrophic for different amino acids, and serine is believed to be the major carbon substrate of *L. pneumophila* (George *et al.*, 1980). Yet, the genome of *L. pneumophila* reveals the possibility of other nutrients as carbon sources, and complete pathways for carbohydrate metabolism are encoded (Chien *et al.*, 2004). Indeed, glucose was found to be metabolized by *L. pneumophila* (Eylert *et al.*, 2010), but the full metabolic capacities of *L. pneumophila* are still not explored.

The aim of this thesis was the investigation of the glycerol and inositol metabolism of *L. pneumophila* and its relevance for extra- and intracellular growth of the bacteria. This was done by constructing defined deletion mutants lacking the glycerol-3-phosphate dehydrogenase GlpD, the putative inositol transporter Lpg1653 or the putative inositol dehydrogenase IolG and by performing different extra- and intracellular growth assays with these mutants. To this end, a newly developed *Legionella* minimal growth medium was employed. Using the technique of isotopologue profiling the metabolism of glycerol was investigated in detail and also compared with the catabolism of the known carbon substrates glucose and serine. The putative inositol degradation cluster *lpg1653-lpg1649* of *L. pneumophila* was identified by sequence homology, and the function of Lpg1653 as inositol transporter was tested using radioactive ^{14}C-inositol. The expression of *iolT* and the whole inositol degradation cluster was to be tested with an unstable GFP variant in different *L. pneumophila* deletion mutants. Finally, the accessibility of the LCV for carbon substrates was investigated using a fluorescent glucose analogue.

2. Materials and Methods

2.1 Materials

2.1.1 Laboratory Equipment

Item	Model	Manufacturer
Amix-Viewer software	v 3.9.22	Bruker Biospin (Rheinstetten)
Autoclave	Sterimaquet	Maquet (Rastatt)
Autoclave	Varioklav classic	H+P (Oberschleissheim)
Cell homogenizer		Isobiotec (Heidelberg)
Benchtop centrifuge	5417R	Eppendorf (Hamburg)
Centrifuge	3-30K	Sigma-Aldrich (St. Louis)
Centrifuge	5810	Eppendorf (Hamburg)
Centrifuge	Heraeus Megafuge 40R	Thermo Fisher Scientific (Waltham)
CO_2 incubator	Heraeus HeraCell 240	Thermo Fisher Scientific (Waltham)
Colony counter	Countermat flash	IUL (Barcelona)
Confocal microscope	TCS SP5	Leica (Mannheim)
Cryogenic freezer box	Mr. Frosty^{Tm} freezing container	Thermo Fisher Scientific (Waltham)
Culture microscope	Axiovert 25	Zeiss (Oberkochen)
Diaphragm vacuum pump	MZ 2C	Vacuubrand (Wertheim)
Electrophoresis chamber	Mini-Subcell GT	Bio-Rad (Munich)
Electroporation device	GenePulser Xcell	Bio-Rad (Munich)
Freeze-dryer	Alpha 2-4 LD plus	Christ (Osterrode)
Gas chromatograph / Mass spectrometer	QP2010 Plus	Shimadzu (Kyoto)
GC / MS analysis software	Lab Solution Software	Shimadzu (Kyoto)
Gel imaging system	GelDoc EQ	Bio-Rad (Munich)

Hot plate magnetic stirrer	RCT basic	IKA (Staufen)
Ice machine	AF30	Scotsman (Vernon Hills)
Incubation cabinet	Multitron Pro	Infors HT (Sulzemoos)
Incubation cabinet	Forma Orbital Shaker	Thermo Fisher Scientific (Waltham)
Incubator	BF 400	Binder (Tuttlingen)
Incubator	Heraeus BR6000	Thermo Fisher Scientific (Waltham)
Incubator	Heraeus Function Line	Thermo Fisher Scientific (Waltham)
Incubator	IPP400	Memmert (Schwabach)
Incubator	IPP500	Memmert (Schwabach)
Liquid scintilation and luminescence counter	Trilux 1450 Micro Beta	Perkin Elmer (Waltham)
Microplate reader	Fluostar Optima	BMG Labtech (Ortenberg)
Mixer	Vortex-Genie 2	IKA (Staufen)
NMR spectrometer	AVANCE-II 600	Bruker Biospin (Rheinstetten)
PCR cycler	T3	Biometra (Goettingen)
pH meter	Level 1	inoLab (Weilheim)
Pipettes	Pipetman	Gilson (Middleton)
Pipettor	Pipetus	Hirschmann (Eberstadt)
Power supply	PAC100	Bio-Rad (Munich)
Precision balance	BP61-S	Sartorius (Goettingen)
Precision balance	PG2002-S	Mettler-Toledo (Greifensee)
Ribolyser		Hybaid (Cambridge)
Spectrophotometer	Helios Epsilon	Thermo (Waltham)
Spectrophotometer	NanoDrop ND-1000	PeqLab (Erlangen)
Suspension mixer	CMV	Fröbel (Lindau)

Thermal mixer	Thermomixer comfort	Eppendorf (Hamburg)
UV-transilluminator		Bachofer (Reutlingen)
Water bath	Wasserbad 1005	GFL (Burgwedel)

Standard laboratory equipment was used in addition to the listed items.

2.1.2 Chemicals and Consumables

Item	Supplier
1 kb plus DNA ladder	Life Technologies (Grand Island)
1.5 mL reaction tubes	Eppendorf (Hamburg)
2-NBDG	Sigma-Aldrich (St. Louis)
4 mL scintillation vials	Perkin Elmer (Waltham)
5 mm glass tubes ST-500	Norell (Marion)
13 mL plastic tubes	Sarstedt (Nürnbrecht)
15 mL reaction tubes	Greiner (Frickenhausen)
50 mL reaction tubes	Greiner (Frickenhausen)
6-well plates	TPP (Trasadingen)
24-well plates	TPP (Trasadingen)
96-well plates	TPP (Trasadingen)
96-well plates black, clear bottom	Perkin Elmer (Waltham)
ACES	AppliChem (Darmstadt)
Acetonitrile	Sigma-Aldrich (St. Louis)
Activated charcoal powder	Fluka (Buchs)
Agar	BD Biosciences (Franklin Lakes)
Agarose	Biozym (Hessisch Oldendorf)
Amiloride hydrochloride hydrate	Sigma-Aldrich (St. Louis)
Bacteriological peptone	Oxoid (Wesel)
Bacto proteose peptone	BD Biosciences (Franklin Lakes)
Bacto yeast extract	BD Biosciences (Franklin Lakes)

BBL yeast extract	BD Biosciences (Franklin Lakes)
$CaCl_2$ x 2 H_20	Roth (Karlsruhe)
Cell culture flasks	TPP (Trasadingen)
Cellulose acetate membrane filter disks (pore size 0.2 µm)	Roth (Karlsruhe)
Cellulose nitrate membrane filter disks (pore size 0.45 µm)	Roth (Karlsruhe
Chloroquine diphosphate	Sigma-Aldrich (St. Louis)
Cryogenic freezing tubes	Thermo (Waltham)
Cuvettes	Brand GmbH (Wertheim)
Cytochalasin B	Sigma-Aldrich (St. Louis)
D_2O	Euriso-Top (St-Aubin)
D(+)-glucose monohydrate	Fluka (Buchs)
D(+)-glucose-6-phosphate sodium salt	Sigma Aldrich (St. Louis)
DMSO	Merck (Darmstadt)
DNA purification kit	Macherey-Nagel (Dueren)
dNTP mix	Thermo Fisher Scientific (Waltham)
DreamTaq green PCR master mix (2x)	Thermo Fisher Scientific (Waltham)
EcoLume scintillation cocktail	MP Biomedicals (Santa Ana)
EDTA (disodium salt)	Sigma-Aldrich (St. Louis)
EGTA	Roth (Karlsruhe)
Electroporation cuvette (2 – 4 mm gap)	Bio-Rad (Munich)
Ethanol	Roth (Karlsruhe)
FCS	Life Technologies (Grand Island)
Filtropur 0.2 µm filter units	Sarstedt (Nürnbrecht)
FeN_3O_9 x 9 H_2O	Sigma-Aldrich (St. Louis)
Fe-pyrophosphate hydrate ($Fe_4O_{21}P_6$)	Sigma-Aldrich (St. Louis)
Glycerol	Roth (Karlsruhe)
Glycine	MP Biomedicals (Eschwege)
HCl	Roth (Karlsruhe)

HEPES	Roth (Karlsruhe)
Inositol	Roth (Karlsruhe)
KH_2PO_4	Fluka (Buchs)
L-arginine	Merck (Darmstadt)
L-aspartate	Sigma-Aldrich (St. Louis)
LB agar Lennox	Invitrogen (Carlsbad)
LB broth base Lennox	Invitrogen (Carlsbad)
L-cysteine	Sigma-Aldrich (St. Louis)
L-glutamate	Sigma-Aldrich (St. Louis)
L-glutamine	Life Technologies (Grand Island)
L-histidine	Roth (Karlsruhe)
L-isoleucine	Merck (Darmstadt)
L-leucine	Roth (Karlsruhe)
L-lysine	Sigma-Aldrich (St. Louis)
L-methionine	Merck (Darmstadt)
LoFlo	ForMedium (Norfolk)
L-phenylalanine	Roth (Karlsruhe)
L-proline	Roth (Karlsruhe)
L-serine	Roth (Karlsruhe)
L-threonine	Roth (Karlsruhe)
L-tryptophane	Sigma-Aldrich (St. Louis)
L-tyrosine	AppliChem (Darmstadt)
Luer lock syringes	Hartenstein (Würzburg)
L-valine	Roth (Karlsruhe)
Methanol	Roth (Karlsruhe)
$MgCl_2$ x 6 H_20	Roth (Karlsruhe)
$MgSO_4$ x 7 H_20	Merck (Darmstadt)
Millex 0.2 µm filters	Milipore (Billerica)
N-methyl-N-[trimethylsilyl]-trifluoroacetamide	Sigma-Aldrich (St. Louis)

N-[tert-butyldimethyl-silyl]-N-methyl-trifluoroacetamide	Sigma-Aldrich (St. Louis)
NH_4Cl	Fluka (Buchs)
NaCl	Roth (Karlsruhe)
Na_2HPO_4	Fluka (Buchs)
NaOH	Roth (Karlsruhe)
PFA	Sigma-Aldrich (St. Louis)
Poly-L-lysine	Sigma-Aldrich (St. Louis)
Phusion polymerase	Thermo Fisher Scientific (Waltham)
Rapid flow filter units	Hartenstein (Würzburg)
Restriction enzymes	Thermo Fisher Scientific (Waltham)
RPMI 1640	Life Technologies (Grand Island)
Saponin	Sigma Aldrich (St. Louis)
Sodium citrate x 2 H_2O	Fluka (Buchs)
Sucrose	Roth (Karlsruhe)
T4 DNA ligase	New England Biolabs (Ipswich)
Tert-butyl-dimethyl-silylchlorid	Sigma-Aldrich (St. Louis)
Trimethylsilyl propanoic acid	Sigma-Aldrich (St. Louis)
Tryptone / peptone from casein	Roth (Karlsruhe)
[U-$^{13}C_6$]glucose	Sigma-Aldrich (St. Louis)
[U-$^{13}C_3$]glycerol	Sigma-Aldrich (St. Louis)
[U-$^{13}C_3$]serine	Sigma-Aldrich (St. Louis)
[U-$^{14}C_6$]inositol	American Radiolabeled Chemicals (St. Louis)
Vectashield mounting medium	Vector Laboratories (Cambridgeshire)
Whatman glass microfiber filter	GE Healthcare (Little Chalfont)
Yeast extract	BD Biosciences (Franklin Lakes)

Standard laboratory materials and reagents were used in addition to the listed items.

2.1.3 Media and Buffers

Deionised, distilled H_2O was used in all recipes and protocols.

2.1.3.1 *Legionella pneumophila*

Charcoal Yeast Extract (CYE) Agar (Feeley *et al.*, 1979)

Component	Amount/Litre	Supplier
ACES	10 g	AppliChem
Bacto yeast extract	10 g	BD Biosciences
Activated charcoal powder p.a. puriss	2 g	Fluka
Agar	15 g	BD Biosciences
L-cysteine	0.4 g in 10 ml H_2O	Sigma
FeN_3O_9 x 9 H_2O	0.25 g in 10 ml H_2O	Sigma
Antibiotic		
Chloramphenicol	5 mg	Roth
Kanamycin	10 mg	Roth

Dissolve ACES and yeast extract in 950 ml H_2O, adjust pH to 6.9 using 10 M KOH and then fill up to 1 l with H_2O. Weigh out charcoal and agar into a Schott bottle, followed by the ACES/yeast extract solution. Add a stirbar and autoclave the medium. After sterilisation, let the solution cool down to 50°C. Add filter-sterilized L-cysteine and then the $Fe(NO_3)_3$ solution (10 ml each per 1 l agar). This has to be done dropwise to prevent precipitation. Add antibiotic solutions as required. Distribute the homogenised mixture into standard petri dishes. Let the plates dry for 1 day at room temperature. Store at 4°C in the dark.

ACES Yeast Extract (AYE) Medium (Horwitz and Maxfield, 1984)

Component	Amount/Litre	Supplier
ACES	10 g	AppliChem
Bacto yeast extract	10 g	BD Biosciences
L-cysteine	0.4 g in 10 ml H_2O	Sigma
FeN_3O_9 x 9 H_2O	0.25 g in 10 ml H_2O	Sigma

Antibiotic		
Chloramphenicol	5 mg	Roth
Kanamycin	50 mg	Roth

Dissolve ACES and yeast extract in 950 ml H_2O. Dissolve L-cysteine and $Fe(NO_3)_3$ in 10 ml H_2O each separately. Now dropwise add the cysteine solution while stirring, followed by the iron solution. Adjust pH to 6.9 using 10 M KOH, then fill up to 1 l with H_2O. If necessary add antibiotics at the indicated concentrations. Filter the medium through a layer of 7 glass fiber filters and repeat the procedure once. At last, sterilise the medium using a 0.2 µm filter cartouche and store it at 4°C in the dark.

Chemically Defined Medium (CDM) adapted from (Ristroph *et al.*, 1981)

Component	**Amount/Litre**	**Supplier**
ACES	10 g	AppliChem
L-arginine	350 mg	Merck
L-cysteine	400 mg	Sigma
L-isoleucine	470 mg	Merck
L-leucine	640 mg	Roth
L-methionine	200 mg	Merck
L-threonine	330 mg	Roth
L-valine	480 mg	Roth
L-serine	650 mg	Roth
L-proline	115 mg	Roth
L-phenylalanine	350 mg	Roth
L-aspartate	510 mg	Sigma
L-glutamate	600 mg	Sigma
L-histidine	150 mg	Roth
L-lysine	650 mg	Sigma

L-tryptophane	100 mg	Sigma
L-tyrosine	400 mg	AppliChem
NH_4Cl	315 mg	Fluka
NaCl	50 mg	Roth
$CaCl_2$ x 2 H_2O	25 mg	Roth
KH_2PO_4	1180 mg	Fluka
$MgSO_4$ x 7 H_2O	70 mg	Merck
Fe-pyrophosphate hydrate	250 mg	Sigma

Weigh out all components, except Fe-pyrophosphate, and dissolve them in 950 ml H_2O. Adjust pH to 6.5 using 10 M KOH. Now dissolve Fe-pyrophosphate, fill up to 1 l with H_2O, filter sterilise and store at 4°C in the dark. The medium can be stored for up to 3 weeks.

Minimal Defined Medium (MDM)

Component	**Amount/Litre**	**Supplier**
ACES	10 g	AppliChem
L-arginine	350 mg	Merck
L-cysteine	400 mg	Sigma
L-isoleucine	470 mg	Merck
L-leucine	640 mg	Roth
L-methionine	200 mg	Merck
L-threonine	330 mg	Roth
L-valine	480 mg	Roth
L-serine	650 mg	Roth
L-proline	115 mg	Roth
L-phenylalanine	350 mg	Roth
NH_4Cl	315 mg	Fluka
NaCl	50 mg	Roth

$CaCl_2$ x 2 H_2O	25 mg	Roth
KH_2PO_4	1180 mg	Fluka
$MgSO_4$ x 7 H_2O	70 mg	Merck
Fe-pyrophosphate hydrate	250 mg	Sigma

Weigh out all components, except Fe-pyrophosphate, and dissolve them in 950 ml H_2O. Adjust pH to 6.5 using 10 M KOH. Now dissolve Fe-pyrophosphate, fill up to 1 l with H_2O, filter sterilise and store at 4°C in the dark. The medium can be stored for up to 3 weeks.

Carbon Enriched Minimal Defined Medium (CE MDM)

The recipe is identical to MDM but additionally 4.6 g (= 3.7 ml) glycerol and 1.98 g D-glucose monohydrate are added. All components, except Fe-pyrophosphate are dissolved in 950 ml H_2O. Adjust pH to 6.5 using 10 M KOH. Now dissolve Fe-pyrophosphate, filter sterilise and store at 4°C in the dark. The medium can be stored for up to 3 weeks.

2.1.3.2 *Escherichia coli*

Luria-Bertani (LB) Agar

Component	**Amount/Litre**	**Supplier**
LB agar Lennox	32 g	Invitrogen
Antibiotic		
Ampicillin	100 mg	Roth
Chloramphenicol	30 mg	Roth
Kanamycin	30 mg	Roth

Dissolve LB agar in 1 l H_2O, autoclave and let cool down to 50°C before pouring plates. Add antibiotics at indicated concentrations if necessary. Let plates dry for 1 day and store at 4°C in the dark.

Luria-Bertani (LB) Medium

Component	Amount/Litre	Supplier
Luria Bertani broth base Lennox	20 g	Invitrogen

Dissolve LB broth base in 1 l H_2O, autoclave and let cool down to 50°C. Add antibiotics at indicated concentrations as for LB agar. Store at room temperature.

Transformation Buffer 1 (TFB1) for Chemically Competent *E. coli*

Component	Amount/Litre	Supplier
Potassium acetate	2.82 g (30 mM)	Roth
KCl	7.46 g (100 mM)	Roth
$CaCl_2$ x 2 H_2O	1.48 g (10 mM)	Roth
MnCl	6.3 g (50 mM)	Roth
Glycerol	150 ml (15%)	Roth

Dissolve all components in 950 ml H_2O and adjust pH to 5.8 using 0.2 M acetic acid. Fill up to 1 l and filter sterilise the buffer. Store 40 ml aliquots at -20°C.

Transformation Buffer 2 (TFB2) for Chemically Competent *E. coli*

Component	Amount/Litre	Supplier
MOPS	0.42 g (10 mM).	Roth
$CaCl_2$ x 2 H_2O	1.11 g (75 mM)	Roth
KCl	0.074 g (10 mM)	Roth
Glycerol	15 ml (15%)	Roth

Dissolve all components in 950 ml H_2O and adjust pH to 6.5 using KOH. Fill up to 1 l and filter sterilise the buffer. Store 4 ml aliquots at -20°C.

2.1.3.3 *Dictyostelium discoideum*

HL5 medium (Watts and Ashworth, 1970)

Component	Amount/Litre	Supplier
D(+)-glucose monohydrate	11 g	Fluka
BBL yeast extract	5 g	BD Biosciences
Bacto proteose peptone	5 g	BD Biosciences
Bacteriological peptone	5 g	Oxoid
Na_2HPO_4	0.355 g (2.5 mM)	Fluka
KH_2PO_4	0.34 g (2.5 mM)	Fluka

Weigh out all components in 950 ml H_2O and adjust pH to 6.5 with 1 M KOH or 1 M HCl. Fill up to 1 l, autoclave and store at 4°C.

SorC Buffer (Malchow *et al.*, 1972)

Component	Amount/Litre	Supplier
Na_2HPO_4	0.28 g (2 mM)	Fluka
KH_2PO_4	2.04 g (15 mM)	Fluka
$CaCl_2$ x 2 H_2O	7.35 mg (50 µM)	Roth

Dissolve Na_2HPO_4 and KH_2PO_4 in 950 ml H_2O and adjust pH to 6.0 using 1 M KOH. Then add $CaCl_2$ x 2 H_2O, fill up to 1 l with H_2O, autoclave and store at 4°C.

Homogenisation buffer (Derre and Isberg, 2004)

Component	Amount/Litre	Supplier
HEPES	4.77 g (20 mM)	Roth
Sucrose	85.58 g (250 mM)	Roth
EGTA	0.19 g (0.5 mM)	Roth

Dissolve all components in 950 ml H_2O, adjust pH to 7.2 with 1 M HCl or 1 M NaOH, fill up to 1 l with H_2O, filter sterilise the buffer and store at 4°C.

2.1.3.4 *Acanthamoeba castellanii*

PYG Medium (Moffat and Tompkins, 1992)

Component	Amount/Litre	Supplier
Bacto proteose peptone	20 g	BD BioSciences
BBL yeast extract	1 g	BD BioSciences
$MgSO_4$ x 7 H_2O	10 ml (of a 0.4 M stock)	Roth
$CaCl_2$ x 2 H_2O	8 ml (of a 0.05 M stock)	Roth
Sodium citrate x 2 H_2O	3.4 ml (of a 1 M stock)	Roth
$Fe(NH_4)_2$ x 7 H_2O	20 mg	Roth
Na_2HPO_4	10 ml (of a 0.25 M stock)	Roth
KH_2PO_4	10 ml (of a 0.25 M stock)	Fluka
D(+)-glucose monohydrate	19.8 g	Fluka

Dissolve proteose peptone and yeast extract in 900 ml H_2O. Prepare and sterilise stocks of all other components and add the indicated amounts. Adjust the pH to 6.5 with 1 M HCl, then add 50 ml of a 2 M glucose solution (= 19.8 g glucose monohydrate in 50 ml H_2O). Fill up to 1 l. Filter the medium through a layer of 7 glass fiber filters and repeat the procedure once. At last, sterilise the medium using a 0.2 µm filter cartouche and store it at 4°C.

LoFlo Medium

Component	Amount/Litre	Supplier
LoFlo base	16.8 g	ForMedium

Dissolve LoFlo base in water, autoclave and store at room temperature.

Ac Buffer (Moffat and Tompkins, 1992)

Component	Amount/Litre	Supplier
$MgSO_4$ x 7 H_2O	985.9 mg (4 mM)	Oxoid
$CaCl_2$	44 mg (0.4 mM)	BD

Sodium citrate x 2 H_2O	999 mg (3.4 mM)	AppliChem
Na_2HPO_4 x 7 H_2O	86 mg (0.05 mM)	Fluka
KH_2PO_4	2.5 mg (2.5 mM)	Fluka
NH_4Cl	2.6 mg (0.05 mM)	Fluka
$FeSO_4$	7.55 mg (0.05 mM)	Merck

Dissolve all components in 950 ml H_2O, adjust pH to 6.5 using 1 M HCl, fill up to 1 l, autoclave and store at 4°C.

2.1.3.5 RAW 264.7 Macrophages

Phosphate-Buffered Saline (PBS) (10 x stock solution)

Component	Amount/Litre	Supplier
$MgSO_4$ x 7 H_2O	80 g	AppliChem
$CaCl_2$	2 g	Fluka
Sodium citrate x 2 H_2O	14.2 g	Fluka
Na_2HPO_4 x 7 H_2O	2.4 g	Fluka

Dissolve all components in 950 ml H_2O, adjust pH to 7.4 with 1 M NaOH or 1 M HCl, fill up to 1l, autoclave and store at room temperature.

2.1.4 Strains, Plasmids, Oligonucleotides and Antibodies

Strain	Relevant properties*	Reference
E. coli		
TOP10		Invitrogen
L. pneumophila		
JR32	Virulent *L. pneumophila* serogroup 1 strain Philadelphia	(Sadosky *et al.*, 1993)
GS3011 (Δ*icmT*)	*L. pneumophila* JR32 *icmT3011*::Km	(Segal and Shuman, 1998)
CM01 (Δ*glpD*)	*L. pneumophila* JR32 *glpD*::Km	This study
CM02 (Δ*iolT*)	*L. pneumophila* JR32 *lpg1653*::Km	This study

CM03 (Δ*iolG*)	*L. pneumophila* JR32 *lpg1652*::Km	This study
AK01 (Δ*lqsT*)	*L. pneumophila* JR32 *lqsT*::Km	(Kessler *et al.*, 2013)
AK02 (Δ*lqsS*- Δ*lqsT*)	*L. pneumophila* JR32 *lqsS-lqsT*::Km	(Kessler *et al.*, 2013)
NT02 (Δ*lqsA*)	*L. pneumophila* JR32 *lqsA*::Km	(Tiaden *et al.*, 2010)
NT03 (Δ*lqsR*)	*L. pneumophila* JR32 *lqsR*::Km	(Tiaden *et al.*, 2007)
NT05 (Δ*lqsS*)	*L. pneumophila* JR32 *lqsS*::Km	(Tiaden *et al.*, 2010)
LM1376 (Δ*rpoS*)	*L. pneumophila* JR32 *rpoS*4::Tn903dGent	(Hales and Shuman, 1999b)
A. castellanii		ATCC 30234
D. discoideum		
Ax3		(Zhou *et al.*, 1995)
RAW 264.7	Murine macrophage cell line	ATCC TIB-71

* Abbreviations: Km, kanamycin.

Plasmids	**Description***	**Reference**
pCM003	pLAW344, *iolT*::Km	This study
pCM004	pMMB207C-*gfp*(ASV)	This study
pCM007	pMMB207C-p*iolT-gfp*(ASV)	This study
pCM018	pLAW344, *glpD*::Km	This study
pCM020	pCR33-M45-*iolT*	This study
pCM021	pCR33-M45-*glpD*	This study
pCM022	pLAW344, *iolG*::Km	This study
pCR033	*Legionella* expression vector, Δ*mobA*, RBS, M45-(Gly)5, Cm (=pMMB207C-RBS-M45)	(Weber *et al.*, 2006)
pJBA132	pUC18-*luxR*-P_{luxI}-RBS-*gfp*(ASV)	(Andersen *et al.*, 2001)
pLAW344	*oriT* (RK2), *oriR* (ColE1), *sacB*, Cm, Ap	(Wiater *et al.*, 1994b)
pMMB207C	*Legionella* expression vetor, Δ*mobA*, -RBS, Cm	(Weber *et al.*, 2006)
pNT028	pMMB207C, *gfp* (constitutive)	(Tiaden *et al.*, 2007)
pSW001	pMMB207C-RBS-*dsred* (constitutive *dsred*)	(Mampel *et al.*, 2006)
pUC4K	*oriR* (pBR322), Ap, MCS::Km	Amersham

*Abbreviations: Ap, ampicillin; Cm. chloramphenicol; Km, kanamycin

Oligonucleotide	Sequnce (5' – 3')*	Description
glpD-BamHI-sen-Kompl	GGAGATGGATCCATGGATCAGGTTTTTGATG	*glpD* for complementation
glpD-SalI-ant-Kompl	TTGATGGTCGACTTAGTGAAATACGAGCTC	*glpD* for complementation
glpD-LB-XbaI-sen	TATGCTTCTAGAAAACTGGTTTATCACCTGTATTGAG	500 bp 5'-flanking region of *glpD*
glpD-LB-SalI-ant	GAACTAGTCGACGCTATTGACCAGGGAACAAG	500 bp 5'-flanking region of *glpD*
glpD-RB-SalI-sen	CAGCATGTCGACTTGTTGCGCCAATTCTTTTA	500 bp 3'-flanking region of *glpD*
glpD-RB-XbaI-ant	CAAAAATCTAGAGAATCAGGTGGGTTGGTGTC	500 bp 3'-flanking region of *glpD*
iol-660-sen-Seq	TACTGGGGAGTAGTTTGTGTGC	seq. primer of *iolT*
iol-1347-sen-Seq	TCAGTGGTACTTTGATCGCA	seq. primer of *iolT*
iol-2051-sen-Seq	CATCTCGAACAAATTATTACAGCG	seq. primer of *iolT*
iol-2744-sen-Seq	GATGGACTACAAGCCTTGCG	seq. primer of *iolT*
iol-3459-sen-Seq	TATGCGATTTGATTGTTGGG	seq. primer of *iolT*
iol-7042-ant-Seq	GAAGTCGTAAGCAATTCGGC	seq. primer of *iolT*
iol-6351-ant-Seq	CCCAATCCCTCTGCGTACT	seq. primer of *iolT*
iol-5655-ant-Seq	AAAGCCCATTTGGAAGCTGT	seq. primer of *iolT*
iol-4942-ant-Seq	TTTTTGTTTGGCATAGGCG	seq. primer of *iolT*
iol-4241-ant-Seq	AAAATAAATTTTCGTTTTCCGTTTC	seq. primer of *iolT*
iolG-1400up-sen	ATGAACAAGGGAATGAAC	seq. primer of *iolG*
iolG-511-sen	ATATTTATGGACATGTCT	seq. primer of *iolG*
iolG-451-sen	CGAATTACTTCTCGTGAT	seq. primer of *iolG*
iolG-301-ant	TATCTCTTCTTCATTCAA	seq. primer of *iolG*
iolG-1400down-ant	GTCTAACTCAAGCATATTAGA	seq. primer of *iolG*
iolG-850bp-up	CCGCTGGATAATGATTAA	seq. primer of *iolG*
iolG-850bp-down	GATTTTGCCTGTAATAGA	seq. primer of *iolG*
iolG-LB-XbaI-sen	GGCCAGTCTAGAATAATATTCAGCAGGAATTG	800 bp 5'-flanking region of *iolG*
iolG-LB-SalI-ant	TTTCATGTCGACTCCATAATTAAATTAAATTTTGC	800 bp 5'-flanking region of *iolG*
iolG-RB-SalI-sen	AGTTGAGTCGACTATGAAACAGTTTCCCGG	800 bp 3'-flanking region of *iolG*

iolG-RB-XbaI-ant	CGAGCATCTAGATCTCCTAATTTAACAAC	800 bp 5'-flanking region of *iolG*
iolT-400bp-XbaI-ant	TCCCTTTCTAGAGTAACTATCTGTCCCTAATG	P_{iolT} 400 bp for pCM007
iolT-BamHI-sen-Kompl	ACAGATGGATCCATGAACAAGGGAATGAAC	*iolT* for complementation
iolT-SalI-ant-Kompl	TCTTTTGTCGACTTAATCCATAATTAAATTAAATTTTGC	*iolT* for complementation
iolT-LB-XbaI-sen	AATATGTCTAGACAATTGTCTTTGGCAGCAGA	500 bp 5'-flanking region of *iolT*
iolT-LB-SalI-ant	CTGTTCGTCGACGATGTTATCACGGCCAGGTT	500 bp 5'-flanking region of *iolT*
iolT-RB-SalI-sen	TCGAATGTCGACAGTAGGTGCGGGAAGAATTG	500 bp 3'-flanking region of *iolT*
iolT-RB-XbaI-ant	TCAAGGTCTAGATATTGAGGTTTTGCGCCATC	500 bp 3'-flanking region of *iolT*

* Restriction sites are underlined

Antibody	**Origin**	**Label**	**Supplier**
anti-SidC	rabbit	none	affinity-purified (Weber *et al.*, 2006)
anti-rabbit IgG	donkey	DYLight650	Abcam (Cambridge)
anti-rabbit IgG	bovine	Rhodamine	Santa Cruz (Dallas)

2.2 Methods

2.2.1 *Legionella pneumophila*

2.2.1.1 Cultivation of *Legionella pneumophila*

Bacterial strains are listed in section 2.1.4. *L. pneumophila* strains were grown from glycerol stocks for 2-3 days on CYE agar plates. Bacteria were suspended from CYE agar plates to a starting OD_{600} of 0.1 in AYE broth using a 13 ml plastic tube and then grown at 37°C on a turning wheel. Bacteria reached infectious state after approximately 21-22 h at OD_{600} of 3.0. Cells were checked for motility and homogeneity of shape with an inverted light microscope (40x objective).

For growth experiments in chemically defined medium (CDM), minimal defined medium (MDM) or carbon enriched minimal defined medium (CE MDM), bacteria were resuspended from CYE agar plates to a starting OD_{600} of 0.1 in CDM and grown at 37°C on a turning wheel to a maximum OD_{600} of 1.0. Cultures were diluted to OD_{600} of 0.1 in CDM, MDM or CE MDM and further incubated for 48 h at 37°C on a turning wheel.

Cultures and agar plates were supplemented with chloramphenicol (Cm, 5 µg/ml) or kanamycin (Km, 50 µg/ml in broth or 10 µg/ml in agar plates), if necessary. See section 2.1.3.1 for media recipes.

2.2.1.2 *Legionella pneumophila* Glycerol Stocks

L. pneumophila liquid cultures were grown approximately 18 h at 37°C, mixed 1:2 with sterile 50% glycerol in cryo tubes, frozen in liquid nitrogen and stored at -80°C.

2.2.1.3 Preparing Electrocompetent *Legionella pneumophila*

L. pneumophila was resuspended from AYE agar plates to a starting OD_{600} of 0.1 in AYE medium and grown at 37°C to prestationary growth phase. 1 ml of that culture was added to 30 ml AYE in a baffled flask. The culture was grown to an OD_{600} between 0.3 and 0.5, cooled on ice, then washed three times with sterile, ice-cold 10% glycerol (10 ml, 2.5 ml, and 160 µl). Aliquots of 25 µl were frozen in liquid nitrogen and stored at -80°C until use.

2.2.1.4 Transformation of *Legionella pneumophila* by Electroporation

25 µl electro-competent *L. pneumophila* (section 2.2.1.3) were thawed on ice, mixed with 100 ng of plasmid and incubated on ice for 2 min. The bacteria were transferred into a 2 mm gap electroporation cuvette and electroporation occurred at 2.5 kV, 200 Ω and 25 µF. Bacteria were washed out of the cuvette with 600 µl AYE, given into a 1.5 ml reaction tube and incubated at 37°C and 800 rpm in a shaking incubator. After 5 h cells were plated on selective CYE agar plates.

2.2.2 *Escherichia coli*

2.2.2.1 Inoculation, Growth and Storage

E. coli strains were grown from glycerol stocks on LB agar plates at 37°C overnight. Liquid cultures were made in LB liquid medium and incubated at 37°C on a turning wheel. Agar plates and medium were supplemented with chloramphenicol (Cm, 30 µg/ml, kanamycin (Km, 30 µg/ml) or ampicilin (Ap, 100 µg/ml) if required. See section 2.1.3.2 for media recipies.

2.2.2.2 Glycerol Stocks of *Escherichia coli*

A mature liquid culture of *E. coli* was mixed 1:2 with sterile 50% glycerol in cryo tubes, frozen in liquid nitrogen and stored at -80°C.

2.2.2.3 Preparation of Chemocompetent *Escherichia coli*

1 ml of a late-exponential culture of *E. coli* strain TOP10 was added to a baffled flask containing 100 ml LB medium. The flask was incubated at 37°C and 180 rpm in an incubation cabinet, until the culture reached an OD_{600} of 0.5. Cells were cooled on ice and centrifuged at 2100 x g for 10 min at 4°C. The pellet was resuspended in 40 ml ice-cold TFB1 (section 2.1.3.2) and again centrifuged. The pellet was then resuspended in 4 ml ice-cold TFB2 (section 2.1.3.2), aliquots of 50 µl were made, frozen in liquid nitrogen and stored at -80°C.

2.2.2.4 Transformation of Competent Cells by Heat Shock

Chemocompetent *E. coli* cells (section 2.2.2.3) were thawed on ice, mixed with with 50-100 ng plasmid and incubated on ice for 20 min. The bacteria were then incubated at 42°C for 1 min,

placed on ice shortly and mixed with 800 µl LB medium. After incubating the cells at 37°C and 800 rpm in a shaking incubator for 1 h, bacteria were plated onto selective LB agar.

2.2.3 *Dictyostelium discoideum*

2.2.3.1 Cultivation of *Dictyostelium discoideum*

D. discoideum was grown axenically at 23°C in HL5 medium (section 2.1.3.3). 1 x 10^4 cells/ml were seeded into 75 cm^2 tissue culture flasks containing 10 ml HL5 medium. After 2-3 days at 23°C or when cells reached 80% confluence, cells were subcultured by removing the old medium, adding 10 ml new HL5 medium and tapping off the cells. Cells were diluted 1:100 in 10 ml HL5, transferred to a new cell culture flask and again incubated at 23°C.

2.2.3.2 Storage of *Dictyostelium discoideum*

D. discoideum was grown to 80% confluence in one 75 cm^2 cell culture flask. Old medium was removed and cells were resuspended in 9 ml freezing medium consisting of 80% HL5, 10% FCS and 10% DMSO. Aliquots of 1 ml were distributed into cryo tubes and placed in a cryogenic freezer box filled with isopropanol, which was precooled for 1 h at 4°C. Cells were frozen at -80°C overnight in this box and subsequently stored in liquid nitrogen. When removing cells from cryogenic storage, the aliquots were rapidly thawed and immediately transferred to 9 ml HL5 in a 15 ml reaction tube. Cells were centrifuged once at 500 x g for 10 min and resuspended in 10 ml HL5 to remove DMSO. The cells were transferred to a cell culture flask and incubated at 23°C.

2.2.4 *Acanthamoeba castellanii*

2.2.4.1 Cultivation of *Acanthamoeba castellanii*

A. castellanii cells were cultivated in 10 ml PYG medium (section 2.1.3.4) in 75 cm^2 cell culture flasks. When cells reached 80% confluence, cells were subcultured by removing the old medium, adding 10 ml new PYG medium and tapping off the cells. Cells were diluted 1:100 in 10 ml PYG, transferred to a new cell culture flask and again incubated at 23°C.

2.2.4.2 Storage of *Acanthamoeba castellanii*

A.castellanii was grown to 80% confluence in one 75 cm^2 cell culture flask. Old medium was removed and cells were resuspended in 9 ml freezing medium consisting of 80% PYG, 10% FCS

and 10% DMSO. Aliquots of 1 ml were distributed into cryo tubes and placed in a cryogenic freezer box filled with isopropanol, which was precooled for 1 h at 4°C. Cells were frozen at -80°C overnight in this box and subsequently stored in liquid nitrogen. When removing cells from cryogenic storage, the aliquots were rapidly thawed and immediately transferred to 9 ml PYG in a 15 ml reaction tube. Cells were centrifuged once at 500 x g for 10 min and resuspended in 10 ml PYG to remove DMSO. The cells were transferred to a cell culture flask and incubated at 23°C.

2.2.5 RAW 264.7 Macrophages

2.2.5.1 Cultivation of RAW 264.7 Macrophages

Murine RAW 264.7 macrophages were grown in 10 ml RPMI 1640 medium containing 2 mM L-glutamine and 10% heat-inactivated FCS in a 75 cm^2 cell culture flask at 37°C in a humidified atmosphere containing 5% CO_2. When cells reached 90% confluence, old medium was removed, 10 ml new RPMI 1640 medium was added and cells were removed mechanically from the culture flask with a cell scraper. Cells were diluted 1:10 in 10 ml RPMI 1640 medium, transferred to a new cell culture flask and further incubated at 37°C and 5% CO_2.

2.2.5.1 Storage of RAW 264.7 Macrophages

Murine RAW 264.7 macrophages were grown to 90% confluence in one 75 cm^2 cell culture flask. Old medium was removed and cells were resuspended in 9 ml freezing medium consisting of 70% RPMI 1640, 20% FCS and 10% DMSO. Aliquots of 1 ml were distributed into cryo tubes and placed in a cryogenic freezer box filled with isopropanol, which was precooled for 1 h at 4°C. Cells were frozen at -80°C overnight in this box and subsequently stored in liquid nitrogen. When removing cells from cryogenic storage, the aliquots were rapidly thawed and immediately transferred to 9 ml RPMI 1640 medium in a 15 ml reaction tube. Cells were centrifuged once at 500 x g for 10 min and resuspended in 10 ml RPMI 1640 medium to remove DMSO. The cells were transferred to a cell culture flask and incubated at 37°C in a humidified atmosphere containing 5% CO_2.

2.2.6 Construction of Vectors for Allelic Exchange, Gene Expression and GFP-Reporter Assays

Standard protocols were used for cloning regarding PCR, restriction digest and ligation. Plasmids were isolated using kits from Macherey-Nagel. All PCR fragments and plasmids were sequenced (GATC, Konstanz). Primer and plasmids are listed in section 2.1.4.

The allelic exchange vectors pCM003, pCM018 and pCM022 were constructed in a four-way ligation using 0.5-0.8 kB of 5' and 0.5-0.8 kB of 3' flanking regions of *iolT* (pCM003), *glpD* (pCM018) and *iolG* (pCM022), respectively, and a Km resistance cassette from vector pUC4K. For flanking regions of *iolT,* primer pairs *iolT*-LB-XbaI-sen, *iolT*-LB-SalI-ant and *iolT*-RB-SalI-sen and *iolT*-RB-XbaI-ant were used. For flanking regions of *glpD,* primer pairs *glpD*-LB-XbaI-sen, *glpD*-LB-SalI-ant and *glpD*-RB-SalI-sen*, glpD*-RB-XbaI-ant were used. For flanking regions of *iolG,* primer pairs *iolG*-LB-XbaI-sen, *iolG*-LB-SalI-ant and *iolG*-RB-SalI-sen, *iolG*-RB-XbaI-ant were used. Amplified PCR products of these flanking regions were digested using the restriction enzymes SalI and XbaI. Plasmid pUC4K was digested with SalI yielding a 1.4 kB fragment containing the Km resistance cassette. Plasmid pLAW344 was digested using the restriction enzyme XbaI. Corresponding flanking regions and the Km resistance cassette were cloned into vector pLAW344 in a four-way ligation and transformed into *E. coli* TOP10. Cells were plated on LB agar containing Km to select for the Km resistance cassette. Plasmids were reisolated from single colonies, analysed by restriction digestion and sequenced.

Vectors pCM020 and pCM021 for complementation of the mutant strains Δ*iolT* and Δ*glpD* were constructed using primer pairs *iolT*-BamHI-sen-Kompl, *iolT*-SalI-ant-Kompl or *glpD*-BamHI-sen-Kompl, *glpD*-SalI-ant-Kompl, respectively. PCR products were digested using BamHI and SalI, cloned into pCR033 and transformed into *E. coli* TOP10. Cells were plated on LB agar plates containing Cm, plasmids were reisolated from single colonies, analysed by restriction digestion and sequenced.

For the construction of plasmid pCM004, an instable form of GFP, GFP(ASV), was used. For that, plasmid pJBA132 was digested using XbaI and HindIII, yielding a 0.75 kB fragment containing *gfp*(ASV). This was cloned into plasmid pMMB207C and transformed into *E. coli* TOP10. Cells were plated on LB agar plates containing Cm, plasmids were reisolated from single colonies, analysed by restriction digestion and sequenced. The 400 bp promotor region of *iolT* was amplified using primer *iolT*-400bp-SacI-sen and *iolT*-400bp-XbaI-ant. The PCR product and plasmid pCM004 were digested using SacI and XbaI, ligated and transformed into *E. coli* TOP10.

Cells were plated on LB agar plates containing Cm, plasmids were reisolated from single colonies, analysed by restriction digestion and sequenced.

2.2.7 Construction of Chromosomal Deletion Mutant Strains CM01, CM02 and CM03

Allelic exchange by double homologous recombination using counter-selection on sucrose was performed as described (Wiater *et al.*, 1994a; Tiaden *et al.*, 2007). To construct mutants CM01 (Δ*glpD*), CM02 (Δ*iolT*) and CM03 (Δ*iolG*), *L. pneumophila* JR32 was transformed with pCM018, pCM003 or pCM022, respectively. Cells were plated on CYE plates containing Km and incubated for 5 days at 30°C. Km^R colonies were selected and grown overnight in AYE broth containing Km (50 µg/ml). Cells were spotted on CYE plates with Km (10 µg/ml), CYE plates with Km (10 µg/ml) and 2% sucrose and CYE plates with Cm (5 µg/ml) and grown at 30°C to select for $Cm^S/Km^R/Suc^R$ colonies. Double-cross-over events and thus deletion mutants were confirmed by PCR and sequenced.

2.2.8 Extracellular Growth Assays

To investigate the influence of different carbon soures on extracellular growing bacteria, *L. pneumophila* wild-type and mutants Δ*glpD*, Δ*iolT* or Δ*iolG* were resuspended from CYE agar plates. Overnight cultures were inoculated with a starting OD_{600} of 0.1 in CDM and grown at 37°C to an OD_{600} of maximum 1.0. Cultures were then diluted to OD_{600} = 0.1 in CDM or MDM. Glycerol or inositol at specific concentrations were added and cultures were further incubated for 48 h at 37°C. The optical density was assessed at defined intervals.

2.2.9 Intracellular Replication of *Legionella pneumophila*

Intracellular replication of *L. pneumophila* was assessed using fluorescence-based single round assays and by determining the cfu. For single round assays a previously published protocol was used (Harrison *et al.*, 2013). In brief: *A. castellanii* were grown in PYG medium and seeded out in 96-well plates such that 4 x 10^5 cells were present in each well. Plates were incubated overnight at 23°C to allow replication and resulted in a cell number of 8 x 10^5 cells per well. PYG medium was then exchanged with LoFlo medium. *L. pneumophila* strains harbouring plasmid pNT28 and constantly expressing GFP were resuspended from AYE plates to a starting OD_{600} of 0.1 in AYE/Cm (5µg/ml) and grown overnight at 37°C to an OD_{600} of 3. Bacteria were diluted in LoFlo medium (ForMedium), and amoeba were infected with *L. pneumophila*

(MOI 20). Infections were synchronised by centrifugation at 500 x g for 10 min. Glycerol, inositol or serine were added 4 h post infection to certain wells, and infected amoeba were incubated at 30°C. GFP fluorescence was measured in a plate spectrophotometer at specific intervals.

Murine RAW 264.7 macrophages were grown in RPMI medium containing 5% FCS at 37°C/5% CO_2. Infections were performed as described for assays with *A. castellanii*, but bacteria were diluted in RPMI medium prior to infection, and plates were incubated at 37°C/5% CO_2. As the culture media used for these assays do not support growth of *L. pneumophila*, GFP fluorescence did only reflect intracellular replication.

Intracellular growth of *L. pneumophila* was also assessed by determining the cfu. Specifically, *A. castellanii* or RAW 264.7 macrophages were suspended in PYG or RPMI medium, respectively. 2 x 10^4 cells per well were seeded into 96-well plates and incubated at 23°C (*A. castellanii*) or 37°C and 5% CO_2 (RAW 264.7 macrophages) overnight, such that 4 x 10^4 cells per well were present the next day. PYG medium was exchanged with AC buffer and RPMI medium was exchanged with fresh RPMI 1640 medium. Cells were then infected with *L. pneumophila* (MOI 0.1) and infection was synchronized by centrifugation at 500 x g for 10 min. Cells were further incubated for 1 h, then washed with AC buffer or RPMI medium. Glycerol, inositol or serine was added 4 h post infection to certain wells. For complementation of the Δ*glpD* phenotype, mutant Δ*glpD* harbouring plasmid pCM021 was grown overnight with 1 mM IPTG to induce expression of *glpD*. Infection and further treatment followed as described above. After 48 h (RAW 264.7 macrophages) or 72 h (*A. castellanii*), cells were lysed with 0.8% saponin and appropriate dilutions were plated on CYE agar plates to determine the cfu.

2.2.10 Intracellular Growth of *Legionella pneumophila* in Coinfection Assays

L. pneumophila wild-type and mutant strains to be tested were resuspended from CYE plates in AYE broth to a starting OD_{600} of 0.1 and incubated at 37°C untill the cultures reached an OD_{600} of 3. Prior to infection *A. castellanii* cells were seeded in a 96-well plate in AC buffer, such that each well contained 5 x 10^4 cells. The plate was incubated for at least 1 h at 30°C. *A. castellanii* was then infected at a 1:1 ratio with *L. pneumophila* wild-type and mutant strain Δ*glpD*, Δ*iolT* or Δ*iolG* respectively (MOI 0.01 each). Infection was synchronised by centrifugation at 500 x g for 10 min, and the plate was incubated at 37°C for 1 h. AC buffer was changed and the plate further incubated at 37°C for three days. After three days fresh amoeba were seeded into a new 96-well

plate (5 x 10^4 cells per well) and incubated at 30°C for 1 h. Supernatant from the old 96-well plate was harvested and remaining cells in the wells were lysed with 0.8% saponin. Supernatant and lysate was combined, diluted 1:1000 and used to infect the fresh amoeba (50 µl per 200 µl amoeba culture). Aliquots of combined supernatant and lysate were plated on CYE agar plates and plates containing Km in parallel to determine cfu and to distinguish between wild-type and Km-resistant mutant bacteria. The freshly infected 96-well plate was further incubated at 37°C for another three days, then lysis and reinfection was repeated. Five rounds of infection were performed in total.

2.2.11 Isotopologue Profiling of Extracellularly Growing *Legionella pneumophila*

L. pneumophila wild-type or mutant Δ*glpD* were resuspended from CYE agar plates, diluted in CDM to a starting OD_{600} of 0.1 and grown overnight at 37°C such that the optical density was not higher than 1.0 the next day. Bacteria were then diluted to an OD_{600} of 0.1 in 100 ml MDM containing 50 mM [U-$^{13}C_3$]glycerol and incubated in an incubation cabinet at 37°C and 180 rpm for 48 h. An aliquot was then plated on CYE agar plates and cells were harvested by centrifugation at 3500 x g and 4°C for 15 min. The resulting cell pellet was washed twice with 50 ml ice-cold AC buffer and once with 1 ml ice-cold AC-buffer, autoclaved at 120°C for 20 min, freeze-dried and then stored at -20°C until analysis.

For time course experiments with different carbon substrates, *L. pneumophila* wild-type was grown overnight in CDM with a starting OD_{600} of 0.1. The bacteria were then diluted to a starting OD_{600} of 0.1 in CE MDM that contained either 50 mM [U-$^{13}C_3$]glycerol, 11 mM [U-$^{13}C_6$]glucose or 6 mM [U-$^{13}C_3$]serine as labelled precursor and then cultivated in an incubation cabinet at 37°C and 180 rpm. After 12, 24, 36 and 48 h, 30 ml samples were taken, optical density was determined at 600 nm and an aliquot was plated on CYE agar plates. Samples were then centrifuged, washed, autoclaved, freeze-dried and stored as described above.

2.2.12 Isotopologue Profiling of *Legionella pneumophila* Growing in *Acanthamoeba castellanii*

For every bacterial strain to be tested, *A. castellanii* was grown in PYG medium in eight 75 cm^2 cell culture flasks to 80% confluence (~2 x 10^7 cells per flask). *L. pneumophila* wild-type or mutant Δ*glpD* were grown in AYE to infectious state. *A. castellanii* was then infected at an MOI 50 with either wild-type or Δ*glpD,* and infection was synchronised by centrifugation of the

cell culture flasks at 500 x g for 10 min. Flasks were incubated at 37°C for 1 h, then cells were washed once with 10 ml pre-warmed AC buffer to remove extracellular bacteria, overlaid with 10 ml fresh AC buffer and further incubated at 37°C. 50 mM [U-$^{13}C_3$]glycerol, 11 mM [U-$^{13}C_6$]glucose or 6 mM [U-$^{13}C_3$]serine was added to the flasks 5 h post infection and cells were further incubated at 37°C for another 10 h.

Cells were then released from the flasks using a cell scraper, transferred to 50 ml reaction tubes, frozen at -80°C for 30 min and then thawed to room temperature to lyse the host cells. To harvest the eukaryotic fraction F1, the suspension was centrifuged at 200 x g and 4°C for 10 min. The supernatant was transferred to new 50 ml reaction tubes and the pellet, representing F1, was washed twice with 50 ml and once with 1 ml ice-cold AC buffer. The supernatant harvested after the first centrifugation was then centrifuged at 3500 x g and 4°C for 15 min. The emerging cell pellet contained *L. pneumophila* bacteria and represented fraction 2 (F2). The supernatant was again harvested and transferred to new 50 ml reaction tubes. The cell pellet of F2 was washed twice with 50 ml and once with 1 ml ice-cold AC buffer. Supernatant of F2 was filtered through 0.22 µm pore filters to remove remaining bacteria, mixed with TCA to a final concentration of 10% and then incubated on ice for 1 h. The suspension was then centrifuged at 4600 x g and 4°C for 30 min. The supernatant was taken off, and the resulting pellet (F3) contained cytosolic proteins of *A. castellanii*. Pellets of F1, F2 and F3 were autoclaved at 120°C for 20 min, freeze-dried and stored at -20°C until analysis. Samples of F1 and F2 were subjected to microscopy and aliquots were plated on CYE agar plates.

2.2.13 Sample Preparation of Protein-Derived Amino Acids, DAP and PHB for GC/MS

Sample preparations and GC/MS measurements for isotopologue profiling (sections 2.2.13-2.2.16) were performed by Ina Häuslein in the laboratory of Prof. Dr. Wolfgang Eisenreich (TU München) and evaluated by Christian Manske and Ina Häuslein at the Max von Pettenkofer-Institute (LMU München).

1 mg of bacterial cell pellet (section 2.2.11) or 1 mg of the fractions F1 and F2 (section 2.2.12) were resuspended in 0.5 ml 6 M hydrochloric acid and incubated at 105°C for 24 h. The samples were dried under a stream of nitrogen and the residual pellet was dissolved in 200 µl acetic acid. A cation exchange column of Dowex 50Wx8 (H+ form, 200-400 mesh, 5 x 10 mm) was washed with 1 ml methanol and 1 ml ultrapure water and then used to purify the samples. To this end, the column was developed with 2 ml distilled water, resulting in eluate 1, and then with 1 ml 4 M

ammonium hydroxide, resulting in eluate 2. The eluates were then dried under a stream of nitrogen at 70°C.

Eluate 1 was dissolved in 100 µl N-methyl-N-(trimethylsilyl)-trifluoroacetamide and incubated at 40°C and 110 rpm in a shaking incubator for 30 min. This procedure resulted in trimethylsilyl (TMS) derivatives of 3-hydroxybutyric acid derived from polyhydroxybutyrate (PHB) that were used for GC/MS analysis.

The dried residual sample of eluate 2 was dissolved in 50 µl dry acetonitrile and 50 µl N-(tert-butyldimethyl-silyl)-N-methyl-trifluoroacetamide containing 1% tert-butyl-dimethyl-silylchlorid and incubated at 70°C for 30 min. The resulting mixture of tert-butyl-dimethylsilyl derivates (TBDMS) of amino acids and DAP was used for further GC/MS analysis. Due to acid degradation, the amino acids tryptophan and cysteine could not be detected with this method. Furthermore, the hydrolysis condition led to the conversion of glutamine and asparagine to glutamate and aspartate.

2.2.14 Sample Preparation of Methanol-Soluble Metabolites for GC/MS

5 mg freeze-dried bacterial pellet (section 2.2.11) was resuspended in 1 ml cold methanol, and 0.8 g of 0.25-0.5 mm glass beeds were added. The cells were lysed mechanically using a ribolyser. The lysate was centrifuged at 2300 x g for 10 min, and the supernatant was transferred to a new reaction tube and then dried under a stream of nitrogen. The residual sample was then dissolved in 50 µl dry acetonitrile and 50 µl N-(tert-butyldimethyl-silyl)-N-methyl-trifluoroacetamide containing 1% tert-butyl-dimethyl-silylchlorid and kept at 70°C for 30 min. This procedure resulted in a mixture of tert-butyl-dimethylsilyl (TBDMS) derivatives of polar metabolites and fatty acids that were subjected to GC/MS analysis.

2.2.15 Sample Preparation of Mannose for GC/MS

5 mg freeze-dried bacterial pellet (section 2.2.11) or 1 mg of fraction F1 or fraction F2 (section 2.2.12) were dissolved in 0.5 ml 3 M methanolic HCl and incubated at 80°C overnight. The solution was cooled to room temperature; the supernatant was transferred to a new reaction tube and then dried under a stream of nitrogen. The residual sample was then dissolved in a mixture of 1 ml acetone and 20 µl concentrated H_2SO_4 and incubated at room temperature for 1 h. Then 2 ml saturated NaCl solution and 2 ml saturated Na_2CO_3 were added and the mixture was extracted two times with 3 ml ethyl acetate. The organic phases were harvested and dried under a stream of

nitrogen. The residue was dissolved in a mixture of 100 µl ethyl acetate and 100 µl acetic anhydride and incubated overnight at 60°C. The sample was again dried under a stream of nitrogen and finally dissolved in 100 µl anhydrous ethyl acetate. The resulting mixture of diisopropylidene/acetate derivatives was used for further GC/MS analysis

2.2.16 Gas Chromatography/Mass Spectrometry and Isotopologue Analysis

Samples from sections 2.2.13-2.2.15 were analyzed by GC/MS using a QP2010 Plus gas chromatograph/mass spectrometer equipped with a 30 m long and 0.25 mm wide silica capillary column with 0.25 µm film thickness and a quadrupole detector working with 70 eV electron impact ionization. 0.1 to 6 µl of sample was injected in 1:5 split mode with an helium inlet pressure of 70 kPa , an interface temperature of 260°C and a sampling rate of 0.5 s. All samples were measured three times (technical replicates).

To analyse amino acids (section 2.2.13) the silica column was held at 150°C for 3 min and then developed with an upward gradient of 7°C/min to a final temperature of 280°C that again was held for 3 min. The following amino acids with corresponding retention times in brackets were detected and isotopologue calculations were performed with m/z $[M-57]^+$ or m/z $[M-85]^+$: alanine (6.7 min), glycine (7.0 min), valine (8.5 min), leucine (9.1 min), isoleucine (9.5 min), proline (10.1 min), serine (13.2 min), phenylalanine (14.5 min), aspartate (15.4 min), glutamate (16.8 min), lysine (18.1 min), histidine (20.4 min) and tyrosine (21.0 min).

To detect diaminopimelic acid (DAP) (section 2.2.13) the column was held at 280°C for 3 min and then with an upward temperature gradient of 10°C/min to a final temperature of 300°C that was again held for 3 min. The TBDMS-derivative of DAP was detected at a retention time of 6.2 min and isotopologue calculations were performed with m/z $[M-57]^+$.

To analyse 3-hydroxybutyric acid derived from polyhydroxybutyrate (PHB) (section 2.2.13), the column was held at 70°C for 3 min and then developed with a first upward temperature gradient of 10°C/min to a final temperature of 150°C and afterwards with a second upward temperature gradient of 50°C min^{-1} to a final temperature of 280°C that was held for 3 min. The TMS-derivative of 3-hydroxybutyric acid, was detected at a retention time of 9.1 min, and isotopologue calculations were performed with m/z $[M-15]^+$.

For the analysis of methanol-soluble metabolites (section 2.2.14) the column was heated at 100°C for 2 min and then developed with a first upward temperature gradient of 3°C/min to a final temperature of 234°C, a second upward temperature gradient of 1°C/min to a final temperature of

237°C, and a third upward temperature gradient of 3°C/min to a final temperature of 260°C. TBDMS-derivatives of lactate with retention times in brackets were detected and isotopologue calculations were performed with m/z $[M-57]^+$: lactate (17.8 min), 3-hydroxybutyric acid (21.6 min), succinic acid (27.5 min), fumaric acid (28.7 min), malic acid (39.1 min), palmitic acid (44.0 min), stearic acid (49.4 min) and citric acid (53.25 min).

For diisopropylidene/acetate derivatives of sugars (section 2.2.15) the column was heated at 150°C for 3 min and then developed with a first temperature gradient of 10°C/min to a final temperature of 220°C, and with a second temperature gradient of 50°C/min to a final temperature of 280°C that was held for 3 min. Isotopologue calculations were performed with m/z 287 $[M-15]^+$, a fragment which still contained all C-atoms of mannose.

Data was collected and analysed using LabSolution software. The analysis involved the determination of unlabeled derivatized metabolites, determination of isotopologue distributions of labelled metabolites and correction of ^{13}C-incorporation with regard to the natural abundances of ^{13}C-isotopes in the derivatized metabolites. Retention times and mass fragments of derivatized metabolites that were used for all isotopologue calculations are documented in Supplementary Table 5.1.

With the isotopologue profiling method it is possible to reconstruct the reaction pathways of certain substrates, as different metabolic pathways often lead to the same intermediates of central metabolism, e.g. pyruvate, acetyl-CoA, glyceraldehyde-3-phosphate and so on. Metabolic intermediates, derived from fully ^{13}C-labelled substrates have defined ^{13}C-patterns or isotopologue profiles depending on the metabolic pathway they are derived from. Pyruvate for example, a compound with three carbon atoms, can have one, two or three ^{13}C-labelled C-atoms. The mass of pyruvate would change with each ^{13}C-atom making it heavier than unlabeled pyruvate. The method of MS does not allow determining the exact position of these labelled C-atoms but can draw conclusions regarding the number of labelled C-atoms in a compound depending on the mass of the compound. Pyruvate for example could have a mass with one, two or three more nucleons depending on the number of ^{13}C-labelled atoms, which would be annotated M+1, M+2 or M+3 in the isotopologue profile. From the percentage of these mass fragments the overall enrichment in a compound can be estimated.

2.2.17 Radioactive Labelling of *Legionella pneumophila*

L. pneumophila JR32, Δ*iolT* or Δ*iolG* were grown in AYE broth to an OD_{600} of 2.8. For complementation of Δ*iolT* the mutant was grown in AYE broth with 1 mM IPTG to allow expression of *iolT*. The cultures were then supplemented with 10 mM inositol that was spiked with 1% of a 1:10 dilution [U-$^{14}C_6$]inositol (specific activity of 300 mCi/mmol). The cells were then further incubated at 37°C with gentle shaking, and 200 µl samples were taken after 0, 10, 20, 30, 60 and 90 minutes. The samples were filtered through cellulose acetate (CA) filter disks (pore size 0.25 µm), and filters were washed three times with PBS. Filter-associated radioactivity was determined in a liquid scintillation counter with EcoLume scintillation cocktail.

In another experimental setup, *L. pneumophila* JR32 and Δ*rpoS* were grown in AYE broth. 200 µl samples were taken at OD_{600} of 0.5, 1.0, 2.0 and 3.0. Cells were then incubated with 10 mM inositol spiked with 1% of a 1:10 dilution of [U-$^{14}C_6$]inositol for 30 min and then filtered, washed and measured as described above.

For determining protein-associated radioactivity, *L. pneumophila* JR32, Δ*iolT* or Δ*iolG* were grown in AYE broth to an OD_{600} of 2.0. Cultures were then supplemented with 10 mM inositol spiked with 1% of a 1:10 dilution of [U-$^{14}C_6$]inositol and further incubated at 37°C with gentle shaking. 200 µl samples were taken after 0, 2, 4, 6 and 8 hours, mixed with 1 ml 50% trichloroacetic acid and incubated on ice for 1 h. Samples were then filtered through cellulose nitrate filter disks (pore size: 0.45 µm) and filters were washed three times with PBS. Filter-associated radioactivity was determined in a liquid scintillation counter with EcoLume scintillation cocktail.

2.2.18 GFP Reporter Experiments

L. pneumophila JR32, Δ*rpoS* or *lqs* mutant strains, harbouring plasmid pCM007 were grown overnight in AYE/Cm broth to an OD_{600} of 1.5-2.0. Bacteria were then diluted in AYE/Cm to an initial OD_{600} of 0.1 in a black 96-well clear bottom plate, and 10 mM inositol or 6 mM serine was added to assigned wells. The plate was then incubated in a shaking incubator at 37°C and 600 rpm for 24 h. Every hour the optical densitiy and GFP fluorescence was measured using a microtitre plate reader.

2.2.19 Uptake of 2-NBDG and (Immuno-) Fluorescence Experiments

2.5 x 10^5 cells of *D. discoideum* in 0.5 ml HL5 medium were seeded onto poly-L-lysine coated sterile coverslips in a 24-well plate and incubated overnight at 23°C, such that around 5 x 10^5 cells were present on each coverslip. Cells were infected with *L. pneumophila* wild-type, Δ*iolT*, Δ*iolG* or Δ*icmT* harbouring plasmid pSW001 (constitutive *dsRed* expression) at a MOI of 10. Infection was synchronized by centrifugation at 500 x g for 10 min. Cells were incubated for 1 h at 25°C, then supernatant was taken off and 0.5 ml SorC (*D. discoideum*) per well was added. After that, 20 µM 2-Deoxy-2[(7-nitro-2,1,3-benzoxadiazol-4-yl)amino]-D-glucose (2-NBDG), a fluorescent glucose analog, was added and cells were further incubated at 25°C for 30 min. The cells were washed with SorC or PBS, and cover slips were then mounted on glass slides using Vectashield supplemented with 1 µg/ml DAPI to stain DNA. The samples were analyzed using a Leica TCS SP5 confocal microscope (HCX PLAPO CS, objective 63x/1.4-0.60 oil).

When homogenisation of infected cells was necessary for immuno-fluorescence microscopy, cells were treated as follws: 8.5 x 10^5 *D. discoideum* cells per well were seeded in a 6-well plate, grown overnight and infected with the desired strain at an MOI of 25. For each strain, three wells were used. Infection was performed at 25°C for 1 h, then cells were washed with SorC and 20 µM 2-NBDG was added. Cells were further incubated for 30 min at 25°C, washed with SorC, suspended in homogenisation buffer (section 2.1.3.3) and lysed by nine passages through a cell homogeniser using an exclusion size of 8 µm. This step was performed on ice. The homogenate was then centrifuged onto poly-L-lysine coated cover slips, followed by an antibody stain against SidC. To this end, coverslips were incubated with blocking solution (5% calf serum in SorC) for 1 h and then incubated with 30 µl of an antibody against SidC (diluted 1:100 in blocking solution) for 1 h at room temperature. Cover slips were washed three times with SorC, and then 30 µl of appropriate secondary antibodies coupled to DyLight650 or Rhodamine (diluted 1:200 in blocking solution) were added and incubated for 30 min with the samples. Cover slips were washed with SorC and then mounted onto glass slides using Vectashield.

3. Results

3.1 Designing a New Chemically Defined *Legionella* Growth Medium

One goal of this thesis was the examination of inositol and glycerol as carbon sources for *L. pneumophila* by applying different growth assays and isotopologue profiling. For this purpose a new *Legionella* growth medium was developed based on a chemically defined medium (Ristroph *et al.*, 1981) with minor adjustments (Eylert *et al.*, 2010) (see section 2.1.3.1 for composition). The aim was to reduce the available amino acids to an extent that growth was still feasible but *de novo* synthesis of several amino acids by the bacteria would be necessary to allow protein synthesis. The growth of *L. pneumophila* depends on certain essential amino acids like arginine, cysteine, isoleucine, leucine, methionine, threonine and valine, while serine is believed to be the major carbon substrate for *L. pneumophila* during extracellular growth (Tesh and Miller, 1981; Eylert *et al.*, 2010). This is in line with our findings, showing that a medium that only contained these essential amino acids or chemically defined medium (CDM) without serine did not sustain growth of *L. pneumophila*, and the bacteria did not replicate within the course of 48 h (Figure 3.1 A). Interestingly, the addition of serine to the essential amino acid medium did also not restore growth, showing that even if serine is the major carbon substrate of *L. pneumophila*, it is not sufficient as a sole source of carbon and energy (Figure 3.1 A). Subsequently, single non-essential amino acids were depleted from the medium and it was observed that leaving out histidine, lysine, proline, tryptophan or aspartate did not alter growth compared to CDM after 48 h (Figure 3.1. B). Furthermore, in media without aspartate and histidine or aspartate and tryptophan the bacteria did reach optical densities comparable to growth in CDM, but depletion of lysine or proline in addition to aspartate significantly reduced growth (Figure 3.1 B). As a next step, a medium was used that lacked all amino acids, which had no significant growth altering effect in the previous experiments, namely histidine, aspartate, tryptophan, lysine and glutamate. This medium (DM) did not allow the bacteria to reach optical densities as high as in CDM after 72 h of growth (Figure 3.1 C), but it still allowed replication efficient enough for the bacteria to produce the brown pigment and apparently reach the transmissive state as judged by shape and motility of the cells (data not shown).

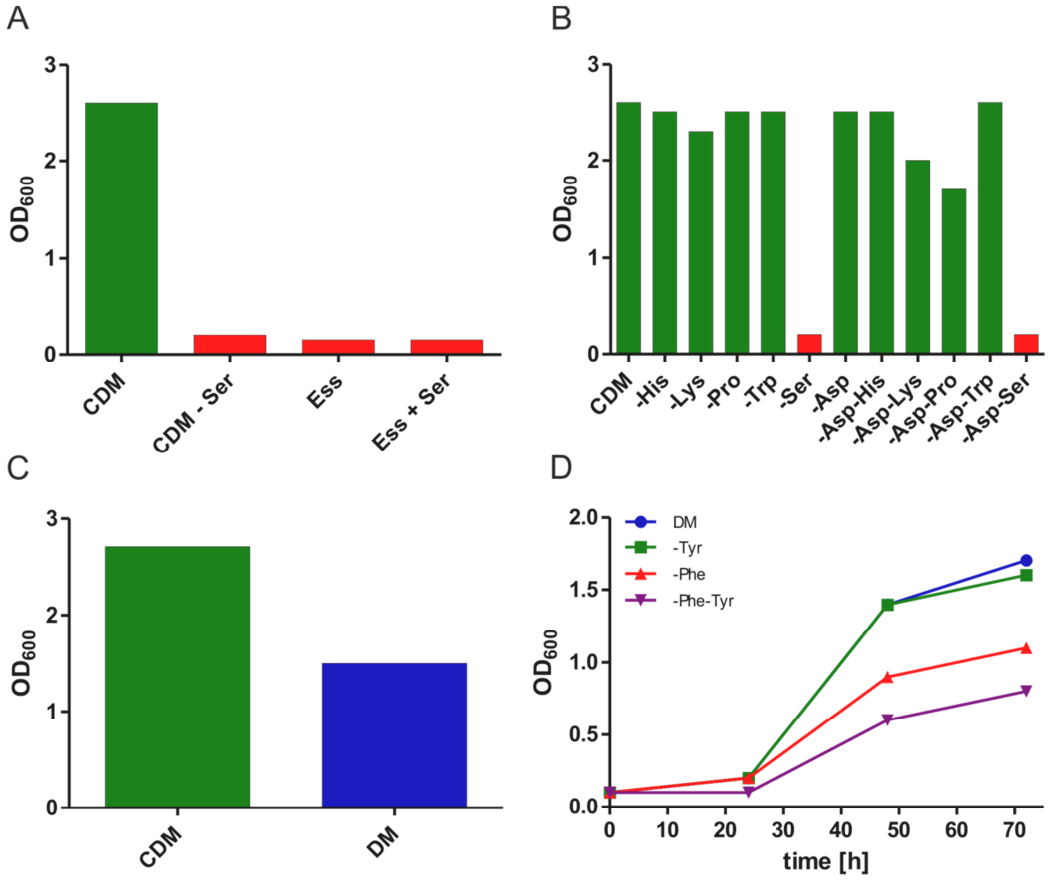

Figure 3.1: Designing a new *Legionella* growth medium. *L. pneumophila* wild-type was grown, in all experiments, at 37°C with a starting OD_{600} of 0.1. Growth in CDM, CDM without serine, a medium only containing essential amino acids (Ess) or additional serine (Ess + Ser) was assessed after 48 h (**A**). Defined media lacking single amino acids or pairs of amino acids were compared, and the optical density was measured after 48 h of growth (**B**). Comparison of optical densities after 72 h of growth in CDM and defined medium (DM) lacking His, Lys, Asp, Trp and Glu (**C**). Growth curve comparison of *L. pneumophila* wild-type grown in DM and DM lacking Tyr, Phe or Phe and Tyr (**D**). Amino acids are shown in three letter code (adapted from Häuslein, Manske *et al.*, 2015).

Finally, the impact of aromatic amino acids on *L. pneumophila* growth was assessed. A medium without tyrosine supported growth comparable to growth in DM over the course of 72 h. Depletion of phenylalanine and phenylalanine and tyrosine on the other side significantly reduced growth (Figure 3.1 D). Phenylalanine seems to be more important for *L. pneumophila* than tyrosine, as this amino acid can also be directly synthesized from phenylalanine in the reaction catalyzed by phenylalanine hydroxylase (*phhA*). This is why the final new defined medium contained phenylalanine, but not tyrosine. Salt composition and iron concentration was not altered compared to CDM, but the new medium was depleted of aspartate, glutamate, histidine, lysine, tryptophan and tyrosine in the end. This new medium was named minimal defined medium (MDM) (for composition see section 2.1.3.1).

3.2 Analysis of the Glycerol Metabolism of *Legionella pneumophila*

3.2.1 Glycerol Promotes Intracellular Growth of *Legionella pneumophila*

Early studies using radiolabeled glycerol and bacteria grown in defined medium suggested that glycerol might be metabolized by *L. pneumophila* (Tesh *et al.*, 1983). Furthermore, the transcriptome of *L. pneumophila* growing inside human macrophages showed that the expression of glycerol kinase (*lpg1414*) and glycerol-3-phosphate dehydrogenase (*glpD*) was 2- or almost 4-fold upregulated compared to bacteria growing in broth, indicating that glycerol might play a role during intracellular growth of *L. pneumophila* (Faucher *et al.*, 2011).

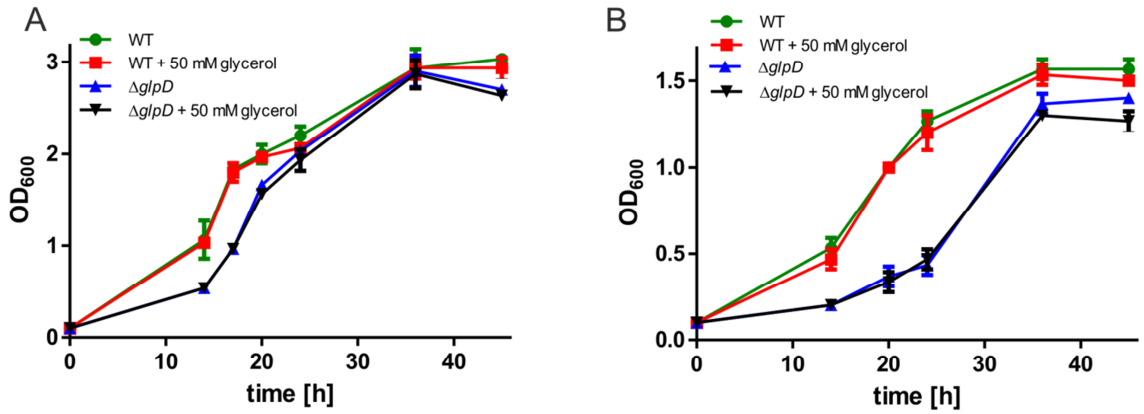

Figure 3.2: Glycerol has no influence on extracellularly growing *L. pneumophila*. Extracellular growth of *L. pneumophila* wild-type (WT) and Δ*glpD* in CDM (**A**) or MDM (**B**) with and without 50 mM glycerol. Bacteria were diluted to a starting OD_{600} of 0.1, glycerol was added at the beginning of the experiment and optical density at 600 nm was determined at the time points indicated. Graphs are representatives of three independent experiments. Shown are mean and SD of triplicates (adapted from Häuslein, Manske *et al.*, 2015).

Using defined media, glycerol had no influence on extracellularly growing *Legionella* (Figure 3.2). The addition of 50 mM glycerol to *L. pneumophila* wild-type or Δ*glpD* growing in CDM (Figure 3.2 A) or MDM (Figure 3.2 B) did not lead to altered growth compared to untreated bacteria. In AYE broth, growth of wild-type and mutant Δ*glpD* was indistinguishable (data not shown), but the mutant did grow slower in MDM and exhibited a longer lag phase than the wild-type although it did reach optical densities comparable to wild-type bacteria after 48 h of growth (Figure 3.2 B). As for wild-type, the addition of 50 mM glycerol did not influence growth of Δ*glpD*.

The impact of glycerol on intracellularly growing *L. pneumophila* was assessed using fluorescence-based assays, colony-forming units (cfu) and coinfection experiments (see sections 2.2.9 and 2.2.10). The glycerol-3-phosphate dehydrogenase GlpD is not essential for successful

replication of *L. pneumophila,* as the mutant strain Δ*glpD* did grow like wild-type in all intracellular replication assays (Figure 3.3 A-C). When glycerol was added to infected macrophages 4 h post infection, higher cell numbers were obtained for wild-type *L. pneumophila* in stationary growth phase indicated by higher fluorescence levels (Figure 3.3 A) and a greater number of cfu after 48 h of intracellular growth (Figure 3.3 B).

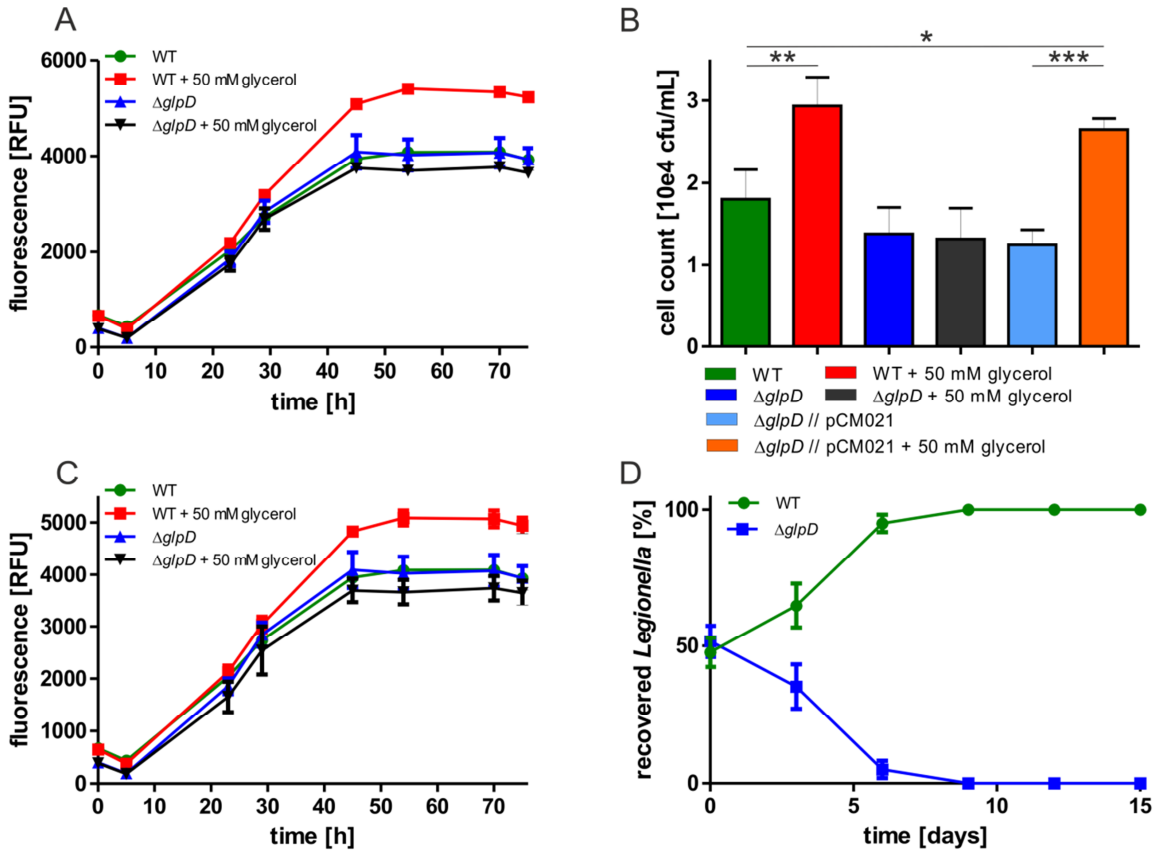

Figure 3.3: Glycerol promotes intracellular growth of *L. pneumophila*. Murine macrophages were infected (MOI 20) with *L. pneumophila* wild-type (WT) or Δ*glpD* harboring plasmid pNT28 (constitutive GFP expression). 50 mM glycerol was added 4 h post infection and replication was determined by fluorescence (**A**). For cfu-assays, murine macrophages were infected (MOI 0.1) with *L. pneumophila* wild-type (WT), Δ*glpD* or Δ*glpD* harbouring plasmid pCM021 (expression of *glpD*). 50 mM glycerol was added 4 h post infection, cells were lysed 48 h post infection and cfu were determined (1 way ANOVA test with Dunett`s multiple comparison test: p* < 0.05, p*** < 0.0001) (**B**). *A. castellanii* was infected (MOI 20) with *L. pneumophila* wild-type (WT) or Δ*glpD* harbouring pNT28. Glycerol was added 4 h post infection and replication was determined by fluorescence (**C**). For coinfection assays, *A. castellanii* were infected with *L. pneumophila* wild-type (WT) and Δ*glpD* at a 1:1 ratio (MOI 0.01 each). Cells were lysed three days post infection and bacteria were used to infect fresh amoeba. Cell numbers were determined by cfu (**D**). Data in (**A**)-(**D**) are representatives of three independent experiments. Mean and SD of triplicates are shown (adapted from Häuslein, Manske *et al*., 2015).

When comparing the intracellular growth curves of wild-type bacteria with and without glycerol, it was evident that the addition of glycerol did not lead to faster intracellular growth, as the levels

of fluorescence were comparable with and without glycerol (Figure 3.3 A). However, it rather seemed that glycerol might be used in later stages of intracellular growth, as fluorescence and therefore the number of intracellular bacteria increased in the late exponential growth phase leading to higher cell numbers in the stationary growth phase (Figure 3.3 A). This positive growth effect of glycerol was dependent on GlpD as it was not observed in the Δ*glpD* mutant and the phenotype could be complemented by providing *glpD* on a plasmid (Figure 3.3 B). The influence of glycerol on intracellular growing *L. pneumophila* was also analyzed in infected *A. castellanii*. Previous studies of the *L. pneumophila* transcriptome during intracellular replication in *A. castellanii* showed the upregulation of *glpD* and *lpg1414* in a similar way than during growth in macrophages (Brüggemann *et al.*, 2006), although not as pronounced. Nevertheless, addition of 50 mM glycerol to infected amoeba 4 h post infection promoted growth of *L. pneumophila* dependent on *glpD* (Figure 3.3 C). These results indicate that glycerol has a growth stimulating effect on *L. pneumophila* growing in different host cells. Lastly, coinfections of *A. castellanii* with wild-type and mutant Δ*glpD* showed that the mutant had a replication disadvantage compared to wild-type bacteria as it was outcompeted within 6 days (Figure 3.3 D), although it had no growth defect in all other intracellular assays. Glycerol might therefore be not essential for intracellular growth, but the metabolism of glycerol seems to provide a certain growth advantage to *L. pneumophila*.

3.2.2 Deciphering the Metabolism of Glycerol *in vitro*

Although glycerol had no apparent effect on extracellular growing bacteria (section 3.2.1), analyzed glycerol metabolism by *L. pneumophila* using isotopologue profiling, a method based on the incorporation of ^{13}C-atoms derived from labelled precursors, e.g. [U-$^{13}C_3$]glycerol (U meaning that all C-atoms in glycerol are ^{13}C-labelled). Metabolism of these precursors leads to ^{13}C-enrichment in amino acids and intermediates of central metabolism, allowing the determination of the overall enrichment and isotopologue composition in these metabolites by GC/MS (see section 2.2.16 for details, especially regarding the evaluation of different mass fragments in the isotopologue profiles). The ^{13}C-excess of a metabolite indicates how much of that metabolite in the bacterial cell was ^{13}C-labelled. The isotopologue profile, on the other hand, describes the relative fraction of isotopologues within that ^{13}C-labelled metabolite population and specifies how many C-atoms of a metabolite were ^{13}C-labelled. The first experiments with *L. pneumophila* grown in AYE or CDM did not result in significant ^{13}C-enrichment in any

metabolite measured (data not shown). MDM (see section 3.1) was therefore used in all further isotopologue experiments. *L. pneumophila* wild-type and mutant Δ*glpD* were grown in MDM in presence of 50 mM [U-$^{13}C_3$]glycerol as precursor for isotopologue profiling. The bacteria were grown for 48 h, so that they reached the stationary growth phase, as determined in extracellular growth experiments (Figure 3.2 B). Cells were harvested and the overall ^{13}C-enrichment in amino acids, PHB, lactate, fatty acids, intermediates of the TCA cycle and mannose was measured.

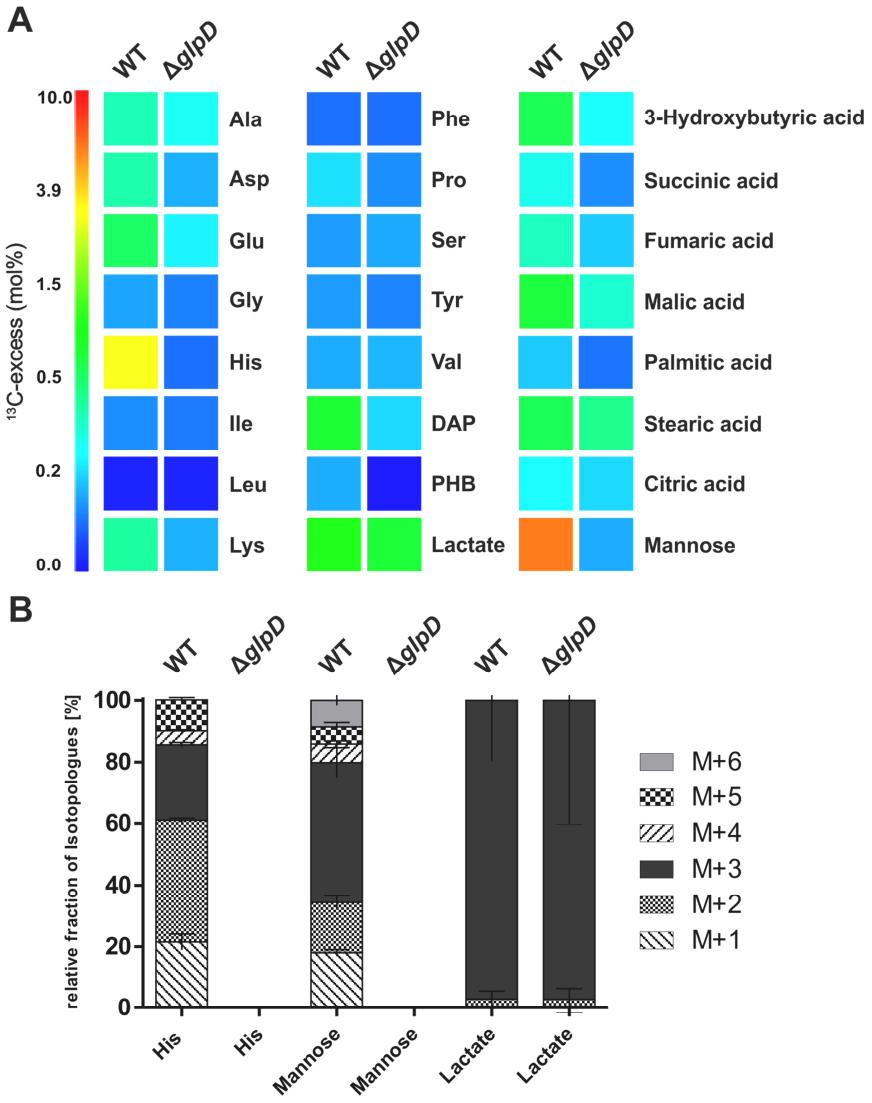

Figure 3.4: Glycerol metabolism of *L. pneumophila in vitro*. *L. pneumophila* wild-type (WT) and Δ*glpD* were grown in MDM containing 50 mM [U-$^{13}C_3$]glycerol and incubated at 37°C for 48 h. Cells were harvested, and the ^{13}C-excess (in mol% as color map) of protein-derived amino acids, diaminopimelic acid (DAP), polyhydroxybutyrate (PHB), methanol-soluble metabolites and mannose was quantified by GC/MS (**A**). The relative fractions (in %) of ^{13}C-isotopologues (M+1 to M+6) of histidine, mannose and lactate from *L. pneumophila* WT and Δ*glpD* were determind (**B**). Amino acids are shown in three letter code. Mean and SD from three independent experiments is shown. For numerical values refer to Supplementary Tables 5.2 and 5.3 (Published in Häuslein, Manske *et al.*, 2015).

Growth in MDM indeed showed that glycerol was metabolized by *L. pneumophila* in a *glpD*-dependent manner (Figure 3.4 A). Significant label (here defined as a ^{13}C-excess greater than 0.5%) was detected in lactate (0.97%), DAP (0.74%), malic acid (0.70%), 3-hydroxybutyric acid (0.61%), stearic acid (0.60%) and glutamate (0.55%). However, the highest enrichment was found in histidine (3.01%) and in mannose (5.75%), which allowed certain conclusions regarding the metabolism of glycerol (Figure 3.4 A). Fructose or rather fructose-6-phosphate and fructose-1,6-bisphosphate are central metabolites of gluconeogenesis. Mannose or mannose-6-phosphate, which were measured here, are synthesized from fructose-6-phosphate in the reaction of mannose-6-phosphate isomerase (*lpg2374*) (only mannose could be detected here, as sample preparation for isotopologue profiling resulted in dephosphorylation of sugars, see section 2.2.15). The isotopologue profile of mannose mainly displayed M+3 (~ 46%) and to a minor extent M+6 (~ 8.6%), reflecting how fully labelled ^{13}C-glycerol entered central metabolism at the stage of dihydroxyacetone-phosphate/glyceraldehyde-3-phosphate, then being converted to fructose-1,6-bisphosphate in the reverse reaction of fructose-1,6-bisphosphate aldolase and further on to fructose-6-phosphate and finally mannose-6-phosphate (Figure 3.4 B). M+3 label in mannose is therefore derived from the fusion of one fully labeled and one unlabeled glyceraldehyde-3-phosphate molecule and M+6 accordingly via the conversion of two fully labeled molecules.

Histidine is synthesized from ribose-5-phosphate within the PPP. The enrichment in histidine (Figure 3.4 A) shows that glycerol was first shuffled into gluconeogenesis and then into the PPP, where histidine was derived from. As *L. pneumophila* does not have a 6-phosphogluconate-dehydrogenase, only the non-oxidative parts of the PPP can take place. Hence, the key metabolite for entry into the PPP would not be glucose-6-phosphate but rather fructose-6-phosphate. This is in line with the observed isotopologue pattern of histidine (Figure 3.4 B). The isotopologue profile of histidine showed a large M+2 fraction (~ 40%) and a large M+3 fraction (~ 25%), both derived from transketolase reactions between glyceraldehyde-3-phosphate and fructose-6-phosphate (Figure 3.4 B). Section 4.2, Figure 4.1 outlines detailed information of carbon flow towards mannose and histidine, and provides explanations for the observed isotopologue profiles of these metabolites.

No significant incorporation of ^{13}C-label into any of the metabolites mentioned above was measured for the *glpD* mutant. This demonstrated that the metabolism of glycerol was entirely dependent on GlpD. Interestingly, only lactate was significantly ^{13}C-enriched (0.71%, Figure

3.4 A) in the mutant strain, and the isotopologue profile of lactate was identical for both wild-type and the mutant, showing only completely M+3 labelled lactate (Figure 3.4 B). No enrichment was measurable in essential amino acids (Ile, Leu, Ser, Val), alanine as derivative of pyruvate, amino acids derived from the TCA cycle (Asp, Lys, Pro) and generally in intermediates of the TCA cycle (succinic, fumaric and citric acid) for wild-type or the mutant strain (Figure 3.4 A). Taken together, these results showed that glycerol was predominantly metabolized in the gluconeogenic pathway and the PPP by *L. pneumophila*. The numerical values of ^{13}C-excess and isotopologue profiles are shown in Supplementary tables 5.2 and 5.3 respectively.

3.2.3 Time-dependent Glycerol Metabolism in Comparison to Other Carbon Substrates

The metabolism of glycerol was assessed in relation to other carbon sources. As it is known that serine and glucose are metabolized by *L. pneumophila in vitro* (Eylert *et al.*, 2010), the metabolism of these carbon sources was chosen to be compared to glycerol. The newly developed MDM contains 6 mM serine as an essential amino acid. In the following experiments, the medium was further enriched by adding 11 mM glucose and 50 mM glycerol. One of these carbon sources, serine, glucose or glycerol, was added as ^{13}C-labelled compound and cells were harvested after 12 h, 24 h, 36 h or 48 h. Based on the findings from extracellular growth experiments in MDM, these time points were chosen to represent early exponential (12 h), exponential (24 h), late exponential (36 h) and stationary (48 h) growth phase (compare section 3.2.1). The ^{13}C-enrichment in protein derived amino acids, DAP, PHB, polar metabolites and mannose was determined for all substrates used. The new adjusted medium was termed “carbon enriched minimal defined medium” (CE MDM).

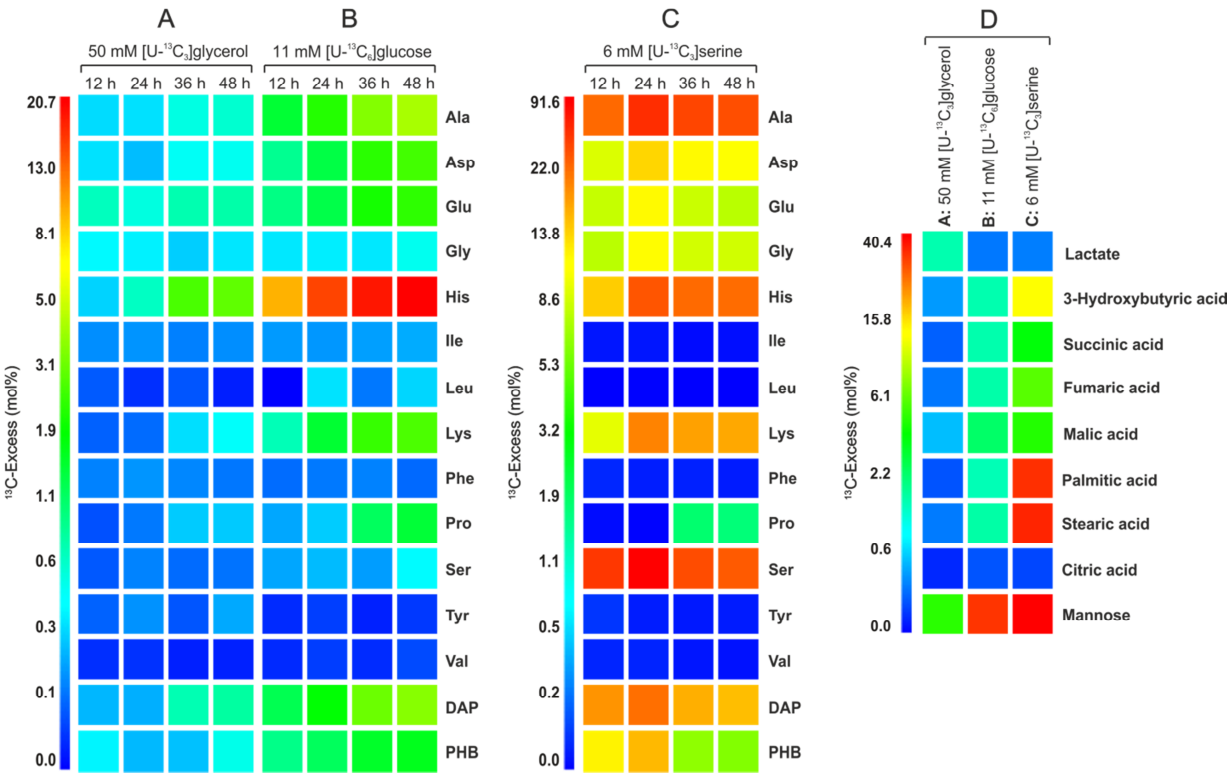

Figure 3.5: ^{13}C-excess (in mol%) in amino acids, polar metabolites and mannose of *L. pneumophila* wild-type grown in CE MDM. *L. pneumophila* wild-type was grown in CE MDM with either 50 mM [U-$^{13}C_3$]glycerol (**A**), 11 mM [U-$^{13}C_6$]glucose (**B**) or 6 mM [U-$^{13}C_3$]serine (**C**) as precursor. After 12 h, 24 h, 36 h and 48 h, samples were taken and incorporation of ^{13}C-label into protein derived amino acids, DAP and PHB (**A-C**) for all time points was determined. Incorporation of label into methanol-soluble metabolites and mannose was determined only after 48 h of growth (**D**). Color map correlates to mean and SD of three independent experiments. For numerical values refer to Supplementary Tables 5.4, 5.5 and 5.6 (Published in Häuslein, Manske *et al*., 2015).

As in the *in vitro* experiments in MDM with ^{13}C-glycerol as carbon source, growth in CE MDM resulted in incorporation of ^{13}C-label into histidine (3.00% after 48 h) and mannose (4.51% after 48 h) (Figure 3.5 A, D). Histidine and mannose were by far the highest labelled metabolites with ^{13}C-glycerol as precursor. To a minor extent, ^{13}C-label was also found in lactate (1.44%), DAP (0.80%), glutamate (0.77%), alanine (0.61%), malic acid (0.55%), PHB (0.52%) and aspartate (0.49%) after 48 h of growth (Figure 3.5 A, D). Significant label in any metabolite was only found after 36 h and 48 h of growth with glycerol as labelled precursor, indicating that glycerol was only used in late exponential and stationary growth phase. The isotopologue patterns for histidine, lactate and mannose were determined (Figure 3.6). Similar to growth in MDM, the pattern of lactate was completely M+3. The isotopologue pattern of histidine showed a large M+3 fraction (31.66%), and large M+1 (22.48%) and M+2 portions (35.70%). The largest isotopologue in mannose was also M+3 (40.59%), reflecting how glycerol was directly used to

make fructose and then mannose. The large M+1 and M+2 fractions in histidine are again derived from transketolase reactions with glyceraldehyde-3-phosphate and fructose-6-phosphate as precursor (Figure 3.6). In summary, also in the presence of glucose as additional carbon source, glycerol was metabolized by *L. pneumophila* in the gluconeogenic pathway and the PPP to produce histidine and mannose.

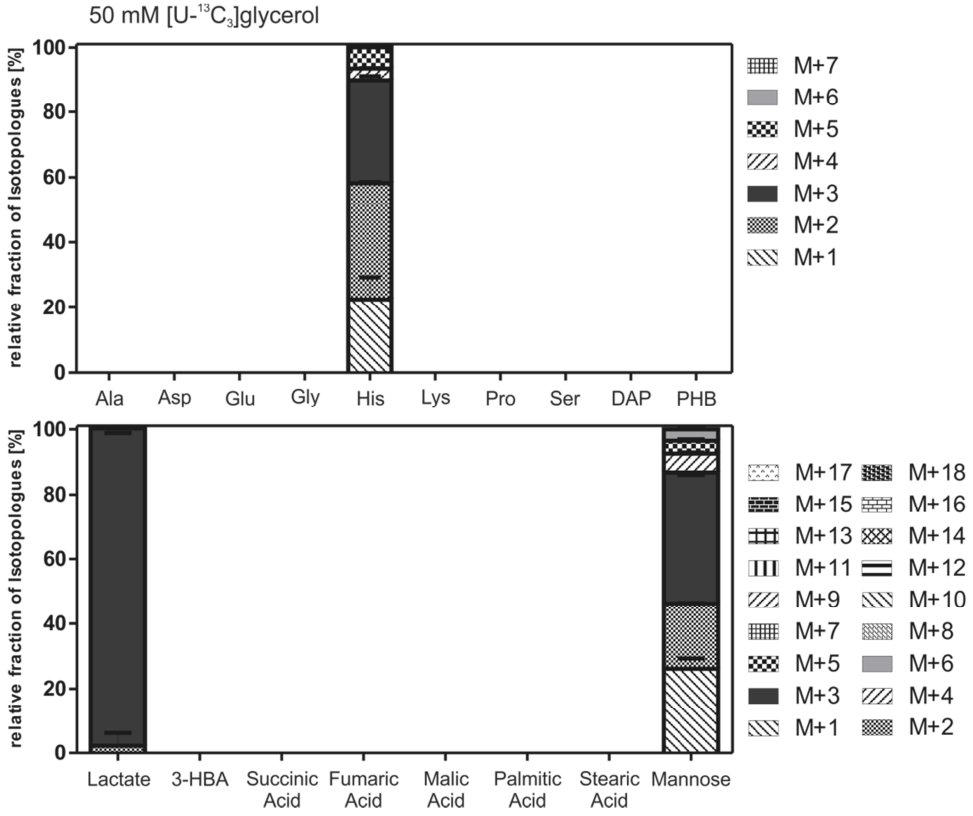

Figure 3.6: Isotopologue profiles of metabolites from experiments with [U-$^{13}C_3$]glycerol as precursor. Patterns of metabolites from growth experiments with *L. pneumophila* wild-type in CE MDM with 50 mM [U-$^{13}C_3$]glycerol as precursor that showed significant enrichment after 48 h are shown. A minimum of 1.00% ^{13}C-enrichment was chosen as threshold here. Columns indicate the relative fraction (in %) of isotopologues (M+1 to M+18) from three technical replicates. For numerical values refer to Supplementary Tables 5.7 and 5.8 (Adapted from Häuslein, Manske *et al*., 2015).

Glucose as precursor rendered the highest label in histidine (20.72%) and mannose (31.88%) after 48 h of growth (Figure 3.5 B, D). Additionally, several other metabolites were also significantly labelled with ^{13}C-glucose as precursor; the threshold here was defined as 1% incorporation. After 48 h of growth, alanine (4.26%), aspartate (2,61%), glutamate (2.36%), lysine (2.73%), proline (1.43%), DAP (3.64%), PHB (1.64%), 3-hydroxybutyric (1.45%), succinic (1.46%), fumaric (1.50%), malic (2.16%), palmitic (1.38%) and stearic acid (1.52%) were significantly ^{13}C-labelled (Figure 3.5 B, D). Significantly labelled metabolites were already

found after 12 h of growth, especially histidine was already highly labelled at early stages of growth (9.16% after 12 h) and the ^{13}C-excess was constantly rising over time (Figure 3.5 B). The isotopologue pattern of mannose revealed the route of glucose catabolism. The largest portion of mannose was M+3 (30.20%) and M+6 (31.50%) labelled, while histidine was, like in the experiments with glycerol, mainly M+2 (37.25%) and M+3 (21.61%) labelled with a greater portion of M+5 (14.62%) (Figure 3.7).

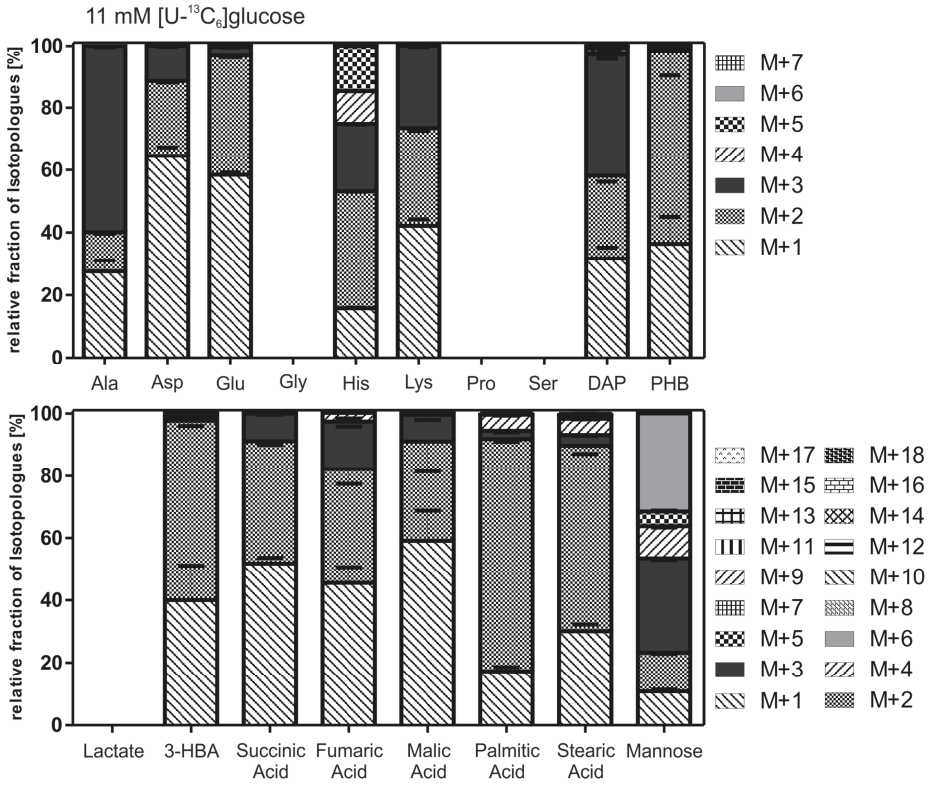

Figure 3.7: Isotopologue profiles of metabolites from experiments with [U-^{13}C$_6$]glucose as precursor. Patterns of metabolites from growth experiments with *L. pneumophila* wild-type in CE MDM with 11 mM [U-^{13}C$_6$]glucose as precursor that showed significant enrichment after 48 h are shown. A minimum of 1.00% ^{13}C-enrichment was chosen as threshold here. Columns indicate the relative fraction (in %) of isotopologues (M+1 to M+18) from three technical replicates. For numerical values refer to Supplementary Tables 5.7 and 5.8 (Adapted from Häuslein, Manske *et al*., 2015).

The major route of glucose metabolism for *L. pneumophila* is the ED pathway (Eylert *et al.*, 2010; Harada *et al.*, 2010), where glucose enters central metabolism on the stages of glyceraldehyde-3-phosphate and pyruvate, two C3-bodies. Mannose is then derived from gluconeogenesis with fructose-6-phosphate as precursor (M+3 and M+6), and labelled fructose-6-phosphate is also used for the reactions of the PPP where histidine is derived from. The M+5

isotopologue in histidine is the result of the greater portion of fully labelled fructose, of which fully labelled ribose-5-phosphate, the precursor for histidine, is derived from. The main flow of carbon from glucose is directed to mannose and histidine, but to a small amount also in the direction of the TCA cycle, as seen by the ^{13}C-enrichment in TCA intermediates and amino acids (Figure 3.5 B, D). Intermediates of the TCA (succinic, fumaric and malic acid) and amino acids derived from the TCA cycle (Asp and Glu) were mainly M+1 and M+2 labelled (Figure 3.7). The latter derived from fully labeled acetyl-CoA entering the TCA cycle, while the single label could be a result of a decarboxylation reaction of α-ketoglutarate dehydrogenase or multiple rounds of TCA cycle, where unlabeled acetyl-CoA was transferred onto labelled oxaloacetate. Glucose was used in part also for fatty acid synthesis (1.38% palmitic and 1.52% stearic acid labelled) (Figure 3.5 D), but the isotopologue pattern of these fatty acids was mainly M+2 (74.65% and 59.60%, respectively), showing the minor carbon flow from glucose to acetyl-CoA, the metabolic precursor for fatty acid synthesis (Figure 3.7). Alanine, as a direct derivative of pyruvate, was consequentially mainly M+3 (59.89%) labelled (Figure 3.7). In summary, glucose was, like glycerol, predominantly used for gluconeogenesis and PPP, but to a small amount also fed into the TCA cycle and fatty acid synthesis.

Serine was the carbon source that was used most effectively by *L. pneumophila*. When fed with [U-$^{13}C_3$]serine as precursor, ^{13}C-enrichment could be detected in the same metabolites as in the time series experiments with labelled glucose (Figure 3.5 C, D).

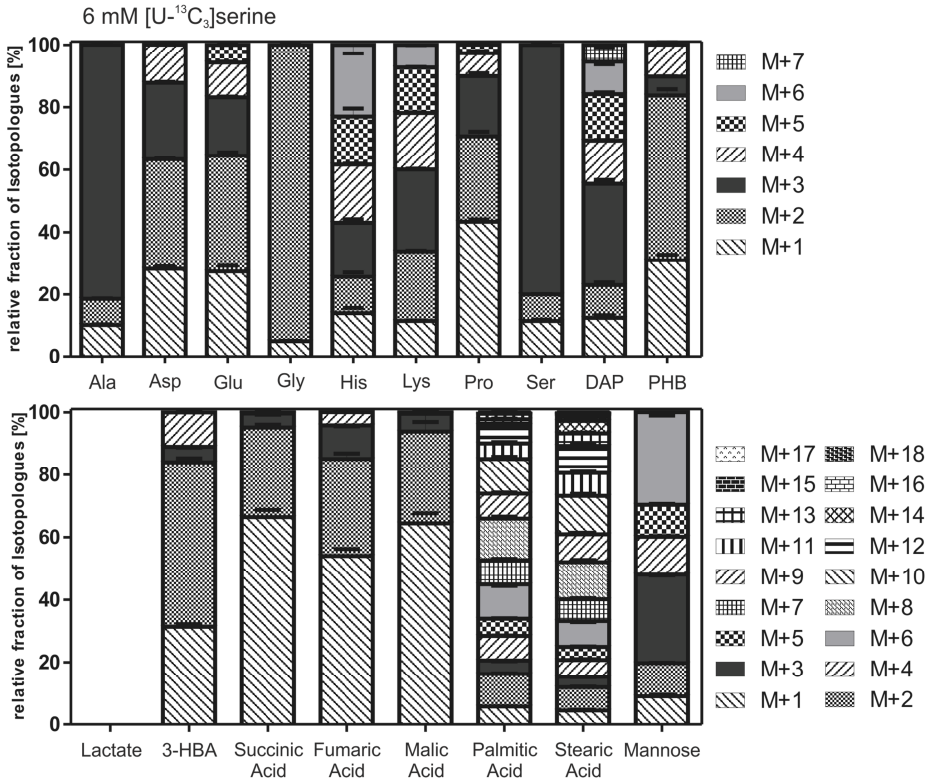

Figure 3.8: Isotopologue profiles of metabolites from experiments with [U-$^{13}C_3$]serine as precursor. Patterns of metabolites from growth experiments with *L. pneumophila* wild-type in CE MDM with 6 mM [U-$^{13}C_3$]serine as precursor that showed significant enrichment after 48 h are shown. A minimum of 1.00% ^{13}C-enrichment was chosen as threshold here. Columns indicate the relative fraction (in %) of isotopologues (M+1 to M+18) from three technical replicates. For numerical values refer to Supplementary Tables 5.7 and 5.8 (Adapted from Häuslein, Manske *et al*., 2015).

Additionally, glycine, proline and of course serine were ^{13}C-labelled. The overall excess in all metabolites measured was much higher than in experiments with glycerol or glucose as precursors, confirming the central role of serine as carbon source for *L. pneumophila*. Interestingly, the enrichment in all metabolites peaked at 24 h and dropped steadily afterwards (Figure 3.5 C). Significantly labelled metabolites after 24 h of growth were serine (91.61%), alanine (74.60%), histidine (62.05%), DAP (55.02%), lysine (50.22%), PHB (39.16%), aspartate (34.34%), glutamate (29.00%) and glycine (28.58%). After 48 h also polar metabolites and mannose were found to be highly ^{13}C-enriched, ranging between 3.53% enrichment in succinic acid and 40.40% in mannose (Figure 3.5 D). The isotopologue pattern of mannose was comparable with that derived from experiments with ^{13}C-glucose and showed large M+3 (28.34%) and M+6 (29.67%) labelled portions (Figure 3.8). Furthermore, histidine was highly

^{13}C-enriched, and the pattern was comparable to that from experiments with glucose, which shows that carbon flow from serine did also occur into gluconeogenesis and the PPP (Figure 3.8). However, the overwhelming part of label was found in metabolites derived from the lower parts of glycolysis and the TCA cycle, which illustrates how serine was preferably used by *L. pneumophila*.

Glycine, as a direct derivative of serine, was almost completely M+2 (95.02%) labelled, which shows its direct synthesis from serine in the reaction catalyzed by serine hydroxymethyltransferase (*glyA*) (Figure 3.8). Alanine is again mainly M+3 labelled (81.43%), as it is synthesized from pyruvate (Figure 3.8). Glutamate was highly ^{13}C-enriched (29.00% after 24 h), and the pattern reflects high flux from serine into acetyl-CoA, which then enters the TCA cycle. In addition to M+1 (27.39%) and M+2 (37.11%), and like in experiments with glucose as precursor, also M+3 (18.62%), M+4 (11.16%) and M+5 (5.71%) label was measured in glutamate (Figure 3.8), indicating that α-ketoglutarate, the precursor of glutamate, had to be enriched with a more complex isotopologue pattern as well. This is only possible, when a higher flux of labelled metabolites is directed into the TCA cycle. Proline is made directly from glutamate, and consistently, the isotopologue pattern of proline was almost identical to that of glutamate (Figure 3.8). Label in proline was only found after 36 h and 48 h of growth, but not in earlier stages (Figure 3.5 C). As part of the growth medium, proline was apparently taken up and used efficiently by *L. pneumophila* and was only then synthesized *de novo* after it was consumed from the medium.

Aspartate is made from oxaloacetate, which is an intermediate of the TCA cycle, or directly synthesized from pyruvate in the reaction catalyzed by pyruvate carboxylase (*lpg0466*). The M+3 (24.48%) isotopologue that was measured for aspartate is the result of the direct synthesis from pyruvate, while the M+1 (28.29%), M+2 (35.03%) and M+4 (12.44%) families are the result of one or more rounds of TCA cycle, resulting in differentially labelled oxaloacetate (Figure 3.8). DAP is synthesized from aspartate and pyruvate, so the M+3 (32.48%) fraction in DAP was presumably again derived from fully labelled pyruvate. All other isotopologue fractions resulted from differentially labelled pyruvate and aspartate (Figure 3.8). Lysine is then made from DAP in a decarboxylation reaction, so all fractions except M+7 were also found in the isotopologue pattern of lysine (Figure 3.8).

The aforementioned high flux of serine into acetyl-CoA and the TCA cycle is also reflected in the isotopologue profile of the fatty acids palmitic and stearic acid, which mainly showed M+2,

M+4, M+6, M+8, M+10 and M+12 labelling (Figure 3.8). Acetyl-CoA is the precursor of the C2-building blocks of fatty acids, and the fractional profile therefore is the result of a large number of fully labelled acetyl-CoA molecules. This was different from the results obtained with ^{13}C-glucose as precursor, where mostly M+2 label was detected in the fatty acids, proving a low flow of labelled acetyl-CoA into fatty acid biosynthesis (Figure 3.7). Taken together, serine was, compared to glycerol and glucose, used as the most efficient carbon substrate and catabolized most efficiently in the lower parts of glycolysis and the TCA cycle. The numerical values of ^{13}C-excess and isotopologue profiles of all time course experiments are shown in Supplementary Tables 5.4-5.6 and 5.7-5.8, respectively.

3.2.4 Phosphorylated Metabolites are Preferred Substrates for *Legionella pneumophila*

As CE MDM contained glycerol and glucose as carbon sources in addition to serine, which could not be omitted as an essential amino acid, it was tested if glycerol and glucose influenced each others metabolism. To that end, time course experiments with *L. pneumophila* wild-type growing in MDM with 50 mM [U-$^{13}C_3$]glycerol or 50 mM [U-$^{13}C_3$]glycerol and 11 mM glucose (Figure 3.9 A) and also experiments in MDM containing 11 mM [U-$^{13}C_6$]glucose or 11 mM [U-$^{13}C_6$]glucose and 50 mM glycerol (Figure 3.9 B) were performed. Cells were cultured for 48 h, samples were taken after 12 h, 24 h, 36 h and 48 h, and ^{13}C-excess was determined. As histidine was always the highest labelled amino acid in previous experiments, only the ^{13}C-excess in histidine was compared here.

In experiments with ^{13}C-glycerol, the addition of glucose led to a drop of 20-25% in ^{13}C-enrichment in histidine (Figure 3.9 A). Significant label in histidine was again only measured after 36 h of growth. This showed that glycerol was also metabolized in the presence of glucose, but that glucose had an influence on the metabolism of glycerol. In labelling experiments with ^{13}C-glucose, the addition of glycerol did not lead to significant changes in ^{13}C-excess in histidine (Figure 3.9 B). Therefore, glycerol and glucose seem to be co-metabolized independently by *L. pneumophila* with glucose as the preferred carbon substrate.

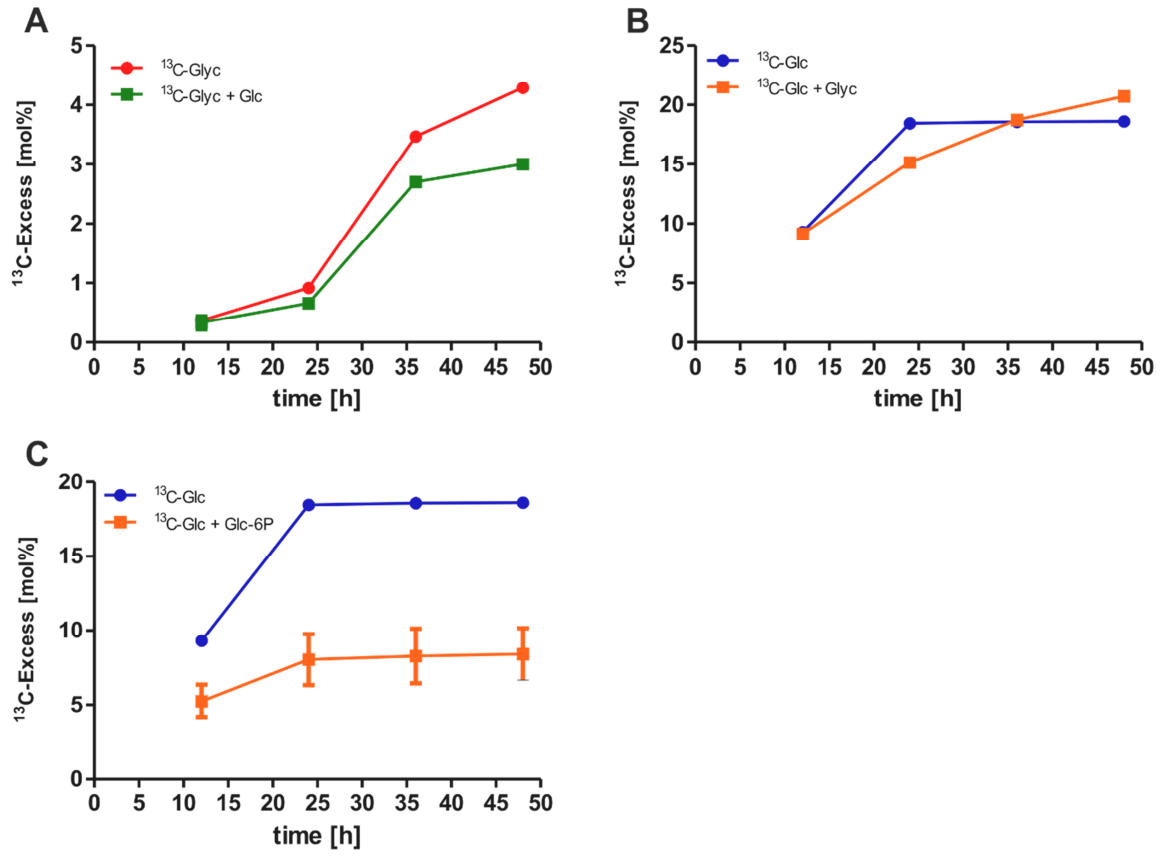

Figure 3.9: Co-metabolism of glycerol and glucose by *L. pneumophila* and phosphorylated sugars as preferred substrates. *L. pneumophila* wild-type was grown in MDM with either 50 mM [U-$^{13}C_3$]glycerol (**^{13}C-Glyc**) or 50 mM [U-$^{13}C_3$]glycerol and 11 mM glucose (**Glc**) (**A**), 11 mM [U-$^{13}C_6$]glucose (**^{13}C-Glc**) or 11 mM [U-$^{13}C_6$]glucose and 50 mM glycerol (**Glyc**) (**B**) or 11 mM [U-$^{13}C_6$]glucose and 11 mM glucose-6-phosphate (**Glc-6P**) (**C**). After 12 h, 24 h, 36 h and 48 h samples were taken and incorporation of ^{13}C-label into histidine (**A-C**) for all time points was determined. Shown are mean and SD of three technical replicates. For numerical values refer to Supplementary Table 5.9.

An interesting observation was made, when growth with 11 mM ^{13}C-glucose alone was compared to growth with 11 mM ^{13}C-glucose and 11 mM unlabeled glucose-6-phosphate present in the medium at the same time. The addition of phosphorylated glucose led to a significant drop in ^{13}C-enrichment in histidine over the time course of the experiment (Figure 3.9 C). ^{13}C-excess dropped over 50% compared to experiments with labelled glucose alone, while the extracellular growth *per se* was not affected. This observation allows the conclusion that phosphorylated carbohydrates might be the better substrates for *L. pneumophila*. The numerical values of ^{13}C-excess of co-metabolism experiments are shown in Supplementary Table 5.9.

3.2.5 Metabolism of Glycerol, Glucose and Serine is Restricted to Certain Pathways

For a better overview of the time-dependent metabolism of glycerol, glucose and serine, four metabolites were chosen that were not present in CE MDM medium and therefore had to be synthesized *de novo* by *L. pneumophila*. Furthermore, the four metabolites were chosen to represent different metabolic pathways and/or intermediates. Alanine, with pyruvate as precursor, histidine, derived from the PPP, diaminopimelic acid (DAP), synthesized through the TCA and from pyruvate, as well as PHB, with acetyl-CoA as precursor, were chosen, and ^{13}C-excess in these metabolites was followed over 48 h. The following graphs are based on the data obtained in section 3.2.3 from time-series experiments in CE MDM with ^{13}C-glycerol, ^{13}C-glucose or ^{13}C-serine as precursors.

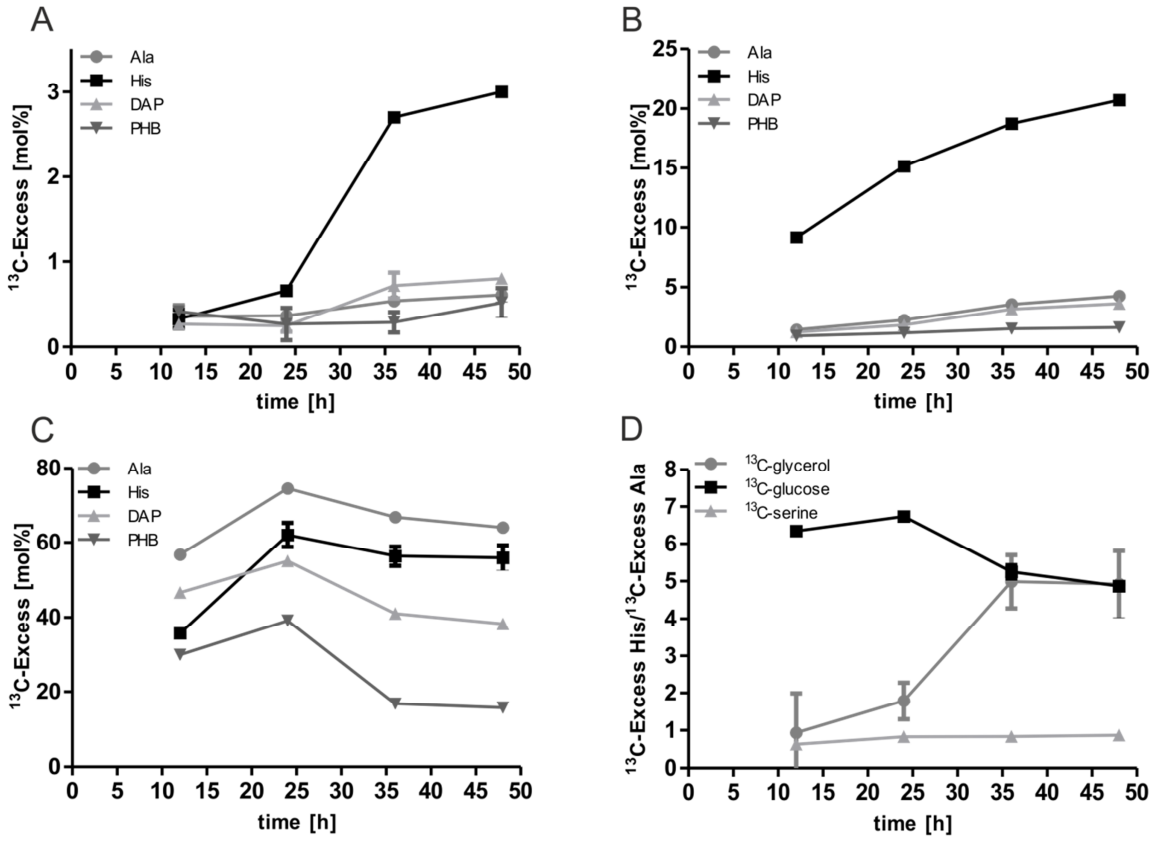

Figure 3.10 Analysis of carbon flux from different substrates into metabolic markers. The ^{13}C-enrichment in alanine, histidine, DAP and PHB over time of *L. pneumophila* wild-type grown in CE MDM with 50 mM [U-$^{13}C_3$]glycerol (**A**), 11 mM [U-$^{13}C_6$]glucose (**B**) or 6 mM [U-$^{13}C_3$]serine (**C**) as precursor was compared. The ratio of ^{13}C-excess in histidine to ^{13}C-excess in alanine with ^{13}C-glycerol, ^{13}C-glucose or ^{13}C-serine as substrate reveals carbon fluxes into gluconeogenesis/PPP or the TCA cycle (**D**). For numerical values refer to Supplementary Table 5.10 (Published in Häuslein, Manske *et al*., 2015).

Histidine was the highest labelled metabolite, when growing with ^{13}C-glycerol as precursor and label was only detected after 36 h and 48 h of growth (Figure 3.10 A). Glycerol was therefore only used in later stages of *L. pneumophila* growth. With ^{13}C-glucose as precursor, histidine was also the highest labelled metabolite that was monitored here. However, incorporation of ^{13}C-label into histidine did occur already at early time points (12 h) and increased continuously over time. The overall enrichment in all metabolites was also higher compared to experiments with ^{13}C-glycerol (Figure 3.10 B). ^{13}C-enrichment in all metabolites from experiments with ^{13}C-serine as precursor peaked already after 24 h and dropped steadily afterwards. Alanine was the highest labelled metabolite, and the overall excess in all metabolites was much higher compared to the experiments with ^{13}C-glycerol and ^{13}C-glucose (Figure 3.10 C). Serine was therefore used as the most effective carbon source here, which was metabolized during all growth phases. Glycerol, on the other hand, is obviously only used in the stationary growth phase, while glucose is used continuously, but mainly as precursor for histidine synthesis.

To illustrate how a carbon substrate was preferably used by *L. pneumophila*, the ratio of ^{13}C-excess in histidine and ^{13}C-excess in alanine was plotted against time (Figure 3.10 D). A high ratio indicated that carbon flux was mainly directed towards the PPP, while a small value indicated flow towards the lower parts of glycolysis, as alanine is made from pyruvate, and into the TCA cycle. Serine as precursor yielded a ratio that stayed below 1 throughout the course of the experiment, indicating that carbon flow from serine was mainly directed towards the TCA. The complete opposite was observed for carbon flow from glucose. Here, the ratio was high, indicating a preferred flow into the PPP towards histidine. The ratio was dropping slightly after 36 h, when glycerol was also used as a carbon substrate. Also here the ratio was high, indicating that the carbon flow from glycerol was also mainly directed towards the PPP. The low ratio that was observed for glycerol at 12 h and 24 h was a result of the low overall enrichments in alanine and histidine and does not indicate that the carbon flow was directed towards the TCA, as significant enrichments with ^{13}C-glycerol as precursor were only obtained after 36 h of growth (Figure 3.10 D). These results clearly showed that glycerol and glucose were not as efficiently used as a carbon source by *L. pneumophila* as serine and that the flow from these substrates was mainly restricted towards gluconeogenesis and the PPP, while the flow from serine was preferentially directed towards the TCA cycle.

3.2.6 *In vivo* Metabolism of Glycerol Leads to the Synthesis of Mannose

The role that glycerol and other substrates play for the intracellular metabolism of *L. pneumophila* was examined in infected *A. castellanii*. Previous studies already showed that *L. pneumophila* imported labeled amino acids from *A. castellanii* fed with ^{13}C-glucose prior to infection (Schunder *et al.*, 2014). One goal of present study was to test, if it is possible that a carbon substrate added to infected cells might be used directly by intracellular *L. pneumophila*. To this end, *A. castellanii* was infected with either *L. pneumophila* wild-type or Δ*glpD* (see section 2.2.12). [U-$^{13}C_3$]glycerol, [U-$^{13}C_6$]glucose or [U-$^{13}C_3$]serine was added to the infected amoebae 5 h post infection. After 15 h the cells were lysed and a protocol was used to separate the bacteria from eukaryotic cell debris (Schunder *et al.*, 2014). This protocol yielded three fractions: one with eukaryotic cell debris/components (F1), one containing *L. pneumophila* (F2) and one comprised of soluble proteins/factors (F3). The ^{13}C-excess and isotopologue patterns of protein-derived amino acids, DAP, PHB and mannose were determined for all fractions, but since F1 and F3 yielded identical results, only F1 was considered here. All amino acids that had been measured in previous experiments were also analyzed, but for the sake of simplicity, only amino acids that yielded significant enrichments are shown (Ala, Asp, Glu, Gly, Ser). Fatty acids and TCA intermediates could not be monitored, as these metabolites would have required sample sizes (bacterial cell mass) that were not obtainable with *in vivo* assays. Samples were subjected to microscopy and aliquots were plated on CYE agar plates to check for bacterial contaminations of F1 as well as purity of F2. Additionally, the amount of DAP, as a compound specific for bacteria, was monitored in F1. DAP never exceeded 10%, so it was concluded that bacterial contamination in this fraction was below that value. All infections were performed in AC buffer, which does not contain any nutrients, so the used precursors were the only available carbon substrates in these assays. To check if the infection with *L. pneumophila* would influence the metabolism of *A. castellanii*, uninfected amoebae were used and fed with ^{13}C-glycerol, ^{13}C-glucose or ^{13}C-serine.

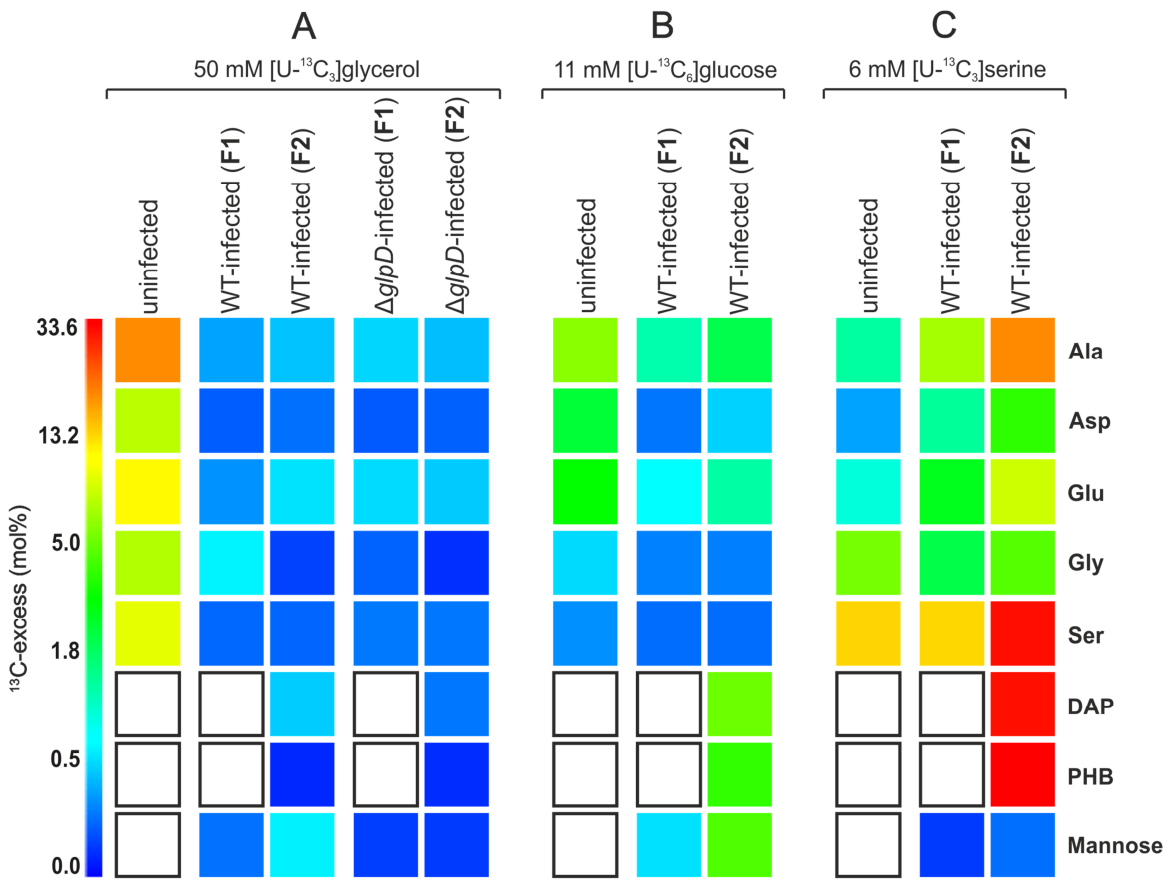

Figure 3.11: ^{13}C-excess in amino acids, DAP, PHB and mannose of *L. pneumophila* grown in *A. castellanii*. Amoeba were infected (MOI 50) with *L. pneumophila* wild-type (WT), mutant Δ*glpD* or used uninfected. 50 mM [U-$^{13}C_3$]glycerol (**A**), 11 mM [U-$^{13}C_3$]glucose (**B**) or 6 mM [U-$^{13}C_3$]serine (**C**) was added 5 h post infection. Cells were lysed 15 h post infection and eukaryotic cell debris (**F1**) and *L. pneumophila* cells (**F2**) were separated. ^{13}C-excess (in mol%) of Ala, Asp, Glu, Gly, Ser, DAP, PHB and mannose was analyzed. Data shown corresponds to mean and SD of two independent experiments. For numerical values refer to Supplementary Table 5.11 (Published in Häuslein, Manske *et al*., 2015).

Glycerol seems to be a favoured carbon substrate for *A. castellanii*, as the amoeba did incorporate ^{13}C-label from glycerol effectively into all amino acids measured, alanine (17.83%) and glutamate (10.65%) being the examples with the highest ^{13}C-enrichment (Figure 3.11 A). Intriguingly, upon infection with *L. pneumophila* wild-type or mutant Δ*glpD*, the incorporation dropped so drastically that no significant enrichment in any amino acid in F1 was detectable anymore. Furthermore, no label in the amino acids measured was detectable in fractions F2 of wild-type and Δ*glpD* infected *A. castellanii* (Figure 3.11 A). Uninfected amoeba fed with ^{13}C-glucose did incorporate significant amounts of ^{13}C-label into alanine (5.98%), aspartate (2.33%) and glutamate (3.09%) (Figure 3.11 B). Again, upon infection with *L. pneumophila*, there was a significant drop in ^{13}C-incorporation in F1, but under these conditions alanine

(2.06%), glutamate (1.28 %), DAP (5.18%) and PHB (3.91%) were found to be enriched in ^{13}C-label in fraction F2. With 5.18% ^{13}C-excess DAP was the highest labelled metabolite in F2 of wild-type infected amoeba (Figure 3.11 B). Serine was not as efficiently metabolized by *A. castellanii* as for example glycerol (Figure 3.11 C). The amoeba did take up ^{13}C-serine, but it was apparently used directly for protein synthesis for the most part and not metabolized. The highest ^{13}C-enrichment was found in protein-derived serine (12.63%) and its direct derivative glycine (5.43%). When infected, significant higher enrichment was observed in fraction F1, especially in alanine (6.85%), aspartate (1.36%) and glutamate (2.66%), while the incorporation levels into serine stayed at the same level as for uninfected amoeba (12.52%) (Figure 3.11 C). High ^{13}C-enrichments were also detected in F2 of wild-type infected amoeba fed with serine. Under these conditions, DAP, PHB and serine each reached levels over 30.00 %. Serine was, similar to results *in vitro*, used for synthesis of amino acids, as high ^{13}C-incorporation did occur into all amino acids measured, especially alanine with 17.90% enrichment. In all *in vivo* experiments, no label occurred in histidine in any *L. pneumophila* containing fractions (F2), suggesting that this amino acid is intracellularly not synthesized *de novo,* but taken up from the host cell.

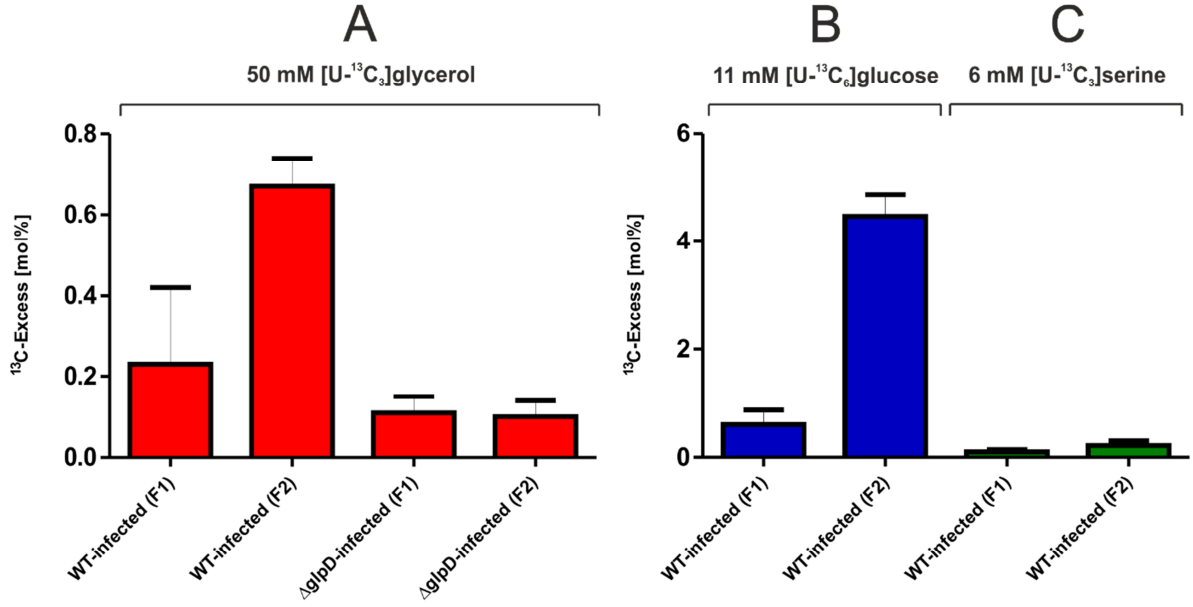

Figure 3.12: Analysis of mannose from *L. pneumophila* grown in *A. castellanii*. Amoebae were infected (MOI 50) with *L. pneumophila* wild-type (WT) or Δ*glpD*. 50 mM [U-$^{13}C_3$]glycerol (**A**), 11 mM [U-$^{13}C_3$]glucose (**B**) or 6 mM [U-$^{13}C_3$]serine (**C**) was added 5 h post infection. Cells were lysed 15 h post infection and eukaryotic cell debris (**F1**) and *L. pneumophila* cells (**F2**) were separated. ^{13}C-excess of mannose in F1 and F2 was analyzed. Mean and SD of two independent experiments are shown. For numerical values refer to Supplementary Table 5.11 (Published in Häuslein, Manske *et al*., 2015).

Anyway, the most interesting conclusions were drawn from analyzing mannose. Fraction F2 of wild-type infected amoeba fed with ^{13}C-glycerol resulted in a significant label in mannose (Figure 3.12 A). Significantly less label was detected in fraction F1. Furthermore, almost no label in mannose was measured in F1 and F2 of Δ*glpD* infected amoeba, showing that enrichment in wild-type F2 was dependent on GlpD (Figure 3.12 A). Also, the eukaryotic fraction F1 of wild-type infected *A. castellanii* fed with ^{13}C-glucose did not yield significant label in mannose, whereas mannose in fraction F2 was highly enriched (4.47%) (Figure 3.12 B). Experiments with ^{13}C-serine as precursor resulted in no incorporation into mannose, neither in F1 nor in F2 (Figure 3.12 C).

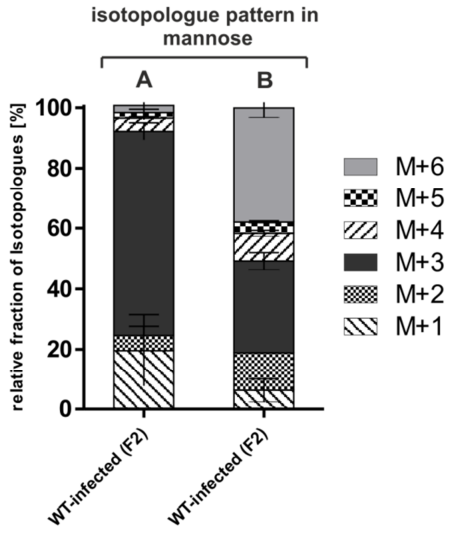

Figure 3.13: Isotopologue pattern of mannose from *L. pneumophila* wild-type grown in *A. castellanii*. The isotopologue pattern of mannose from *Legionella* containing fractions F2 of wild-type infected *A. castellanii* fed with [U-$^{13}C_3$]glycerol (**A**) or [U-$^{13}C_6$]glucose (**B**) are shown. Columns indicate the relative fraction (in %) of ^{13}C-isotopologues (M+1 to M+6). Data shown represent mean and SD of two independent experiments. For numerical values refer to Supplementary Table 5.12 (Adapted from Häuslein, Manske *et al*., 2015).

The isotopologue pattern of mannose from *in vivo* experiments with ^{13}C-glycerol as precursor revealed that the sugar was mostly M+3 (~ 68%) labelled, suggesting that glycerol was directly used for gluconeogenesis to make fructose and subsequently mannose (Figure 3.13 A). The pattern reflected that of mannose from *in vitro* experiments relatively well (compare Figure 3.4 B). Furthermore, the lack of significant label in mannose with *L. pneumophila* Δ*glpD* proved that ^{13}C-incorporation into mannose was a result of direct uptake of glycerol into the LCV and direct synthesis of mannose from glycerol by *L. pneumophila* (Figure 3.12 A). The isotopologue

pattern of mannose from *in vivo* experiments with ^{13}C-glucose was also almost identical to that of *L. pneumophila* grown in CE MDM (compare Figure 3.7), displaying mainly M+3 (~ 30%) and M+6 (~ 38%) (Figure 3.13 B). Furthermore, as no incorporation in F1 was detectable here (Figure 3.12 B), it was concluded that also glucose was taken up directly from the host cell (M+6) and metabolized by the bacteria (M+3). The numerical values of ^{13}C-excess and isotopologue profiles of all *in vivo* experiments are documented in Supplementary Tables 5.11 and 5.12, respectively.

Taken together, it was shown that glycerol also serves intracellularly as a carbon substrate and is used exclusively for anabolic reactions by *L. pneumophila*, similar to results obtained *in vitro*. Glycerol and glucose can reach the bacteria inside the LCV without being metabolized by the amoeba, expanding the intracellular diet of *L. pneumophila* from only amino acids to sugars as additional carbon source. The absence of label in mannose, when fed with ^{13}C-serine, suggests that, similar to growth *in vitro*, flow of carbon from different substrates might be preferentially directed to certain pathways by intracellular growing *L. pneumophila*.

3.3 Analysis of the Inositol Metabolism of *Legionella pneumophila*

3.3.1 A Putative Inositol Degradation Cluster in the Genome of *Legionella pneumophila*

Myo-inositol (here referred to as "inositol") is used as the sole source of carbon by many bacteria, including *Bacillus subtilis* (Yoshida *et al.*, 2008), *Lactococcus casei* (Colas *et al.*, 2015) or *Salmonella enterica* (Kröger and Fuchs, 2009). Genes involved in inositol catabolism are organized in operons in these organisms (see section 1.3.2 for details). Interestingly, also the genome of *L. pneumophila* harbors a group of genes putatively involved in inositol metabolism (Figure 3.14).

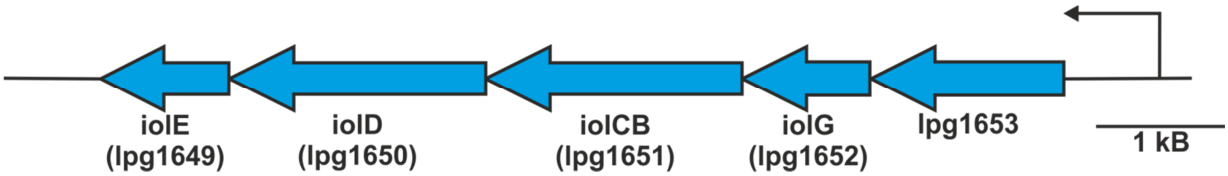

Figure 3.14: The *lpg1653- lpg1649* operon of *L. pneumophila*. The gene cluster contains five genes predicted to be involved in inositol metabolism, including the putative inositol transporter Lpg1653, and the inositol catabolism proteins IolG, IolCB, IolD and IolE.

The gene cluster of interest is located in a 7 kB large region on the *L. pneumophila* chromosome and contains five genes, *lpg1653-lpg1649*. The genes are organized in an operon as predicted by the DOOR^2 database of prokaryotic operons (Mao *et al.*, 2009) and the prokaryotic operon database (http://operons.ibt.unam.mx/OperonPredictor/) with a predicted promoter in the 400 bp region between the genes *lpg1653* and *lpg1654*. The proteins in this operon are annotated as IolG (*lpg1652*), a *myo*-inositol-2-dehydrogenase, IolCB (*lpg1651*), a combined 5-dehydro-2-deoxygluconokinase and 5-deoxy-glucuronate isomerase protein, IolD (*lpg1650*), an inositol catabolism hydrolase protein and IolE (*lpg1649*), an inosose dehydratase. These proteins show sequence identities between 30% and 50% with the corresponding proteins of *B. subtilis* and *S. enterica*. The first gene in the *lpg1653-lpg1649* operon is annotated as D-xylose proton symporter and shares some homology to the inositol transporter proteins IolT of *B. subtilis* and *S. enterica* (Figure 3.14). The operon is found in several *L. pneumophila* strains including Philadelphia 1, Paris, Lens, Corby and Alcoy and is also present in the genome of *L. longbeachae*. Therefore, *Legionella* spp. are probably able to metabolize inositol.

The only proteins missing in the genome of *L. pneumophila* that were described to be involved in inositol metabolism in other organisms, are the bisphosphate aldolase IolJ and the malonate-semialdehyde-dehydrogenase IolA (see section 1.3.2). Interestingly, also no homologue of the

major regulator protein IolR is found by sequence homology in the genome of *L. pneumophila*. Thus, the expression of the *iol* operon seems to be regulated differently than in *B. subtilis* (Yoshida *et al.*, 2008) or *S. enterica* (Kröger and Fuchs, 2009).

3.3.2 Characterization of Lpg1653 as an Inositol Transporter and Utilization of Inositol by *Legionella pneumophila*

To test whether *L. pneumophila* can metabolize inositol, the role of the putative inositol degradation cluster was assessed using different growth assays. To this end, mutant strains lacking *lpg1653*, the putative inositol transporter, or lacking *iolG* (*lpg1652*), the inositol dehydrogenase, were constructed. Growth of these mutants was monitored in different media in presence or absence of inositol. In AYE broth, growth of wild-type, Δ*lpg1653* or Δ*iolG* was indistinguishable, and the addition of 10 mM inositol did not alter growth of any strain tested (data not shown). The *lpg1653* mutant grew like wild-type bacteria in CDM and MDM and again, the addition of 10 mM inositol did not influence the growth of either strain (Figure 3.15 A, B). Even though inositol did not have a growth-stimulating effect in all media tested, it was analyzed whether *L. pnumophila* can take up and utilize inositol. To this end, the bacteria were grown to late exponential growth phase and then incubated with radiolabelled ^{14}C-inositol. Cells were spun onto filter disks, washed, and cell-associated radioactivity on the filters was determined using a liquid scintillation counter. Indeed, wild-type bacteria did take up ^{14}C-inositol; cell associated radioactivity was maximum after 30 min (Figure 3.15 C). On the other hand, no cell-associated radioactivity was measured for the *lpg1653* mutant. This uptake defect was complemented by expressing *lpg1653* from a plasmid (pCM020) (Figure 3.15 C). Thus, Lpg1653 was identified as an inositol transporter, and the protein was termed IolT in reference to the described inositol transporters from *B. subtilis* and *S. enterica* (Yoshida *et al.*, 2008; Kröger *et al.*, 2010).

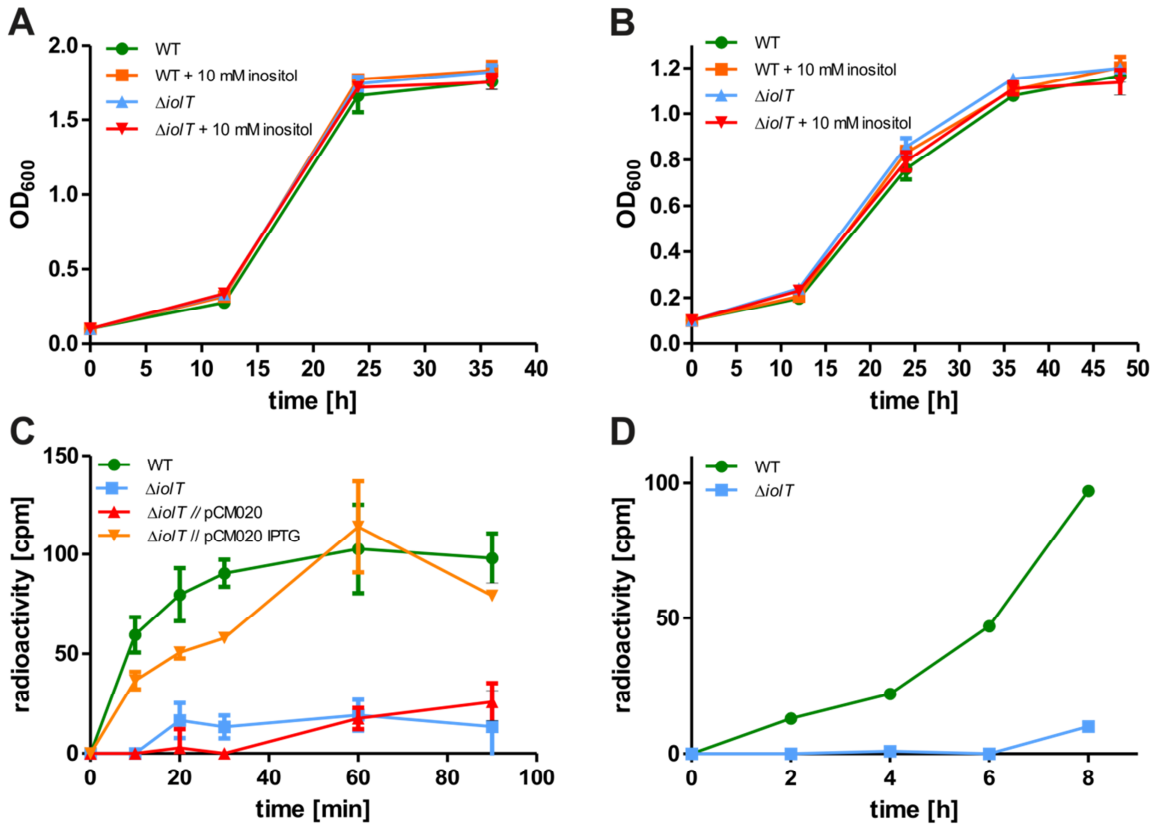

Figure 3.15: Characterization of *L. pneumophila* IolT as an inositol transporter. Extracellular growth of *L. pneumophila* wild-type (WT) and mutant Δ*iolT* (Δ*lpg1653*) in CDM (**A**) or MDM (**B**) with and without 10 mM inositol. Optical density at 600 nm was determined at the time points indicated. *L. pneumophila* WT, Δ*iolT* or Δ*iolT* harbouring plasmid pCM020 (*iolT* under control of P_{tac}) were grown to late exponential growth phase, 10 mM inositol mixed with 1% [U-$^{14}C_6$]inositol was added, and cells were further incubated. After 0, 10, 20, 30, 60 and 90 minutes, samples were taken, cells were spun onto cellulose acetate filter disks, and cell-associated radioactivity was measured using a liquid scintillation counter (**C**). *L. pneumphila* WT or mutant Δ*iolT* were grown to exponential growth phase, 10 mM inositol mixed with 1% [U-$^{14}C_6$]inositol was added, and cells were further incubated. After 0, 2, 4, 6 and 8 h samples were taken and mixed with 50% trichloroacetic acid. Samples were incubated on ice for 1 h, spun onto cellulose nitrate filter disks, washed, and filter-associated radioactivity was determined using a liquid scintillation counter (**D**). Data in (**A**)-(**D**) are representatives of three independent experiments. Mean and SD of triplicates are shown (**A**)-(**C**).

To test, whether inositol was catabolized and incorporated into cell matter by *L. pneumophila* radioactive inositol was used. To this end, exponentially growing *L. pneumophila* were incubated with ^{14}C-inositol for several hours. Every two hours, samples were taken and mixed with trichloroacetic acid to precipitate proteins. The samples were then spun onto cellulose nitrate filter disks, and incorporation of radioactivity into the acid-insoluble fraction was measured using a liquid scintillation counter. For wild-type bacteria, radioactivity was rising steadily over time,

indicating that inositol was also used as precursor for macromolecules, while no radioactivity was detectable in the acid-insoluble fractions of an *iolT* mutant (Figure 3.15 D).

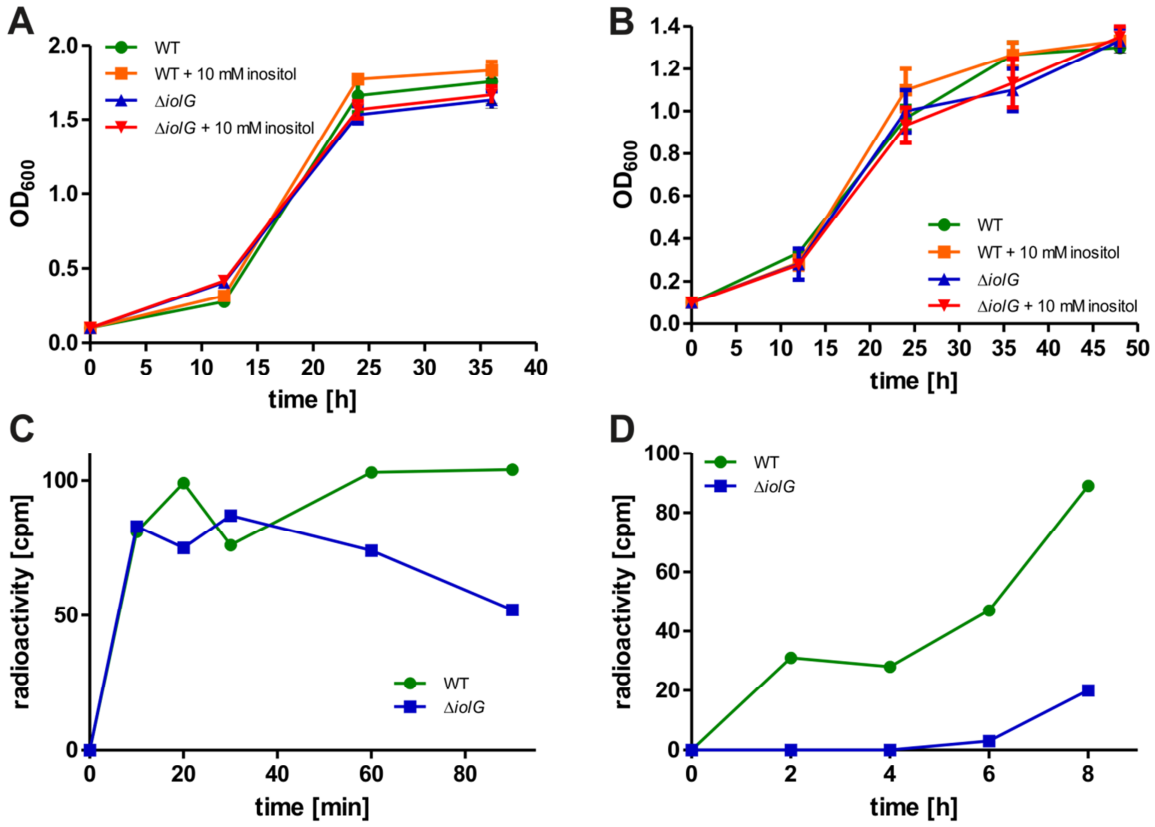

Figure 3.16: Inositol metabolism of *L. pneumophila* in dependence of IolG. Extracellular growth of *L. pneumophila* wild-type (WT) and mutant Δ*iolG* in CDM (**A**) or MDM (**B**) with and without 10 mM inositol. Optical density at 600 nm was determined at the time points indicated. *L. pneumophila* WT or Δ*iolG* were grown to late exponential growth phase, 10 mM inositol mixed with 1% [U-$^{14}C_6$]inositol was added and cells were further incubated. After 0, 10, 20, 30, 60 and 90 minutes, samples were taken. Cells were spun onto cellulose acetate filter disks and cell-associated radioactivity was measured using a liquid scintillation counter (**C**). *L. pneumphila* WT or Δ*iolG* were grown to exponential growth phase, 10 mM inositol mixed with 1% [U-$^{14}C_6$]inositol was added and cells were further incubated. After 0, 2, 4, 6 and 8 h samples were taken and mixed with 50% trichloroacetic acid. Samples were incubated on ice for 1 h, spun onto cellulose nitrate filter disks, washed, and filter-associated radioactivity was determined using a liquid scintillation counter (**D**). Data in (**A**)-(**D**) are representatives of three independent experiments. Mean and SD of triplicates are shown (**A**)-(**B**).

An *L. pneumophila* Δ*iolG* mutant strain was characterized in the same way as Δ*iolT* by growth in different media and determination of uptake and usage of ^{14}C-inositol. Again, the mutant lacking the inositol dehydrogenase IolG grew like wild-type bacteria in CDM and MDM, and the addition of 10 mM inositol did not alter growth of the bacteria (Figure 3.16 A, B). By using ^{14}C-inositol, it was shown that the *iolG* mutant was able to transport inositol (Figure 3.16 C), but was not able to use inositol as precursor for macromolecules, as no radioactivity was detected in

the acid insoluble fractions of Δ*iolG* (Figure 3.16 D). The mutant strain was therefore able to transport inositol, but could not metabolize it.

In summary, we showed that *L. pneumophila* possesses a gene cluster (*lpg1653-lpg1649*), which is used to metabolize inositol, and IolT (Lpg1653) was identified as an inositol transporter. Inositol did not stimulate growth of *L.* pneumophila, but was used as precursor for macromolecules.

3.3.3 Expression of *iolT* is Regulated by RpoS and the Availability of Serine

In *B. subtilis*, the expression of all genes linked to inositol metabolism is regulated by IolR, which represses the expression of *iol* genes in absence of inositol (Yoshida *et al.*, 2008). No homologue for IolR was found in the genome of *L. pneumophila*, so the expression of the *iol* gene cluster has to be regulated differently. As no other promotor as the *iolT* promotor is predicted within the operon (see section 3.3.1), a reporter plasmid was constructed with an unstable GFP variant (ASV) under control of P_{iolT} (pCM007). This reporter was used to test the expression of *iolT* and hence the whole *iol* operon under different conditions.

The addition of 10 mM inositol did not alter the expression of *iolT* as measured by GFP fluorescence levels in wild-type bacteria (Figure 3.17 A). Therefore, the expression of *iolT* seems not to be regulated by the availability of inositol. Interestingly, the addition of 6 mM serine to AYE broth did result in higher expression levels of *iolT*, shifting the expression maximum from around 14 h to around 16 h of growth (Figure 3.17 A). The highest expression levels of *iolT* were therefore obtained in the late exponential growth phase of *L. pneumophila*.

The Lqs system is known to be part of the stationary-phase regulatory network of *L. pneumophila* (Tiaden *et al.*, 2007). To assess whether the Lqs system regulates the expression of the *iol* operon, the expression of *iolT* was also tested in a mutant strain lacking the response regulator LqsR. Here, no differences compared to wild-type bacteria were detectable and again, addition of inositol had no influence on the expression of *iolT*, while 6 mM serine did enhance the expression (Figure 3.17 B). This was also analyzed in other *lqs* mutants, but the same results as for wild-type were obtained for Δ*lqsA*, Δ*lqsS*, Δ*lqsT* and Δ*lqsS-ΔlqsT* mutants (Figure 3.18). Therefore, the expression of *iolT* is not regulated by the *lqs* system of *L. pneumophila*.

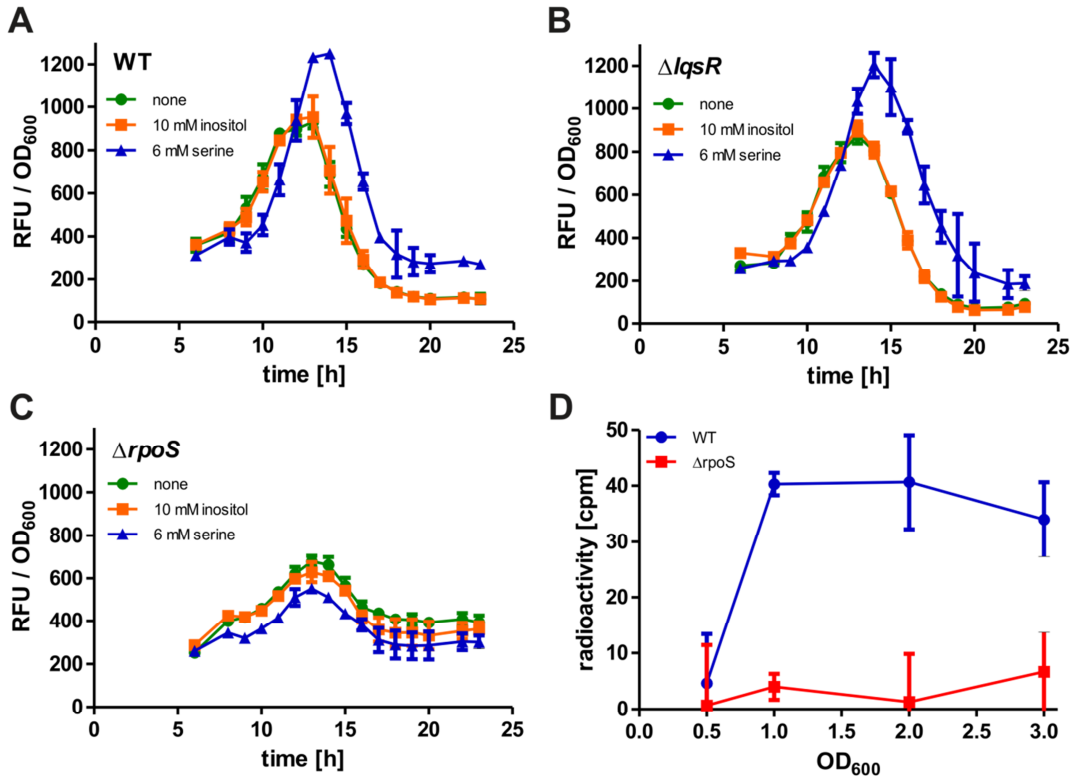

Figure 3.17: Expression of *iolT* is regulated by RpoS and the availability of serine. Exponentially growing cultures of *L. pneumophila* wild-type (WT) (**A**), Δ*lqsR* (**B**) or Δ*rpoS* (**C**) harboring plasmid pCM007 (unstable GFP (ASV) under control of P_{iolT}) were diluted to a starting OD_{600} of 0.1 in AYE broth. Cells were grown at 37°C with 10 mM inositol, 6 mM serine or without the addition of additional nutrients (**A**)-(**C**). Optical density at 600 nm and GFP fluorescence was measured every hour for 24 h and results were plotted with RFU as a function of OD_{600} over time (**A**)-(**C**). *L. pneumophila* WT or mutant Δ*rpoS* were grown to an OD_{600} of 0.5, 1.0, 2.0 and 3.0. At that points, samples were taken and 10 mM inositol mixed with 1% [U-$^{14}C_6$]inositol was added and the bacteria were further incubated for 30 min. Cells were spun onto cellulose acetate filter disks, washed and filter-associated radioactivity was determined in a liquid scintillation counter (**D**). Data in (**A**)-(**D**) are representatives of three independent experiments. Mean and SD of triplicates are shown.

The sigma factor RpoS is a central regulator of intracellular replication and differentiation in *L. pneumophila* and regulates many genes in stationary growth phase (Zusman *et al.*, 2002; Hovel-Miner *et al.*, 2009). To test whether RpoS controls the expression of the *iol* operon, the P_{iolT} reporter construct was transformed into a *L. pneumophila* Δ*rpoS* mutant strain. Expression levels of *iolT* in the *rpoS* mutant strain were significantly lower compared to wild-type bacteria. Also, the addition of serine had no influence on the expression of *iolT* in the Δ*rpoS* strain anymore (Figure 3.17 C). Therefore, *iolT* seems to be regulated by RpoS. This finding was confirmed in experiments measuring the uptake of ^{14}C-inositol at different stages of *L. pneumophila* growth. At an OD_{600} of 0.5 (early exponential growth phase), wild-type and Δ*rpoS* did not transport inositol, as no cell-associated radioactivity was measured for either strain

(Figure 3.17 D). However, while for wild-type bacteria increased radioactivity was detectable at OD_{600} of 1.0 (exponential growth phase), 2.0 (late exponential growth phase) and 3.0 (stationary growth phase), no cell-associated radioactivity was measured for Δ*rpoS* at all time points (Figure 3.17 D). In summary, these results show that the growth phase- and serine-dependent expression of *iolT* is regulated by RpoS. Highest levels of *iolT* expression were obtained in the late exponential growth phase, but *L. pneumophila* was able to transport inositol already at earlier stages of its growth cycle.

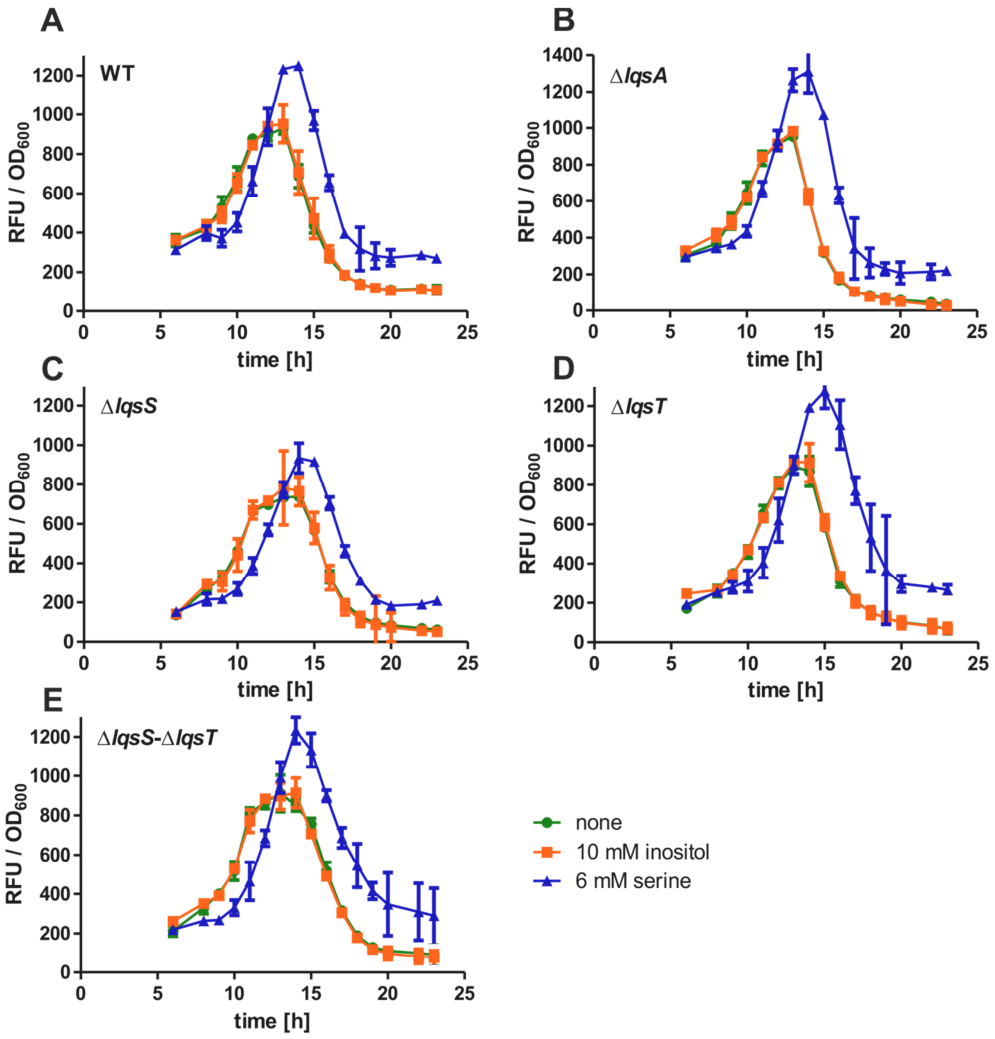

Figure 3.18: **Expression of *iolT* is not regulated by *lqs* genes.** Exponentially growing cultures of *L. pneumophila* wild-type (WT) (**A**), Δ*lqsA* (**B**), Δ*lqsS* (**C**), Δ*lqsT* (**D**) or Δ*lqsS*-Δ*lqsT* (**E**) harboring plasmid pCM007 (unstable GFP (ASV) under control of P_{iolT}) were diluted to a starting OD_{600} of 0.1 in AYE broth. Cells were grown at 37°C with 10 mM inositol, 6 mM serine or without additional nutrients (**A**)-(**E**). Optical density at 600 nm and GFP fluorescence was measured every hour for 24 h, and results were plotted with RFU as a function of OD_{600} over time (**A**)-(**E**). Data are representatives of three independent experiments. Mean and SD of triplicates are shown.

3.3.4 Inositol Promotes Intracellular Growth of *Legionella pneumophila*

Similar to genes involved in glycerol metabolism (see section 3.2.1), the expression of genes of the *iol* cluster was upregulated upon intracellular growth of *L. pneumophila* in human macrophages (Faucher *et al.*, 2011). The genes, except the inositol transporter *iolT*, were 2-fold upregulated showing that also inositol might play a role during intracellular growth of *L. pneumophila.* Moreover, the IolBC genes, encoding the combined transferase kinase protein of *L. pneumophila* were also almost 2-fold upregulated in post-exponential growth phase compared to exponential growth phase.

The impact of inositol on intracellular growth of *L. pneumophila* was assessed using colony forming units (cfu), fluorescence based assays, as well as co-infection assays (see sections 2.2.9 and 2.2.10). Addition of 20 mM inositol concomitant with infection or 2 h or 4 h post infection to infected *A. castellanii* cells, yielded higher bacterial cell numbers based on increased fluorescence levels (Figure 3.19 A-C). This was dependent on *iolT*, and addition of inositol to Δ*iolT* did not result in higher fluorescence levels, but the mutant grew like wild-type (Figure 3.19 A-C). Inositol did not lead to faster growth of exponentially growing bacteria, but did lead to higher cell numbers after 24 h and at later time points of infection, suggesting that inositol might, like glycerol, only be used in later stages of infection (Figure 3.19 A-C). Addition of 20 mM inositol to *L. pneumophila* wild-type growing in *A. castellanii* or murine macrophages did also result in a greater number of cfu after 72 or 48 h of intracellular growth, respectively (Figure 3.19 D, E). This positive growth effect was not observed for the *iolT* mutant, although the mutant was not impaired in intracellular growth *per se* (Figure 3.19 D, E). However, the mutant was slowly outcompeted by wild-type bacteria in co-infection assays within 15 days, indicating that the *iolT* mutant had a fitness disadvantage compared to the wild-type strain, although *iolT* was not essential for intracellular growth (Figure 3.19 F).

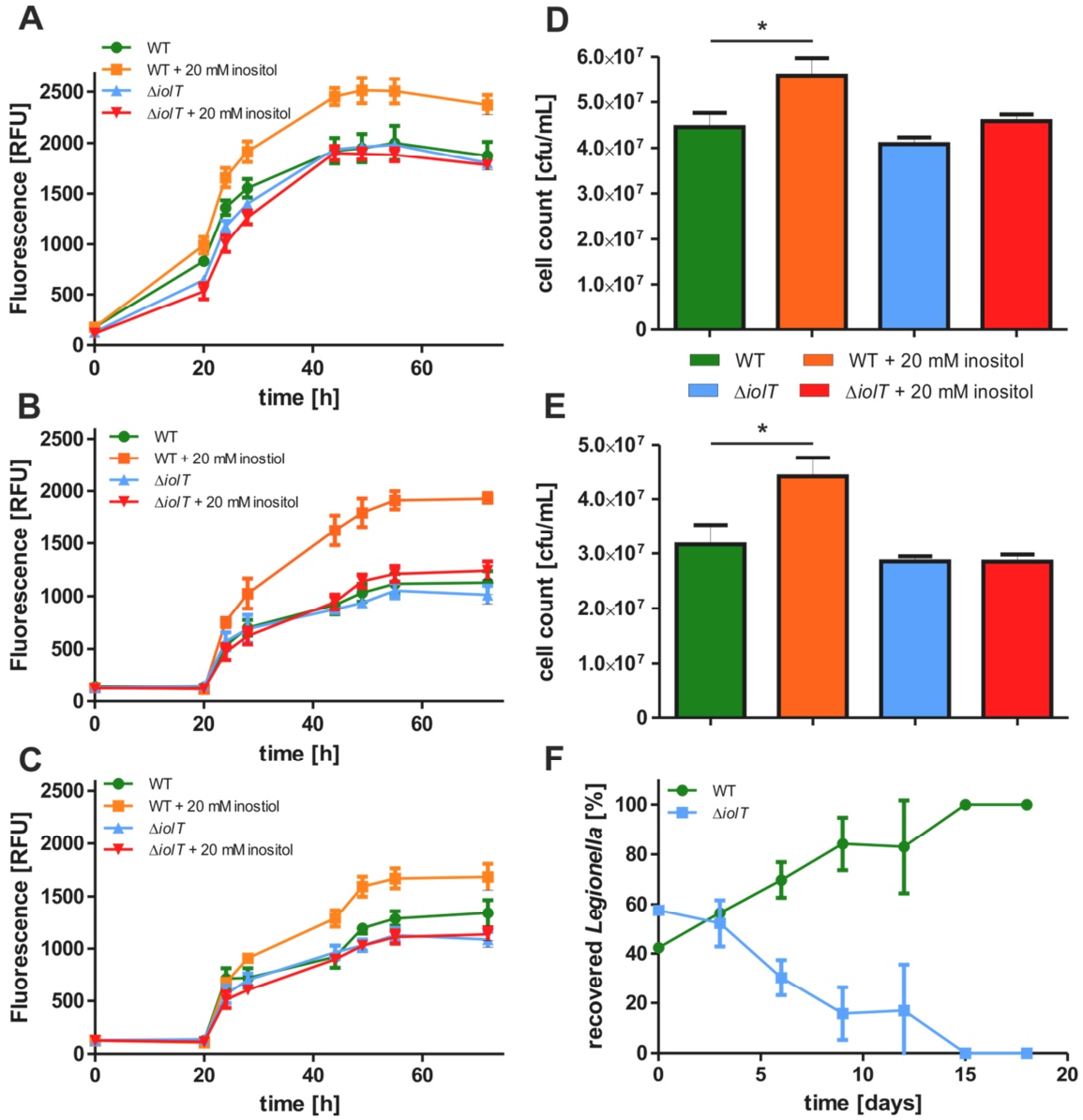

Figure 3.19: Inositol promotes intracellular growth of *L. pneumophila* dependent on *iolT*. *A. castellanii* was infected (MOI 20) with *L. pneumophila* wild-type (WT) or Δ*iolT* harbouring plasmid pNT28 (constitutive GFP expression). 20 mM inositol was added concomitant with infection (**A**), 2 h (**B**) or 4 h post infection (**C**), and intracellular replication was determined by fluorescence. *A. castellanii* (**D**) or murine macrophages (**E**) were infected (MOI 0.1) with *L. pneumophila* WT or mutant strain Δ*iolT*. 20 mM inositol was added 4 h post infection, cells were lysed 72 h (**D**) or 48 h (**E**) post infection, and cfu were determined by plating out appropriate dilutions on CYE agar plates (Student´s t-test *$p < 0.05$). For co-infection assays, *A. castellanii* was infected with *L. pneumophila* WT and Δ*iolT* at a 1:1 ratio (MOI 0.01 each). Cells were lysed three days post infection and bacteria were used to infect fresh amoeba. Cell numbers were determined by cfu (**F**). Data in (**A**)-(**F**) are representatives of three independent experiments. Mean and SD of triplicates are shown.

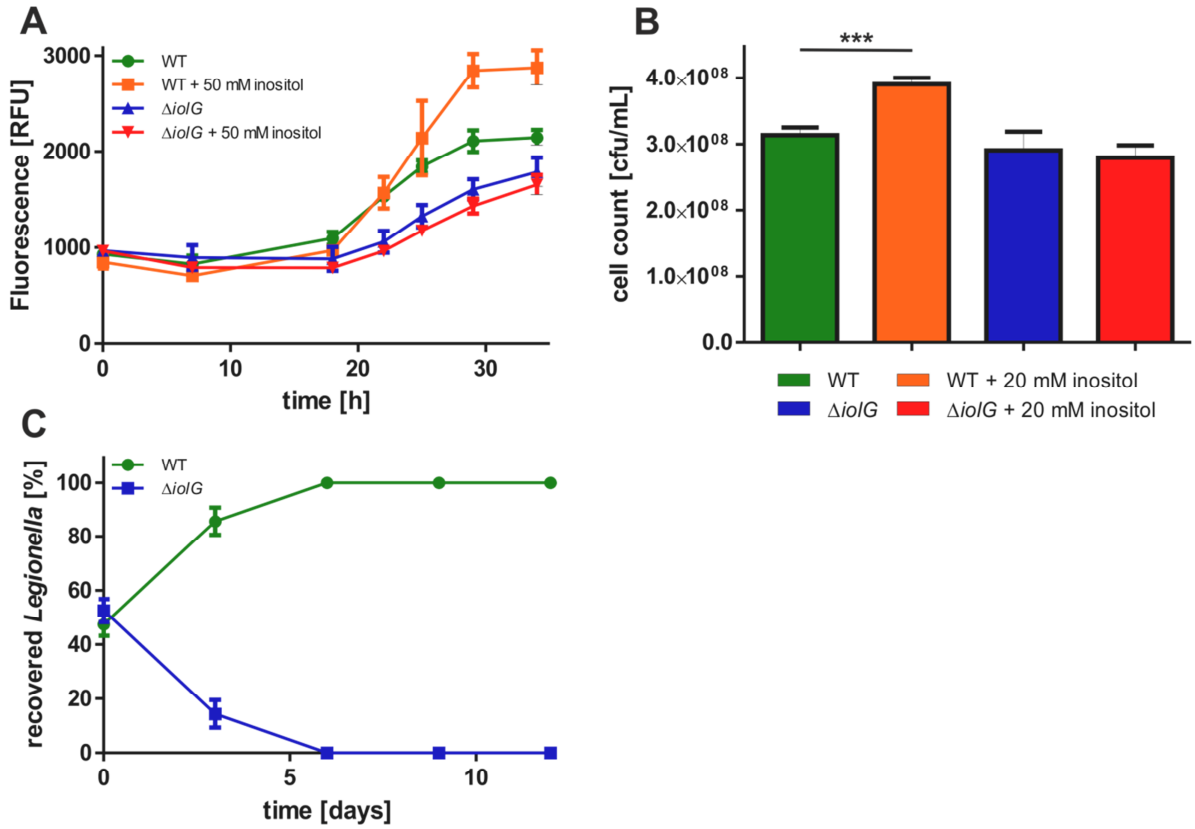

Figure 3.20: Inositol promotes intracellular growth of *L. pneumophila* dependent on *iolG*. *A. castellanii* was infected (MOI 20) with *L. pneumophila* wild-type (WT) or Δ*iolG* harbouring plasmid pNT28 (constitutive GFP expression). 50 mM inositol was added 4 h post infection and replication was determined by fluorescence (**A**). *A. castellanii* was infected (MOI 0.1) with *L. pneumophila* WT or mutant strain Δ*iolG*. 20 mM inositol was added 4 h post infection, cells were lysed 72 h post infection and cfu were determined by plating out appropriate dilutions on CYE agar plates (**B**) (Student´s t-test ***$p < 0.001$). For co-infection assays, *A. castellanii* was infected with *L. pneumophila* WT and Δ*iolG* at a 1:1 ratio (MOI 0.01 each). Cells were lysed three days post infection and bacteria were used to infect fresh amoeba. Cell numbers were determined by cfu (**C**). Data in (**A**)-(**C**) are representatives of three independent experiments. Mean and SD of triplicates are shown.

The intracellular growth of *L. pneumophila* in presence or absence of inositol was also tested in the Δ*iolG* mutant strain. While the addition of inositol to wild-type bacteria resulted in higher fluorescence levels (Figure 3.20 A) and higher cfu numbers (Figure 3.20 B), the addition of inositol to Δ*iolG* did not. The mutant did intracellularly grow like wild-type but was outcompeted by the wild-type strain within 6 days in co-infection assays (Figure 3.20 C). In summary, inositol had a positive effect on intracellular growth of *L. pneumophila*, resulting in higher cell numbers. The observed phenotype was dependent on the inositol transporter IolT or the inositol dehydrogenase IolG, and the mutant strains were outcompeted by wild-type bacteria. Therefore,

inositol is likely a carbon source of *L. pneumophila* during intracellular growth in different host cells.

3.3.5 Analysis of Substrate Uptake into LCVs of Infected Host Cells

As inositol had a positive effect on intracellular growth of *L. pneumophila*, the question was whether this was a result of the direct metabolism of inositol by the bacteria or an indirect effect, where the host cells metabolized inositol and the bacteria then benefited from more available metabolites like amino acids. One prerequisite for the direct metabolism of inositol or any other substrate by *L. pneumophila* would be the accessibility of the LCV for substrates supplied from the outside to infected host cells.

To test whether substrates reach the LCV, we added a fluorescent glucose analogue, 2-(N-(7-Nitrobenz-2-oxa-1,3-diazol-4-yl)amino)-2-deoxyglucose (2-NBDG) to infected *D. discoideum* cells 1 h post infection. Subsequently, we monitored by fluorescence microscopy whether 2-NBDG can reach the bacteria inside the LCV or not. Indeed, when *D. discoideum* was infected with either wild-type, or Δ*iolT* or Δ*iolG* mutant bacteria, the amoeba did take up 2-NBDG and the glucose analogue was found in close proximity to the intracellular bacteria as seen by green fluorescence surrounding the bacteria (Figure 3.21 A). This was quantified by counting 2-NBDG positive LCVs in whole infected amoeba, and it was found that around 60% of all LCVs were positive for the fluorescent glucose analogue. No difference between wild-type, Δ*iolT* or Δ*iolG* was observed (Figure 3.21 B). The LCV was therefore accessible for the substrate added to infected cells. When *D. discoideum* was infected with an Δ*icmT* mutant and 2-NBDG was added 1 h post infection, significantly less 2-NBDG-positive LCVs were found. Only around 30% of all *Legionella*-containing compartments that were counted were 2-NBDG-positive, showing that uptake of 2-NBDG was in part dependent on a functional T4SS.

These findings were also confirmed by monitoring LCVs in homogenates from *D. discoideum* infected with wild-type *L. pneumophila*. The infected cells were homogenized after incubation with 2-NBDG, washed thoroughly and then stained for SidC, a *L. pneumophila* effector protein specifically found on LCV membranes. Again, a high number of 2-NBDG-positive LCVs was determined (Figure 3.22). As the samples were washed several times in the course of the experiments, the observed fluorescence had to be inside membrane-confined compartments, confirming that 2-NBDG was taken up into the LCVs of infected host cells.

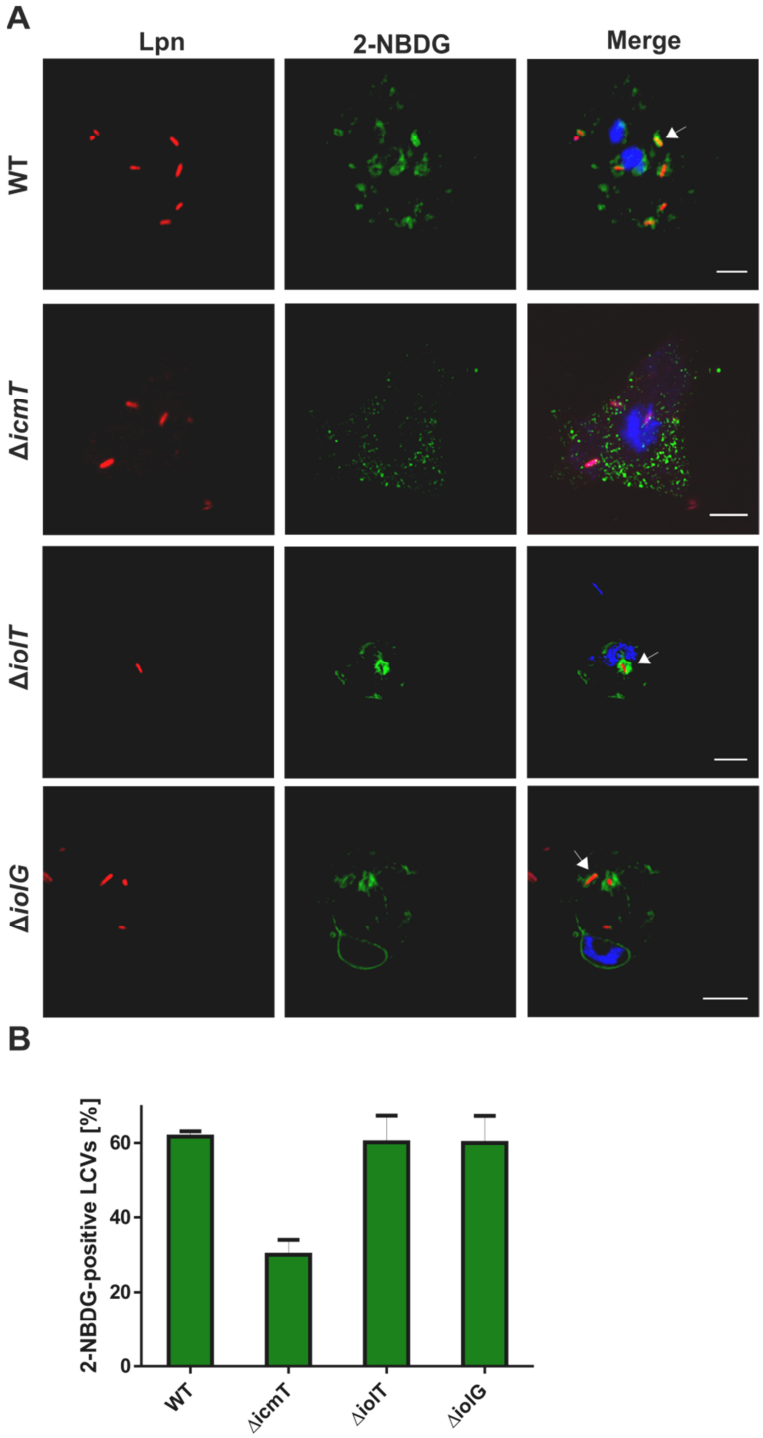

Figure 3.21: Accumulation of 2-NBDG in LCVs within *D. discoideum*. *D. discoideum* was infected (MOI 10) with *L. pneumophila* (Lpn) wild-type (WT), Δ*icmT*, Δ*iolT* or Δ*iolG* harbouring plasmid pSW001 (constitutive *dsred* expression) for 1 h. Cells were washed and incubated with 20 µM 2-NBDG for 30 min. After that, cells were washed, fixed with PFA, stained with DAPI and subjected to fluorescence microscopy. 2-NBDG-positive LCVs are marked with white arrows; scale bars 5 µm (**A**). The number of 2-NBDG-positive LCVs was quantified from three independent experiments. At least 50 LCVs were counted per experiment (**B**). The pictures shown are representatives of at least three independent experiments.
Abbreviations: **Lpn**, *Legionella pneumophila*; **2-NBDG**, 2-(N-(7-Nitrobenz-2-oxa-1,3-diazol-4-yl)amino)-2-deoxyglucose.

In summary, the LCV is accessible for substrates after infection, suggesting that inositol and other substrates can reach the bacteria inside the compartment and can subsequently be metabolized directly by *L. pneumophila*. This notion is in agreement with the finding that the observed positive growth effect inside different host cells was dependent on IolT and IolG (see section 3.3.4). The fact that the vacuole containing the Δ*icmT* mutant did not take up 2-NBDG as efficiently as the other strains tested indicates that the acquisition of substrates from the host cell might be dependent on the T4SS-induced communication with the endosomal network of the host cell. This might occur through macropinocytotic processes and vesicle fusion events and/or through host cell transporters that could facilitate the uptake of different substrates into the LCV.

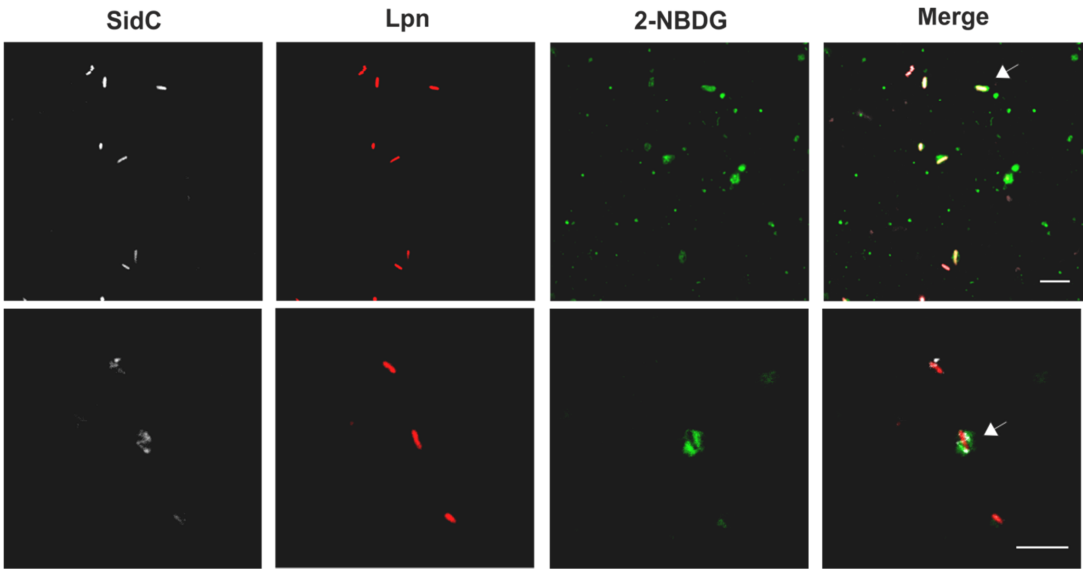

Figure 3.22: 2-NBDG-positive LCVs in homogenates from *L. pneumophila*-infected amoeba. *D. discoideum* was infected (MOI 10) with *L. pneumophila* wild-type (WT) harbouring plasmid pSW001 (constitutive *dsred* expression) for 1 h. Cells were washed and further incubated with 20 µM 2-NBDG for 30 min. Cells were washed and homogenized using a ball homogenizer with 8 µm exclusion size. Samples were then fixed with PFA on poly-L-lysine coated coverslips and stained for SidC. Samples were subjected to fluorescence microscopy. White arrows indicate 2-NBDG-positive LCVs. Scale bars: 5 µm.
Abbreviations: **Lpn**, *Legionella pneumophila*; **2-NBDG**, 2-(N-(7-Nitrobenz-2-oxa-1,3-diazol-4-yl)amino)-2-deoxyglucose.

4. Discussion

The knowledge about the metabolism of *L. pneumophila* was restricted for some time to the preference of amino acids for nutrition. In particular, it was neglected what possibilities the intracellular milieu could offer for the bacteria and how metabolism could influence the course of the infection. This study now documents that *L. pneumophila* metabolizes glycerol and inositol *in vitro* as well as *in vivo*. Furthermore it shows that amino acids like serine and carbohydrates like glucose and glycerol have particular metabolic fates when being metabolized by the bacteria, a principle that also seems to be employed by other intracellular pathogens like *L. monocytogenes* or *M. tuberculosis* to ensure effective and successful intracellular replication.

4.1 The Metabolism of Inositol by *Legionella pneumophila* and its Regulation

The genome of *L. pneumophila* harbors a cluster of genes associated with the catabolism of inositol, which are organized in an operon (see section 3.3.1). However, no gene for the bisphosphate aldolase *iolJ* and the malonate semialdehyde dehydrogenase *iolA* are found within the operon or elsewhere in the genome. The Kyoto Encyclopedia of Genes and Genomes (KEGG) predicts that MmsA (Lpg0129) catalyzes the reaction of IolA in *L. pneumophila* (http://www.genome.jp/kegg/kegg2.html). IolA normally converts malonate semialdehyde into acetyl-CoA, releasing CO_2 and producing one molecule $NADH/H^+$ in the course. However, MmsA is annotated as a methylmalonate semialdehyde dehydrogenase that oxidizes methylmalonate semialdehyde to propionyl-CoA, producing one molecule $NADH/H^+$ in the process. Whether the inositol catabolism in *L. pneumophila* produces methylmalonate or malonate semialdehyde is not known. However, the enzyme corresponding to MmsA in *B. subtilis* was found to catalyze both reactions with methylmalonate semialdehyde and malonate semialdehyde as substrates, producing propionyl- and acetyl-CoA, respectively (Stines-Chaumeil *et al.*, 2006; Talfournier *et al.*, 2011). *L. pneumophila* MmsA shares some homologies with *B. subtilis* MmsA, and it is possible that the *Legionella* enzyme also has a wider substrate spectrum than just methylmalonate semialdehyde.

A substitution for the missing IolJ on the other hand is harder to find. IolJ catalyzes the aldolase reaction with 2-deoxy-5-keto-D-gluconate-6-phosphate as substrate, which yields one molecule dihydroxyacetone phosphate and the aforementioned malonate semialdehyde. *S. enterica* also has no homologue of *iolJ* in its genome, but other than *L. pneumophila* can grow on inositol as sole

source of carbon and energy (Kröger and Fuchs, 2009). At this point, it is not possible to propose multi-substrate specificities of other aldolases that could make up for the missing IolJ. It is possible that *L. pneumophila* employs a novel inositol catabolic pathway as shown for *Thermotoga maritima* (Rodionova *et al.*, 2013). However, this is not likely as all other enzymes in the *iol* cluster resemble enzymes that were described in *B. subtilis* and *S. enterica*. Indeed, *L. pneumophila* seems to metabolize inositol as suggested in experiments performed with radioactive ^{14}C-inositol (see section 3.3.2). While the addition of inositol did not have a growth stimulating effect in different chemically defined media, upon incubation of the bacteria with ^{14}C-inositol, radioactivity was efficiently incorporated into the acid-insoluble fraction of the cell indicating that inositol is used as a precursor for macromolecules. As this was dependent on IolT and IolG one can assume that this was by virtue of inositol metabolism (see section 3.3.2). Further investigations on the fate of inositol in the bacterial cell would help to elucidate the mechanisms of inositol metabolism and could also clarify, if and how inositol contributes to the bipartite metabolism of *L. pneumophila* (see section 4.3).

The inositol metabolism in other bacteria like *B. subtilis*, *S. enterica* or *L. casei* is regulated by the repressor protein IolR (Yebra *et al.*, 2007; Yoshida *et al.*, 2008; Kröger *et al.*, 2010). In the absence of inositol, IolR binds to the operator sites of regulated genes and blocks their transcription. If inositol is available, a catabolic intermediate of inositol metabolism acts as a derepressor of IolR. The regulator detaches from the operator sites, thus allowing expression of inositol metabolism genes and the transporter gene *iolT* (Yoshida *et al.*, 1997; Yoshida *et al.*, 2008). No homologue of IolR is found in the genome of *L. pneumophila*, and accordingly, the addition of inositol had no influence on the expression of *iolT* (see section 3.3.3). However, the expression of *iolT* was up-regulated by the addition of serine and down-regulated in a Δ*rpoS* mutant (see section 3.3.3).

Availability of nutrients, especially amino acids, constitutes an important factor for *L. pneumophila* for the regulation of the phenotypic switch between replication and transmission and vice versa. As long as amino acids are available, expression of virulence traits is repressed (Byrne and Swanson, 1998), and only when nutrients become limiting the bacteria will undergo a transcriptional switch and express virulence traits (see also section 1.2.4). Transporters of the Pht family, like the threonine transporter PhtA or the valine transporter PhtJ, were shown to be essential for the intracellular differentiation to the replicative form (Sauer *et al.*, 2005; Chen *et al.*, 2008). Furthermore, arginine is important for the switch to replication inside the host. The

availability of arginine allows the expression of genes that are repressed by the regulator ArgR in absence of the amino acid. The regulator is crucial for maximal intracellular replication in *A. castellanii* (Hovel-Miner *et al.*, 2010).

It is currently not known, whether serine also acts on regulatory proteins and how it influences gene expression patterns of *L. pneumophila*, but as the amino acid is a major carbon source for the bacteria, a role for serine in the regulatory network of *Legionella* is likely. The effect of serine on gene expression might also be indirect and linked to the overall metabolic state of the bacterial cell. As long as amino acids are not limiting, the ppGpp-synthase RelA is not activated. The second ppGpp-synthase of *L. pneumophila*, SpoT, senses the metabolic condition of the cell through the state of fatty acid biosynthesis and is activated by a reduction in the rate of fatty acid biosynthesis. As long as this is not the case, SpoT acts as a ppGpp-hydrolase and assures that the transmissive phenotype is not expressed and bacteria can replicate (Dalebroux *et al.*, 2009; Edwards *et al.*, 2009). Isotopologue profiling with ^{13}C-serine as precursor showed high carbon flux from serine into fatty acids, and therefore, a high rate of fatty acid biosynthesis occurs when serine was present (see section 3.2.3). This in consequence would lead to ppGpp-hydrolase activity of SpoT, which could also influence the second regulator of inositol metabolism, the alternative sigma factor RpoS.

In a *L. pneumophila rpoS* deletion mutant, the expression of *iolT* was drastically reduced and also serine did not enhance the expression anymore (see section 3.3.3). In line with these results is the finding of Trigui *et al.* who observed the downregulation of *iolG* in an *rpoS* mutant upon extracellular growth in water (Trigui *et al.*, 2015). In *E. coli* RpoS is believed to be the central stress sigma factor as Δ*rpoS* mutants of *E. coli* are much more sensitive to stress (Hengge-Aronis, 1993; 2002). An *L. pneumophila* Δ*rpoS* mutant, on the other hand, retains stress resistance, but is not able to replicate inside protozoan hosts anymore (Hales and Shuman, 1999b; Hovel-Miner *et al.*, 2009). Therefore, RpoS is believed to be a key regulator of genes associated with intracellular multiplication in *L. pneumophila* (Hovel-Miner *et al.*, 2009). RpoS regulates a plethora of genes including Icm/Dot-translocated effector proteins, small regulatory RNAs as well as two component systems, and is mainly associated with virulence related genes. However, RpoS was also shown to positively regulate genes associated with carbohydrate metabolism during exponential growth (Hovel-Miner *et al.*, 2009), and inositol transport was also highest in exponential growth phase (see section 3.3.3). At that point the ppGpp concentration in the cell is low due to the availability of nutrients (e.g. serine) and the resulting ppGpp-hydrolase activity of

SpoT. When nutrients become limiting and ppGpp concentrations rise, the stability and activity of RpoS will change and the expression profile switches to the transmissive pattern (Zusman *et al.*, 2002; Hovel-Miner *et al.*, 2009). This link might explain the observed interplay of serine and RpoS in the regulation of inositol metabolism in the exponential growth phase of *L. pneumophila*. Regulatory proteins downstream of RpoS could also be responsible for the regulation of inositol metabolism. RpoS controls the expression of the arginine repressor ArgR. The expression of *argR* was twelve-fold upregulated in Δ*rpoS*, and thus, the intracellular growth defect of Δ*rpoS* might be due to the inability of the bacteria to express the *arg* regulon upon infection (Hovel-Miner *et al.*, 2009; Hovel-Miner *et al.*, 2010). ArgR does not regulate the *iol* operon of *L. pneumophila* (Hovel-Miner *et al.*, 2010), but the observed downregulation of *iolT* in Δ*rpoS* could be due to the disturbed expression of one or several other regulators downstream of RpoS. The *Legionella* quorum sensing system (Lqs) might be one of those regulators, as it was shown that the expression of *iolG* was two-fold upregulated in a mutant lacking the two sensor kinases LqsS and LqsT in stationary growth phase (Kessler *et al.*, 2013). Moreover, the *lqs* system is regulated by RpoS (Tiaden *et al.*, 2007) and could therefore be responsible for the downregulation of the *iol* operon in stationary growth phase.

The overall picture of regulatory processes regarding inositol metabolism is still vague, but the involvement of RpoS suggests that the carbohydrate could be used as an intracellular carbon source by *L. pneumophila*. Indeed, inositol promoted intracellular growth dependent on IolT and IolG in *A. castellanii* and murine macrophages (see section 3.3.4). Furthermore, mutants lacking the inositol transporter IolT or the inositol dehydrogenase IolG had a severe fitness disadvantage compared to wild-type bacteria, without being impaired for intracellular growth *per se* (see section 3.3.4). The catabolism of inositol is therefore not essential for intracellular growth of *L. pneumophila*, but provides the bacteria with certain fitness benefits. As the observed positive growth effect of inositol was dependent on the inositol transporter IolT and also on IolG, one can assume that it was due to the direct metabolism of inositol inside the host cell and not due to a secondary effect, where inositol was metabolized by the host and the bacteria would then profit from host metabolites, such as amino acids or glucose. Also, the transcriptome of *L. pneumophila* growing in macrophages suggests that inositol is used as a carbon source by the bacteria, since the expression of *iolG* and *iolCB* was over two-fold upregulated compared to exponentially growing bacteria (Faucher *et al.*, 2011). Inositol might therefore serve the intracellular nutrition of *L. pneumophila.* The LCV is likely accessible for inositol post infection, as the compound

promoted intracellular growth when added to the infected cells several hours after the infection (see section 4.4).

Other intracellular pathogens also utilize inositol in context with infection. *Mycobacterium* spp. use inositol to synthesize mycothiol that serves many functions including detoxification and protection from oxidative damage. The compound is essential for the bacteria and is discussed as an antitubercular drug target (Movahedzadeh *et al.*, 2004; Nilewar and Kathiravan, 2014). However, it is unclear whether the bacteria import inositol intracellularly or if they rely on *de novo* synthesis, although inositol transporter activity has been proven for *M. smegmatis* at least *in vitro* (Movahedzadeh *et al.*, 2004; Newton *et al.*, 2006). *S. enterica* uses inositol as a source of carbon and energy, and it was shown that the metabolism of inositol is regulated by IolR and the availability of inositol (Kröger and Fuchs, 2009). In addition, bicarbonate/CO_2 acts as a positive regulator of inositol catabolism genes in *Salmonella*, which is believed to be an adaption to a life in the gut, where bicarbonate concentrations exceed those that were sufficient to initiate transcription of inositol genes. The interplay between IolR and bicarbonate/CO_2 supposedly assures that inositol concentrations are high enough before gene expression is initiated (Kröger *et al.*, 2011). It is not known to date whether *S. enterica* also metabolizes inositol upon intracellular growth or just uses the carbohydrate as an extracellular carbon and energy source.

Taken together, available evidence indicates that inositol is metabolized by *L. pneumophila*, preferably during intracellular growth, although also extracellular uptake and metabolism of inositol was shown. These results extend the proven metabolic capacities of *L. pneumophila* by another carbon source and help to understand the nutrition of *Legionella* spp. particularly inside host cells.

4.2 The Metabolism of Glycerol by *Legionella pneumophila*

A defined *L. pneumophila* deletion mutant lacking the glycerol-3-phosphate dehydrogenase GlpD was constructed in this study and used to analyze the metabolism of glycerol under extra- and intracellular conditions. As predicted by transcriptome data (Faucher *et al.*, 2011), glycerol had no influence on the extracellular growth of wild-type or Δ*glpD* similar to inositol (see section 4.1). The *glpD* mutant exhibited a somewhat longer lag-phase than wild-type bacteria, but reached similar optical densities after 48 h growth in different chemically defined media (see section 3.2.1). The reason for that might be a disturbed energy balance and/or a disturbed phospholipid biosynthesis within the cell. Glycerol-3-phosphate is a precursor for the

biosynthesis of phospholipids. The *glpD* mutant could still produce glycerol-3-phosphate from glycerol in the reaction catalyzed by glycerol kinase Lpg1414, which is an ATP consuming reaction. In *E. coli* it was shown that GlpD is a central enzyme at the junction of respiration, glycolysis and phospholipid biosynthesis and important for the energy homeostasis of the cell, as it is an integral part of the electron transport chain in the inner membrane of *E. coli* (Yeh *et al.*, 2008). The conversion of glycerol-3-phosphate to dihydroxyacetone phosphate is not only important for glycolysis, but also delivers $FADH_2$ for the respiratory chain. The longer lag-phase of *L. pneumophila* Δ*glpD* might therefore also reflect a disturbed energy homeostasis, which would require certain adaptions to allow efficient cell growth and division. Nothing is known about membrane association and regulation of GlpD in *L. pneumophila* so far. Intracellularly, glycerol promoted growth of wild-type *L. pneumophila* in murine macrophages and *A. castellanii*, which was dependent on GlpD. In competition experiments, the mutant had a significant growth disadvantage compared to wild-type, although the mutant was not impaired in intracellular growth *per se* (see section 3.2.1). This suggested that glycerol might preferentially be used as an intracellular carbon source by *L. pneumophila*, but isotopologue profiling showed that glycerol was used in later growth phases also in broth, although it did not enhance extracellular growth (see section 3.2.1, 3.2.2 and 3.2.3).

The genomes of *L. pneumophila* (Cazalet *et al.*, 2004; Chien *et al.*, 2004; Steinert *et al.*, 2007) and *L. longbeachae* (Cazalet *et al.*, 2010; Kozak *et al.*, 2010) encode a complete glycolytic and ED pathway, as well as an incomplete PPP lacking 6-phosphogluconate dehydrogenase and the transaldolase. Glucose was already described as a carbon substrate for *L. pneumophila* and is preferentially metabolized via the ED pathway (Eylert *et al.*, 2010; Harada *et al.*, 2010). The data presented in this thesis now prove activity of the gluconeogenic pathway as well as the PPP, as ^{13}C-incorporation from labelled glycerol, glucose or serine occurred into mannose and histidine (see section 3.2.2 and 3.2.3). Mannose or rather mannose-6-phosphate is derived from fructose-6-phosphate in the reaction catalyzed by the mannose-6-phsophate isomerase RfbA, and therefore, depends on the gluconeogenic production of fructose-6-phosphate, at least with serine and glycerol as precursors. An integral enzyme of gluconeogenesis is fructose-1,6-bisphosphatase that converts fructose-1,6-bisphosphate to fructose-6-phosphate, which serves as precursor in mannose biosynthesis. An enzyme with homology to known fructose-1,6-bisphosphatases is not found in the genomes of *Legionella* spp., and only phosphofructokinase, the enzyme catalyzing the forward reaction, is annotated (Cazalet *et al.*, 2004; Chien *et al.*, 2004; Cazalet *et al.*, 2010).

Yet, the flow of ^{13}C-label into mannose, especially from serine and glycerol as substrate, and the fact that mannose was mainly M+3 and M+6 labelled in all isotopologue experiments indicates activity of the gluconeogenic pathway. An earlier study also described that the enzymatic activity of fructose-1,6-bisphophatase in *L. pneumophila* cell extracts was ten-fold higher than that of phosphofructokinase, clearly indicating that carbon flow is favorably directed towards gluconeogenesis rather than glycolysis (Keen and Hoffman, 1984). Also, when analyzing the phosphofructokinase of *L. pneumophila*, encoded by *lpg1913* (alias *pfkA*), it becomes evident that PfkA of *L. pneumophila* bears homology to eukaryotic and bacterial PfkA enzymes that use pyrophosphate rather than ATP as cofactor and are therefore reversible (Arimoto *et al.*, 2002; Costa dos Santos *et al.*, 2003). Taken together, the available data suggests that PfkA of *L. pneumophila* might also function as an enzyme catalyzing the forward (glycolytic) as well as the reverse (gluconeogenic) reaction between fructose-6-phosphate and fructose-1,6-bisphosphate.

Fructose-6-phosphate, together with glyeraldehyde-3-phosphate, is then the central metabolite for entry into the PPP, as *L. pneumophila* does not have a 6-phosphogluconate-deghydrogenase, an essential enzyme for the oxidative part of the PPP. Since histidine was found to be ^{13}C-enriched in all *in vitro* isotopologue experiments, the non-oxidative part of the PPP is active, as histidine is derived from ribose-5-phosphate. Another enzyme missing in the genome of *Legionella* spp. is the transaldolase enzyme (Cazalet *et al.*, 2004; Chien *et al.*, 2004; Cazalet *et al.*, 2010). Figure 4.1 shows the essential reactions of the “incomplete” PPP of *L. pneumophila* and illustrates where ^{13}C-label in mannose and histidine was presumably derived from.

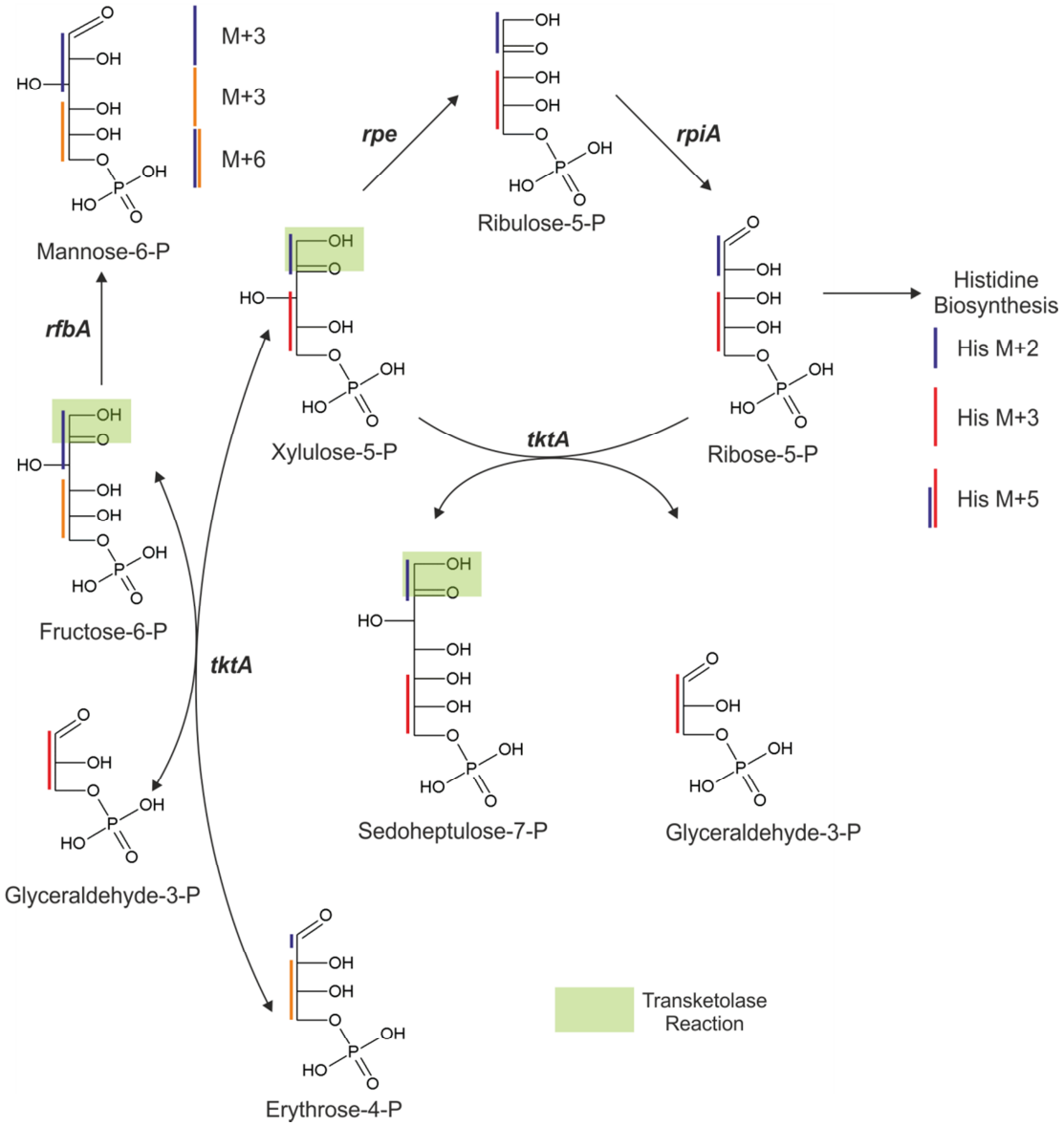

Figure 4.1: The PPP of *L. pneumophila* and occurrence of ^{13}C-label in mannose and histidine. Shown are transketolase reactions (**green rectangles**) between fructose-6-phosphate and glyceraldehyde-3-phosphate for the interconversion of sugars for cell wall biosynthesis and histidine synthesis. ^{13}C-label in mannose-6-phosphate and histidine is depicted by colored bars depending on the position and the precursor, the ^{13}C-label was presumably derived from.
Genes: ***rfbA,*** mannose-6-phosphate isomerase; ***rpe***, ribulose-5-phosphate epimerase; ***rpiA***, ribulose-5-phosphate isomerase; ***tktA***, transketolase.

The transketolase TktA transfers a C_2-fragment from fructose-6-phosphate onto glyceraldehyde-3-phosphate, resulting in erythrose-4- and xylulose-5-phosphate. In another transketolase reaction a C_2-fragment from xylulose-5-phosphate is transferred onto ribose-5-phosphate, resulting in seduheptulose-7-phosphate and glyceraldehyde-3-phosphate (Figure 4.1). As ribose-5-phosphate cannot be made from glucose-6-phosphate in *L. pneumophila*, because of the missing

6-phosphogluconate-dehydrogenase, it is presumably synthesized from xylulose-5-phosphate in the reactions of ribulose-5-phosphate epimerase (Rpe) and isomerase (RpiA). This non-oxidative branch of the PPP is sufficient for the interconversion of sugars that are needed for the synthesis of cell wall components, purines and pyrimidines, but cannot provide $NADPH/H^+$. However, as *L. pneumophila* employs the ED pathway for glucose catabolism (Eylert *et al.*, 2010; Harada *et al.*, 2010), the bacteria can synthesize $NADPH/H^+$ via this pathway.

In all isotopologue profiling experiments, at least with ^{13}C-glycerol and ^{13}C-glucose as precursors, histidine was mainly M+2 and M+3 labelled, indicating that either two or three C-atoms were labelled (see section 3.2.2. and 3.2.3). To a lesser extent also a fraction of M+5 labelled histidine appeared. Figure 4.1 shows where these entities of labelled histidines were derived from. With ^{13}C-glycerol as precursor, a part of the intracellular pool of glyceraldehyde-3-phosphate will be fully labelled (M+3). Fructose-6-phosphate might be unlabeled, or M+3 or M+6 labelled, depending on the label of glyceraldehyde-3-phosphate and dihydroxyacetone phosphate. M+3-label in histidine is then presumably derived from fully labelled glyceraldehyde-3-phosphate and unlabeled fructose-6-phosphate, resulting in three labelled carbon atoms in ribose-5-phosphate (Figure 4.1, red line). M+2 labelled histidine is derived from unlabeled glyceraldehyde-3-phosphate and fructose-6-phosphate, which has been M+3-labelled at the C-atoms that are transferred in the reaction of the transketolase and further onto ribose-5-phosphate in the reactions of the ribulose-5-phosphate epimerase and isomerase (Figure 4.1, blue line). The fraction of M+5 labelled histidine then is a combination of fully labelled glyceraldehyde-3-phosphate and M+3 labelled fructose-6-phosphate (Figure 4.1). Mannose was mainly M+3 and M+6 labelled in all isotopologue profiling experiments. The label is simply derived from M+3 or M+6 labelled fructose-6-phosphate, which is converted to mannose-6-phosphate by RfbA (Figure 4.1).

When the *glpD* mutant was grown *in vitro* with ^{13}C-glycerol as substrate, the only metabolite that was found to be significantly enriched was lactate (see section 3.2.2). This effect was independent of GlpD, as neither histidine nor mannose, that were both ^{13}C-enriched in the wild-type, nor were any other metabolites enriched in the mutant. A possible explanation for this might be the formation of methylglyoxal from glycerol. In *Enterobacteriaceae*, two glycerol assimilatory pathways exist (Subedi *et al.*, 2008). One that involves the phosphorylation of glycerol to glycerol-3-phosphate by a glycerol kinase, followed by the conversion of glycerol-3-phosphate to dihydroxyacetone phosphate catalyzed by a glycerol-3-phosphate dehydrogenase. In

L. pneumophila these reactions are catalyzed by *lpg1414* and *glpD* respectively (Figure 4.2). The second pathway consists of the glycerol dehydrogenase GldA that forms dihydroxyacetone from glycerol, which is then phosphorylated to dihydroxyacetone phosphate in a kinase reaction. Furthermore, dihydroxyacetone can be converted non-enzymatically to methylglyoxal within the cell (Subedi *et al.*, 2008). Methylglyoxal is a byproduct of different metabolic pathways and can also be generated non-enzymatically from glyceraldehyde-3-phosphate or dihydroxyacetone phosphate (Riddle and Lorenz, 1973; Cooper, 1984).

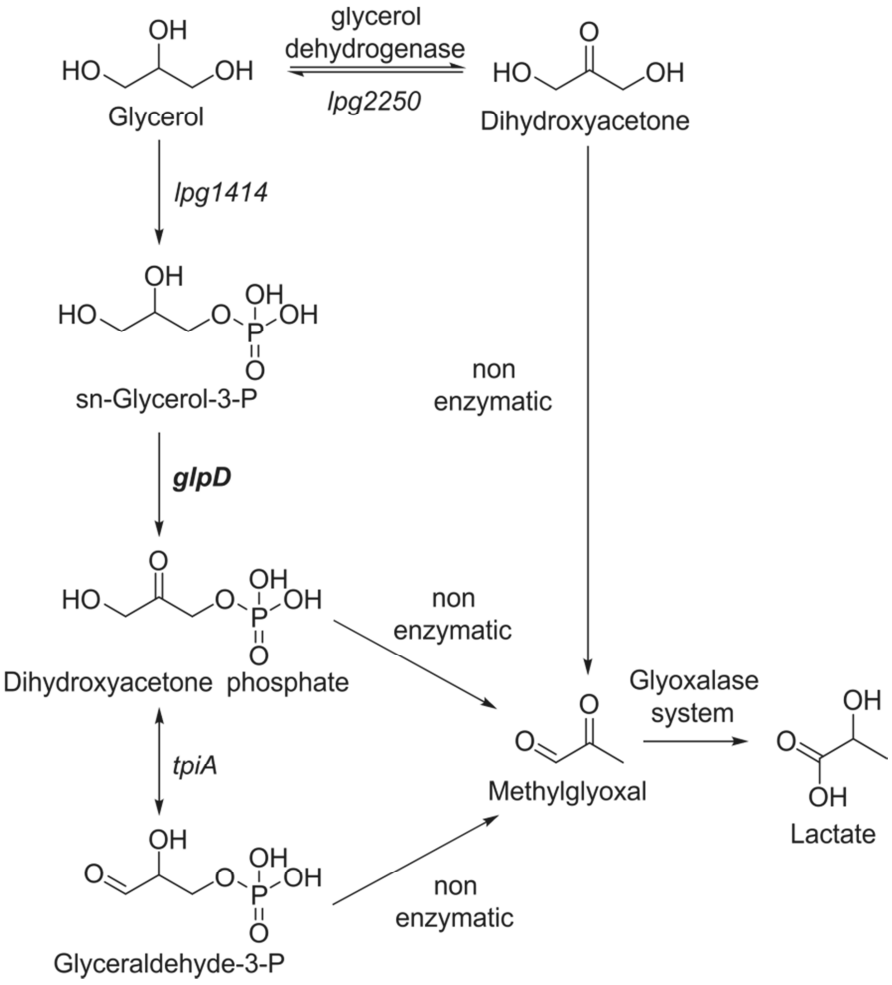

Figure 4.2: Proposed metabolism of methylglyoxal by *L. pneumophila*. Methylglyoxal is a toxic metabolite that can be derived non-enzymatically from dihydroxyacetone phosphate, glyceraldehyde-3-phosphate or dihydroxyacetone. To detoxify methylglyoxal the compound is converted to lactate by the glyoxalase system. In *L. pneumophila* Δ*glpD*, methylglyoxal could be derived from dihydroxyacetone directly made from glycerol, catalyzed by a glycerol dehydrogenase (supposedly *lpg2250*) (Published in Häuslein, Manske *et al.*, 2015).

As methylglyoxal is toxic, it is converted to lactate by the glyoxalase system (Figure 4.2) (Cooper, 1984). The protein Lpg2250 of *L. pneumophila* is annotated as alcohol dehydrogenase with 27% identity to *E. coli* GldA and might be responsible for the formation of dihydroxyacetone in Δ*glpD*. Also, genes for both enzymes of the glyoxalase system (*gloA* and *lpg1295*) are present in the genome of *L. pneumophila*, which would explain the flow from glycerol into lactate in the Δ*glpD* mutant (Figure 4.2).

4.3 The Bipartite Metabolism of *Legionella pneumophila*

The metabolism of glycerol was also compared to that of other carbon sources, namely glucose and serine under *in vitro* growth conditions. Earlier studies already indicated that serine is the preferred carbon substrate for *L. pneumophila* (George *et al.*, 1980; Eylert *et al.*, 2010), which was also confirmed in this work. The amount of ^{13}C-incorporation from ^{13}C-serine was the highest in all experiments compared to experiments with ^{13}C-glycerol and ^{13}C-glucose (see section 3.2.3), which showed the preference for this carbon source. Also, glucose was readily used as a carbon source by *L. pneumophila*, but glycerol was only used in later growth stages, as incorporation of ^{13}C-label was only found after 36 h and 48 h extracellular growth (see section 3.2.2 and 3.2.3). Under extracellular growth conditions, glycerol seems to play only a minor role for *L. pneumophila* metabolism, while glucose and especially serine are preferred carbon sources. The ratio of ^{13}C-excess in histidine as marker of the PPP and alanine as marker of the energy-generating lower part of glycolysis and the flow into the TCA cycle was calculated (see section 3.2.5), and it was found that glycerol and glucose were predominantly used as carbon sources for gluconeogenesis and the PPP, while carbon flow from serine was mainly restricted to the lower parts of glycolysis and the TCA cycle. These findings indicate that the metabolic fate of certain carbon sources is restricted to certain pathways resulting in a bipartite metabolism of *L. pneumophila* (Figure 4.3).

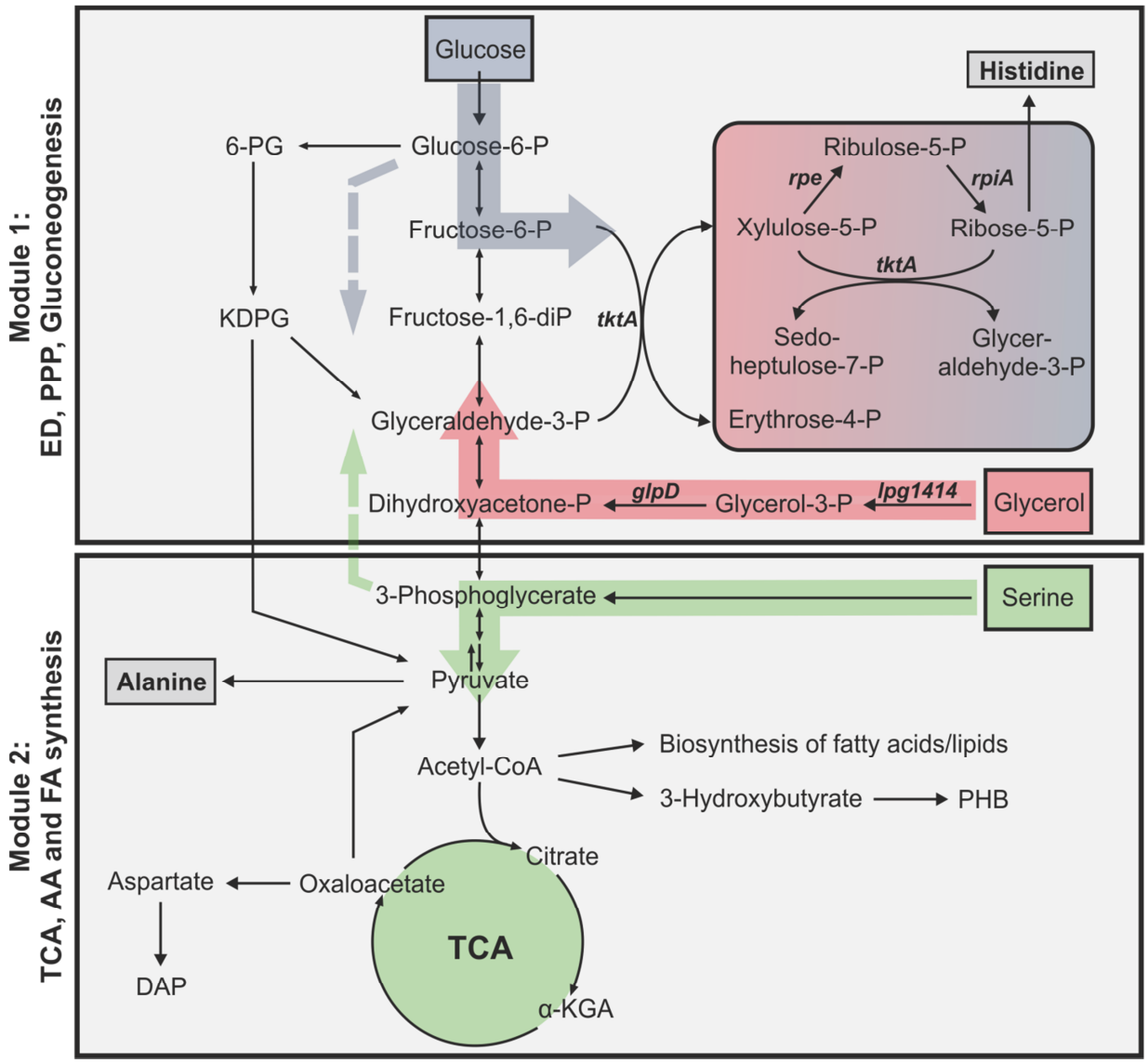

Figure 4.3: The bipartite metabolism of *L. pneumophila*. The metabolism of *L. pneumophila* is divided into two modules. Module 1 containing the ED pathway, gluconeogenesis and the PPP (**red/blue rectangle**) and module 2 containing the TCA cycle (**green cycle**), amino acid (**AA**) and fatty acid (**FA**) synthesis. The thick colored arrows represent the main routes of carbon flow from glucose (**blue**), glycerol (**red**) and serine (**green**). The flow from glucose and glycerol is mainly restricted to the upper part of metabolism in module 1, while serine is mainly used in the lower energy-generating parts of metabolism in module 2. Glucose and serine do also play a minor part in module 2 (**dotted blue arrow**) or module 1 (**dotted green arrow**), respectively (Published in Häuslein, Manske *et al*., 2015).

Abbreviations: 6-PG, 6-phosphogluconate; **KDPG**, 2-keto-3-desoxy-phosphogluconate; **PPP**, pentose phosphate pathway; **PHB**, poly-hydroxybutyrate; **TCA**, tricarbolic acid pathway; **α-KGA**, α-ketoglutaric acid; **DAP**, diaminopimelic acid.

Genes: ***tktA***, transketolase; ***rpe***, ribulose-5-phosphate-epimerase; ***rpiA***, ribulose-5-phosphate-isomerase; ***lpg1414***, glycerol kinase; ***glpD***, glycerol-3-phosphate dehydrogenase.

According to this model, the central carbon metabolism of *L. pneumophila* can be divided into two modules, of which module 1 comprises the ED pathway, the PPP and gluconeogenesis. This module provides $NADPH/H^+$ from reactions of the ED pathway, as well as precursors for anabolic reactions, essential for the synthesis of cell wall components, nucleotides, histidine and aromatic amino acids. Module 2 comprises the lower part of the glycolytic pathway, as well as the TCA cycle and provides precursors for aliphatic amino acids as well as fatty acids and lipids. Importantly, module 2 is the major energy-generating part of metabolism. ATP is synthesized by substrate phosphorylation in the dehydration of glyceraldehyde-3-phosphate to 3-phosphoglycerate and in the reaction of pyruvate kinase resulting in pyruvate. Furthermore, the TCA cycle supplies the cell with $NADH/H^+$ and $FADH_2$, which are used to synthesize ATP by oxidative phosphorylation via aerobic respiration. Accordingly, module 2 is the major energy providing part of metabolism, while module 1 is mainly energy-consuming, but essential for cell wall biosynthesis and hence cell division and proliferation. The experimental data presented here indicate that glucose and glycerol mainly serve module 1, while carbon flow from serine is mainly restricted to module 2 (Figure 4.3). Although this model is mainly based on data obtained from *in vitro* growth assays, *in vivo* data also support a bipartite intracellular metabolism of *L. pneumophila* (see section 3.2.6). Addition of ^{13}C-glycerol to infected *A. castellanii* resulted in a GlpD-dependent incorporation of ^{13}C-label into mannose. The same was observed with ^{13}C-glucose as precursor, but not with ^{13}C-serine, where incorporation of ^{13}C-label occurred into amino acids, DAP and PHB but not into mannose. These findings indicate that the concept of a bipartite metabolism might also apply for intracellularly growing *L. pneumophila*.

At this point, it can only be speculated whether and how inositol fits into this model. Since ^{13}C-inositol is commercially not available, isotopologue profiling experiments could not be performed. Inositol presumably would enter central carbon metabolism at the stages of dihydroxyacetone-phosphate and acetyl-CoA, which would have been shuffled into the TCA cycle and used for fatty acid synthesis. Dihydroxyacetone-phosphate could be used both for gluconeogenesis, but also for energy generation.

The concept of a modular metabolism seems to apply both for extracellular and intracellular growing *L. pneumophila*. Accordingly, glycerol might then also *in vivo* be used in later stages of intracellular growth, based on results obtained from *in vitro* experiments. At late stages of infection, the bacteria will switch from the replicative to the transmissive growth phase, lyse the LCV and eventually the host cell. The disintegration of host cell membranes through secreted

phospholipases might then also be the source of intracellular glycerol (Lang and Flieger, 2011). Other possible intracellular sources of glycerol will be discussed in section 4.4.

Noteworthy, a modular metabolism is also employed by other intracellular bacterial pathogens (Figure 4.4). *L. pneumophila* uses serine for energy generation in the lower parts of glycolysis and the TCA cycle, while glycerol and glucose are employed for gluconeogenesis and the PPP (Figure 4.4 A). *Listeria monocytogenes*, an intracellular pathogen that dwells in the host cell cytoplasm, can grow on different nutrients as sole source of carbon and energy *in vitro*, including glucose and glycerol (Schneebeli and Egli, 2013). *L. monocytogenes* can import amino acids from the host cell, but only uses them directly for protein synthesis (Grubmüller *et al.*, 2014). The major carbon sources for intracellularly growing *Listeria* seem to be glycerol and glucose-6-phosphate, with glycerol being used mainly in the lower parts of glycolysis and the TCA cycle for energy generation and glucose-6-phosphate mainly in the PPP. Glucose, if at all, is only used to a minor extent, and glucose-6-phosphate is the preferred carbon substrate of *L. monocytogenes* (Grubmüller *et al.*, 2014) (Figure 4.4 B). Similar to *Legionella*, *Listeria* also exhibits a bipartite metabolism, but this example also shows how a carbon substrate might be metabolized by different modules depending on the microorganism.

M. tuberculosis, the causative agent of tuberculosis, also exhibits a modular metabolism. *In vitro* studies showed that co-catabolism of different substrates occurs and that depending on the substrate combination the metabolic fate of these nutrients is defined (de Carvalho *et al.*, 2010). *M. tuberculosis* metabolizes glucose, glycerol and acetate at least under *in vitro* conditions. When fed with glucose and acetate, glucose is preferentially metabolized in the PPP and early steps of the glycolytic pathway, while acetate is mainly fed into the TCA cycle. The metabolic fate of glycerol, on the other hand, is dependent on its nutrient partner. When co-catabolized with glucose, the flow of carbon from glycerol is mainly directed towards the TCA cycle. However, when metabolized together with acetate, the flow is directed towards gluconeogenesis and the PPP (de Carvalho *et al.*, 2010) (Figure 4.4 C). The major carbon source during intracellular growth is a C_2-body, which presumably is acetate or acetyl-CoA, derived from β-oxidation of host lipids (Beste *et al.*, 2013). Furthermore, glycolytic C_3-compounds were shown to be carbon sources for *M. tuberculosis*.

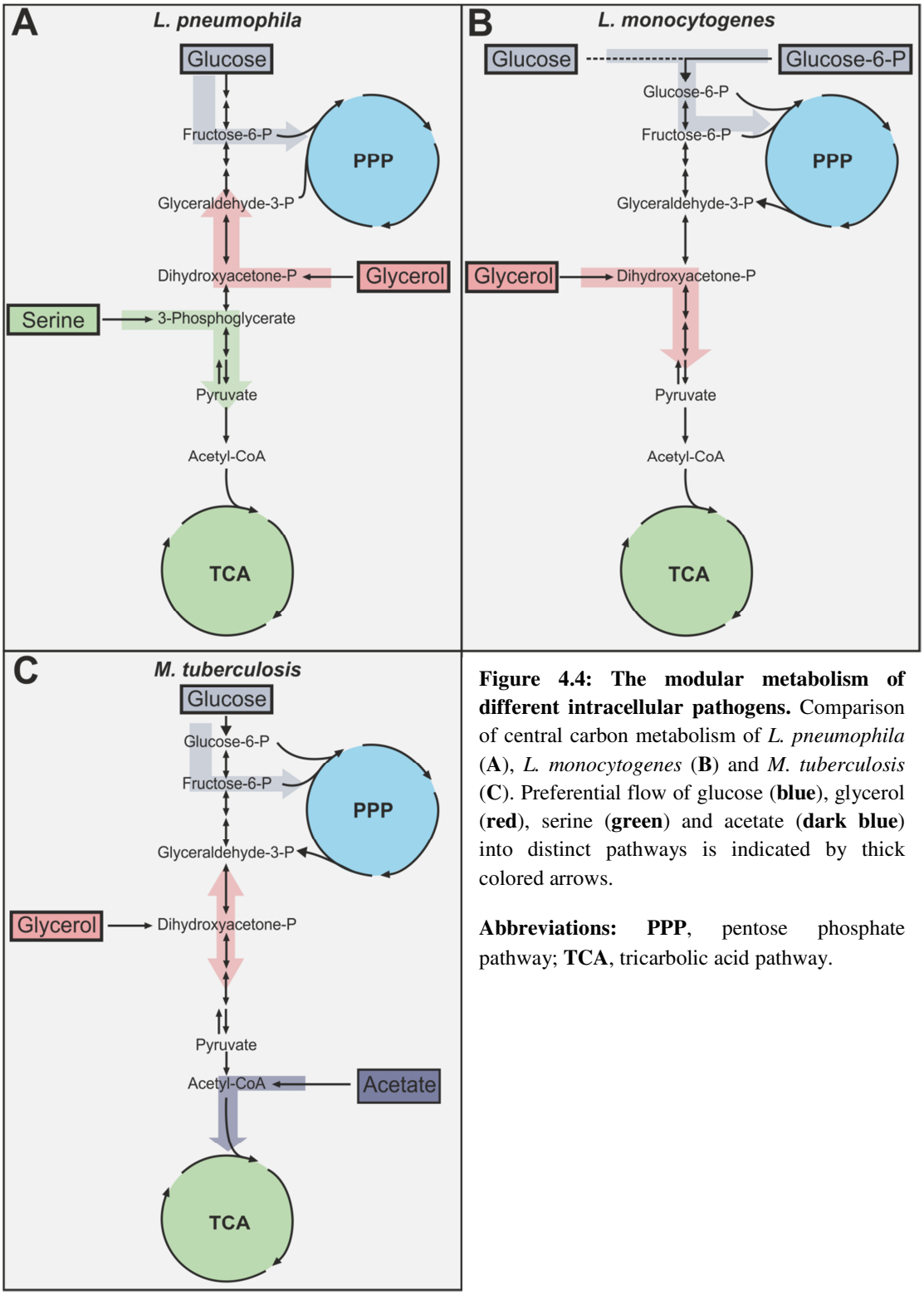

Figure 4.4: The modular metabolism of different intracellular pathogens. Comparison of central carbon metabolism of *L. pneumophila* (**A**), *L. monocytogenes* (**B**) and *M. tuberculosis* (**C**). Preferential flow of glucose (**blue**), glycerol (**red**), serine (**green**) and acetate (**dark blue**) into distinct pathways is indicated by thick colored arrows.

Abbreviations: **PPP**, pentose phosphate pathway; **TCA**, tricarbolic acid pathway.

These C_3-compounds could be derived from amino acids imported from the host cell, but also glycerol or glycerol-3-phosphate were discussed as potential carbon sources *in vivo*. Similar to extracellular growth, co-metabolism of different substrates is also occurring *in vivo* with preferential use of different carbon sources for certain pathways (Beste *et al.*, 2013).

Another pathogen, *S. enterica*, was also found to exploit a large number of different host nutrients in parallel in infected tissues with glycerol being the major carbon source for *in vivo* based on proteomic analysis (Steeb *et al.*, 2013). Furthermore, also during intracellular growth, the bacteria seem to access and rely on several carbon sources for parallel exploitation (Steeb *et al.*, 2013). Currently, no detailed flux analysis for intracellular growing *S. enterica* is available, and it is not known, whether these carbon sources are used for fixed metabolic pathways or not. Taking together all these findings, the concept of a modular metabolism appears to be a general concept for pathogens when replicating within their host cells.

It is striking that glucose or glucose-6-phosphate always seems to be used preferentially through the PPP by *Legionella* and *Listeria* as well as by *Mycobacterium*. For *L. pneumophila*, a metabolic strategy, which relies on amino acids as substrates for energy generation and that uses carbohydrates like glucose mainly for anabolic purposes might put less nutritional stress on the host cell, thus allowing successful and prolonged infection compared to bacteria that would rely on glucose as substrate for energy generation. A reason for this might be that the intracellular level of glucose is a regulator for apoptosis in eukaryotes (Zhao *et al.*, 2008). Apoptosis is initiated through two primary pathways: the mitochondrial, also called intrinsic, pathway and the death receptor, also called extrinsic, pathway (Danial and Korsmeyer, 2004). Glucose was found to directly affect the intrinsic pathway of apoptosis (Zhao *et al.*, 2008). As long as intracellular levels of glucose are normal, anti-apoptotic proteins of the Bcl-2 family prevent cell death. If the intracellular levels of glucose are disturbed, the levels of Bcl-2 regulators decrease (Alves *et al.*, 2006; Zhao *et al.*, 2007) and pro-apoptotic proteins are activated (Chi *et al.*, 2000). Apparently, the status of glucose metabolism also changes prior to cell death (Zhao *et al.*, 2008). The usage of glucose by intracellular pathogens in large amounts would therefore counteract the goal of a successful and prolonged infection of the host cell. This notion is supported by experimental data: *L. monocytogenes* and enteroinvasive *E. coli* both replicate inside the host cell cytoplasm, but use glucose for anabolic reactions (*L. monocytogenes*) or as main substrate for intracellular replication (*E. coli*). Interestingly, *E. coli* kills the same host cell much faster then *L. monocytogenes* (Götz *et al.*, 2010; Grubmüller *et al.*, 2014). The strategy of a bipartite

metabolism seems therefore to be a good adaption of *L. pneumophila* and other intracellular pathogens to an intracellular life-style.

4.4 Substrate Uptake into LCVs

It was shown in this study that *L. pneumophila* is able to metabolise glycerol and inositol *in vitro* and *in vivo*, and it was already known that the bacteria use amino acids, especially serine, and glucose as carbon sources (Eylert *et al.*, 2010; Harada *et al.*, 2010; Schunder *et al.*, 2014). The prerequisite for the *in vivo* metabolism of different substrates is the accessibility of the LCV for nutrients from the host cell cytoplasm, but also for substrates added from the outside to the host. *L. pneumophila* exploits eukaryotic amino acid transporters to facilitate amino acid uptake into the LCV (Wieland *et al.*, 2005). The transporter SLC1A5, which transports serine (Colas *et al.*, 2015), together with solute carrier proteins of the SLC7 family, are found in the proteome of purified LCVs and might facilitate the uptake of serine and other amino acids into the LCV lumen (Hoffmann *et al.*, 2014a). Upon intracellular growth of *L. pneumophila*, many different amino acids are taken up from the host (Schunder *et al.*, 2014), which are then imported into the bacterial cell by one of the various amino acid transporters (see section 1.2.1). In particular, serine is transported into the bacterial cell by the transporter SdaC (Figure 4.5).

This work now provides evidence that glycerol and glucose added to infected cells can directly reach the bacteria inside the LCV and are used as carbon source by intracellular *L. pneumophila*. These results suggest that the LCV is accessible also for other carbon sources. However, the mode of uptake for these substrates is not clear. Glycerol could enter the host cell via diffusion or transport. Transport can be facilitated through aquaglyceroporines, which are common transporters in eukaryotes that take up water and glycerol. Interestingly, these porines were recently also shown to be involved in innate immunity (Zhu *et al.*, 2011). The proteome of purified LCVs suggests that not glycerol but rather glycerol-3-phosphate might be more important for *L. pneumophila in vivo*, since the eukaryotic glycerol kinase (Gk) was identified in the LCV proteome. Gk could phosphorylate cytoplasmic glycerol to glycerol-3-phosphate, which subsequently might be transported by solute carriers of the SLC37 family that are also found in the proteome of LCVs (Hoffmann *et al.*, 2014a). Furthermore, in the genome of *L. pneumophila* only a glycerol-3-phosphate transporter (GlpT) is annotated, suggesting that the bacteria may transport glycerol-3-phosphate rather than glycerol. Another possibility of making glycerol available inside the host might be the exploitation of vesicular bodies by *L. pneumophila*. Lipid

bodies (LBs) are intracellular organelles that are found in all cell types and exhibit a distinctive architecture. LBs consist of a core containing triacylglycerols and sterolesters surrounded by a phospholipid hemimembrane with associated proteins (Tauchi-Sato *et al.*, 2002). These organelles were mainly associated with lipid storage in the past, but are now recognized as being involved in a variety of functions within the eukaryotic cell (Melo and Dvorak, 2012). LBs can fuse with several intracellular organelles including the phagosomes in cells of the immune system (Melo and Dvorak, 2012). Remarkably, *Mycobacterium bovis* and other *Mycobacterium* species were found to actively increase LB formation within their host cells (D'Avila *et al.*, 2006) and LBs as source of nutrients for the pathogens have been discussed (Peyron *et al.*, 2008; Mattos *et al.*, 2011; Barisch *et al.*, 2015). Whether LBs fuse with LCVs is not known, but it is imaginable that LBs could also constitute a nutrient source for *L. pneumophila*. The triacylglycerols released into the LCV lumen could be hydrolysed by type-II secreted phospholipases of *L. pneumophila* (Lang and Flieger, 2011), thus releasing fatty acids and glycerol inside the LCV (Figure 4.5).

Secreted effector proteins of *L. pneumophila* could also play a role in the acquisition of inositol. LppA is a type-IV-translocated phytase of *L. pneumophila* that functions as a hexakisphosphate inositol (phytate) phosphatase in infected phagocytes (Weber *et al.*, 2014a). Phytate is a major phosphorus storage compound in plants and the most abundant organic phosphorus compound in the environment (Turner *et al.*, 2002). Furthermore, an *L. pneumophila* host amoeba, *D. discoideum*, produces phytate in millimolar quantities (Stephens and Irvine, 1990). Phytate is a strong chelator of iron, resistant to hydrolysis and could be used as an intracellular bacteriostatic component, by depriving intracellular pathogens of iron. LppA might promote intracellular replication by removing phytate and making iron available to *L. pneumophila* inside the cell (Weber *et al.*, 2014a). Dephosphorylation of phytate might not only release iron, but would also yield inositol-phosphates or inositol, the sugar backbone of phytate, to be used by the bacteria. Inositol can also be taken up from the environment or be synthesized from glucose (Fischbach *et al.*, 2006). Humans synthesize inositol especially in the kidney in amounts of up to 4 g per day, and the highest amounts are found in the brain (Castillo *et al.*, 2000; Parthasarathy *et al.*, 2006). Inositol transporters of the solute carrier family 5 and family 2 facilitate uptake of inositol in mammalian cells (Klaus *et al.*, 2008) and perhaps, also into the LCV. IolT could then import inositol from the LCV lumen into the bacterial cell (Figure 4.5).

The data presented here also show the direct uptake and metabolism of glucose by *L. pneumophila* growing intracellularly (see section 3.2.6). Glucose is taken up into eukaryotic

cells by members of the Slc2 family of solute carriers (Mueckler and Thorens, 2013) or other major facilitators (Wright *et al.*, 1994). Solute carrier proteins are found in the plasma membrane of all eukaryotic cells (Palmada *et al.*, 2006). The proteome of purified LCVs revealed that also glucose transporters are incorporated into the LCV membrane, for example SLC2A1 (Glut1) and SLC2A6 (Glut6). Interestingly, besides these two glucose transporters, also SLC37A2 is found in the proteome of purified LCVs (Hoffmann *et al.*, 2014a). SLC37A2 is a phosphate-linked glucose-6-phosphate antiporter (Pan *et al.*, 2011) that could be used by *L. pneumophila* to transport glucose-6-phosphate into the LCV. As suggested in the present work, phosphorylated carbohydrates might be the preferred carbon source for *L. pneumophila* (see section 3.2.4), which corresponds to the acquisition of sugar-phosphate transporters and phosphorylating enzymes (see above) into the LCV membrane. Furthermore, the genome of *L. pneumophila* only encodes the hexose-phosphate transporter UhpC, which, for example, is used by the intracellular pathogen *Chlamydia pneumoniae* to transport glucose-6-phosphate (Schwoppe *et al.*, 2002). Also, *L. monocytogenes* relies on glucose-6-phosphate as substrate for intracellular growth (see section 4.3). Thus, perhaps also *L. pneumophila* exploits both, glucose and glucose-6-phosphate, upon intracellular growth (Figure 4.5).

The uptake of these substrates seems to be at least partially dependent on a functional Icm/Dot type IV secretion system. A fluorescent glucose analogue (2-NBDG) was found to be taken up into a high percentage of LCVs harbouring wild-type bacteria or inositol metabolism mutants. An *icmT* mutant on the other hand showed 50 % reduced uptake of 2-NBDG (see section 3.3.5). 2-NBDG has been used to study glucose uptake and metabolism in different organisms, including *E. coli* (Natarajan and Srienc, 1999), yeast (Oh and Matsuoka, 2002), neurons (Itoh *et al.*, 2004) and cancer cell lines (Cheng *et al.*, 2006) and is presumably transported by canonical glucose transporters of the cell (Yamada *et al.*, 2000). Import into wild-type LCVs could therfore be mediated through acquisition of host cell transporters via fusion of the LCV with ER exit site vesicles, which is happening shortly after bacterial uptake (Kagan and Roy, 2002). This vesicular fusion is dependent on the Icm/Dot T4SS, as vacuoles containing *icm/dot* mutants do not acquire ER vesicles as wild-type LCVs do (Kagan and Roy, 2002). The processes that lead to the fusion with these ER exit site vesicles are dependent on small GTPases and the non-canonical pairing of plasma membarane-derived t-SNARES with the ER-resident v-SNARE Sec22b (Arasaki and Roy, 2010; Finsel and Hilbi, 2015). The type IV-secreted effector protein SidM is responsible for this non-canonical SNARE fusion through activation of the small GTPase Rab1 (Arasaki *et al.*,

2012). Other effector proteins are also involved in the acquisition of ER-derived vesicles. The *L. pneumophila* effector protein LseA shows close homology to eukaryotic Qc-SNARE receptor family and is presumably a mediator of membrane fusion in Golgi-associated pathways (King *et al.*, 2015).

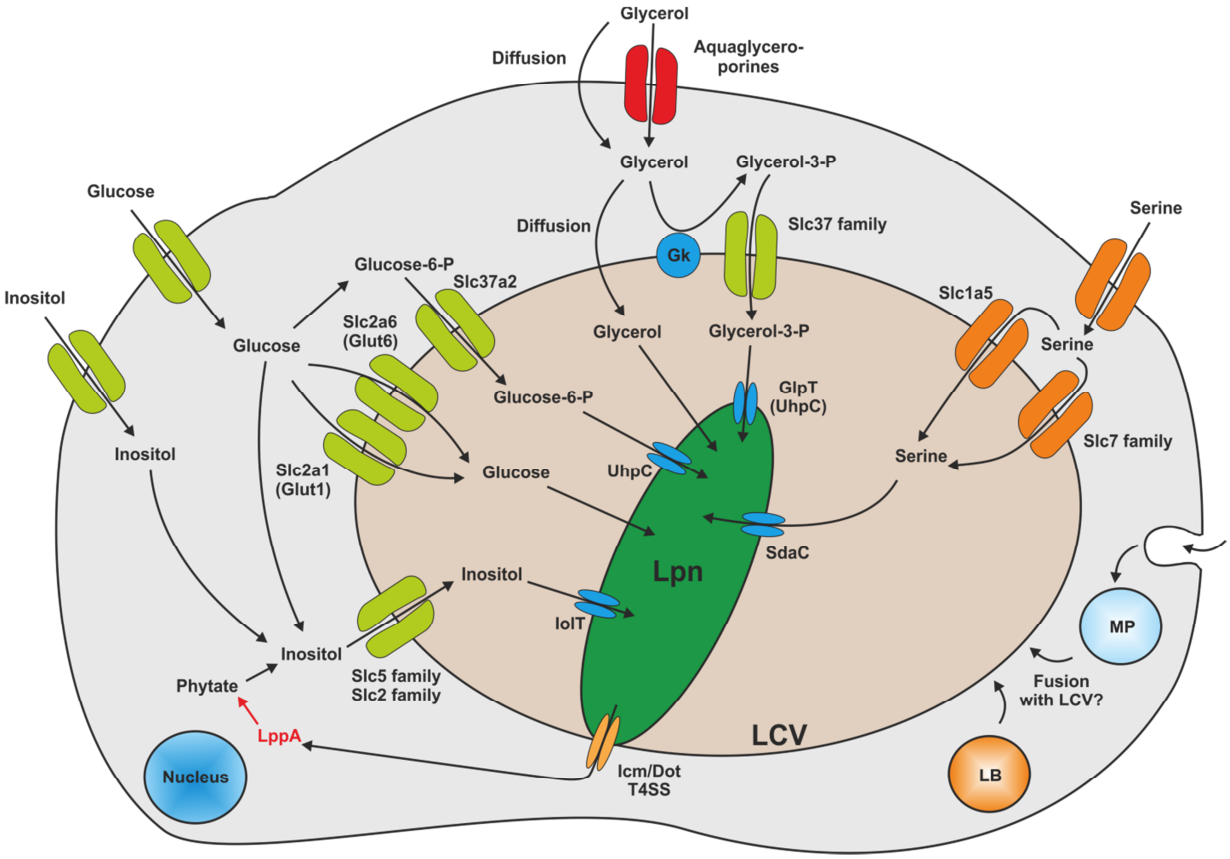

Figure 4.5: Nutrient uptake of *L. pneumphila* inside host cells. *L. pneumophila* has several ways to take up substrates inside its host. Serine is imported into the cell by solute carrier proteins (**orange**) of the Slc1 and Slc7 family, which have been identified on the LCV. SdaC is used as bacterial serine transporter. Glycerol can enter the cell via diffusion, aquaglyceroporines (**red**) or solute carrier (**green**) that could also transport glycerol-3-phosphate, which subsequently might be taken up by the bacteria with the transporter GlpT. Glucose is imported by several solute carrier transporters (**green**) and could reach the bacteria in form of glucose-6-phosphate or unpohosphorylated. The genome of *L. pneumophila* only harbours the glucose-6-phosphate transporter UhpC. Inositol can be derived from *de novo* synthesis with glucose as precursor, from transport via solute carrier (**green**) or from the dephosphorylation of phytate by the *L. pneumophila* type IV-secreted effector LppA. Import into the bacterial cell might be facilitated by IolT. Uptake of nutrients could also occur by fusion of lipid bodies (**LB**) with the LCV or macropinocytotic events (**MP**).
Abbreviations: Gk, glycerol kinase; **LB**, lipid body; **LCV**, *Legionella*-containing vacuole; **Lpn**, *Legionella pneumophila*; **MP**; macropinosome; **T4SS**, type IV secretion system.

A large number of effector proteins are also part of this interaction with the secretory pathway and the ER, for example by accumulating the lipid PtdIns(4)*P* in the LCV membrane and thus anchoring other effector proteins to the LCV (Weber *et al.*, 2014b; Finsel and Hilbi, 2015). An *icm/dot* mutant obviously cannot translocate all these effector proteins, as it does not possess a functional T4SS. This could explain the reduced number of 2-NBDG-positive LCVs in the *icmT* mutant used in this study, as the mutant strain would be unable to redirect host cell transporters to the LCV. For heterotrophic plant cells it was shown that 2-NBDG, and therefore likely glucose as well, can also be taken up by endocytic processes and end up in vesicles and vacuoles (Etxeberria *et al.*, 2005). Thus, endocytic processes like macropinocytosis, could also explain how 2-NBDG might reach *L. pneumophila* inside the host cell. *D. discoideum*, the host cell that was used here to test uptake of 2-NBDG, is able to take up fluid-phase material via macropinocytosis (Hacker *et al.*, 1997) and could therefore also take up 2-NBDG through this process. Interestingly, macropinocytosis was recently also associated with the metabolism in cancer cells, as these cells upregulate macropinocytosis to take up and degrade proteins as amino acid supply (Commisso *et al.*, 2013). Macropinocytosis or other endocytic processes might explain how nutrients are delivered to *L. pneumophila* inside the LCV, especially since our *in vivo* isotopologue profiling experiments showed that the substrates used reached the bacteria presumably unmetabolized (see section 3.2.6). Also other, yet unknown, substrates for *L. pneumophila* might reach the bacteria via this route (Figure 4.5).

Taken together, numerous ways of uptake of different nutrients into the LCV likely exist, but they are far from being understood. Further efforts have to be taken to fully grasp the metabolic capacities that are available for *L. pneumophila* inside its host cell.

4.5 Concluding Remarks

The metabolism of *L. pneumophila* still remains a rather uncharted field, and not much is known about the nutrition of the bacteria, especially *in vivo*. In this study, a new *Legionella* growth medium was developed and used to investigate the metabolism of inositol and glycerol *in vitro* and *in vivo*, as well as upon co-metabolism with the known substrates serine and glucose. The finding that glycerol and glucose were preferentially used for gluconeogenesis or in the upper parts of glycolysis, respectively, and serine was preferentially used for energy generation uncovered that *L. pneumophila* operates a bipartite metabolism. This concept might be a paradigm for intracellular pathogens and seems to be employed to dodge host cell defense programs, otherwise triggered by interfering with central host carbon metabolism. Inositol was found to be metabolized by *L. pneumophila* presumably also *in vivo*. The carbohydrate enhanced intracellular growth of *L. pneumophila.* Furthermore, the expression of the *iol* cluster was regulated by the sigma factor RpoS as well as by nutrient availability. However, the regulation of metabolic processes and the modes of substrate uptake inside the host cell still demands further research. The insights gained thus far might also help to find new therapies for *L. pneumophila*, as the metabolism of pathogens is arising as a promising novel target for developing new and efficient treatments against pathogens (Murima *et al.*, 2014).

Further efforts should therefore be taken to fully grasp the metabolic interplay between *L. pneumophila* and its host cells, because "it is only by understanding the true behavior and requirements of the bacteria when growing *in vivo* that we shall learn how to prevent their multiplication and, hopefully, how to cause their death" (Ratledge, 1976).

5. Supplementary Material

Table 5.1: Retention time (RT) and mass fragments of derivatized metabolites used for isotopologue calculations.

Metabolite	RT [min]	$[M-15]^+$	$[M-57]^+$	$[M-85]^+$
Ala	6.7		m/z 260	
Gly	7.0		m/z 246	
Val	8.5		m/z 288	
Leu	9.1			m/z 274
Ile	9.5			m/z 274
Pro	10.1			m/z 258
Ser	13.2		m/z 390	
Phe	14.5		m/z 336	
Asp	15.4		m/z 418	
Glu	16.8		m/z 432	
Lys	18.1		m/z 431	
His	20.4		m/z 432	
Tyr	21.0		m/z 466	
DAP	6.3		m/z 589	
PHB	9.1	m/z 233		
Lactate	17.8		m/z 261	
3-Hydroxybutyric acid	21.6		m/z 275	
Succinic acid	27.5		m/z 289	
Fumaric acid	28.7		m/z 287	
Malic acid	39.1		m/z 419	
Palmitic acid	44.0		m/z 313	
Stearic acid	49.4		m/z 341	
Citric acid	53.3		m/z 591	
Mannose	8.7	m/z 287		

Table 5.2: ^{13}C-Excess (mol%) from [U-$^{13}C_3$]glycerol at 48 h. ^{13}C-Excess (mol%) of amino acids, DAP, PHB, polar metabolites and mannose from experiments with *L. pneumophila* wild-type and Δ*glpD* grown in MDM supplemented with 50 mM [U-$^{13}C_3$]glycerol for 48 h. Mean and standard deviation from three independent experiments are shown.

50 mM [U-$^{13}C_3$]glycerol	*L. pneumophila* WT	*L. pneumophila ΔglpD*
Ala	0.34% ± 0.04%	0.23% ± 0.21%
Asp	0.36% ± 0.05%	0.12% ± 0.02%
Glu	0.55% ± 0.03%	0.20% ± 0.04%
Gly	0.11% ± 0.04%	0.08% ± 0.02%
His	3.01% ± 0.05%	0.06% ± 0.03%
Ile	0.09% ± 0.01%	0.07% ± 0.02%
Leu	0.01% ± 0.00%	0.01% ± 0.00%
Lys	0.39% ± 0.02%	0.12% ± 0.01%
Phe	0.07% ± 0.01%	0.06% ± 0.01%
Pro	0.18% ± 0.01%	0.09% ± 0.01%
Ser	0.10% ± 0.01%	0.12% ± 0.03%
Tyr	0.10% ± 0.02%	0.08% ± 0.02%
Val	0.12% ± 0.01%	0.13% ± 0.04%
DAP	0.74% ± 0.09%	0.17% ± 0.08%
PHB	0.12% ± 0.06%	0.00% ± 0.00%
Lactate	0.97% ± 0.20%	0.71% ± 0.29%
3-Hydroxybutyric acid	0.61% ± 0.05%	0.22% ± 0.06%
Succinic acid	0.24% ± 0.03%	0.09% ± 0.02%
Fumaric acid	0.32% ± 0.03%	0.15% ± 0.07%
Malic acid	0.70% ± 0.16%	0.29% ± 0.05%
Palmitic acid	0.15% ± 0.01%	0.07% ± 0.02%
Stearic acid	0.60% ± 0.05%	0.44% ± 0.06%
Citric acid	0.21% ± 0.03%	0.17% ± 0.01%
Mannose	5.75% ± 0.65%	0.12% ± 0.08%

Table 5.3: Relative fractions of isotopologues (%) from [U-$^{13}C_3$]glycerol at 48 h. Relative fractions of isotopologues (%) of histidine, lactate and mannose from *L. pneumophila* wild-type and Δ*glpD* grown in MDM supplemented with 50 mM [U-$^{13}C_3$]glycerol for 48 h. M+x represents the mass of the unlabeled metabolite plus x labeled ^{13}C-atoms. Mean and standard deviation from three independent experiments are shown.

L. pneumophila WT + 50 mM [U-$^{13}C_3$]glycerol			
	His	**Lactate**	**Mannose**
M+1	21.5% ± 2.61%	0.00% ± 0.00%	17.93% ± 1.05%
M+2	39.5% ± 0.69%	2.78% ± 2.67%	16.42% ± 2.23%
M+3	24.6% ± 0.8%	97.12% ± 19.66%	45.47% ± 4.86%
M+4	4.6% ± 0.31%		6.10% ± 0.97%
M+5	10.00% ± 0.72%		5.52% ± 1.40%
M+6	0.00% ± 0.00%		8.57% ± 1.56%
L. pneumophila Δ*glpD* + 50 mM [U-$^{13}C_3$]glycerol			
		Lactate	
M+1		0.00% ± 0.00%	
M+2		2.78% ± 3.57%	
M+3		97.22% ± 40.36%	

Table 5.4: Kinetics of ^{13}C-excess (mol%) from [U-$^{13}C_3$]glycerol. ^{13}C-excess (mol%) of amino acids, DAP, PHB, polar metabolites and mannose from time series experiments with *L. pneumophila* wild-type grown in CE MDM supplemented with 50 mM [U-$^{13}C_3$]glycerol.

50 mM [U-$^{13}C_3$]glycerol	**12 h**	**24 h**	**36 h**	**48 h**
Ala	0.36% ± 0.13%	0.37% ± 0.06%	0.54% ± 0.06%	0.61% ± 0.08%
Asp	0.37% ± 0.04%	0.28% ± 0.07%	0.48% ± 0.01%	0.49% ± 0.03%
Glu	0.68% ± 0.05%	0.55% ± 0.04%	0.74% ± 0.01%	0.77% ± 0.02%
Gly	0.44% ± 0.16%	0.41% ± 0.21%	0.32% ± 0.18%	0.38% ± 0.15%
His	0.33% ± 0.11%	0.66% ± 0.03%	2.70% ± 0.02%	3.00% ± 0.05%
Ile	0.19% ± 0.02%	0.20% ± 0.04%	0.16% ± 0.01%	0.19% ± 0.03%
Leu	0.11% ± 0.02%	0.05% ± 0.02%	0.10% ± 0.05%	0.03% ± 0.03%
Lys	0.12% ± 0.03%	0.13% ± 0.03%	0.36% ± 0.02%	0.46% ± 0.01%
Phe	0.17% ± 0.02%	0.20% ± 0.08%	0.18% ± 0.04%	0.15% ± 0.06%
Pro	0.09% ± 0.04%	0.15% ± 0.02%	0.31% ± 0.03%	0.31% ± 0.02%
Ser	0.10% ± 0.07%	0.17% ± 0.05%	0.13% ± 0.06%	0.14% ± 0.06%
Tyr	0.12% ± 0.03%	0.19% ± 0.02%	0.10% ± 0.04%	0.24% ± 0.07%
Val	0.05% ± 0.02%	0.05% ± 0.05%	0.03% ± 0.01%	0.03% ± 0.03%
DAP	0.27% ± 0.03%	0.25% ± 0.07%	0.72% ± 0.15%	0.80% ± 0.05%
PHB	0.42% ± 0.03%	0.27% ± 0.19%	0.29% ± 0.12%	0.52% ± 0.17%
Lactate				1.44% ± 0.05%
3-Hydroxybutyric acid				0.41% ± 0.06%
Succinic acid				0.22% ± 0.01%
Fumaric acid				0.29% ± 0.03%
Malic acid				0.55% ± 0.14%
Palmitic acid				0.19% ± 0.02%
Stearic acid				0.30% ± 0.01%
Citric acid				0.08% ± 0.01%
Mannose				4.51% ± 0.12%

Table 5.5: Kinetics of ^{13}C-excess (mol%) from [U-$^{13}C_6$]glucose. ^{13}C-Excess (mol%) of amino acids, DAP, PHB, polar metabolites and mannose from time series experiments with *L. pneumophila* wild-type grown in CE MDM supplemented with 11 mM [U-$^{13}C_6$]glucose.

11 mM [U-$^{13}C_6$]glucose	**12 h**	**24 h**	**36 h**	**48 h**
Ala	1.44% ± 0.03%	2.25% ± 0.02%	3.57% ± 0.10%	4.26% ± 0.07%
Asp	0.88% ± 0.02%	1.32% ± 0.07%	2.31% ± 0.03%	2.61% ± 0.04%
Glu	0.94% ± 0.03%	1.30% ± 0.02%	2.08% ± 0.03%	2.36% ± 0.01%
Gly	0.39% ± 0.05%	0.40% ± 0.03%	0.39% ± 0.06%	0.50% ± 0.04%
His	9.16% ± 0.08%	15.15% ± 0.04%	18.74% ± 0.05%	20.72% ± 0.01%
Ile	0.21% ± 0.02%	0.20% ± 0.01%	0.22% ± 0.01%	0.25% ± 0.01%
Leu	0.00% ± 0.00%	0.37% ± 0.33%	0.15% ± 0.02%	0.34% ± 0.36%
Lys	0.71% ± 0.00%	1.46% ± 0.04%	2.47% ± 0.05%	2.73% ± 0.04%
Phe	0.13% ± 0.02%	0.15% ± 0.03%	0.17% ± 0.03%	0.13% ± 0.03%
Pro	0.24% ± 0.04%	0.32% ± 0.02%	1.17% ± 0.05%	1.43% ± 0.04%
Ser	0.23% ± 0.10%	0.28% ± 0.03%	0.22% ± 0.06%	0.44% ± 0.01%
Tyr	0.04% ± 0.01%	0.07% ± 0.02%	0.03% ± 0.01%	0.06% ± 0.01%
Val	0.04% ± 0.04%	0.07% ± 0.01%	0.04% ± 0.02%	0.08% ± 0.01%
DAP	1.24% ± 0.14%	1.85% ± 0.13%	3.18% ± 0.08%	3.64% ± 0.08%
PHB	0.92% ± 0.11%	1.17% ± 0.14%	1.53% ± 0.17%	1.64% ± 0.20%
Lactate				0.29% ± 0.03%
3-Hydroxybutyric acid				1.45% ± 0.08%
Succinic acid				1.46% ± 0.03%
Fumaric acid				1.50% ± 0.14%
Malic acid				2.16% ± 0.28%
Palmitic acid				1.38% ± 0.03%
Stearic acid				1.52% ± 0.03%
Citric acid				0.19% ± 0.05%
Mannose				31.88% ± 0.08%

Table 5.6: Kinetics of ^{13}C-excess (mol%) from [U-$^{13}C_3$]serine. ^{13}C-Excess (mol%) of amino acids, DAP, PHB, polar metabolites and mannose from time series experiments with *L. pneumophila* wild-type grown in CE MDM supplemented with 6 mM [U-$^{13}C_3$]serine.

6 mM [U-$^{13}C_3$]serine	**12 h**	**24 h**	**36 h**	**48 h**
Ala	56.77% ± 0.37%	74.60% ± 0.62%	66.83% ± 0.26%	64.03% ± 0.28%
Asp	23.90% ± 0.17%	34.34% ± 0.19%	28.94% ± 0.14%	28.20% ± 0.15%
Glu	21.57% ± 0.02%	29.00% ± 0.38%	21.99% ± 0.10%	20.38% ± 0.05%
Gly	20.53% ± 0.14%	28.58% ± 0.27%	22.94% ± 0.18%	22.72% ± 0.05%
His	35.79% ± 1.13%	62.05% ± 3.23%	56.35% ± 2.55%	55.88% ± 3.32%
Ile	0.09% ± 0.01%	0.09% ± 0.00%	0.04% ± 0.01%	0.06% ± 0.02%
Leu	0.00% ± 0.00%	0.01% ± 0.01%	0.00% ± 0.00%	0.00% ± 0.00%
Lys	25.24% ± 0.12%	50.22% ± 0.22%	43.86% ± 0.21%	42.45% ± 0.21%
Phe	0.17% ± 0.06%	0.13% ± 0.02%	0.14% ± 0.02%	0.12% ± 0.01%
Pro	0.05% ± 0.04%	0.01% ± 0.02%	4.70% ± 0.14%	4.45% ± 0.06%
Ser	71.13% ± 0.17%	91.61% ± 0.17%	64.59% ± 0.20%	60.83% ± 0.30%
Tyr	0.25% ± 0.05%	0.12% ± 0.08%	0.11% ± 0.04%	0.12% ± 0.04%
Val	0.16% ± 0.05%	0.16% ± 0.08%	0.09% ± 0.02%	0.07% ± 0.02%
DAP	46.62% ± 0.17%	55.02% ± 0.12%	41.05% ± 0.21%	38.31% ± 0.24%
PHB	29.97% ± 0.51%	39.16% ± 0.56%	16.75% ± 0.21%	15.70% ± 0.67%
Lactate				0.31% ± 0.11%
3-Hydroxybutyric acid				12.45% ± 0.31%
Succinic acid				3.53% ± 0.09%
Fumaric acid				5.63% ± 0.27%
Malic acid				4.34% ± 0.19%
Palmitic acid				32.64% ± 1.73%
Stearic acid				34.26% ± 1.93%
Citric acid				0.15% ± 0.01%
Mannose				40.40% ± 0.59%

Table 5.7: Relative fractions of isotopologues (%) of amino acids, DAP and PHB from time series experiments. *L. pneumophila* wild-type was grown in CE MDM supplemented with either (**i**) 50 mM [U-$^{13}C_3$]glycerol, (**ii**) 11 mM [U-$^{13}C_6$]glucose or (**iii**) 6 mM [U-$^{13}C_3$]serine as precursor. Shown are isotopologue profiles (in %) of 48 h time points from time series experiments. M+x represents the mass of the unlabeled metabolite plus x labeled ^{13}C-atoms. Mean and standard deviation from three independent experiments are shown.

i) 50 mM [U-$^{13}C_3$]glycerol										
	Ala	**Asp**	**Glu**	**Gly**	**His**	**Lys**	**Pro**	**Ser**	**DAP**	**PHB**
M+1					22.48% ± 6.77%					
M+2					35.70% ± 0.40%					
M+3					31.66% ± 1.30%					
M+4					3.66% ± 0.12%					
M+5					6.53% ± 0.15%					
M+6					0.00% ± 0.00%					
M+7										
ii) 11 mM [U-$^{13}C_6$]glucose										
	Ala	**Asp**	**Glu**	**Gly**	**His**	**Lys**	**Pro**	**Ser**	**DAP**	**PHB**
M+1	27.55% ± 3.52%	64.50% ± 2.70%	58.44% ± 0.67%		15.81% ± 0.14%	42.17% ± 2.04%			31.66% ± 3.54%	36.39% ± 8.65%
M+2	12.52% ± 0.44%	24.08% ± 0.48%	38.30% ± 0.48%		37.35% ± 0.18%	31.25% ± 0.86%			26.49% ± 1.97%	61.95% ± 7.95%
M+3	59.89% ± 0.57%	11.45% ± 0.29%	2.92% ± 0.13%		21.61% ± 0.08%	26.67% ± 0.42%			38.98% ± 1.39%	0.83% ± 0.72%
M+4		0.00% ± 0.00%	0.04% ± 0.07%		10.62% ± 0.13%	0.00% ± 0.00%			0.60% ± 1.05%	0.98% ± 0.42%
M+5			0.38% ± 0.01%		14.62% ± 0.12%	0.00% ± 0.00%			1.42% ± 0.44%	
M+6					0.00% ± 0.00%	0.00% ± 0.00%			0.80% ± 0.16%	
M+7									0.06% ± 0.06%	
iii) 6 mM [U-$^{13}C_3$]serine										
	Ala	**Asp**	**Glu**	**Gly**	**His**	**Lys**	**Pro**	**Ser**	**DAP**	**PHB**
M+1	10.19% ± 0.15%	28.29% ± 0.77%	27.39% ± 1.90%	4.97% ± 0.15%	13.37% ± 1.71%	11.45% ± 0,16%	43.36% ± 0.76%	11.45% ± 0.39%	12.44% ± 0.86%	31.06% ± 1.73%
M+2	8.39% ± 0.16%	35.03% ± 0.42%	37.11% ± 1.01%	95.03% ± 0.30%	11.62% ± 1.43%	22.42% ± 0.29%	27.34% ± 1.48%	8.51% ± 0.11%	10.54% ± 0.87%	52.63% ± 1.99%
M+3	81.43% ± 0.45%	24.48% ± 0.29%	18.62% ± 0.23%		17.43% ± 1.11%	26.21% ± 0.20%	19.25% ± 0.86%	80.04% ± 0.39%	32.48% ± 1.26%	6.08% ± 0.05%
M+4		12.22% ± 0.05%	11.16% ± 0.27%		18.59% ± 0.33%	18.09% ± 0.19%	7.31% ± 0.62%		13.83% ± 0.26%	10.24% ± 0.79%
M+5			5.71% ± 0.13%		15.43% ± 2.57%	14.54% ± 0.15%	2.79% ± 0.33%		14.88% ± 0.55%	
M+6					22.95% ± 2.80%	7.27% ± 0.08%			10.39% ± 0.88%	
M+7									5.43% ± 0.73%	

Table 5.8: Relative fractions of isotopologues (mol%) of polar metabolites and mannose from time-series experiments. *L. pneumophila* wild-type was grown in CE MDM supplemented with either (**i**) 50 mM [U-$^{13}C_3$]glycerol, (**ii**) 11 mM [U-$^{13}C_6$]glucose or (**iii**) 6 mM [U-$^{13}C_3$]serine as precursor. Shown are isotopologue profilies (in %) of 48 h time points from time series experiments. M+x represents the mass of the unlabeled metabolite plus x labeled ^{13}C-atoms. Mean and standard deviation from three independent experiments are shown.

i) 50 mM [U-$^{13}C_3$]glycerol								
	Lactate	**3-HBA**	**Succinic acid**	**Fumaric acid**	**Malic acid**	**Palmitic acid**	**Stearic acid**	**Mannose**
M+1	0.00% ± 0.00%							26.16% ± 3.13%
M+2	2.77% ± 3.94%							20.00% ± 0.18%
M+3	97.99% ± 1.40%							40.59% ± 0.71%
M+4								5.81% ± 0.35%
M+5								3.89% ± 0.42%
M+6								3.53% ± 0.21%
ii) 11 mM [U-$^{13}C_6$]glucose								
	Lactate	**3-HBA**	**Succinic acid**	**Fumaric acid**	**Malic acid**	**Palmitic acid**	**Stearic acid**	**Mannose**
M+1		39.96% ± 11.04%	51.77% ± 1.85%	45.44% ± 5.08%	59.08% ± 9.73%	17.20% ± 1.35%	30.10% ± 2.07%	10.82% ± 0.58%
M+2		57.71% ± 1.69%	39.37% ± 1.16%	36.78% ± 4.81%	31.97% ± 9.58%	74.65% ± 0.84%	59.60% ± 2.63%	12.42% ± 0.41%
M+3		1.19% ± 1.07%	8.86% ± 0.37%	15.21% ± 1.58%	8.55% ± 1.70%	2.64% ± 0.52%	3.41% ± 0.21%	30.20% ± 0.46%
M+4		1.20% ± 0.35%	0.08% ± 0.14%	2.73% ± 1.75%	0.38% ± 0.66%	5.09% ± 0.23%	5.24% ± 0.25%	10.33% ± 0.37%
M+5						0.26% ± 0.01%	0.41% ± 0.04%	4.76% ± 0.23
M+6						0.12% ± 0.02%	0.60% ± 0.02%	31.50% ± 0.50%
M+7						0.00% ± 0.00%	0.05% ± 0.01%	
M+8						0.00% ± 0.00%	0.13% ± 0.03%	
M+9						0.00% ± 0.00%	0.00% ± 0.00%	
M+10						0.00% ± 0.00%	0.00% ± 0.00%	
M+11						0.00% ± 0.00%	0.00% ± 0.00%	
M+12						0.00% ± 0.00%	0.02% ± 0.01%	
M+13						0.00% ± 0.00%	0.01% ± 0.00%	
M+14						0.00% ± 0.00%	0.00% ± 0.00%	
M+15						0.00% ± 0.00%	0.01% ± 0.00%	
M+16						0.00% ± 0.00%	0.01% ± 0.00%	
M+17							0.00% ± 0.00%	

M+18							0.00% ± 0.00%	
iii) 6 mM [U-$^{13}C_3$]serine								
	Lactate	**3-HBA**	**Succinic acid**	**Fumaric acid**	**Malic acid**	**Palmitic acid**	**Stearic acid**	**Mannose**
M+1		31.33% ± 0.85%	66.47% ± 2.22%	54.02% ± 2.24%	64.47% ± 3.18%	5.74% ± 0.08%	4.47% ± 0.18%	9.05% ± 0.46%
M+2		52.67% ± 1.29%	28.62% ± 0.97%	31.04% ± 1.79%	29.39% ± 6.86%	10.50% ± 0.20%	7.48% ± 0.24%	10.68% ± 0.16%
M+3		4.97% ± 0.23%	4.50% ± 0.34%	10.78% ± 0.27%	5.69% ± 2.66%	4.37% ± 0.24%	3.38% ± 0.09%	28.34% ± 0.29%
M+4		10.98% ± 0.152	0.35% ± 0.15%	4.22% ± 0.44%	0.40% ± 0.70%	7.79% ± 0.20%	5.41% ± 0.26%	12.11% ± 0.19%
M+5						5.53% ± 0.14%	4.18% ± 0.14%	10.16% ± 0.30%
M+6						10.98% ± 0.48%	8.26% ± 0.36%	29.67% ± 1.05%
M+7						7.80% ± 0.40%	6.95% ± 0.33%	
M+8						13.24% ± 0.62%	11.92% ± 0.69%	
M+9						7.99% ± 0.37%	8.87% ± 0.54%	
M+10						11.12% ± 0.69%	12.29% ± 0.65%	
M+11						5.01% ± 0.41%	7.37% ± 0.39%	
M+12						5.92% ± 0.42%	8.66% ± 0.52%	
M+13						1.80% ± 0.15%	4.03% ± 0.31%	
M+14						1.75% ± 0.17%	4.02% ± 0.235	
M+15						0.25% ± 0.02%	1.28% ± 0.11%	
M+16						0.21% ± 0.03%	1.09% ± 0.09%	
M+17							0.19% ± 0.02%	
M+18							0.14% ± 0.01%	

Table 5.9: Kinetics of ^{13}C-excess (mol%) in histidine from co-metabolism experiments with glycerol and glucose as precursor. *L. pneumophila* wild-type was grown in MDM supplemented with either 50 mM [U-$^{13}C_3$]glycerol or 50 mM [U-$^{13}C_3$]glycerol and 11 mM glucose, 11 mM [U-$^{13}C_6$]glucose or 11 mM [U-$^{13}C_6$]glucose and 50 mM glycerol or 11 mM [U-$^{13}C_6$]glucose or 11 mM [U-$^{13}C_6$]glucose and 11 mM glucose-6-phosphate.

^{13}C-excess [mol%] in histidine	**12 h**	**24 h**	**36 h**	**48 h**
50mM [U-$^{13}C_3$]glycerol	0.37% ± 0.04%	0.92% ± 0.08%	3.47% ± 0.09%	4.29% ± 0.04%
50mM [U-$^{13}C_3$]glycerol + 11mM glucose	0.33% ± 0.11%	0.66% ± 0.03%	2.70% ± 0.02%	3.00% ± 0.05%
11mM [U-$^{13}C_6$]glucose	9.31% ± 0.04%	18.45% ± 0.03%	18.57% ± 0.02%	18.61% ± 0.04%
11mM [U-$^{13}C_6$]glucose + 50mM glycerol	9.16% ± 0.08%	15.15% ± 0.04%	18.74% ± 0.05%	20.72% ± 0.01%
11mM [U-$^{13}C_6$]glucose	9.31% ± 0.04%	18.45% ± 0.03%	18.57% ± 0.02%	18.61% ± 0.04%
11mM [U-$^{13}C_6$]glucose + 11mM glucose-6-phosphate	5.24% ± 1.12%	8.04% ± 1.72%	8.28% ± 1.84%	8.41% ± 1.75%

Table 5.10: Ratio of ^{13}C-excess in histidine to ^{13}C-excess in alanine calculated from time series experiments with *L. pneumophila* wild-type grown in CE MDM with either 50 mM [U-$^{13}C_3$]glycerol, 11 mM [U-$^{13}C_6$]glucose or 6 mM [U-$^{13}C_3$]serine as precursor. Shown is the ratio of means from samples taken after 12, 24, 36 or 48 h. Standard deviation was calculated from the highest possible (**+**) and the lowest possible (**-**) value.

Ratio: ^{13}C-Excess [mol%] **His**/^{13}C-Excess [mol%] **Ala**												
	12 h	**+**	**-**	**24 h**	**+**	**-**	**36 h**	**+**	**-**	**48 h**	**+**	**-**
50 mM [U-$^{13}C_3$]glycerol	0.94	1.05	0.48	1.79	0.49	0.34	4.99	0.71	0.56	4.92	0.89	0.67
11 mM [U-$^{13}C_6$]glucose	6.34	0.21	0.20	6.74	0.07	0.07	5.25	0.17	0.16	4.87	0.08	0.08
6 mM [U-$^{13}C_3$]serine	0.63	0.02	0.02	0.83	0.05	0.05	0.84	0.04	0.04	0.87	0.06	0.06

Table 5.11: ^{13}C-Excess (mol%) of alanine, aspartate, glutamate, glycine, serine, DAP, PHB and mannose from experiments with uninfected *A. castellanii* and *A. castellanii* infected with *L. pneumophila* wild-type or Δ*glpD*. Infections were supplemented with either (**i**) 50 mM [U-$^{13}C_3$]glycerol, (**ii**) 11 mM [U-$^{13}C_6$]glucose or (**iii**) 6 mM [U-$^{13}C_3$]serine 5 h post infcection. Cells were lysed and fractionated 15 h post infection, resulting in fraction 1 (**F1**), containing eukaryotic cell debris and fraction 2 (**F2**), containing *L. pneumophila* bacteria.

i) 50 mM [U-$^{13}C_3$]glycerol					
	uninfected	WT-infected (**F1**)	WT-infected (**F2**)	Δ*glpD*-infected (**F1**)	Δ*glpD*-infected (**F2**)
Ala	17.83% ± 0.28%	0.37% ± 0.19%	0.48% ± 0.14%	0.55% ± 0.22%	0.46% ± 0.11%
Asp	7.51% ± 0.37%	0.18% ± 0.13%	0.22% ± 0.08%	0.17% ± 0.09%	0.19% ± 0.05%
Glu	10.65% ± 0.06%	0.32% ± 0.10%	0.61% ± 0.26%	0.58% ± 0.24%	0.51% ± 0.18%
Gly	7.22% ± 0.18%	0.68% ± 0.89%	0.12% ± 0.10%	0.19% ± 0.14%	0.08% ± 0.10%
Ser	9.26% ± 0.18%	0.20% ± 0.11%	0.20% ± 0.05%	0.25% ± 0.03%	0.24% ± 0.02%
DAP			0.52% ± 0.04%		0.24% ± 0.03%
PHB			0.06% ± 0.03%		0.07% ± 0.10%
Mannose		0.23% ± 0.19%	0.67% ± 0.07%	0.11% ± 0.04%	0.10% ± 0.04%
ii) 11 mM [U-$^{13}C_6$]glucose					
	uninfected	WT-infected (**F1**)	WT-infected (**F2**)		
Ala	5.98% ± 0.12%	1.22% ± 0.16%	2.06% ± 0.44%		
Asp	2.33% ± 0.04%	0.24% ± 0.00%	0.54% ± 0.17%		
Glu	3.09% ± 0.07%	0.74% ± 0.16%	1.28% ± 0.39%		
Gly	0.57% ± 0.22%	0.27% ± 0.17%	0.27% ± 0.07%		
Ser	0.31% ± 0.06%	0.22% ± 0.01%	0.22% ± 0.02%		
DAP			5.18% ± 1.30%		
PHB			3.91% ± 1.11%		
Mannose		0.60% ± 0.27%	4.47% ± 0.40%		
iii) 6 mM [U-$^{13}C_3$]serine					
	uninfected	WT-infected (**F1**)	WT-infected (**F2**)		
Ala	1.32% ± 0.07%	6.85% ± 1.07%	17.90% ± 0.44%		
Asp	0.37% ± 0.09%	1.36% ± 0.50%	3.82% ± 0.05%		
Glu	0.93% ± 0.10%	2.66% ± 1.35%	8.18% ± 0.05%		
Gly	5.43% ± 0.15%	2.11% ± 0.59%	4.64% ± 0.11%		
Ser	12.63% ± 0.08%	12.52% ± 2.21%	31.51% ± 0.16%		
DAP			31.35% ± 0.23%		
PHB			33.64% ± 1.00%		
Mannose		0.10% ± 0.04%	0.22% ± 0.08%		

Table 5.12: Relative fraction of isotopologues in mannose (%) from fraction 2 of *in vivo* infection and separation experiments. *A. castellanii* cells were either fed with (**i**) 50 mM [U-$^{13}C_3$]glycerol or (**ii**) 11 mM [U-$^{13}C_6$]glucose. M+x represents the mass of the unlabeled metabolite plus x labeled ^{13}C-atoms. Mean and standard deviation from two independent experiments are shown.

Relative fraction of isotopologues in mannose		
	i) 50 mM [U-$^{13}C_3$]glycerol	**ii) 11 mM [U-$^{13}C_6$]glucose**
M+1	19.59% ± 11.87%	6.25% ± 3.84%
M+2	4.97% ± 3.03%	12.51% ± 0.07%
M+3	67.67% ± 2.80%	30.37% ± 2.80%
M+4	4.38% ± 0.51%	9.12% ± 0.97%
M+5	1.80% ± 1.09%	3.81% ± 0.40%
M+6	2.35% ± 1.67%	37.86% ± 3.11%

Literature

Abdel-Nour, M., Duncan, C., Low, D.E., and Guyard, C. (2013). Biofilms: the stronghold of *Legionella pneumophila*. *Int J Mol Sci* 14**,** 21660-21675.

Abdel-Nour, M., Duncan, C., Prashar, A., Rao, C., Ginevra, C., Jarraud, S., Low, D.E., Ensminger, A.W., Terebiznik, M.R., and Guyard, C. (2014). The *Legionella pneumophila* collagen-like protein mediates sedimentation, autoaggregation, and pathogen-phagocyte interactions. *Appl Environ Microbiol* 80**,** 1441-1454.

Abdelhady, H., and Garduno, R.A. (2013). The progeny of *Legionella pneumophila* in human macrophages shows unique developmental traits. *FEMS Microbiol Lett* 349**,** 99-107.

Al-Bana, B.H., Haddad, M.T., and Garduno, R.A. (2014). Stationary phase and mature infectious forms of *Legionella pneumophila* produce distinct viable but non-culturable cells. *Environ Microbiol* 16**,** 382-395.

Al-Khodor, S., Kalachikov, S., Morozova, I., Price, C.T., and Abu Kwaik, Y. (2009). The PmrA/PmrB two-component system of *Legionella pneumophila* is a global regulator required for intracellular replication within macrophages and protozoa. *Infect Immun* 77**,** 374-386.

Allard, K.A., Dao, J., Sanjeevaiah, P., Mccoy-Simandle, K., Chatfield, C.H., Crumrine, D.S., Castignetti, D., and Cianciotto, N.P. (2009). Purification of Legiobactin and importance of this siderophore in lung infection by *Legionella pneumophila*. *Infect Immun* 77**,** 2887-2895.

Allard, K.A., Viswanathan, V.K., and Cianciotto, N.P. (2006). *lbtA* and *lbtB* are required for production of the *Legionella pneumophila* siderophore legiobactin. *J Bacteriol* 188**,** 1351-1363.

Alli, O.A., Gao, L.Y., Pedersen, L.L., Zink, S., Radulic, M., Doric, M., and Abu Kwaik, Y. (2000). Temporal pore formation-mediated egress from macrophages and alveolar epithelial cells by *Legionella pneumophila*. *Infect Immun* 68**,** 6431-6440.

Altman, E., and Segal, G. (2008). The response regulator CpxR directly regulates expression of several *Legionella pneumophila icm/dot* components as well as new translocated substrates. *J Bacteriol* 190**,** 1985-1996.

Alves, N.L., Derks, I.A., Berk, E., Spijker, R., Van Lier, R.A., and Eldering, E. (2006). The Noxa/Mcl-1 axis regulates susceptibility to apoptosis under glucose limitation in dividing T cells. *Immunity* 24**,** 703-716.

Andersen, J.B., Heydorn, A., Hentzer, M., Eberl, L., Geisenberger, O., Christensen, B.B., Molin, S., and Givskov, M. (2001). gfp-based N-acyl homoserine-lactone sensor systems for detection of bacterial communication. *Appl Environ Microbiol* 67**,** 575-585.

Anderson, A., and Cooper, R.A. (1969). Gluconeogenesis in *Escherichia coli* The role of triose phosphate isomerase. *FEBS Lett* 4**,** 19-20.

Andreini, C., Bertini, I., Cavallaro, G., Holliday, G.L., and Thornton, J.M. (2008). Metal ions in biological catalysis: from enzyme databases to general principles. *J Biol Inorg Chem* 13**,** 1205-1218.

Arasaki, K., and Roy, C.R. (2010). *Legionella pneumophila* promotes functional interactions between plasma membrane syntaxins and Sec22b. *Traffic* 11**,** 587-600.

Arasaki, K., Toomre, D.K., and Roy, C.R. (2012). The *Legionella pneumophila* Effector DrrA Is Sufficient to Stimulate SNARE-Dependent Membrane Fusion. *Cell Host Microbe* 11**,** 46-57.

Arimoto, T., Ansai, T., Yu, W., Turner, A.J., and Takehara, T. (2002). Kinetic analysis of PPi-dependent phosphofructokinase from *Porphyromonas gingivalis*. *FEMS Microbiol Lett* 207**,** 35-38.

Aurass, P., Schlegel, M., Metwally, O., Harding, C.R., Schroeder, G.N., Frankel, G., and Flieger, A. (2013). The *Legionella pneumophila* Dot/Icm-secreted effector PlcC/CegC1 together with PlcA and PlcB promotes virulence and belongs to a novel zinc metallophospholipase C family present in bacteria and fungi. *J Biol Chem* 288**,** 11080-11092.

Bachman, M.A., and Swanson, M.S. (2001). RpoS co-operates with other factors to induce *Legionella pneumophila* virulence in the stationary phase. *Mol Microbiol* 40**,** 1201-1214.

Bandyopadhyay, P., Lang, E.A., Rasaputra, K.S., and Steinman, H.M. (2013). Implication of the VirD4 coupling protein of the Lvh type 4 secretion system in virulence phenotypes of *Legionella pneumophila*. *J Bacteriol* 195**,** 3468-3475.

Bandyopadhyay, P., Liu, S., Gabbai, C.B., Venitelli, Z., and Steinman, H.M. (2007). Environmental mimics and the Lvh type IVA secretion system contribute to virulence-related phenotypes of *Legionella pneumophila*. *Infect Immun* 75**,** 723-735.

Barisch, C., Paschke, P., Hagedorn, M., Maniak, M., and Soldati, T. (2015). Lipid droplet dynamics at early stages of *Mycobacterium marinum* infection in *Dictyostelium*. *Cell Microbiol* 17**,** 1332-1349.

Becker, K.W., and Skaar, E.P. (2014). Metal limitation and toxicity at the interface between host and pathogen. *FEMS Microbiol Rev* 38**,** 1235-1249.

Bellinger-Kawahara, C., and Horwitz, M.A. (1990). Complement component C3 fixes selectively to the major outer membrane protein (MOMP) of *Legionella pneumophila* and mediates phagocytosis of liposome-MOMP complexes by human monocytes. *J Exp Med* 172**,** 1201-1210.

Belyi, Y., Jank, T., and Aktories, K. (2011). Effector glycosyltransferases in *Legionella*. *Front Microbiol* 2**,** 76.

Bender, J., Rydzewski, K., Broich, M., Schunder, E., Heuner, K., and Flieger, A. (2009). Phospholipase PlaB of *Legionella pneumophila* represents a novel lipase family: protein residues essential for lipolytic activity, substrate specificity, and hemolysis. *J Biol Chem* 284**,** 27185-27194.

Beste, D.J., Noh, K., Niedenfuhr, S., Mendum, T.A., Hawkins, N.D., Ward, J.L., Beale, M.H., Wiechert, W., and McFadden, J. (2013). ^{13}C-flux spectral analysis of host-pathogen metabolism reveals a mixed diet for intracellular *Mycobacterium tuberculosis*. *Chem Biol* 20**,** 1012-1021.

Boshuizen, H.C., Neppelenbroek, S.E., Van Vliet, H., Schellekens, J.F., Den Boer, J.W., Peeters, M.F., and Conyn-Van Spaendonck, M.A. (2001). Subclinical *Legionella* infection in workers near the source of a large outbreak of Legionnaires disease. *J Infect Dis* 184**,** 515-518.

Brenner, D.J., Steigerwalt, A.G., and Mcdade, J.E. (1979). Classification of the Legionnaires' disease bacterium: *Legionella pneumophila*, *genus novum, species nova*, of the family *Legionellaceae*, *familia nova*. *Ann Intern Med* 90**,** 656-658.

Brombacher, E., Urwyler, S., Ragaz, C., Weber, S.S., Kami, K., Overduin, M., and Hilbi, H. (2009). Rab1 guanine nucleotide exchange factor SidM is a major phosphatidylinositol 4-phosphate-binding effector protein of *Legionella pneumophila*. *J Biol Chem* 284**,** 4846-4856.

Brown, L., Gentry, D., Elliott, T., and Cashel, M. (2002). DksA affects ppGpp induction of RpoS at a translational level. *J Bacteriol* 184**,** 4455-4465.

Brüggemann, H., Hagman, A., Jules, M., Sismeiro, O., Dillies, M.A., Gouyette, C., Kunst, F., Steinert, M., Heuner, K., Coppee, J.Y., and Buchrieser, C. (2006). Virulence strategies for infecting phagocytes deduced from the *in vivo* transcriptional program of *Legionella pneumophila*. *Cell Microbiol* 8**,** 1228-1240.

Burns, D.L. (2003). Type IV transporters of pathogenic bacteria. *Curr Opin Microbiol* 6**,** 29-34.

Burnside, D.M., Wu, Y., Shafaie, S., and Cianciotto, N.P. (2015). The *Legionella pneumophila* siderophore legiobactin is a polycarboxylate that is identical in structure to rhizoferrin. *Infect Immun*.

Byrd, T.F., and Horwitz, M.A. (2000). Aberrantly low transferrin receptor expression on human monocytes is associated with nonpermissiveness for *Legionella pneumophila* growth. *J Infect Dis* 181**,** 1394-1400.

Byrne, B., and Swanson, M.S. (1998). Expression of *Legionella pneumophila* virulence traits in response to growth conditions. *Infect Immun* 66**,** 3029-3034.

Carvalho, F.R., Nastasi, F.R., Gamba, R.C., Foronda, A.S., and Pellizari, V.H. (2008). Occurrence and diversity of *Legionellaceae* in polar lakes of the Antarctic peninsula. *Curr Microbiol* 57**,** 294-300.

Castillo, M., Smith, J.K., and Kwock, L. (2000). Correlation of *myo*-inositol levels and grading of cerebral astrocytomas. *AJNR Am J Neuroradiol* 21**,** 1645-1649.

Cazalet, C., Gomez-Valero, L., Rusniok, C., Lomma, M., Dervins-Ravault, D., Newton, H.J., Sansom, F.M., Jarraud, S., Zidane, N., Ma, L., Bouchier, C., Etienne, J., Hartland, E.L., and Buchrieser, C.

(2010). Analysis of the *Legionella longbeachae* genome and transcriptome uncovers unique strategies to cause Legionnaires' disease. *PLoS Genetics* 6**,** e1000851.

Cazalet, C., Rusniok, C., Brüggemann, H., Zidane, N., Magnier, A., Ma, L., Tichit, M., Jarraud, S., Bouchier, C., Vandenesch, F., Kunst, F., Etienne, J., Glaser, P., and Buchrieser, C. (2004). Evidence in the *Legionella pneumophila* genome for exploitation of host cell functions and high genome plasticity. *Nat Genet* 36**,** 1165-1173.

Chang, B., Kura, F., Amemura-Maekawa, J., Koizumi, N., and Watanabe, H. (2005). Identification of a novel adhesion molecule involved in the virulence of *Legionella pneumophila*. *Infect Immun* 73**,** 4272-4280.

Charpentier, X., Kay, E., Schneider, D., and Shuman, H.A. (2011). Antibiotics and UV radiation induce competence for natural transformation in *Legionella pneumophila*. *J Bacteriol* 193**,** 1114-1121.

Chatfield, C.H., and Cianciotto, N.P. (2007). The secreted pyomelanin pigment of *Legionella pneumophila* confers ferric reductase activity. *Infect Immun* 75**,** 4062-4070.

Chatfield, C.H., Mulhern, B.J., Burnside, D.M., and Cianciotto, N.P. (2011). *Legionella pneumophila* LbtU acts as a novel, TonB-independent receptor for the legiobactin siderophore. *J Bacteriol* 193**,** 1563-1575.

Chatfield, C.H., Mulhern, B.J., Viswanathan, V.K., and Cianciotto, N.P. (2012). The major facilitator superfamily-type protein LbtC promotes the utilization of the legiobactin siderophore by *Legionella pneumophila*. *Microbiology* 158**,** 721-735.

Chen, D.E., Podell, S., Sauer, J.D., Swanson, M.S., and Saier, M.H., Jr. (2008). The phagosomal nutrient transporter (Pht) family. *Microbiology* 154**,** 42-53.

Chen, J., De Felipe, K.S., Clarke, M., Lu, H., Anderson, O.R., Segal, G., and Shuman, H.A. (2004). *Legionella* effectors that promote nonlytic release from protozoa. *Science* 303**,** 1358-1361.

Cheng, Z., Levi, J., Xiong, Z., Gheysens, O., Keren, S., Chen, X., and Gambhir, S.S. (2006). Near-infrared fluorescent deoxyglucose analogue for tumor optical imaging in cell culture and living mice. *Bioconjug Chem* 17**,** 662-669.

Chi, M.M., Pingsterhaus, J., Carayannopoulos, M., and Moley, K.H. (2000). Decreased glucose transporter expression triggers BAX-dependent apoptosis in the murine blastocyst. *J Biol Chem* 275**,** 40252-40257.

Chien, M., Morozova, I., Shi, S., Sheng, H., Chen, J., Gomez, S.M., Asamani, G., Hill, K., Nuara, J., Feder, M., Rineer, J., Greenberg, J.J., Steshenko, V., Park, S.H., Zhao, B., Teplitskaya, E., Edwards, J.R., Pampou, S., Georghiou, A., Chou, I.C., Iannuccilli, W., Ulz, M.E., Kim, D.H., Geringer-Sameth, A., Goldsberry, C., Morozov, P., Fischer, S.G., Segal, G., Qu, X., Rzhetsky, A., Zhang, P., Cayanis, E., De Jong, P.J., Ju, J., Kalachikov, S., Shuman, H.A., and Russo, J.J. (2004). The genomic sequence of the accidental pathogen *Legionella pneumophila*. *Science* 305**,** 1966-1968.

Cianciotto, N.P. (2007). Iron acquisition by *Legionella pneumophila*. *Biometals* 20**,** 323-331.

Cirillo, S.L., Bermudez, L.E., El-Etr, S.H., Duhamel, G.E., and Cirillo, J.D. (2001). *Legionella pneumophila* entry gene *rtxA* is involved in virulence. *Infect Immun* 69**,** 508-517.

Colas, C., Grewer, C., Otte, N.J., Gameiro, A., Albers, T., Singh, K., Shere, H., Bonomi, M., Holst, J., and Schlessinger, A. (2015). Ligand Discovery for the Alanine-Serine-Cysteine Transporter (ASCT2, SLC1A5) from Homology Modeling and Virtual Screening. *PLoS Comput Biol* 11**,** e1004477.

Commisso, C., Davidson, S.M., Soydaner-Azeloglu, R.G., Parker, S.J., Kamphorst, J.J., Hackett, S., Grabocka, E., Nofal, M., Drebin, J.A., Thompson, C.B., Rabinowitz, J.D., Metallo, C.M., Vander Heiden, M.G., and Bar-Sagi, D. (2013). Macropinocytosis of protein is an amino acid supply route in Ras-transformed cells. *Nature* 497**,** 633-637.

Cooper, R.A. (1984). Metabolism of methylglyoxal in microorganisms. *Annu Rev Microbiol* 38**,** 49-68.

Costa Dos Santos, A., Seixas Da-Silva, W., De Meis, L., and Galina, A. (2003). Proton transport in maize tonoplasts supported by fructose-1,6-bisphosphate cleavage. Pyrophosphate-dependent phosphofructokinase as a pyrophosphate-regenerating system. *Plant Physiol* 133**,** 885-892.

Csete, M., and Doyle, J. (2004). Bow ties, metabolism and disease. *Trends Biotechnol* 22**,** 446-450.

D'Auria, G., Jimenez-Hernandez, N., Peris-Bondia, F., Moya, A., and Latorre, A. (2010). Legionella pneumophila pangenome reveals strain-specific virulence factors. *BMC Genomics* 11**,** 181.

D'Avila, H., Melo, R.C., Parreira, G.G., Werneck-Barroso, E., Castro-Faria-Neto, H.C., and Bozza, P.T. (2006). *Mycobacterium bovis* bacillus Calmette-Guerin induces TLR2-mediated formation of lipid bodies: intracellular domains for eicosanoid synthesis *in vivo*. *J Immunol* 176**,** 3087-3097.

Dalebroux, Z.D., Edwards, R.L., and Swanson, M.S. (2009). SpoT governs *Legionella pneumophila* differentiation in host macrophages. *Mol Microbiol* 71**,** 640-658.

Dalebroux, Z.D., Yagi, B.F., Sahr, T., Buchrieser, C., and Swanson, M.S. (2010). Distinct roles of ppGpp and DksA in *Legionella pneumophila* differentiation. *Mol Microbiol* 76**,** 200-219.

Danial, N.N., and Korsmeyer, S.J. (2004). Cell death: critical control points. *Cell* 116**,** 205-219.

De Carvalho, L.P., Fischer, S.M., Marrero, J., Nathan, C., Ehrt, S., and Rhee, K.Y. (2010). Metabolomics of *Mycobacterium tuberculosis* reveals compartmentalized co-catabolism of carbon substrates. *Chem Biol* 17**,** 1122-1131.

Debroy, S., Dao, J., Soderberg, M., Rossier, O., and Cianciotto, N.P. (2006). *Legionella pneumophila* type II secretome reveals unique exoproteins and a chitinase that promotes bacterial persistence in the lung. *Proc Natl Acad Sci U S A* 103**,** 19146-19151.

Declerck, P. (2010). Biofilms: the environmental playground of *Legionella pneumophila*. *Environ Microbiol* 12**,** 557-566.

Derre, I., and Isberg, R.R. (2004). *Legionella pneumophila* replication vacuole formation involves rapid recruitment of proteins of the early secretory system. *Infect Immun* 72**,** 3048-3053.

Di Paolo, G., and De Camilli, P. (2006). Phosphoinositides in cell regulation and membrane dynamics. *Nature* 443**,** 651-657.

Donachie, W.D., and Begg, K.J. (1970). Growth of the bacterial cell. *Nature* 227**,** 1220-1224.

Drozanski, W. (1956). Fatal bacterial infection in soil amoebae. *Acta Microbiol Pol* 5**,** 315-317.

Duncan, C., Prashar, A., So, J., Tang, P., Low, D.E., Terebiznik, M., and Guyard, C. (2011). Lcl of *Legionella pneumophila* is an immunogenic GAG binding adhesin that promotes interactions with lung epithelial cells and plays a crucial role in biofilm formation. *Infect Immun* 79**,** 2168-2181.

Edwards, R.L., Dalebroux, Z.D., and Swanson, M.S. (2009). *Legionella pneumophila* couples fatty acid flux to microbial differentiation and virulence. *Mol Microbiol* 71**,** 1190-1204.

Ensminger, A.W., and Isberg, R.R. (2010). E3 ubiquitin ligase activity and targeting of BAT3 by multiple *Legionella pneumophila* translocated substrates. *Infect Immun* 78**,** 3905-3919.

Ensminger, A.W., Yassin, Y., Miron, A., and Isberg, R.R. (2012). Experimental evolution of *Legionella pneumophila* in mouse macrophages leads to strains with altered determinants of environmental survival. *PLoS Pathog* 8**,** e1002731.

Entner, N., and Doudoroff, M. (1952). Glucose and gluconic acid oxidation of *Pseudomonas saccharophila*. *J Biol Chem* 196**,** 853-862.

Etxeberria, E., Gonzalez, P., Tomlinson, P., and Pozueta-Romero, J. (2005). Existence of two parallel mechanisms for glucose uptake in heterotrophic plant cells. *J Exp Bot* 56**,** 1905-1912.

Ewann, F., and Hoffman, P.S. (2006). Cysteine metabolism in *Legionella pneumophila*: characterization of an L-cystine-utilizing mutant. *Appl Environ Microbiol* 72**,** 3993-4000.

Eylert, E., Herrmann, V., Jules, M., Gillmaier, N., Lautner, M., Buchrieser, C., Eisenreich, W., and Heuner, K. (2010). Isotopologue profiling of *Legionella pneumophila*: role of serine and glucose as carbon substrates. *J Biol Chem* 285**,** 22232-22243.

Faucher, S.P., Mueller, C.A., and Shuman, H.A. (2011). *Legionella pneumophila* transcriptome during intracellular multiplication in human macrophages. *Front Microbiol* 2**,** 60.

Faulkner, G., and Garduno, R.A. (2002). Ultrastructural analysis of differentiation in *Legionella pneumophila*. *J Bacteriol* 184**,** 7025-7041.

Feeley, J.C., Gibson, R.J., Gorman, G.W., Langford, N.C., Rasheed, J.K., Mackel, D.C., and Baine, W.B. (1979). Charcoal-yeast extract agar: primary isolation medium for *Legionella pneumophila*. *J Clin Microbiol* 10**,** 437-441.

Fields, B.S. (1996). The molecular ecology of *Legionellae*. *Trends Microbiol* 4**,** 286-290.

Fields, B.S., Benson, R.F., and Besser, R.E. (2002). *Legionella* and Legionnaires' disease: 25 years of investigation. *Clin Microbiol Rev* 15**,** 506-526.

Fields, B.S., Fields, S.R., Loy, J.N., White, E.H., Steffens, W.L., and Shotts, E.B. (1993). Attachment and entry of *Legionella pneumophila* in *Hartmannella vermiformis*. *J Infect Dis* 167**,** 1146-1150.

Finsel, I., and Hilbi, H. (2015). Formation of a pathogen vacuole according to *Legionella pneumophila*: how to kill one bird with many stones. *Cell Microbiol* 17**,** 935-950.

Fischbach, A., Adelt, S., Muller, A., and Vogel, G. (2006). Disruption of inositol biosynthesis through targeted mutagenesis in *Dictyostelium discoideum*: generation and characterization of inositol-auxotrophic mutants. *Biochem J* 397**,** 509-518.

Flydal, M.I., Chatfield, C.H., Zheng, H., Gunderson, F.F., Aubi, O., Cianciotto, N.P., and Martinez, A. (2012). Phenylalanine hydroxylase from *Legionella pneumophila* is a thermostable enzyme with a major functional role in pyomelanin synthesis. *PLoS One* 7**,** e46209.

Fonseca, M.V., Sauer, J.D., Crepin, S., Byrne, B., and Swanson, M.S. (2014). The *phtC-phtD* locus equips *Legionella pneumophila* for thymidine salvage and replication in macrophages. *Infect Immun* 82**,** 720-730.

Franco, I.S., Shohdy, N., and Shuman, H.A. (2012). The *Legionella pneumophila* effector VipA is an actin nucleator that alters host cell organelle trafficking. *PLoS Pathog* 8**,** e1002546.

Fraser, D.W., Tsai, T.R., Orenstein, W., Parkin, W.E., Beecham, H.J., Sharrar, R.G., Harris, J., Mallison, G.F., Martin, S.M., Mcdade, J.E., Shepard, C.C., and Brachman, P.S. (1977). Legionnaires' disease: description of an epidemic of pneumonia. *N Engl J Med* 297**,** 1189-1197.

Fuche, F., Vianney, A., Andrea, C., Doublet, P., and Gilbert, C. (2015). Functional type 1 secretion system involved in *Legionella pneumophila* virulence. *J Bacteriol* 197**,** 563-571.

Gal-Mor, O., and Segal, G. (2003a). Identification of CpxR as a positive regulator of *icm* and *dot* virulence genes of *Legionella pneumophila*. *J Bacteriol* 185**,** 4908-4919.

Gal-Mor, O., and Segal, G. (2003b). The *Legionella pneumophila* GacA homolog (LetA) is involved in the regulation of icm virulence genes and is required for intracellular multiplication in *Acanthamoeba castellanii*. *Microb Pathog* 34**,** 187-194.

Garduno, R.A., Garduno, E., Hiltz, M., and Hoffman, P.S. (2002). Intracellular growth of *Legionella pneumophila* gives rise to a differentiated form dissimilar to stationary-phase forms. *Infect Immun* 70**,** 6273-6283.

Gaspar, A.H., and Machner, M.P. (2014). VipD is a Rab5-activated phospholipase A1 that protects *Legionella pneumophila* from endosomal fusion. *Proc Natl Acad Sci U S A*.

Gebran, S.J., Yamamoto, Y., Newton, C., Klein, T.W., and Friedman, H. (1994). Inhibition of *Legionella pneumophila* growth by gamma interferon in permissive A/J mouse macrophages: role of reactive oxygen species, nitric oxide, tryptophan, and iron(III). *Infect Immun* 62**,** 3197-3205.

George, J.R., Pine, L., Reeves, M.W., and Harrell, W.K. (1980). Amino acid requirements of *Legionella pneumophila*. *J Clin Microbiol* 11**,** 286-291.

Glick, T.H., Gregg, M.B., Berman, B., Mallison, G., Rhodes, W.W., Jr., and Kassanoff, I. (1978). Pontiac fever. An epidemic of unknown etiology in a health department: I. Clinical and epidemiologic aspects. *Am J Epidemiol* 107**,** 149-160.

Goody, P.R., Heller, K., Oesterlin, L.K., Muller, M.P., Itzen, A., and Goody, R.S. (2012). Reversible phosphocholination of Rab proteins by *Legionella pneumophila* effector proteins. *EMBO J* 31**,** 1774-1784.

Götz, A., Eylert, E., Eisenreich, W., and Goebel, W. (2010). Carbon metabolism of enterobacterial human pathogens growing in epithelial colorectal adenocarcinoma (Caco-2) cells. *PLoS One* 5**,** e10586.

Grubmüller, S., Schauer, K., Goebel, W., Fuchs, T.M., and Eisenreich, W. (2014). Analysis of carbon substrates used by *Listeria monocytogenes* during growth in J774A.1 macrophages suggests a bipartite intracellular metabolism. *Front Cell Infect Microbiol* 4**,** 156.

Hacker, U., Albrecht, R., and Maniak, M. (1997). Fluid-phase uptake by macropinocytosis in *Dictyostelium*. *J Cell Sci* 110 (Pt 2)**,** 105-112.

Hägele, S., Kohler, R., Merkert, H., Schleicher, M., Hacker, J., and Steinert, M. (2000). *Dictyostelium discoideum*: a new host model system for intracellular pathogens of the genus *Legionella*. *Cell Microbiol* 2**,** 165-171.

Hales, L.M., and Shuman, H.A. (1999a). *Legionella pneumophila* contains a type II general secretion pathway required for growth in amoebae as well as for secretion of the Msp protease. *Infect Immun* 67**,** 3662-3666.

Hales, L.M., and Shuman, H.A. (1999b). The *Legionella pneumophila rpoS* gene is required for growth within *Acanthamoeba castellanii*. *J Bacteriol* 181**,** 4879-4889.

Hammer, B.K., and Swanson, M.S. (1999). Co-ordination of *Legionella pneumophila* virulence with entry into stationary phase by ppGpp. *Mol Microbiol* 33**,** 721-731.

Hammer, B.K., Tateda, E.S., and Swanson, M.S. (2002). A two-component regulator induces the transmission phenotype of stationary-phase *Legionella pneumophila*. *Mol Microbiol* 44**,** 107-118.

Haneburger, I., and Hilbi, H. (2013). Phosphoinositide lipids and the *Legionella* pathogen vacuole. *Curr Top Microbiol Immunol* 376**,** 155-173.

Hao, C., Wang, L., Gao, Y., Zhang, L., and Dong, H. (2010). Microbial diversity in acid mine drainage of Xiang Mountain sulfide mine, Anhui Province, China. *Extremophiles* 14**,** 465-474.

Harada, E., Iida, K., Shiota, S., Nakayama, H., and Yoshida, S. (2010). Glucose metabolism in *Legionella pneumophila*: dependence on the Entner-Doudoroff pathway and connection with intracellular bacterial growth. *J Bacteriol* 192**,** 2892-2899.

Harrison, C.F., Kicka, S., Trofimov, V., Berschl, K., Ouertatani-Sakouhi, H., Ackermann, N., Hedberg, C., Cosson, P., Soldati, T., and Hilbi, H. (2013). Exploring anti-bacterial compounds against intracellular *Legionella*. *PLoS One* 8**,** e74813.

Hengge-Aronis, R. (1993). Survival of hunger and stress: the role of *rpoS* in early stationary phase gene regulation in *E. coli*. *Cell* 72**,** 165-168.

Hengge-Aronis, R. (2002). Signal transduction and regulatory mechanisms involved in control of the sigma(S) (RpoS) subunit of RNA polymerase. *Microbiol Mol Biol Rev* 66**,** 373-395, table of contents.

Herrmann, V., Eidner, A., Rydzewski, K., Bladel, I., Jules, M., Buchrieser, C., Eisenreich, W., and Heuner, K. (2011). GamA is a eukaryotic-like glucoamylase responsible for glycogen- and starch-degrading activity of *Legionella pneumophila*. *Int J Med Microbiol* 301**,** 133-139.

Hilbi, H., Hoffmann, C., and Harrison, C.F. (2011a). *Legionella* spp. outdoors: colonization, communication and persistence. *Environ Microbiol Rep* 3**,** 286–296.

Hilbi, H., Segal, G., and Shuman, H.A. (2001). Icm/Dot-dependent upregulation of phagocytosis by *Legionella pneumophila*. *Mol Microbiol* 42**,** 603-617.

Hilbi, H., Weber, S., and Finsel, I. (2011b). Anchors for effectors: subversion of phosphoinositide lipids by *Legionella*. *Front Microbiol* 2**,** 91.

Hoffmann, C., Finsel, I., Otto, A., Pfaffinger, G., Rothmeier, E., Hecker, M., Becher, D., and Hilbi, H. (2014a). Functional analysis of novel Rab GTPases identified in the proteome of purified *Legionella*-containing vacuoles from macrophages. *Cell Microbiol* 16**,** 1034-1052.

Hoffmann, C., Harrison, C.F., and Hilbi, H. (2014b). The natural alternative: protozoa as cellular models for *Legionella* infection. *Cell Microbiol* 16**,** 15-26.

Holden, E.P., Winkler, H.H., Wood, D.O., and Leinbach, E.D. (1984). Intracellular growth of *Legionella pneumophila* within *Acanthamoeba castellanii* Neff. *Infect Immun* 45**,** 18-24.

Hookey, J.V., Saunders, N.A., Fry, N.K., Birtles, R.J., and Harrison, T.G. (1996). Phylogeny of *Legionellaceae* based on small-subunit ribosomal DNA sequences and proposal of *Legionella* lytica comb nov for *Legionella*-Like amoebal pathogens. *International Journal of Systematic Bacteriology* 46**,** 526-531.

Horenkamp, F.A., Mukherjee, S., Alix, E., Schauder, C.M., Hubber, A.M., Roy, C.R., and Reinisch, K.M. (2014). *Legionella pneumophila* subversion of host vesicular transport by SidC effector proteins. *Traffic*.

Horwitz, M., and Maxfield, F. (1984). *Legionella pneumophila* inhibits acidification of its phagosome in human monocytes. *J Cell Biol* 99**,** 105-114.

Horwitz, M.A. (1983). Formation of a novel phagosome by the Legionnaires' disease bacterium (*Legionella pneumophila*) in human monocytes. *J Exp Med* 158**,** 1319-1331.

Hovel-Miner, G., Faucher, S.P., Charpentier, X., and Shuman, H.A. (2010). ArgR-regulated genes are derepressed in the *Legionella*-containing vacuole. *J Bacteriol* 192**,** 4504-4516.

Hovel-Miner, G., Pampou, S., Faucher, S.P., Clarke, M., Morozova, I., Morozov, P., Russo, J.J., Shuman, H.A., and Kalachikov, S. (2009). SigmaS controls multiple pathways associated with intracellular multiplication of *Legionella pneumophila*. *J Bacteriol* 191**,** 2461-2473.

Hsu, F., Zhu, W., Brennan, L., Tao, L., Luo, Z.Q., and Mao, Y. (2012). Structural basis for substrate recognition by a unique *Legionella* phosphoinositide phosphatase. *Proc Natl Acad Sci U S A* 109**,** 13567-13572.

Hubber, A., and Roy, C.R. (2010). Modulation of host cell function by *Legionella pneumophila* type IV effectors. *Annu Rev Cell Dev Biol* 26**,** 261-283.

Isaac, D.T., Laguna, R.K., Valtz, N., and Isberg, R.R. (2015). MavN is a *Legionella pneumophila* vacuole-associated protein required for efficient iron acquisition during intracellular growth. *Proc Natl Acad Sci U S A* 112**,** E5208-5217.

Itoh, Y., Abe, T., Takaoka, R., and Tanahashi, N. (2004). Fluorometric determination of glucose utilization in neurons *in vitro* and *in vivo*. *J Cereb Blood Flow Metab* 24**,** 993-1003.

James, B.W., Mauchline, W.S., Fitzgeorge, R.B., Dennis, P.J., and Keevil, C.W. (1995). Influence of iron-limited continuous culture on physiology and virulence of *Legionella pneumophila*. *Infect Immun* 63**,** 4224-4230.

Johnson, W., Varner, L., and Poch, M. (1991). Acquisition of iron by *Legionella pneumophila*: role of iron reductase. *Infect Immun* 59**,** 2376-2381.

Jones, S.C., Price, C.T., Santic, M., and Abu Kwaik, Y. (2015). Selective requirement of the shikimate pathway of *Legionella pneumophila* for intravacuolar growth within human macrophages but not within *Acanthamoeba*. *Infect Immun* 83**,** 2487-2495.

Joseph, B., Mertins, S., Stoll, R., Schar, J., Umesha, K.R., Luo, Q., Muller-Altrock, S., and Goebel, W. (2008). Glycerol metabolism and PrfA activity in *Listeria monocytogenes*. *J Bacteriol* 190**,** 5412-5430.

Kagan, J.C., and Roy, C.R. (2002). *Legionella* phagosomes intercept vesicular traffic from endoplasmic reticulum exit sites. *Nat Cell Biol* 4**,** 945-954.

Kagan, J.C., Stein, M.P., Pypaert, M., and Roy, C.R. (2004). *Legionella* subvert the functions of Rab1 and Sec22b to create a replicative organelle. *J Exp Med* 199**,** 1201-1211.

Keen, M.G., and Hoffman, P.S. (1984). Metabolic pathways and nitrogen metabolism in *Legionella pneumophila*. *Curr Microbiol* 11**,** 81-88.

Kessler, A., Schell, U., Sahr, T., Tiaden, A., Harrison, C., Buchrieser, C., and Hilbi, H. (2013). The *Legionella pneumophila* orphan sensor kinase LqsT regulates competence and pathogen-host interactions as a component of the LAI-1 circuit. *Environ Microbiol* 15**,** 646-662.

King, N.P., Newton, P., Schuelein, R., Brown, D.L., Petru, M., Zarsky, V., Dolezal, P., Luo, L., Bugarcic, A., Stanley, A.C., Murray, R.Z., Collins, B.M., Teasdale, R.D., Hartland, E.L., and Stow, J.L. (2015). Soluble NSF attachment protein receptor molecular mimicry by a *Legionella pneumophila* Dot/Icm effector. *Cell Microbiol* 17**,** 767-784.

Klaus, F., Palmada, M., Lindner, R., Laufer, J., Jeyaraj, S., Lang, F., and Boehmer, C. (2008). Up-regulation of hypertonicity-activated *myo*-inositol transporter SMIT1 by the cell volume-sensitive protein kinase SGK1. *J Physiol* 586**,** 1539-1547.

Konopka, A. (1984). Microbial growth: growth of the bacterial cell. *Science* 224**,** 738-739.

Koubar, M., Rodier, M.H., and Frere, J. (2013). Involvement of minerals in adherence of *Legionella pneumophila* to surfaces. *Curr Microbiol* 66**,** 437-442.

Kozak, N.A., Buss, M., Lucas, C.E., Frace, M., Govil, D., Travis, T., Olsen-Rasmussen, M., Benson, R.F., and Fields, B.S. (2010). Virulence factors encoded by *Legionella longbeachae* identified on the basis of the genome sequence analysis of clinical isolate D-4968. *J Bacteriol* 192**,** 1030-1044.

Kröger, C., and Fuchs, T.M. (2009). Characterization of the *myo*-inositol utilization island of *Salmonella enterica* serovar Typhimurium. *J Bacteriol* 191**,** 545-554.

Kröger, C., Srikumar, S., Ellwart, J., and Fuchs, T.M. (2011). Bistability in *myo*-inositol utilization by *Salmonella enterica* serovar Typhimurium. *J Bacteriol* 193**,** 1427-1435.

Kröger, C., Stolz, J., and Fuchs, T.M. (2010). *myo*-Inositol transport by *Salmonella enterica* serovar Typhimurium. *Microbiology* 156**,** 128-138.

Lang, C., and Flieger, A. (2011). Characterisation of *Legionella pneumophila* phospholipases and their impact on host cells. *Eur J Cell Biol* 90**,** 903-912.

Lang, C., Rastew, E., Hermes, B., Siegbrecht, E., Ahrends, R., Banerji, S., and Flieger, A. (2012). Zinc metalloproteinase ProA directly activates *Legionella pneumophila* PlaC glycerophospholipid:cholesterol acyltransferase. *J Biol Chem* 287**,** 23464-23478.

Lei, X.G., Weaver, J.D., Mullaney, E., Ullah, A.H., and Azain, M.J. (2013). Phytase, a new life for an "old" enzyme. *Annu Rev Anim Biosci* 1**,** 283-309.

Liles, M.R., Edelstein, P.H., and Cianciotto, N.P. (1999). The prepilin peptidase is required for protein secretion by and the virulence of the intracellular pathogen *Legionella pneumophila*. *Mol Microbiol* 31**,** 959-970.

Liles, M.R., Scheel, T.A., and Cianciotto, N.P. (2000). Discovery of a nonclassical siderophore, legiobactin, produced by strains of *Legionella pneumophila*. *J Bacteriol* 182**,** 749-757.

Lomma, M., Dervins-Ravault, D., Rolando, M., Nora, T., Newton, H.J., Sansom, F.M., Sahr, T., Gomez-Valero, L., Jules, M., Hartland, E.L., and Buchrieser, C. (2010). The *Legionella pneumophila* F-box protein Lpp2082 (AnkB) modulates ubiquitination of the host protein parvin B and promotes intracellular replication. *Cell Microbiol* 12**,** 1272-1291.

Lu, H., and Clarke, M. (2005). Dynamic properties of *Legionella*-containing phagosomes in *Dictyostelium* amoebae. *Cell Microbiol* 7**,** 995-1007.

Lynch, D., Fieser, N., Gloggler, K., Forsbach-Birk, V., and Marre, R. (2003). The response regulator LetA regulates the stationary-phase stress response in *Legionella pneumophila* and is required for efficient infection of *Acanthamoeba castellanii*. *FEMS Microbiol Lett* 219**,** 241-248.

Malchow, D., Nagele, B., Schwarz, H., and Gerisch, G. (1972). Membrane-bound cyclic AMP phosphodiesterase in chemotactically responding cells of *Dictyostelium discoideum*. *Eur J Biochem* 28**,** 136-142.

Mampel, J., Spirig, T., Weber, S.S., Haagensen, J.a.J., Molin, S., and Hilbi, H. (2006). Planktonic replication is essential for biofilm formation by *Legionella pneumophila* in a complex medium under static and dynamic flow conditions. *Appl Environ Microbiol* 72**,** 2885-2895.

Manske, C., and Hilbi, H. (2014). Metabolism of the vacuolar pathogen *Legionella* and implications for virulence. *Front Cell Infect Microbiol* 4**,** 125.

Mao, F., Dam, P., Chou, J., Olman, V., and Xu, Y. (2009). DOOR: a database for prokaryotic operons. *Nucleic Acids Res* 37**,** D459-463.

Mattos, K.A., Lara, F.A., Oliveira, V.G., Rodrigues, L.S., D'avila, H., Melo, R.C., Manso, P.P., Sarno, E.N., Bozza, P.T., and Pessolani, M.C. (2011). Modulation of lipid droplets by *Mycobacterium leprae* in Schwann cells: a putative mechanism for host lipid acquisition and bacterial survival in phagosomes. *Cell Microbiol* 13**,** 259-273.

McDade, J.E., Shepard, C.C., Fraser, D.W., Tsai, T.R., Redus, M.A., and Dowdle, W.R. (1977). Legionnaires' disease: isolation of a bacterium and demonstration of its role in other respiratory disease. *N Engl J Med* 297**,** 1197-1203.

Melo, R.C., and Dvorak, A.M. (2012). Lipid body-phagosome interaction in macrophages during infectious diseases: host defense or pathogen survival strategy? *PLoS Pathog* 8**,** e1002729.

Moffat, J.F., and Tompkins, L.S. (1992). A quantitative model of intracellular growth of *Legionella pneumophila* in *Acanthamoeba castellanii*. *Infect Immun* 60**,** 296-301.

Molofsky, A.B., and Swanson, M.S. (2003). *Legionella pneumophila* CsrA is a pivotal repressor of transmission traits and activator of replication. *Mol Microbiol* 50**,** 445-461.

Molofsky, A.B., and Swanson, M.S. (2004). Differentiate to thrive: lessons from the *Legionella pneumophila* life cycle. *Mol Microbiol* 53**,** 29-40.

Morash, M.G., Brassinga, A.K., Warthan, M., Gourabathini, P., Garduno, R.A., Goodman, S.D., and Hoffman, P.S. (2009). Reciprocal expression of integration host factor and HU in the

developmental cycle and infectivity of *Legionella pneumophila*. *Appl Environ Microbiol* 75**,** 1826-1837.

Movahedzadeh, F., Smith, D.A., Norman, R.A., Dinadayala, P., Murray-Rust, J., Russell, D.G., Kendall, S.L., Rison, S.C., Mcalister, M.S., Bancroft, G.J., Mcdonald, N.Q., Daffe, M., Av-Gay, Y., and Stoker, N.G. (2004). The *Mycobacterium tuberculosis ino1* gene is essential for growth and virulence. *Mol Microbiol* 51**,** 1003-1014.

Mueckler, M., and Thorens, B. (2013). The SLC2 (GLUT) family of membrane transporters. *Mol Aspects Med* 34**,** 121-138.

Mukherjee, S., Liu, X., Arasaki, K., Mcdonough, J., Galan, J.E., and Roy, C.R. (2011). Modulation of Rab GTPase function by a protein phosphocholine transferase. *Nature* 477**,** 103-106.

Müller, A., Hacker, J., and Brand, B.C. (1996). Evidence for apoptosis of human macrophage-like HL-60 cells by *Legionella pneumophila* infection. *Infect Immun* 64**,** 4900-4906.

Murga, R., Forster, T.S., Brown, E., Pruckler, J.M., Fields, B.S., and Donlan, R.M. (2001). Role of biofilms in the survival of *Legionella pneumophila* in a model potable-water system. *Microbiology* 147**,** 3121-3126.

Murima, P., McKinney, J.D., and Pethe, K. (2014). Targeting bacterial central metabolism for drug development. *Chem Biol* 21**,** 1423-1432.

Nash, T.W., Libby, D.M., and Horwitz, M.A. (1984). Interaction between the Legionnaires' disease bacterium (*Legionella pneumophila*) and human alveolar macrophages. Influence of antibody, lymphokines, and hydrocortisone. *J Clin Invest* 74**,** 771-782.

Nasrallah, G.K., Abdelhady, H., Tompkins, N.P., Carson, K.R., and Garduno, R.A. (2014). Deletion of *potD*, encoding a putative spermidine-binding protein, results in a complex phenotype in *Legionella pneumophila*. *Int J Med Microbiol*.

Nasrallah, G.K., Riveroll, A.L., Chong, A., Murray, L.E., Lewis, P.J., and Garduno, R.A. (2011). *Legionella pneumophila* requires polyamines for optimal intracellular growth. *J Bacteriol* 193**,** 4346-4360.

Natarajan, A., and Srienc, F. (1999). Dynamics of glucose uptake by single *Escherichia coli* cells. *Metab Eng* 1**,** 320-333.

Neunuebel, M.R., Mohammadi, S., Jarnik, M., and Machner, M.P. (2012). *Legionella pneumophila* LidA affects nucleotide binding and activity of the host GTPase Rab1. *J Bacteriol* 194**,** 1389-1400.

Newton, G.L., Ta, P., Bzymek, K.P., and Fahey, R.C. (2006). Biochemistry of the initial steps of mycothiol biosynthesis. *J Biol Chem* 281**,** 33910-33920.

Newton, H.J., Ang, D.K., Van Driel, I.R., and Hartland, E.L. (2010). Molecular pathogenesis of infections caused by *Legionella pneumophila*. *Clin Microbiol Rev* 23**,** 274-298.

Nguyen, T.M., Ilef, D., Jarraud, S., Rouil, L., Campese, C., Che, D., Haeghebaert, S., Ganiayre, F., Marcel, F., Etienne, J., and Desenclos, J.C. (2006). A community-wide outbreak of legionnaires disease linked to industrial cooling towers--how far can contaminated aerosols spread? *J Infect Dis* 193**,** 102-111.

Nilewar, S.S., and Kathiravan, M.K. (2014). Mycothiol: a promising antitubercular target. *Bioorg Chem* 52**,** 62-68.

O'connor, T.J., Adepoju, Y., Boyd, D., and Isberg, R.R. (2011). Minimization of the *Legionella pneumophila* genome reveals chromosomal regions involved in host range expansion. *Proc Natl Acad Sci U S A* 108**,** 14733-14740.

Oh, K.B., and Matsuoka, H. (2002). Rapid viability assessment of yeast cells using vital staining with 2-NBDG, a fluorescent derivative of glucose. *Int J Food Microbiol* 76**,** 47-53.

Ohno, A., Kato, N., Yamada, K., and Yamaguchi, K. (2003). Factors influencing survival of *Legionella pneumophila* serotype 1 in hot spring water and tap water. *Appl Environ Microbiol* 69**,** 2540-2547.

Palmada, M., Boehmer, C., Akel, A., Rajamanickam, J., Jeyaraj, S., Keller, K., and Lang, F. (2006). SGK1 kinase upregulates GLUT1 activity and plasma membrane expression. *Diabetes* 55**,** 421-427.

Pan, C.J., Chen, S.Y., Jun, H.S., Lin, S.R., Mansfield, B.C., and Chou, J.Y. (2011). SLC37A1 and SLC37A2 are phosphate-linked, glucose-6-phosphate antiporters. *PLoS One* 6**,** e23157.

Parthasarathy, L.K., Seelan, R.S., Tobias, C., Casanova, M.F., and Parthasarathy, R.N. (2006). Mammalian inositol 3-phosphate synthase: its role in the biosynthesis of brain inositol and its clinical use as a psychoactive agent. *Subcell Biochem* 39**,** 293-314.

Pearce, M.M., and Cianciotto, N.P. (2009). *Legionella pneumophila* secretes an endoglucanase that belongs to the family-5 of glycosyl hydrolases and is dependent upon type II secretion. *FEMS Microbiol Lett* 300**,** 256-264.

Peyron, P., Vaubourgeix, J., Poquet, Y., Levillain, F., Botanch, C., Bardou, F., Daffe, M., Emile, J.F., Marchou, B., Cardona, P.J., De Chastellier, C., and Altare, F. (2008). Foamy macrophages from tuberculous patients' granulomas constitute a nutrient-rich reservoir for *M. tuberculosis* persistence. *PLoS Pathog* 4**,** e1000204.

Piao, Z., Sze, C.C., Barysheva, O., Iida, K., and Yoshida, S. (2006). Temperature-regulated formation of mycelial mat-like biofilms by *Legionella pneumophila*. *Appl Environ Microbiol* 72**,** 1613-1622.

Pine, L., George, J.R., Reeves, M.W., and Harrell, W.K. (1979). Development of a chemically defined liquid medium for growth of *Legionella pneumophila*. *J Clin Microbiol* 9**,** 615-626.

Poch, M.T., and Johnson, W. (1993). Ferric reductases of *Legionella pneumophila*. *Biometals* 6**,** 107-114.

Poras, H., Duquesnoy, S., Dange, E., Pinon, A., Vialette, M., Fournie-Zaluski, M.C., and Ouimet, T. (2012). Highly sensitive quenched fluorescent substrate of *Legionella* major secretory protein (msp) based on its structural analysis. *J Biol Chem* 287**,** 20221-20230.

Portier, E., Zheng, H., Sahr, T., Burnside, D.M., Mallama, C., Buchrieser, C., Cianciotto, N.P., and Hechard, Y. (2015). *iroT/mavN*, a new iron-regulated gene involved in *Legionella pneumophila* virulence against amoebae and macrophages. *Environ Microbiol* 17**,** 1338-1350.

Prashar, A., Bhatia, S., Gigliozzi, D., Martin, T., Duncan, C., Guyard, C., and Terebiznik, M.R. (2013). Filamentous morphology of bacteria delays the timing of phagosome morphogenesis in macrophages. *J Cell Biol* 203**,** 1081-1097.

Prashar, A., Bhatia, S., Tabatabaeiyazdi, Z., Duncan, C., Garduno, R.A., Tang, P., Low, D.E., Guyard, C., and Terebiznik, M.R. (2012). Mechanism of invasion of lung epithelial cells by filamentous *Legionella pneumophila*. *Cell Microbiol* 14**,** 1632-1655.

Price, C.T., Al-Khodor, S., Al-Quadan, T., Santic, M., Habyarimana, F., Kalia, A., and Kwaik, Y.A. (2009). Molecular mimicry by an F-box effector of *Legionella pneumophila* hijacks a conserved polyubiquitination machinery within macrophages and protozoa. *PLoS Pathog* 5**,** e1000704.

Price, C.T., Al-Quadan, T., Santic, M., Rosenshine, I., and Abu Kwaik, Y. (2011). Host proteasomal degradation generates amino acids essential for intracellular bacterial growth. *Science* 334**,** 1553-1557.

Price, C.T., Jones, S.C., Amundson, K.E., and Kwaik, Y.A. (2010). Host-mediated post-translational prenylation of novel dot/icm-translocated effectors of *Legionella pneumophila*. *Front Microbiol* 1**,** 131.

Price, C.T., and Kwaik, Y.A. (2010). Exploitation of Host Polyubiquitination Machinery through Molecular Mimicry by Eukaryotic-Like Bacterial F-Box Effectors. *Front Microbiol* 1**,** 122.

Rasis, M., and Segal, G. (2009). The LetA-RsmYZ-CsrA regulatory cascade, together with RpoS and PmrA, post-transcriptionally regulates stationary phase activation of *Legionella pneumophila* Icm/Dot effectors. *Mol Microbiol* 72**,** 995-1010.

Ratledge, C. (1976). The physiology of the mycobacteria. *Adv Microb Physiol* 13**,** 115-244.

Ratledge, C., and Dover, L.G. (2000). Iron metabolism in pathogenic bacteria. *Annu Rev Microbiol* 54**,** 881-941.

Rdest, U., Wintermeyer, E., Ludwig, B., and Hacker, J. (1991). Legiolysin, a new hemolysin from *L. pneumophila*. *Zentralbl Bakteriol* 274**,** 471-474.

Recalcati, S., Invernizzi, P., Arosio, P., and Cairo, G. (2008). New functions for an iron storage protein: the role of ferritin in immunity and autoimmunity. *J Autoimmun* 30**,** 84-89.

Reeves, M.W., Pine, L., Hutner, S.H., George, J.R., and Harrell, W.K. (1981). Metal requirements of *Legionella pneumophila*. *J Clin Microbiol* 13**,** 688-695.

Riddle, V.M., and Lorenz, F.W. (1973). Nonenzymic formation of toxic levels of methylglyoxal from glycerol and dihydroxyacetone in Ringer's phosphate suspensions of avian spermatozoa. *Biochem Biophys Res Commun* 50**,** 27-34.

Ristroph, J.D., Hedlund, K.W., and Gowda, S. (1981). Chemically defined medium for *Legionella pneumophila* growth. *J Clin Microbiol* 13**,** 115-119.

Robertson, P., Abdelhady, H., and Garduno, R.A. (2014). The many forms of a pleomorphic bacterial pathogen-the developmental network of *Legionella pneumophila*. *Front Microbiol* 5**,** 670.

Robey, M., and Cianciotto, N.P. (2002). *Legionella pneumophila feoAB* promotes ferrous iron uptake and intracellular infection. *Infect Immun* 70**,** 5659-5669.

Robinson, C.G., and Roy, C.R. (2006). Attachment and fusion of endoplasmic reticulum with vacuoles containing *Legionella pneumophila*. *Cell Microbiol* 8**,** 793-805.

Rodionova, I.A., Leyn, S.A., Burkart, M.D., Boucher, N., Noll, K.M., Osterman, A.L., and Rodionov, D.A. (2013). Novel inositol catabolic pathway in *Thermotoga maritima*. *Environ Microbiol* 15**,** 2254-2266.

Rolando, M., and Buchrieser, C. (2012). Post-translational modifications of host proteins by *Legionella pneumophila*: a sophisticated survival strategy. *Future Microbiol* 7**,** 369-381.

Rowbotham, T.J. (1980). Preliminary report on the pathogenicity of *Legionella pneumophila* for freshwater and soil amoebae. *J Clin Pathol* 33**,** 1179-1183.

Rowbotham, T.J. (1986). Current views on the relationships between amoebae, legionellae and man. *Isr J Med Sci* 22**,** 678-689.

Roy, C.R., and Isberg, R.R. (1997). Topology of *Legionella pneumophila* DotA: an inner membrane protein required for replication in macrophages. *Infect Immun* 65**,** 571-578.

Sabria, M., and Yu, V.L. (2002). Hospital-acquired legionellosis: solutions for a preventable infection. *Lancet Infect Dis* 2**,** 368-373.

Sadosky, A.B., Wiater, L.A., and Shuman, H.A. (1993). Identification of *Legionella pneumophila* genes required for growth within and killing of human macrophages. *Infect Immun* 61**,** 5361-5373.

Sahr, T., Brüggemann, H., Jules, M., Lomma, M., Albert-Weissenberger, C., Cazalet, C., and Buchrieser, C. (2009). Two small ncRNAs jointly govern virulence and transmission in *Legionella pneumophila*. *Mol Microbiol* 72**,** 741-762.

Sakai, H., Iwai, T., Matsubara, C., Usui, Y., Okamura, M., Yatou, O., Terada, Y., Aoki, N., Nishida, S., and Yoshida, K.T. (2015). A decrease in phytic acid content substantially affects the distribution of mineral elements within rice seeds. *Plant Sci* 238**,** 170-177.

Sauer, J.D., Bachman, M.A., and Swanson, M.S. (2005). The phagosomal transporter A couples threonine acquisition to differentiation and replication of *Legionella pneumophila* in macrophages. *Proc Natl Acad Sci U S A* 102**,** 9924-9929.

Schneebeli, R., and Egli, T. (2013). A defined, glucose-limited mineral medium for the cultivation of *Listeria* spp. *Appl Environ Microbiol* 79**,** 2503-2511.

Schoebel, S., Oesterlin, L.K., Blankenfeldt, W., Goody, R.S., and Itzen, A. (2009). RabGDI displacement by DrrA from *Legionella* is a consequence of its guanine nucleotide exchange activity. *Mol Cell* 36**,** 1060-1072.

Schroeder, G.N., Petty, N.K., Mousnier, A., Harding, C.R., Vogrin, A.J., Wee, B., Fry, N.K., Harrison, T.G., Newton, H.J., Thomson, N.R., Beatson, S.A., Dougan, G., Hartland, E.L., and Frankel, G. (2010). Legionella pneumophila strain 130b possesses a unique combination of type IV secretion systems and novel Dot/Icm secretion system effector proteins. *J Bacteriol* 192**,** 6001-6016.

Schunder, E., Gillmaier, N., Kutzner, E., Herrmann, V., Lautner, M., Heuner, K., and Eisenreich, W. (2014). Amino Acid Uptake and Metabolism of *Legionella pneumophila* Hosted by *Acanthamoeba castellanii*. *J Biol Chem*.

Schwoppe, C., Winkler, H.H., and Neuhaus, H.E. (2002). Properties of the glucose-6-phosphate transporter from *Chlamydia pneumoniae* (HPTcp) and the glucose-6-phosphate sensor from *Escherichia coli* (UhpC). *J Bacteriol* 184**,** 2108-2115.

Segal, G., Feldman, M., and Zusman, T. (2005). The Icm/Dot type-IV secretion systems of *Legionella pneumophila* and *Coxiella burnetii*. *FEMS Microbiol Rev* 29**,** 65-81.

Sheehan, K.B., Henson, J.M., and Ferris, M.J. (2005). *Legionella* species diversity in an acidic biofilm community in Yellowstone National Park. *Appl Environ Microbiol* 71**,** 507-511.

Shin, S., and Roy, C.R. (2008). Host cell processes that influence the intracellular survival of *Legionella pneumophila*. *Cell Microbiol* 10**,** 1209-1220.

Solomon, J.M., and Isberg, R.R. (2000). Growth of *Legionella pneumophila* in *Dictyostelium discoideum*: a novel system for genetic analysis of host-pathogen interactions. *Trends Microbiol* 8**,** 478-480.

Spirig, T., Tiaden, A., Kiefer, P., Buchrieser, C., Vorholt, J.A., and Hilbi, H. (2008). The *Legionella* autoinducer synthase LqsA produces an α-hydroxyketone signaling molecule. *J Biol Chem* 283**,** 18113-18123.

Starkenburg, S.R., Casey, J.M., and Cianciotto, N.P. (2004). Siderophore activity among members of the Legionella genus. *Curr Microbiol* 49**,** 203-207.

Steeb, B., Claudi, B., Burton, N.A., Tienz, P., Schmidt, A., Farhan, H., Maze, A., and Bumann, D. (2013). Parallel exploitation of diverse host nutrients enhances *Salmonella* virulence. *PLoS Pathog* 9**,** e1003301.

Steinert, M., Heuner, K., Buchrieser, C., Albert-Weissenberger, C., and Glockner, G. (2007). *Legionella* pathogenicity: genome structure, regulatory networks and the host cell response. *Int J Med Microbiol* 297**,** 577-587.

Stenmark, H. (2009). Rab GTPases as coordinators of vesicle traffic. *Nat Rev Mol Cell Biol* 10**,** 513-525.

Stephens, L.R., and Irvine, R.F. (1990). Stepwise phosphorylation of *myo*-inositol leading to *myo*-inositol hexakisphosphate in *Dictyostelium*. *Nature* 346**,** 580-583.

Stines-Chaumeil, C., Talfournier, F., and Branlant, G. (2006). Mechanistic characterization of the MSDH (methylmalonate semialdehyde dehydrogenase) from *Bacillus subtilis*. *Biochem J* 395**,** 107-115.

Sturgill-Koszycki, S., and Swanson, M.S. (2000). *Legionella pneumophila* replication vacuoles mature into acidic, endocytic organelles. *J Exp Med* 192**,** 1261-1272.

Subedi, K.P., Kim, I., Kim, J., Min, B., and Park, C. (2008). Role of GldA in dihydroxyacetone and methylglyoxal metabolism of *Escherichia coli* K12. *FEMS Microbiol Lett* 279**,** 180-187.

Swanson, M.S., and Isberg, R.R. (1995). Association of *Legionella pneumophila* with the macrophage endoplasmic reticulum. *Infect Immun* 63**,** 3609-3620.

Szeto, L., and Shuman, H.A. (1990). The *Legionella pneumophila* major secretory protein, a protease, is not required for intracellular growth or cell killing. *Infect Immun* 58**,** 2585-2592.

Talfournier, F., Stines-Chaumeil, C., and Branlant, G. (2011). Methylmalonate-semialdehyde dehydrogenase from *Bacillus subtilis*: substrate specificity and coenzyme A binding. *J Biol Chem* 286**,** 21971-21981.

Tatlock, H. (1944). A rickettsia-like organism recovered from guinea pigs. *Proceedings of the Society for Experimental Biology and Medicine* 57**,** 95-98.

Tauchi-Sato, K., Ozeki, S., Houjou, T., Taguchi, R., and Fujimoto, T. (2002). The surface of lipid droplets is a phospholipid monolayer with a unique fatty acid composition. *J Biol Chem* 277**,** 44507-44512.

Taylor, M., Ross, K., and Bentham, R. (2009). Legionella, protozoa, and biofilms: interactions within complex microbial systems. *Microb Ecol* 58**,** 538-547.

Temmerman, R., Vervaeren, H., Noseda, B., Boon, N., and Verstraete, W. (2006). Necrotrophic growth of *Legionella pneumophila*. *Appl Environ Microbiol* 72**,** 4323-4328.

Tesh, M.J., and Miller, R.D. (1981). Amino acid requirements for *Legionella pneumophila* growth. *J Clin Microbiol* 13**,** 865-869.

Tesh, M.J., and Miller, R.D. (1983). Arginine biosynthesis in *Legionella pneumophila*: absence of N-acetylglutamate synthetase. *Can J Microbiol* 29**,** 1230-1233.

Tesh, M.J., Morse, S.A., and Miller, R.D. (1983). Intermediary metabolism in *Legionella pneumophila*: utilization of amino acids and other compounds as energy sources. *J Bacteriol* 154**,** 1104-1109.

Thacker, S.B., Bennett, J.V., Tsai, T.F., Fraser, D.W., Mcdade, J.E., Shepard, C.C., Williams, K.H., Jr., Stuart, W.H., Dull, H.B., and Eickhoff, T.C. (1978). An outbreak in 1965 of severe respiratory illness caused by the Legionnaires' disease bacterium. *J Infect Dis* 138**,** 512-519.

Tiaden, A., Spirig, T., Carranza, P., Bruggemann, H., Riedel, K., Eberl, L., Buchrieser, C., and Hilbi, H. (2008). Synergistic contribution of the *Legionella pneumophila lqs* genes to pathogen-host interactions. *J Bacteriol* 190**,** 7532-7547.

Tiaden, A., Spirig, T., Sahr, T., Walti, M.A., Boucke, K., Buchrieser, C., and Hilbi, H. (2010). The autoinducer synthase LqsA and putative sensor kinase LqsS regulate phagocyte interactions, extracellular filaments and a genomic island of *Legionella pneumophila*. *Environ Microbiol* 12**,** 1243-1259.

Tiaden, A., Spirig, T., Weber, S.S., Bruggemann, H., Bosshard, R., Buchrieser, C., and Hilbi, H. (2007). The *Legionella pneumophila* response regulator LqsR promotes host cell interactions as an element of the virulence regulatory network controlled by RpoS and LetA. *Cell Microbiol* 9**,** 2903-2920.

Tilney, L.G., Harb, O.S., Connelly, P.S., Robinson, C.G., and Roy, C.R. (2001). How the parasitic bacterium *Legionella pneumophila* modifies its phagosome and transforms it into rough ER: implications for conversion of plasma membrane to the ER membrane. *J Cell Sci* 114**,** 4637-4650.

Tison, D.L. (1987). Microbial ecology of *Legionella*. *J Infect Dis* 156**,** 852.

Trigui, H., Dudyk, P., Oh, J., Hong, J.I., and Faucher, S.P. (2015). A regulatory feedback loop between RpoS and SpoT supports the survival of *Legionella pneumophila* in water. *Appl Environ Microbiol* 81**,** 918-928.

Turner, B.L., Paphazy, M.J., Haygarth, P.M., and McKelvie, I.D. (2002). Inositol phosphates in the environment. *Philos Trans R Soc Lond B Biol Sci* 357**,** 449-469.

Urwyler, S., Brombacher, E., and Hilbi, H. (2009). Endosomal and secretory markers of the *Legionella*-containing vacuole. *Commun Integr Biol* 2**,** 107-109.

Vincent, C.D., Friedman, J.R., Jeong, K.C., Buford, E.C., Miller, J.L., and Vogel, J.P. (2006). Identification of the core transmembrane complex of the *Legionella* Dot/Icm type IV secretion system. *Mol Microbiol* 62**,** 1278-1291.

Viner, R., Chetrit, D., Ehrlich, M., and Segal, G. (2012). Identification of two *Legionella pneumophila* effectors that manipulate host phospholipids biosynthesis. *PLoS Pathog* 8**,** e1002988.

Wadowsky, R.M., and Yee, R.B. (1985). Effect of non-*Legionellaceae* bacteria on the multiplication of *Legionella pneumophila* in potable water. *Appl Environ Microbiol* 49**,** 1206-1210.

Warren, W.J., and Miller, R.D. (1979). Growth of Legionnaires disease bacterium (*Legionella pneumophila*) in chemically defined medium. *J Clin Microbiol* 10**,** 50-55.

Watarai, M., Derre, I., Kirby, J., Growney, J.D., Dietrich, W.F., and Isberg, R.R. (2001). *Legionella pneumophila* is internalized by a macropinocytotic uptake pathway controlled by the Dot/Icm system and the mouse *lgn1* locus. *J Exp Med* 194**,** 1081-1096.

Watts, D.J., and Ashworth, J.M. (1970). Growth of myxameobae of the cellular slime mould *Dictyostelium discoideum* in axenic culture. *Biochem J* 119**,** 171-174.

Weber, S., Stirnimann, C.U., Wieser, M., Frey, D., Meier, R., Engelhardt, S., Li, X., Capitani, G., Kammerer, R.A., and Hilbi, H. (2014a). A type IV translocated *Legionella* cysteine phytase counteracts intracellular growth restriction by phytate. *J Biol Chem* 289**,** 34175-34188.

Weber, S., Wagner, M., and Hilbi, H. (2014b). Live-cell imaging of phosphoinositide dynamics and membrane architecture during *Legionella* infection. *MBio* 5**,** e00839-00813.

Weber, S.S., Ragaz, C., and Hilbi, H. (2009). The inositol polyphosphate 5-phosphatase OCRL1 restricts intracellular growth of *Legionella*, localizes to the replicative vacuole and binds to the bacterial effector LpnE. *Cell Microbiol* 11**,** 442-460.

Weber, S.S., Ragaz, C., Reus, K., Nyfeler, Y., and Hilbi, H. (2006). *Legionella pneumophila* exploits PI(4)P to anchor secreted effector proteins to the replicative vacuole. *PLoS Pathog* 2**,** e46.

Weiss, E., Peacock, M.G., and Williams, J.C. (1980). Glucose and glutamate metabolism of *Legionella pneumophila*. *Curr Microbiol* 4**,** 1-6.

Wiater, L.A., Marra, A., and Shuman, H.A. (1994a). *Escherichia coli* F plasmid transfers to and replicates within *Legionella pneumophila*: an alternative to using an RP4-based system for gene delivery. *Plasmid* 32**,** 280-294.

Wiater, L.A., Sadosky, A.B., and Shuman, H.A. (1994b). Mutagenesis of *Legionella pneumophila* using Tn*903*dll*lacZ*: identification of a growth-phase-regulated pigmentation gene. *Mol Microbiol* 11**,** 641-653.

Wieland, H., Ullrich, S., Lang, F., and Neumeister, B. (2005). Intracellular multiplication of *Legionella pneumophila* depends on host cell amino acid transporter SLC1A5. *Mol Microbiol* 55**,** 1528-1537.

Williams, R.J. (2012). Iron in evolution. *FEBS Lett* 586**,** 479-484.

Wright, E.M., Loo, D.D., Panayotova-Heiermann, M., Lostao, M.P., Hirayama, B.H., Mackenzie, B., Boorer, K., and Zampighi, G. (1994). 'Active' sugar transport in eukaryotes. *J Exp Biol* 196**,** 197-212.

Xu, L., Shen, X., Bryan, A., Banga, S., Swanson, M.S., and Luo, Z.Q. (2010). Inhibition of host vacuolar H+-ATPase activity by a *Legionella pneumophila* effector. *PLoS Pathog* 6**,** e1000822.

Yamada, K., Nakata, M., Horimoto, N., Saito, M., Matsuoka, H., and Inagaki, N. (2000). Measurement of glucose uptake and intracellular calcium concentration in single, living pancreatic beta-cells. *J Biol Chem* 275**,** 22278-22283.

Yebra, M.J., Zuniga, M., Beaufils, S., Perez-Martinez, G., Deutscher, J., and Monedero, V. (2007). Identification of a gene cluster enabling *Lactobacillus* casei BL23 to utilize *myo*-inositol. *Appl Environ Microbiol* 73**,** 3850-3858.

Yeh, J.I., Chinte, U., and Du, S. (2008). Structure of glycerol-3-phosphate dehydrogenase, an essential monotopic membrane enzyme involved in respiration and metabolism. *Proc Natl Acad Sci U S A* 105**,** 3280-3285.

Yoshida, K., Yamaguchi, M., Morinaga, T., Kinehara, M., Ikeuchi, M., Ashida, H., and Fujita, Y. (2008). *myo*-Inositol catabolism in *Bacillus subtilis*. *J Biol Chem* 283**,** 10415-10424.

Yoshida, K., Yamamoto, Y., Omae, K., Yamamoto, M., and Fujita, Y. (2002). Identification of two *myo*-inositol transporter genes of *Bacillus subtilis*. *J Bacteriol* 184**,** 983-991.

Yoshida, K.I., Aoyama, D., Ishio, I., Shibayama, T., and Fujita, Y. (1997). Organization and transcription of the *myo*-inositol operon, *iol*, of *Bacillus subtilis*. *J Bacteriol* 179**,** 4591-4598.

Yoshida, K.I., Shibayama, T., Aoyama, D., and Fujita, Y. (1999). Interaction of a repressor and its binding sites for regulation of the *Bacillus subtilis iol* divergon. *J Mol Biol* 285**,** 917-929.

Zamboni, N., Fendt, S.M., Ruhl, M., and Sauer, U. (2009). (13)C-based metabolic flux analysis. *Nat Protoc* 4**,** 878-892.

Zhao, Y., Altman, B.J., Coloff, J.L., Herman, C.E., Jacobs, S.R., Wieman, H.L., Wofford, J.A., Dimascio, L.N., Ilkayeva, O., Kelekar, A., Reya, T., and Rathmell, J.C. (2007). Glycogen synthase kinase 3alpha and 3beta mediate a glucose-sensitive antiapoptotic signaling pathway to stabilize Mcl-1. *Mol Cell Biol* 27**,** 4328-4339.

Zhao, Y., Wieman, H.L., Jacobs, S.R., and Rathmell, J.C. (2008). Mechanisms and methods in glucose metabolism and cell death. *Methods Enzymol* 442**,** 439-457.

Zheng, H., Chatfield, C.H., Liles, M.R., and Cianciotto, N.P. (2013). Secreted pyomelanin of *Legionella pneumophila* promotes bacterial iron uptake and growth under iron-limiting conditions. *Infect Immun* 81**,** 4182-4191.

Zhou, K., Takegawa, K., Emr, S.D., and Firtel, R.A. (1995). A phosphatidylinositol (PI) kinase gene family in *Dictyostelium discoideum*: biological roles of putative mammalian p110 and yeast Vps34p PI3-kinase homologs during growth and development. *Mol Cell Biol* 15**,** 5645-5656.

Zhu, N., Feng, X., He, C., Gao, H., Yang, L., Ma, Q., Guo, L., Qiao, Y., Yang, H., and Ma, T. (2011). Defective macrophage function in aquaporin-3 deficiency. *FASEB J* 25**,** 4233-4239.

Zink, S.D., Pedersen, L., Cianciotto, N.P., and Abu-Kwaik, Y. (2002). The Dot/Icm type IV secretion system of *Legionella pneumophila* is essential for the induction of apoptosis in human macrophages. *Infect Immun* 70**,** 1657-1663.

Zusman, T., Aloni, G., Halperin, E., Kotzer, H., Degtyar, E., Feldman, M., and Segal, G. (2007). The response regulator PmrA is a major regulator of the *icm/dot* type IV secretion system in *Legionella pneumophila* and *Coxiella burnetii*. *Mol Microbiol* 63**,** 1508-1523.

Zusman, T., Gal-Mor, O., and Segal, G. (2002). Characterization of a *Legionella pneumophila relA* insertion mutant and toles of RelA and RpoS in virulence gene expression. *J Bacteriol* 184**,** 67-75.

Danksagung

Nach nun mehr vier Jahren geht meine Doktorandenzeit nun zu Ende. An viel wissenschaftlicher und persönlicher Erfahrung reicher, heißt es nun Danke zu sagen.

Ein besonderer Dank geht dabei an meinen Doktorvater Hubert Hilbi. Nicht nur für die Möglichkeit an diesem interessanten Thema zu forschen, sondern auch für seine fortwährende Unterstützung, angeregte Diskussionen über Filme und Musik und den ein oder anderen Pogo.

Ein großes Dankeschön geht an meine Kooperationspartner Wolfgang Eisenreich und vor allem auch Ina Häuslein, die mit ihren Experimenten und ihrer isotoplogischen Expertise entscheidend für diese Arbeit waren. Danke Ina auch für die eine oder andere erheiternde Kaffeepause.

Großer Dank gebührt auch der gesamten AG Hilbi und allen Nicht-Hilbis des Pettenkofer Instituts für viele tolle Erlebnisse und schöne Feiern. Insbesondere danke ich Ivo Finsel für meine finanziell gesicherte Zukunft in der Behörde oder durch Umsetzung der ein oder anderen Milliarden-Dollar-Idee und Gudrun Pfaffinger für ihre Lebensweisheit und ihren Rat. Alle nicht genannten seien sich meines tiefen Danks bewusst und verzeihen mir, dass ich sie hier nicht namentlich erwähne.

Ich danke natürlich meinen Eltern und meiner gesamten Familie für die Unterstützung während meines Studiums und meiner Promotion, ohne die dieses Unterfangen nicht möglich gewesen wäre.

Zu guter Letzt und doch am eindringlichsten danke ich meiner Frau Franziska, die mir in dieser nicht immer leichten Zeit den Rücken frei gehalten hat, mich unterstützt hat und immer bereit war, meine Sorgen zu teilen und die ein oder andere Schimpftirade zu ertragen, wenn der Frust zu groß wurde. Ich liebe dich sehr, Spatzl! Und jetzt auf ins nächste Abenteuer!